Some Electrical Properties of Alkaline Earth Oxides With Particular Reference to Oxide-Coated Cathodes

Thesis presented for the degree of Ph.D.

At The University of BIRMINGHAM

by

G. S. HIGGINSON, B.A.

Physics Dept.

U.C.N.S.

March, 1957.

CONTENTS

Introduction.

SECTION I

Chapter 1. The Oxide-Coated Cathode 5

Preparation and General Properties 5

Chapter 2 The Mechanism of the Oxide-Coated Cathode 12

Early Theories 12

The Fowler-Wilson Theory of Semiconduction 13

Thermionic Emission from Oxide Cathodes 17

Emission Decay Effects 21

Chapter 3 Apparatus and Experimental Techniques 24

General Arrangements 24

The Vacuum System 24

Measurement of Pressure 25

Experimental Tubes 26

Assembly of an Experimental Tube 27

The Activation Procedure 30

Measurements. 31

SECTION 2

An Investigation of the Conductivity of Oxide-Coated Cathodes.

Chapter 4 Previous Work 32

Surface Electron Traps 38

Chapter 5 Preliminary Experiments 42

Introduction 42

The Conductivity of Oxide Coatings 42

Chapter 5 Contd....

Measurements on BaO coatings 43

Measurements on Mixed Oxide Coatings 48

Summary Table of Activation Energies 50

Discussion of Results 51

Chapter 6 Further Conductivity Measurements on Cathodes BaSr4 - BaSr9 53

Discussion of Results 74

Chapter 7 An Investigation of the Low Temperature Conductivity Effect 79

Theoretical Curves 81

Long Term Activation Experiments 85

Summary of Results 86

Conclusions 87

Chapter 8 Barium Deposition Experiments 90

Discussion of Results 92

SECTION 3

An Investigation of the Effect of Oxygen and Sulphur on the Oxide Coated Cathode

Chapter 9 Previous Work

The Effect of Oxygen on Electron Emission 95

The Effect of Oxygen on Conductivity 96

The Effect of Sulphur on the Electrical Properties of Oxide Cathodes 98

Chapter 10	Experimental Results	
	Introduction	101
	Preliminary Experiments	101
	Discussion of Preliminary Results	103
	Further Oxygen Poisoning Experiments	105
	Sulphur Poisoning Experiments	106
	Sulphur and Oxygen Poisoning Experiments	108
	Discussion of Results of Oxygen and Sulphur Poisoning Experiments	111
Chapter 11	Introduction	114
	Experiments on Cathode BaSr11	114
	Experiments on Cathode BaSr8	116
	Conclusions	118
Chapter 12	Discussion of Results	
	1. Behaviour of the Oxide-Cathode in the High Temperature Region	120
	2. Behaviour of the Oxide-Cathode at temperatures below 700°K	122
	Further Work	126
Appendix I	An A.C. Technique for the measuring of Probe Current-Voltage Characteristics	128
Acknowledgments		135
Bibliography		136

SYNOPSIS

The electrical conductivity and thermionic emission from cathodes coated with barium oxide and a mixture of barium and strontium oxides has been studied as a function of temperature in the range 290° - 1000°K, employing cylindrical diodes containing a probe-wire embedded in the oxide coating.

At temperatures above 500°K the results obtained are in complete agreement with the pore-conduction theory of Loosjes and Vink. At temperatures below 500°K an effect not previously reported is observed. The log I/R vs. I/T curve is not linear in this region but exhibits a bend at ~ 400°K with a lower slope section between 400° and 290°K.

Theoretical curves of a similar shape are obtained by assuming that the conductivity is given by a relation of the kind

$$\sigma = \sigma_0 \exp\left(\frac{-Q}{kT}\right) + \sigma_1 \exp\left(\frac{-L}{kT}\right)$$

which implies that at temperatures below 500°K two conduction mechanisms are operating in parallel. A simple correction is justified which enables a value of Q to be obtained from the experimental curves. Experiments in which barium is deposited upon the cathode suggest that the mechanism with temperature dependence L is one of movement of barium ions over the surfaces of internal crystal grains.

The results of oxygen and sulphur poisoning experiments support the Loosjes and Vink theory and in addition tend to confirm that a surface conduction mechanism is important at lower temperatures. Sulphur poisoning is found to be a reversible effect very similar to oxygen poisoning described by Metson and Shepherd.

INTRODUCTION

This thesis is concerned with studies in the field of solid state physics which are being made at the University College of North Staffordshire under the general direction of Professor F.A.Vick. The work described here forms part of a research programme designed to investigate the properties of oxide-coated cathodes in the light of modern theories of semiconduction.

The experimental work undertaken consists of two allied investigations which assist in the elucidation of the electrical conduction processes occurring in the oxide cathode. The first of these, described in Section 2, is concerned with the variation with temperature of the conductivity of the oxide layer at various stages during the activation of the cathode. For this purpose simple diodes with cylindrical symmetry are employed and the conductivity is measured by means of a probe wire embedded in the coating at a known distance from the core. The temperature range covered by the experiments is large, ranging from 1000°K to room temperature in most cases. The second investigation, described in Section 3, is concerned with the effect of oxygen gas and sulphur vapour on the oxide-cathode at temperatures within this range.

These two sections are preceeded by brief surveys of the relevant literature relating to conductivity measurements and to oxygen and sulphur poisoning experiments. Section 1 forms an introduction to the oxide cathode. A brief Chapter on the preparation and general properties of cathodes is followed by a discussion of some of the theoretical

concepts involved in an investigation of oxide cathode conductivity. This is succeeded by a description of the apparatus employed.

An additional piece of experimental work is described in an Appendix since this was not relevant to the main thesis but consisted entirely in an improvement in technique.

SECTION I

CHAPTER I

THE OXIDE-COATED CATHODE

Preparation and General Properties.

The oxide coated cathode usually consists of one or more of the oxides of the alkaline earth metals, coated on to a metallic base which may be in the form of a wire, strip or tube. The coating thickness is generally of the order of 50 microns.

The cathode may be heated directly by passing current through the coated wire or strip, or indirectly by an insulated heater inserted into the tube.

Several base metals have been employed from time to time; e.g. platinum was in general use before 1929, cathodes then being of the directly heated type. More recently, with the widespread use of indirectly heated cathodes, a less expensive base metal was required and nickel containing small quantities of reducing impurities was found to be satisfactory. One form of nickel often used, 'O' Nickel, has the composition shown in the following table:-

'O' Nickel

Ni	99.5%	Si	0.1%
Co	0.5%	Cu	0.1%
Mg	0.07 - 0.15%	S	0.005%
Mn	0.15%	C	0.04%
Fe	0.2%		

The presence of silicon and magnesium in the nickel base metal causes a reduction during the activation process and facilitates the preparation of satisfactory cathodes.

The maximum thermionic emission from oxide cathodes at the same temperature coated with the three oxides is in the approximate ratio:-

BaO : SrO : CaO :: 100 : 10 : 1

a mixed barium strontium oxide, signified (BaSr)O to indicate that both metals are present in the same crystal lattice, produces a coating which yields a higher emission than one of barium oxide and Grey (1) has shown that a coating of (BaCa)O in optimum proportions, similarly yields a large emission.

The addition of small quantities of calcium oxide to a barium strontium mixture has been found to give increased emission and this mixture is often used commercially. The function of the calcium is not fully understood but it is thought that its presence influences the crystal size of the oxide which as Kawamura (2) and Yamaka (3) have shown is an emission determining factor.

The alkaline earth oxides are unstable in air and so it is necessary to prepare them from stable compounds which may subsequently be converted to the oxides in vacuo. The usual method is to employ the carbonate, or a coprecipitated mixture of carbonates in the case of the mixed oxide, though it is possible to use the nitrate, resinate and in the case of barium the azide in aqueous solution. The carbonate is suspended in a volatile organic solvent; ethyl butyl or amyl acetates are commonly used, and a small quantity of nitrocellulose is added to act as a binder.

Several methods of applying the coating have been developed, the more important ones being spraying, painting, dragging and cataphoresis. The choice of any particular method will depend upon the geometry of the cathode; e.g. dragging or cataphoresis for wire cathodes; painting or spraying for indirectly heated cathodes. The exact composition of the suspension used will vary with the method of application and the requirements of the cathode. A typical preparation designed for spraying is given:-*

Double carbonates	3Kg
Nitro-cellulose (5% in amyl acetate)	1.6 litre
Amyl acetate	1.0 litre
Methyl alcohol	1.8 litre

The final composition of the sprayed coating is influenced by the proportion of air to carbonate suspension used in the spray gun. Also, if the cathode being sprayed is some distance from the gun a fairly rough coating will result. Such a coating is suitable for us in low voltages valves. A wet spray, giving a much smoother coating is preferable for use in high voltage applications, for this reduces the danger of flash-over or arcing from peaks on the cathode surface where the electric field may reach a high value.

When the cathode has been coated it is enclosed in the vacuum tube which is then exhausted to a pressure of 10^{-5} mm.Hg. or less. The glass and metal parts are outgassed by baking and eddy-current heating. During the baking process the nitrocellulose binder is converted to gaseous products which are pumped away. The breakdown process is

* (Source)

initiated by gradually raising the temperature of the cathode. The conversion of the carbonates to oxides is completed at around 950°C.

Following the breakdown process the cathode must be activated before it becomes an efficient electron emitter. This may be accomplished in one of several ways or a combination of these. The temperature of the cathode may be raised to around 1200°C for a few minutes (thermal activation) or a potential applied to the anode (cathode at 900°C) and an emission current drawn which increases to a steady value over a period of several hours, (current activation). A third method of activation is to admit a reducing gas into the valve while the cathode is at 900°C. This method has been employed by several authors: Prescott and Morrison (4), Eisenstein (5) who used methane; and more recently Forman (6) who used ethane to obtain highly activated cathodes. The process has been studied in detail by Wagener (7) who showed that hydrogen, water vapour and methane are all activating gases below 10^{-5} mm.Hg. pressure.

It is generally assumed that the activating process produces free alkaline earth metal in the coating. In thermally activated cathodes impurities in the core metal act as reducing agents, liberating free alkaline earth metal and producing complex compounds at the core-coating interface. Thermal energy alone does not produce activation to any measurable extent for it has been found that cathodes prepared on a pure nickel base are very difficult to activate, while the inclusion of small quantities of silicon and magnesium in the nickel facilitates rapid activation.

The presence of interface compounds formed during activation was first reported by Arnold (8) who noted the presence of $BaPtO_3$ when using platinum as a base metal. Fineman and Eisenstein (9) have made an extensive study of the properties of the interface layers and have found Ba_2SiO_4 and $BaTiO_4$ in the interface of cathodes on nickel cores containing less than 0.5% of Si and Ti respectively. Rocksby (10) has also identified these compounds in the interface using X-ray diffraction analysis.

A theoretical study of the chemical processes occuring during breakdown and activation has been made recently by Rittner (11). Employing a thermodynamical method he was able to indicate the reactions most likely to be favoured under given conditions during the breakdown and subsequent activation operations in the production of a typical cathode. These considerations showed that the breakdown process was a critical one in the processing schedule, for during this time, when the carbonate is being reduced to the oxide with evolution of Co_2, the reducing agent (Mg or Si) in the core may be oxidised rapidly by the carbonate with the release of CO, a side reaction which is highly deleterious. It was also concluded that the rate-determining process during thermal activation is the rate of diffusion of the reducing agent in the nickel base metal. If this is high, then free barium may be produced quickly at relatively high vapour pressures and consequently facilitate the solution of Ba metal in the lattice of the oxide which in turn gives rise to an active cathode. In a current-activated cathode

it is quite probable that electrolysis plays some part; (Ba, Sr Ca)$^{++}$ ions moving through the coating towards the core, while some oxygen ions move to the outer surface of the oxide, form oxygen molecules and are pumped away. This liberation of oxygen molecules during activation has been demonstrated by Becker (12) who used the gas to poison the emission from a tunsten wire. Shepherd (13) used a mass sprectrometer technique and was unable to detect the presence of oxygen ions during activation, showing that the oxygen given off during activation is in the form of neutral molecules.

In addition to the evolution of oxygen, barium and strontium metal and to a lesser extent the oxides are also evaporated from an oxide cathode during activation and subsequent cathode life. Wooten/Ruehle and Moore (14) have shown that the evaporation product from a mixed oxide cathode is largely barium metal with less than 5% strontium; BaO and SrO being evaporated to the extent of 2% and 0.01% respectively. This preferential evaporation of BaO takes place from the outer layers of the coating and in many cases relatively thick layers of BaO deficient coating at the surface have been found (15).

The extent to which excess alkaline earth metal is present in the oxide coating has been the subject of several investigations. The most recent, by Moore, Wooten and Morrison (16) employing careful chemical techniques, has shown that the significant amount of excess metal is not greater than one atom in 10^6 molecules of (BaSr)O in a practical oxide cathode. Even cathodes with very low emission qualities were found to contain this proportion and so it was concluded that the excess metal (Ba) content of an oxide cathode was not necessarily a factor limiting

the performance of the cathode.

At some stage during the activating process the vacuum tube is sealed off from the pump. Emission current is usually drawn prior to sealing off and finally a getter is fired. The active metal surface thus deposited onto the glass of the tube takes up any gas evolved during subsequent activation and operation.

An activated oxide coated cathode consists therefore of a metal core separated from the bulk of the oxide coating by an interface layer and this oxide coating contains an excess of the alkaline earth metal in a concentration of about 10^{17} atoms per c.c.

CHAPTER 2

THE MECHANISM OF THE OXIDE-COATED CATHODE

Early Theories

Early theories of the mechanism of electron-emission from an oxide-coated cathode were based on the concept of reduction of the work function of the base metal by analogy with the thoriated tungsten emitter then in general use. Two theories were current until the advent of the Fowler-Wilson theory of semiconductors. The first put forward by Lowery (17) suggested that the mechanism was essentially an electrolytic one; free barium was formed in the coating and diffused to the interface where it formed a monolayer on the base metal and so reduced the work function. The emitted electrons were said to diffuse through the interstices of the coating, for the oxide itself was regarded as a poor conductor.

The rival theory maintained that a thin film of alkaline earth metal existed on the outer surface of the oxide. This was considered by Becker (18) to be the emission determining factor. The conductivity of the coating was assumed to be sufficiently great for electrons to move from the base metal to the oxide surface.

An experiment by Becker and Sears (19) was designed to distinguish between the two theories. The emission was found to fall by a factor of 10^4 when the oxide coating was removed and this was adjudged to be evidence in favour of the second theory. Later investigations by Darbyshire (20) and Huber and Wagener (21) employing electron diffrac-

tion techniques have failed to identify a surface barium layer and no conclusive evidence for its existence has so far been advanced.

The Fowler-Wilson Theory of Semiconduction.

The major disadvantage under which Lowery, Becker and other authors worked, before 1930, was the absence of any adequate theory of electronic conduction in dielectric materials such as the alkaline earth oxides. This defect was rectified by Wilson (22) in 1931, who extended the band theory of solids to cover the case of impurity semiconductors. According to this theory, two types of impurity semiconductors may be distinguished. In the first (N-type), electrons may be excited into the conduction band of the material from their original positions (at $0^{\circ}K$) in extra energy levels, (donor levels) lying in the forbidden zone between the empty conduction band and the topmost filled band but separated by only a small energy gap (a few eV) from the conduction band. In the second (P-type) of impurity semiconductor, conduction may arise by the virtual movement of positive holes in the topmost filled band which are formed by the transference of electrons from that band into adjacent extra energy levels in the forbidden zone.

Following Fowler (23) the equilibrium conditions in an impurity semiconductor, of either kind, may be calculated. It is assumed that

1. The conduction band is completely empty at $0^{\circ}K$
2. The density of impurity levels is n_b per cc. and these are completely full of carriers at $0^{\circ}K$.

3. The energy gap ΔE between the conduction band and the extra levels is larger than kT i.e. greater than 0.5eV and to a first approximation the energy gap between the conduction band and the filled band E is so large that the contribution of carriers from the full band is negligible.

If the zero of energy is taken at the extra levels, then the chemical potential, μ, or Fermi level is given by

$$\exp\left(\frac{\mu}{kT}\right) = n_b^{1/2}\omega^{1/2}\frac{h^{3/2}}{(2\pi m kT)^{3/4}}\exp\left(\frac{+\Delta E}{2kT}\right) \qquad \text{---------- (1)}$$

where ω is the statistical weight of states in the conduction band i.e. 2.

m is effective mass of an electron in the cond. band

h is Planck's const. and k Boltzmann's const.

This equation shows that to a first approximation the μ-level is midway between the extra levels and the conduction band.

The density of electrons in the conduction band n_f is given by:-

$$n_f = n_b^{1/2}\omega^{1/2}\frac{(2\pi m kT)^{3/4}}{h^{3/2}}\exp\left(\frac{-\Delta E}{2kT}\right) \qquad \text{- - - - - (2)}$$

The specific conductivity σ' of the material is given by

$$\sigma' = n_f e V \qquad \text{- - - - (3)}$$

where V is the mean velocity of the carriers.

If we assume that the mean free path l_o has a constant value, then since V is related to l_o

$$\sigma' = \frac{4 n_f l_o e^2}{3(2\pi m k T)^{1/2}} \qquad \text{---(4)}$$

and sub. for n_f

$$\sigma' = \frac{4}{3} \omega^{1/2} n_b^{1/2} \frac{e^2 l_o}{h^{3/2}} (2\pi m k T)^{1/4} \exp\left(\frac{-\Delta E}{2kT}\right) \qquad \text{---(5)}$$

Provided that $\Delta E \gg kT$, the temperature variation of conductivity will be due to the exponential term

$$\text{i.e.} \quad \sigma' = \sigma'_o \exp\left(\frac{-Q}{kT}\right) \qquad \text{---(6)}$$

This form describes the variation of conductivity with temperature for either type of impurity semiconductor.

The term σ'_o over a limited range of temperature may be regarded as a function only of n_b.

By combining equations (1) and (2) it is possible to express the density of electrons in the conduction band in terms of the Fermi level

$$n_f = \frac{2}{h^3} (2\pi m k T)^{3/2} \exp\left(\frac{-\mu}{kT}\right) \qquad \text{---(7)}$$

Substituting this value in equation(4)

gives $$\sigma' = \frac{8 l_o e^2}{3h^3} (2\pi m k T) \exp\left(\frac{-\mu}{kT}\right) \qquad \text{---(8)}$$

This expression contains the density of impurity centres implicitly in the chemical potential μ.

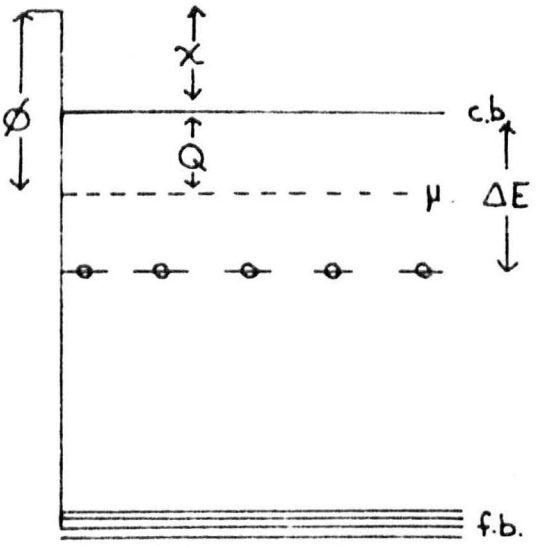

FIG. 2.1

This equation may be compared with the experimental temperature dependence of

$$\sigma' = \sigma'_0 \exp\left(\frac{-Q}{kT}\right)$$

Thus a plot of log σ' vs $1/T$ should if the material behaves as a semiconductor yield a linear variation, from the slope of which the separation of the Fermi level from the conduction band may be determined. This should be $\frac{\Delta E}{2}$ provided the condition that $n_f \ll n_b$ is maintained. This implies that ΔE must be greater than 0.5 eV.

Provided that this condition holds good the slope of the conduction line (Q) is equal to $\frac{\Delta E}{2}$. However if ΔE is small all the donor centres may become ionised at comparatively low temperatures and the condition $n_f \ll n_b$ becomes $n_f \approx n_b$. Under these conditions n_f is constant and the variation of conductivity with temperature is determined by the temperature variance of l_o. At low temperatures in an impurity semiconductor the impurity centres produce a scattering of the electron waves. This leads to a mobility proportional to $T^{3/2}$. Hence if n_f is approximately constant the variation of conductivity with temperature is determined by $\sigma' \propto T^{3/2}$.

For a donor concentration of 10^{17} per cc. a value usually assumed for oxide cathodes, the minimum value of ΔE, below which $n_f \approx n_b$ is 0.3 eV at 500°K.

This implies that conductivity curves with slopes less than 0.15 eV cannot be interpreted on the simple semiconductor basis outlined in the preceeding paragraphs.

Thermionic Emission from Oxide-Coated Cathodes.

One property which has lead to the widespread use of oxide cathodes is the ability to emit a copious supply of electrons at a relatively low temperature. This property has been treated theoretically by Schottky who derived a Richardson type of equation for the emission. This has the form

$$j_o = (1-r) A T^2 \exp\left(\frac{-\phi}{kT}\right) \qquad \text{(9)}$$

where j_o is the saturation current density at temperature T°K

A is $\frac{4\pi m k^2 e}{h^3}$ = 120 amp.cm^{-2} deg.$^{-2}$

r is the mean reflection coefficient for electrons at the surface.

ϕ is the total work function = $\chi + E_o - \mu$

Fig. (2.1) shows that ϕ is the total step from the Fermi level of the base metal to the potential just outside the semiconductor.

μ may be expressed in terms of ΔE and n_b thus:-

$$\mu = E - \frac{\Delta E}{2} + kT \log\left[\frac{n_b h^3}{2(2\pi m kT)^{3/2}}\right]$$

Hence by substituting for $E_o - \mu$ we obtain for j_o

$$j_o = B(1-r) n_b^{1/2} T^{5/4} \exp - \left(\frac{\chi + \frac{\Delta E}{2}}{kT}\right)$$

where $B = \frac{2e(2\pi m kT)^{1/4}}{h^{3/2}}$

A plot of log $j_o/T^{5/4}$ against $1/T$ should yield a value of $\phi = \chi + \frac{\Delta E}{2}$

In practice T^2 is used instead of $T^{5/4}$ and the resulting plot is known as a Richardson line by analogy with the equation for pure metals. This implies the approximation

$$\phi = \chi + \frac{\Delta E}{2}$$

which for most purposes is sufficiently accurate. Owing to the possibility of adsorbed layers on the cathode surface which would vary with temperature, values of ϕ and B obtained in this way have doubtful significance unless the temperature range over which measurements have been made has been restricted.

Attempts have been made using emission data, to estimate the values to be assigned to n_b and r. If r is assumed to be unity and $n_b = 10^{17}$ and ϕ = 1eV -average values for (BaSr)O - then j_o calculated by using equation (9) is considerably greater than the accepted D.C. capabilities of the cathode. Such values of j_o have been found in micro-second pulse measurements by Sproull (24) and Coomes (25), and Wright (26) has found that using such values of j_o obtained in this way, the Richardson line is quite linear to high temperatures.

In the shape of the current voltage curve, when an emission current is being drawn under normal conditions, three well defined regions may be distinguished.

1. Emission in retarding fields
2. Space charge limited emission
3. Emission in accelerating fields

1. Emission in Retarding Fields.

In this region only those electrons will reach the anode which have energies greater than the barrier height imposed between anode and cathode by the retarding voltage. This barrier also includes any contact potential difference between the anode and the cathode.

For a diode with plane parallel electrodes the current density j_r at an applied potential V is given by:-

$$j_r = A(1-r)T^2 C \exp -\left(\frac{V+\phi_a}{kT}\right)$$

This equation is valid for values of V giving a barrier height greater than the work function ϕ of the cathode. For more positive values of V, j_0 is given by equation (9)

A plot of j_r/j_0 vs. V should give a slope of $-e/kT$ which joins a horizontal line when $V + \phi_a = \phi$. Thus ϕ may be found if ϕ_a is known. In practice ϕ_a is unknown and may even change due to contamination by materials evaporated from the cathode.

The current-voltage characteristics are best plotted in the form of log i_a vs. V_a. The retarding region may then be represented by a straight line with gradient related to $1/T$, which becomes horizontal when the applied field changes from a retarding to an accelerating one. Fan (27) and Hung (28) have obtained good agreement between observed emission in retarding fields and that calculated theoretically at temperatures below 1000°K. The latter detected a slight fall below the theoretical line as the 'knee' of the curve was approached. This was interpreted in terms of patches on the surface having slightly

different work functions.

2. Space-charge Limited Emission.

This is not a function of the cathode but rather of the geometry of the anode-cathode assembly. At sufficiently low temperatures, when small emission currents are drawn the space charge effect is absent and there is an abrupt change from the retarding field condition to accelerating field emission.

3. Emission in an Accelerating Field.

Schottky (29) assumed mirror image forces between the cathode and an emitted electron and so deduced the following expression for the current in an accelerating field:-

$$i = i_o \exp\left(\frac{e^{3/2} E^{1/2}}{kT}\right)$$

A plot of log i vs. the square root of the applied field should yield a straight line. This is approximately the case for oxide cathodes but the gradient is several times larger than that predicted by Schottky's equation. This is true both for pulsed and D.C. emission. It was explained by Hung (28) in terms of a patch theory; different areas on the cathode having slightly different work functions, but Wright and Woods (30) have shown this to be an unsatisfactory explanation. They have extended the theory of Morgulis (31) who assumed that the applied field distorted the energy levels near to the surface of the oxide. This extended theory shows that the space charge zone which penetrates the oxide surface and reduces the work function, is dependent upon both the applied field and the current that flows through the diode charac-

teristics as a function of coating parameters which may then be compared with experimental diodes. Good agreement was found with data obtained from Hall effect and conductivity measurements.

Emission Decay Effects.

In many cases when an emission current is drawn from a fully activated cathode a decay occurs from the initial value of anode current. In general such a decay may be attributed to ionic bombardment of the cathode by residual gas in the tube or by material deposited on the anode during processing.

The emission frequently suffers checks if the anode potential is slowly raised during the current activation procedure. Actual decreases may be observed at potential of about 5, 10, and 15 volts. Metson (32) has shown that this is due to the decomposition at the anode surface of such materials as BaO, $BaCl_2$ and $BaSO_4$, by the electron stream. The resulting ions 'poison' the cathode. This process has been treated theoretically by Deb (33). The presence of chlorine on the surface of the cathode, greatly impairing its performance, may be deduced from the work of Vick and Walley (34) who showed that the dominant ions emitted from an oxide cathode during life were those of chlorine. This was thought to have originated from the glass during the baking process.

A further type of emission decay phenomenon is the decrease of current which occurs during pulse operation of a cathode when the pulse is of several microseconds duration. Sproull (24) has suggested that this is due to the migration of surface Ba^{++} ions to the core leading

to a deficiency of such ions near the emitting surface, while Wright (35) considers the change in shape of the interface barrier accompanying this migration to be the major factor. However both Deb and Feaster (36) have pointed out that this decay may also be due to anode contaminants. More recently Nergaard (37) has performed a simple experiment designed to show that during the decay of a pulse some change in conductivity of the oxide also occurs. This is thought to indicate that the seat of the decay mechanism lies in the cathode alone.

The interpretation of this experiment in conjunction with the work of Becker (38) on electrolysis in cathodes and Sproull on decay effects and some further experimental work, lead Nergaard to postulate an entirely new theory for the mechanism of the oxide-coated cathode. This is the first attempt to give a complete theory which will account for the general properties of the oxide cathode and yet will also explain anomalous behaviour reported by many authors. Such behaviour includes the lack of agreement between the measured cathode temperature above 1000°K and that obtained from Shottky and Richardson lines; the decay of anode current under what appears to be emission-limited conditions and the decay of emission under space charge limited conditions.

The theory of advanced by Nergaard is based upon a semiconductor model in which the donors are mobile. The work of Becker and Sears (39) has suggested this donor mobility either in the form of electrolysis or by simple diffusion. Before current is drawn through the coating an equilibrium state ~~pertains~~; the donors are uniformly distributed and the energy diagram is like that shown in fig. 2.2 due to de Vore (40).

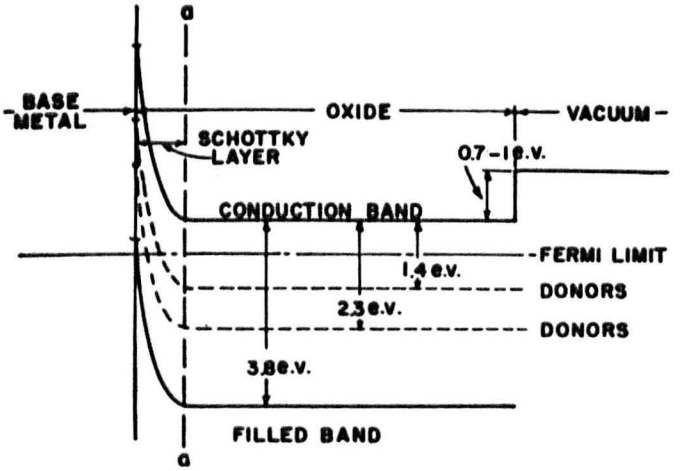

The energy level structure of BaO.

Fig. 2.2.

When a stable current is drawn, the donors electrolyse towards the base metal leaving a donor depletion layer near to the emitting surface. This movement towards the base metal is balanced by back diffusion, so that the donors do not plate out at the core of the cathode. This implies that the position of the Fermi level in the semiconducting oxide is a function of the current drawn. This accounts for the lack of agreement between calculated and measured temperatures. Moreover, under pulsed conditions, when there is not a stable current, the donor distribution will change and if the pulse is long, pulse decay will occur. The recovery after a pulse is the result of donors having diffused back into the depletion layer.

A number of experiments were designed by Nergaard to test the validity of this theory and the results seem to favour such a modal. No extensive criticism of this work has so far been made although a few authors (41) (42) have noted that their results do not accord with a donor depletion layer hypothesis. More recently a theoretical study of the thermodynamics of the reactions which can occur within the oxide layer has led Plumlee (43) to suggest that the donor species is not either excess barium or oxygen vacancies as proposed by many authors but $\bar{O}H$.e radicals. This suggestion is supported by mass spectrometric evidence for the existance of residual partial pressures of water vapour, hydrogen and oxygen in the region of the cathode under normal operating conditions. Such a donor species accords with Nergaard's view of mobile donors since this radical can move from one oxygen ion to another simply by transfer of a proton. Further experimental evidence is required before such a theory can be substantiated.

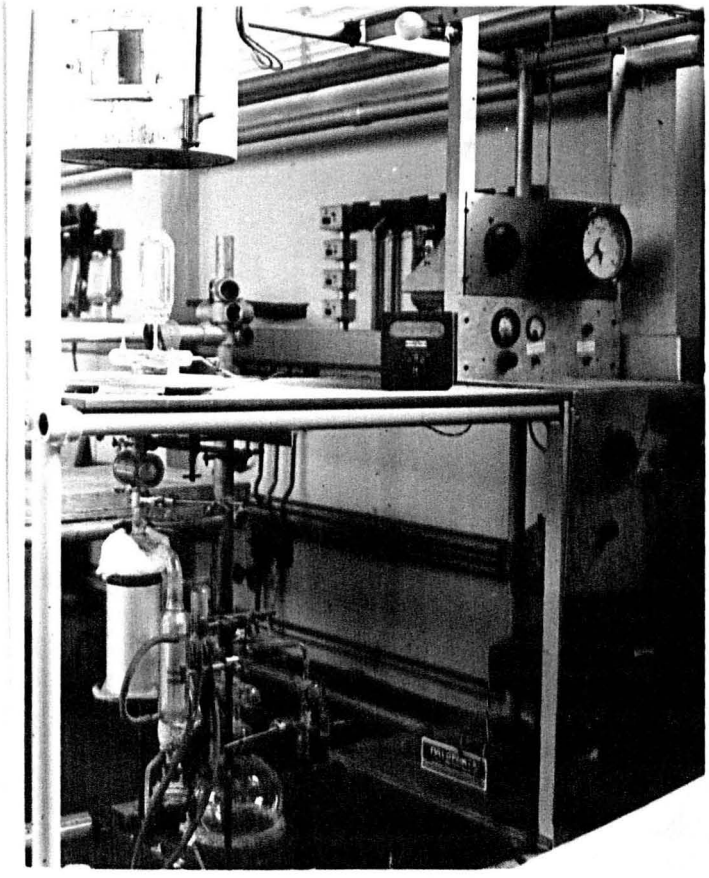

Fig. 3.1.

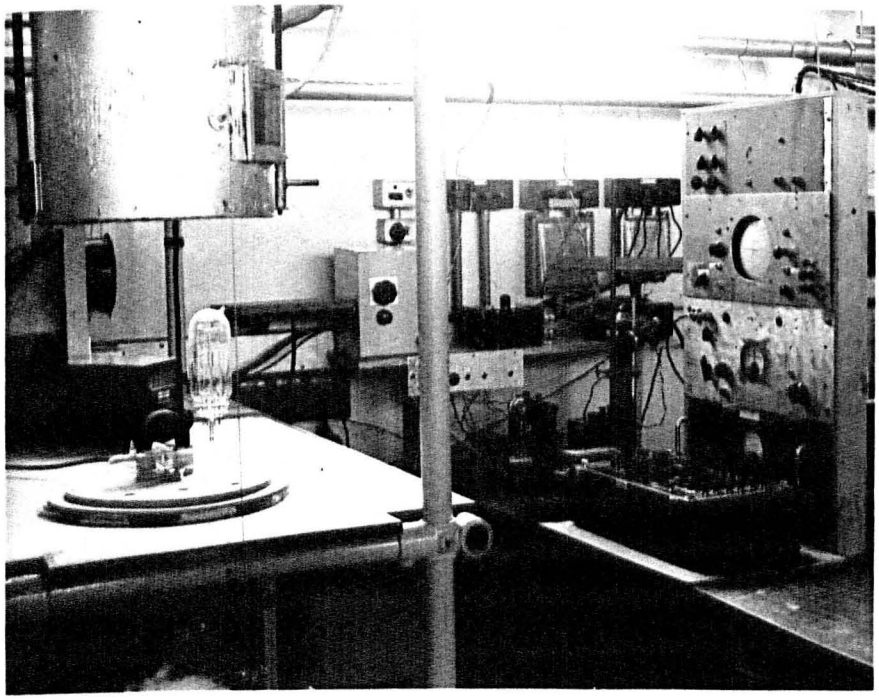

Fig. 3.2

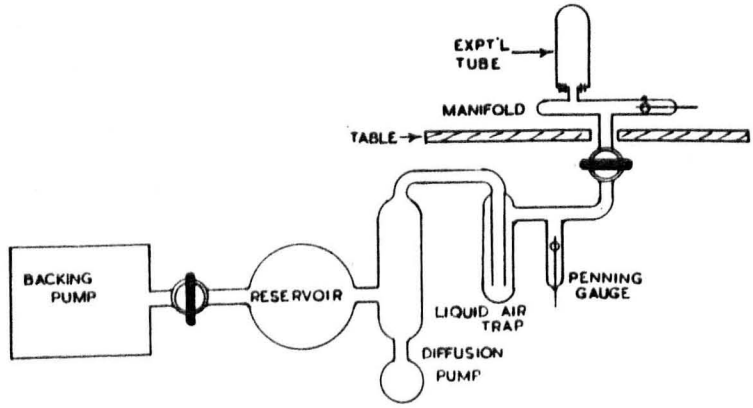
EXPT'L TUBE
MANIFOLD
TABLE
BACKING PUMP
RESERVOIR
LIQUID AIR TRAP
PENNING GAUGE
DIFFUSION PUMP

Fig. 3.3.

CHAPTER 3

APPARATUS AND EXPERIMENTAL TECHNIQUES

3.1 General Arrangements.

The apparatus consists of (a) a vacuum system for the preparation of the experimental tubes and (b) the equipment used in taking the various measurements. The general lay-out is shown in fig. (3.1) and fig. (3.2).

3.2 The Vacuum System.

The production of a very high vacuum is essential for any thermonic work particularly in the case of oxide cathodes. Only then will the thermionic emission be stable and reproducible. Much of the conflicting evidence in earlier work was due to comparative failure in this respect.

The requirements of a vacuum system suitable for the preparation of sealed-off tubes are the ability to remove as quickly as possible the large volume of gas evolved during the activation process and to achieve an ultimate vacuum of better than 10^{-6} mm.Hg.

The vacuum system shown diagramatically in fig. (3.3) was constructed of hard glass and consisted of a single-stage mercury diffusion pump with a maximum speed of the order of 1 litre per second, backed by an Edwards Speedivac two-stage rotary pump. In the interests of maintaining a reasonable pumping speed only one liquid air trap was fitted between the diffusion pump and the experimental tube to condense any mercury vapour diffusing towards the tube; also all the tubing on the high vacuum side was as short and wide as possible. A wide bore tap

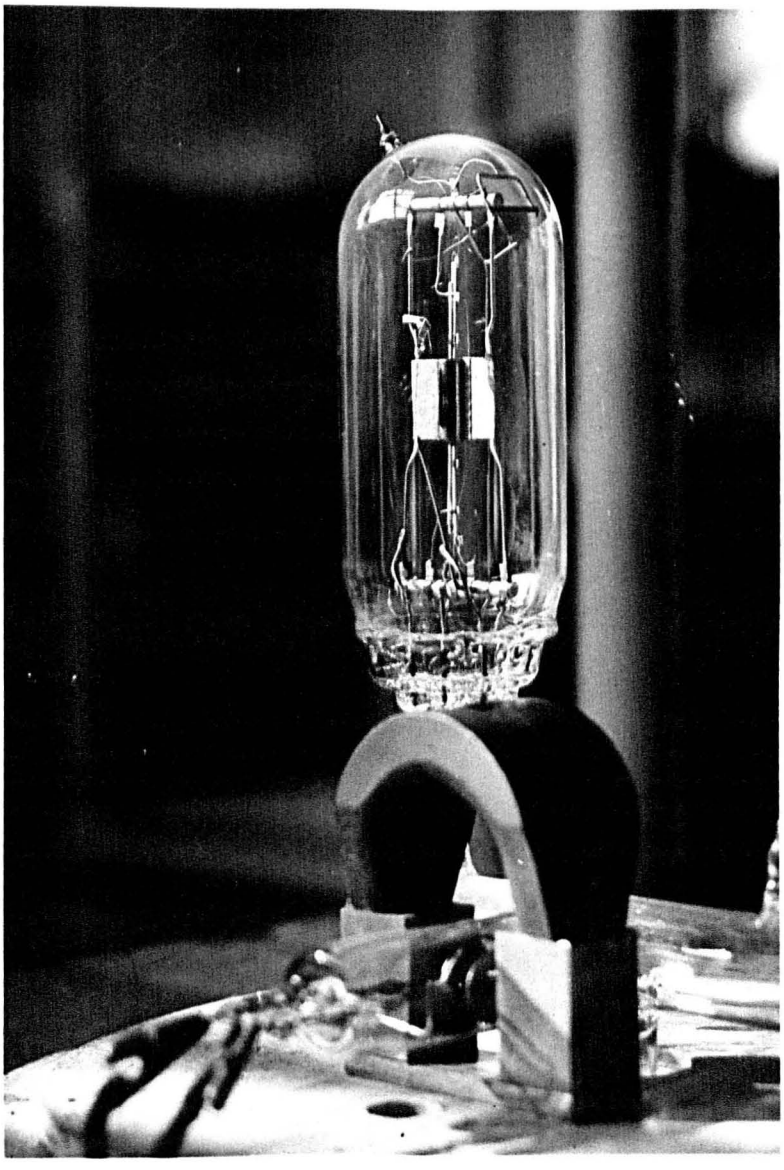

Fig. 3.4.

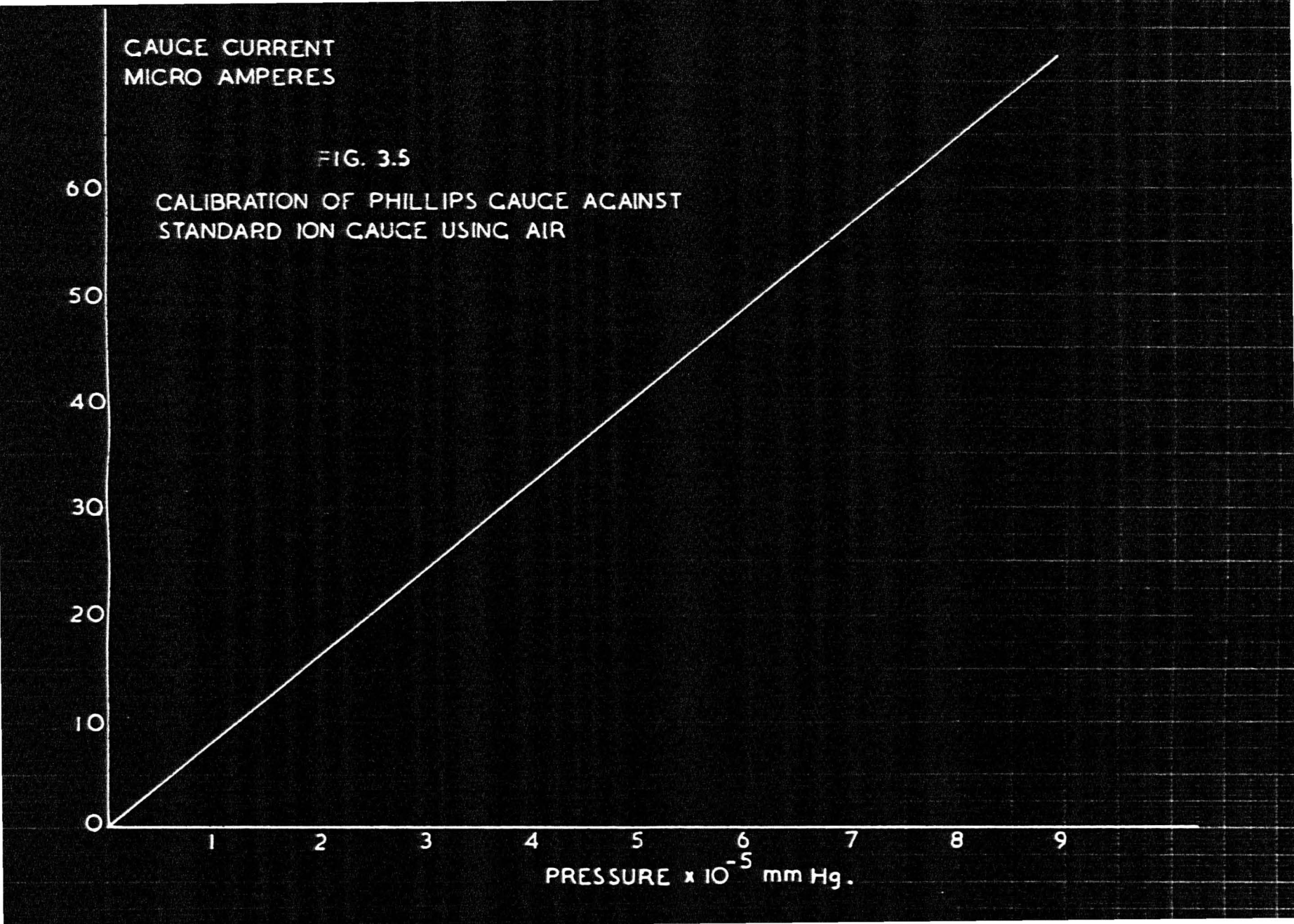

FIG. 3.5

CALIBRATION OF PHILLIPS CAUCE ACAINST STANDARD ION CAUCE USINC AIR

was provided between the experimental tube and the trap in order that during the slow breakdown of the carbonates the tube might be cut off overnight.

To enable a good ultimate vacuum to be obtained provision was made for baking the tubes to a temperature of 400°C by an oven which heated the glass-work to within 3" of the tap. Also parts of the experimental tubes were hydrogen furnaced before assembly and were throughly out-gassed by eddy current heating while the tubes were on the pump.

3.3 Measurement of Pressure

The pressure in the system was measured by Penning or Philips type gauges. Two such gauges were provided, one connected immediately to the manifold to measure the pressure in the experimental tube, and the other between the liquid air trap and tap to enable the pressure to be measured during baking. The gauge fig. (3.4) consists of two flat circular nickel plate cathodes separated by about 1 cm, and a nickel wire loop placed between these which serves as an anode. A constant voltage of 2700v. is applied across the gauge and a magnetic field of 600 oersteds is maintained at right angles to the plates by a small permanent magnet. When the voltage is applied, a discharge in the gauge results, in which the gas ions are accelerated from cathode to anode, following helical trajectories of considerable length owing to the presence of the magnetic field. The resulting ionisation current is measured by a Tinsley multi-range microammeter with a limiting resistor to keep the current below 100 ua. This current gives a good indication of the vacuum in the system and a typical calibration curve is showin in fig. (3.5).

In practice a tube was not sealed off from the pump until the pressure was less than 10^{-6} mm.Hg. i.e. a gauge reading of 1 ua.

3.4 Experimental Tubes.

General Description.

The experimental tubes may be divided into two types, those used for measuring the thermionic emission and conductivity of a particular oxide, and those used for studying the effect of oxygen on the cathode. The latter are essentially the same as the former but contain in addition an oxygen-producing filament coated with barium peroxide. Basically each tube is a cylindrical diode with a helical probe wire embedded in the coating of the cathode to enable conductivity measurements between cathode core and helix to be made. The cathode temperature is measured by means of a tungsten-nickel thermocouple as described by Fan (27).

The electrode assembly is supported by a frame consisting of two vertical 16 S.W.G. nickel wires, length 10 cms., to which the anode is attached, and two ceramic rods, length 35 mm. diam. 4 mm. Metal tags attached to the ceramic rods are used to support nickel wires from the probe, cathode etc., and from these connections are made to the nickel wires of the B7A glass press. The envelope in the poisoning tubes is provided with a side tube at the opposite end to the press through which the tungsten thermocouple lead is brought out. The press and envelope are of C9 glass and are supplied by Messrs. Ediswan Ltd. In addition to the seven leads the press carries a central thick-walled pumping tube of internal diameter 3 mm.

3.5 The Assembly of an Experimental Tube.

The glass envelope and the press are first cleaned in chromic acid, then washed in distilled water and dried. The cathode, which consists of a 2.5 mm. 'O' nickel sleeve of length 7.0 cms. and wall thickness 0.2 mm. is then prepared as follows:-

A tungsten thermocouple wire of diameter 0.095 mm. is passed through the cathode sleeve, together with a copper wire which is a close fit inside the sleeve (a flat is filed on the copper wire to accommodate the thermocouple). A weld is made halfway along the tube and the copper wire withdrawn leaving the tungsten wire welded to the inside of the nickel sleeve. One end of the thermocouple wire is then cut off flush with the cathode end. Two flat nickel ribbons of length about 2 cm. are then welded on the outside of each end of the cathode at distances of 3 mm. and 17 mm. from the ends. These ribbons are bent firmly round ceramic tubes 2.5 cm. long (G.Bray Ltd., Leeds, Cat. No. 2840) which hold and insulate the supports for the probe wire, and are welded close to the ceramics to ensure that the latter are gripped tightly. The supports are 26 S.W.G. pure nickel wire which protrude from the ceramics 2 mm. towards the centre of the cathode. To prevent movement they are anchored at the other end to a metal strip which is firmly fixed round the ceramic 22 S.W.G. nickel cathode leads at each end complete the arrangement fig. (3.6).

A cathode assembly is provided with a tungsten hairpin heater insulated by a double-hole ceramic tube (Bray's Cat.No.2788) and the thermocouple wire is insulated from the nickel tube by means of another ceramic tube length 3.5 cms. (Bray Cat.No.2945).

The heater is used to furnace the cathode in hydrogen for 2 minutes at 1000°C, after which it is allowed to cool in the hydrogen stream for 15 minutes. This ensures that all contamination caused by previous handling is removed. During subsequent operations the cathode is held by tweezers to prevent further contamination.

The cathode is then coated with carbonate suspension over 2 cms. of its central portion in a rotating jig, the ends being shielded by small rubber tubes which are a close fit over the cathode tube. The first coating applied is 40-50 microns thick, and after drying for a short time the helical probe is wound over this coating. The probe wire is .005" in diameter and the method of winding is as follows.

A length of about 7 cm. of probe wire has short pieces of 24 S.W.G. nickel welded to its ends. This facilitates handling and makes location of the probe easier, since it is so thin as to be difficult to see. This assembly is furnaced in hydrogen at 1000°C and the probe wire itself is welded 2 mm. or so from one end to one of the supports of the cathode. It is then allowed to hang from the welded joint, being kept taut by the weight of the thicker wire attached to its other end. By rotating the cathode at a suitable angle several turns of probe wire are wound evenly over the coating and the probe is welded to the second support. Surplus probe wire is removed by pulling. The rest of the coating is then sprayed on, covering the probe and giving a total thickness of about 100 microns. This is measured by projecting an enlarged image of the cathode on to a distance screen and comparing the coated and uncoated portions of the cathode. The magni-

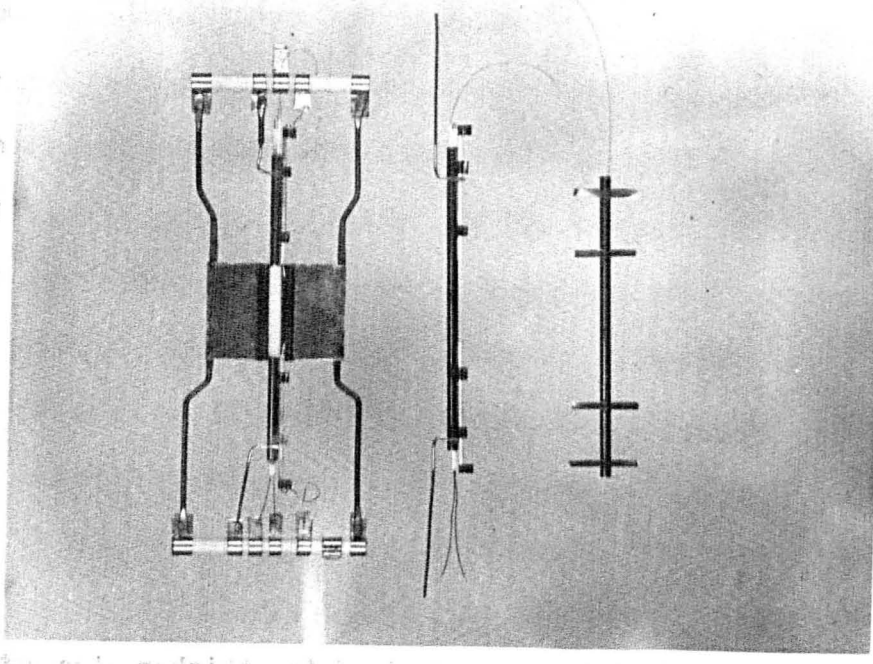

Fig 3.6

fication employed is about 50 and so that coating thickness can be measured and uniform thickness ensured to within ± 5 microns.

After reinserting the heater the cathode is mounted in the frame to which one half of the anode has already been attached. Allowance for thermal expansion is made by the provision of a sliding contact for one of the cathode support wires. The anode is a pure nickel cylinder of diameter 8 mm. and length 2.2 cms., provided with two radial cooling fins 1 cm. wide which also serve to support it on the frame. It is made in two halves; the second half which is welded on at this point does not have cooling fins but in the poisoning tubes has a slit 1.8 cm. x 1 mm. cut in the centre to permit direct evaporation of oxygen onto the cathode at low pressures. Both halves of the anode are hydrogen furnaced before assembly. The oxygen producing fidament, where this is used, is 3.5 cm. long and is held under spring tension at a distance of 1 cm. from the anode slit. This consists of an alumina coated tungsten wire onto which is painted a suspension of pure barium peroxide in amyl acetate to which a trace (5%) of collodion has been added to act as a binder.

The electrode assembly is completed by the addition of two barium getters and connections are made from the frame to the press wires using short lengths of 24 S.W.G. nickel. The tungsten thermocouple wire is furnished with a tungsten lead through the top of the glass envelope. This seal is first made and then the envelope is sealed to the press. The tube is then connected to the manifold of the vacuum system, tested under vacuum, and baked for 4 hours at 400°C.

3.6 The Activation Procedure.

Before heating the cathode, the anode is outgassed by eddy-current heating to a bright red heat. The getters are also pre-heated to prevent further release of gas when they are fired before seal-off.

Experience with this type of tube has shown that since the cathode coating is thicker than those normally used, considerable risk of cracking the coating occurs if the breakdown of the carbonates proceeds too rapidly. This cracking is caused by rapid evolution of gas trapped in the coating and is aggravated by the presence of the probe wire.

In order that a homogeneous coating may be obtained, the evolution of CO_2 during the forming process is controlled by very slowly raising the temperature over a period of 24 hours. This is accomplished automatically by supplying the heater current from a transformer in the primary of which is a variac. The variac is driven by an electric motor and high ratio reduction gearing at the required speed to raise the cathode temperature to about 900°C in the prescribed period. A perfectly satisfactory oxide coating is obtained in this way. The temperature of the cathode is maintained at 900°C (heater $\approx$ 8v) until evolution of CO_2 ceases. The anode is again eddy-current heated to remove gases adsorbed during breakdown. A two minute activation flash to 1050°C is then given (heater voltage 10-11v.) and an emission current drawn at a cathode temperature of 900°C. The getters are fired and the tube sealed off.

At this stage the cathode is subjected to the ageing process by drawing an emission current for several hours with the cathode at 900°C

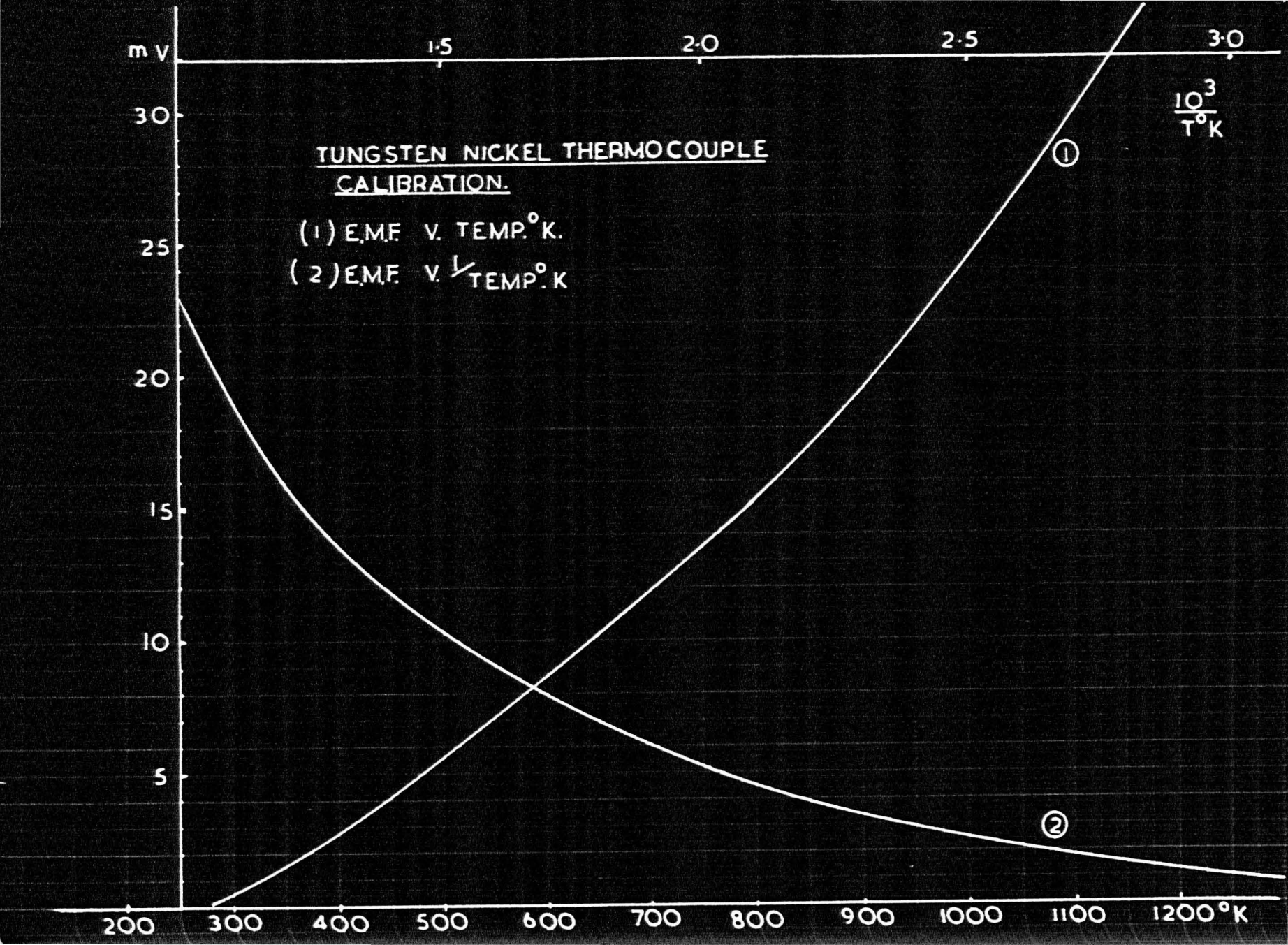
mV
30
25
20
15
10
5
1·5
2·0
2·5
3·0
$\frac{10^3}{T°K}$
TUNGSTEN NICKEL THERMOCOUPLE
CALIBRATION.
(1) E.M.F. V. TEMP.°K.
(2) E.M.F. V. 1/TEMP.°K
①
②
200
300
400
500
600
700
800
900
1000
1100
1200°K

and with 100 volts applied to the anode, until the anode current attains a steady value. At stages during this process, for several tubes complete conductivity vs. temperature measurements are made in order to determine how the conductivity changes during activation.

3.7 Measurements.

All measurements of emission and conductivity are made with reversible d.c. voltages supplies to both anode and probe. Anode currents are measured with a Gambrell galvanometer of sensitivity 1.6×10^{-7} amps per cm. deflection at 1 metre, provided with a universal shunt. Probe currents are measured with a Cambridge Spot Galvanometer of sensitivity 1×10^{-8} amps per scale division.

Conductivity measurements are, in general, made by applying direct voltage of up to 100 mV between cathode core and probe wire with the anode floating.

The cathode temperature is estimated by measuring the E.M.F. generated by the thermocouple using a Muirhead potentiometer. A calibration curve for the nickel-tungsten junction is given in fig. (3.7). Fan (27) claims that with a particular junction the temperature of a cathode may be measured to within $1^{\circ}C$. Experiments in this laboratory however indicate than an accuracy of better than $\pm 2^{\circ}$ is not possible; for the measured E.M.F. is found to depend not only on the junction temperature, but in addition, though to a lesser extent on the tension in the wire, the size of wire used and the degree of hydrogen furnacing to which the junction has been subjected.

SECTION 2

AN INVESTIGATION OF THE CONDUCTIVITY OF OXIDE COATED CATHODES

CHAPTER 4

PREVIOUS WORK

In any investigation of the electrical properties of a semiconductor, the measurement of conductivity must occupy a prominent position. A knowledge of this parameter and particularly its temperature dependence coupled with measurements of thermoelectric power, Hall effect and thermionic and photoemission facilitates the calculation of the position of the energy levels in the semiconductor and thus enables a useful model to be constructed.

Equation (6) in Chapter 2 indicates that over a limited temperature range the expression for the conductivity of a semiconductor may be written

$$\sigma = \sigma_0 \exp\left(\frac{-Q}{kT}\right)$$

where σ_0 is a function of n_b the number of electrons in the donor levels.

Thus a plot of log σ vs. $1/T$ should be linear with slope from which the distance between the conduction band and the donor levels may be found.

Many measurements of the conductivity of oxide cathodes have been made. The diversity of results obtained prior to 1939 is shown in fig. (4.1).

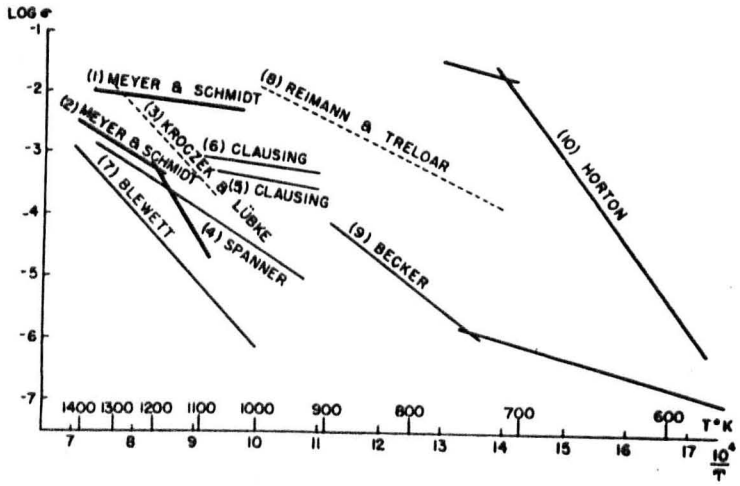

Fig 4.1

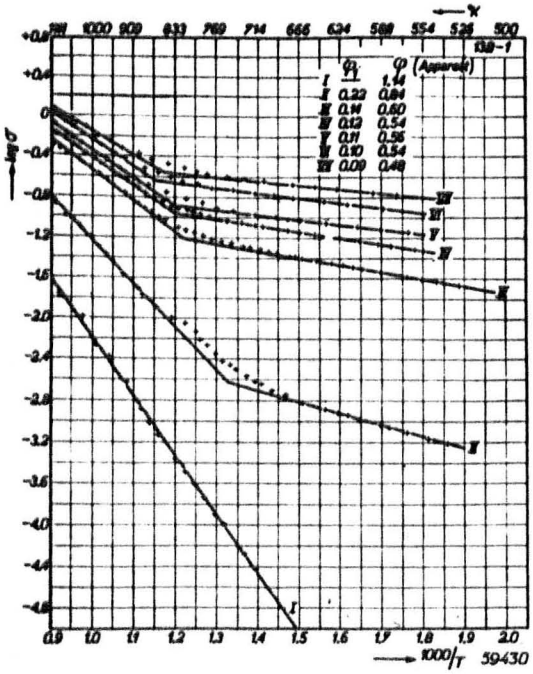

Fig 4.3

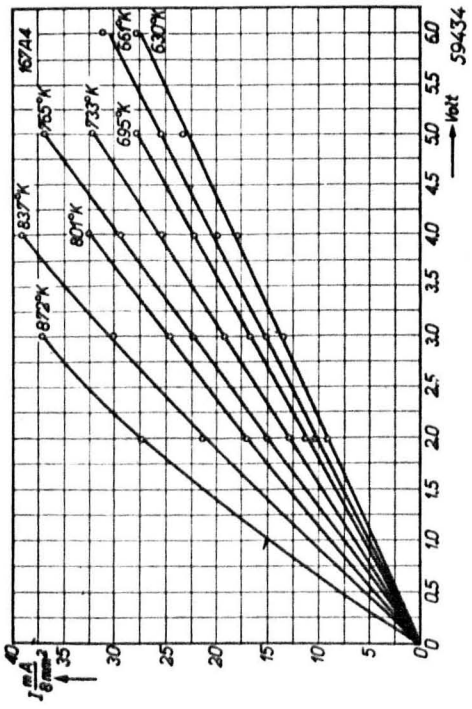

Fig. 4.2.

The use of probes embedded in the cathode in order that emission and conductivity could be measured on one sample, was favoured by several authors. Nishibori and Kawamura (44) in 1940 used this method. The cathode was activated by the evaporation of barium from a separate electrode. A linear dependence of emission current density on conductivity was found and was explained by assuming the invariance of χ with emission. It was concluded that emission was not primarily a surface phenomenon. The resistance of the coating was found to be ohmic and a value of ΔE of 1.4eV for BaO was reported.

In 1949 Loosjes and Vink (45) criticised the use of probe tubes and employed two button cathodes coated with oxide placed face to face. The conductivity of the oxide was determined over the range 300° o 1000° K, potentials of up to 10 volts being applied. Fig. (4.4) shows the form of the I-V curves obtained and fig. (4.3) the $\log\sigma$ vs. $^{1}/_{T}$ curves.

The curvature of the I-V characteristics at higher temperatures together with the definite bend in the conductivity curves was interpreted in terms of two parallel conduction mechanisms operating simultaneously. If the oxide coating is assumed to be a highly porous semiconductor, then at temperatures above 800°K each crystal grain will be surrounded by an electron gas. Conduction will occur predominantly through this gas above 800°K but at much lower temperatures, 300-500°K, the predominant process will be one of conduction through the crystal-crystal contacts in the semiconductor. The activation energy at high tempdratures was found to agree with that obtained from a Richardson plot of the emission and this was taken as further evidence in support of the hypothesis. These emission measurements were made after taking

apart the two button cathodes and inserting an anode an operation which could hardly fail to modify theporous semiconducting oxide to some extent. Furthermore as pointed out by Shepherd (13) it is not clear from the report of Loosjes and Vink just how the high temperature activation energy was calculated.

A recent paper by Japanese authors (46) has claimed to verify the results of Loosjes and Vink in that the high temperature conductivity and Richardson's lines are parallel; but this claim is subject to some doubt for it appears that no correction has been made to the high temperature conductivity slope to account for the parallel low temperature mechanism.

However confirmatory evidence in the favour of the pore conduction hypothesis has been advanced by Young (42) and Forman (47). Young also measured the thermoelectric power of the oxide, employing a similar experimental arrangement to that of Loosjes and Vink. Agreement was found between thermoelectric and conductivity activation energies in the high temperature region. The magnetoresistive effect was also measured; a field of 5600 oersteds decreased the high temperature conductivity by a factor of six whilst the low temperature conductivity was hardly affected.

Forman made simultaneous measurements of the Hall effect and conductivity and accounted for the observed decrease in Hall emf. at high temperatures and the large magnetoresistive effect in terms of the pore conduction hypothesis. A theory based on this hypothesis was developed. It was found to account for all the observed phenomena.

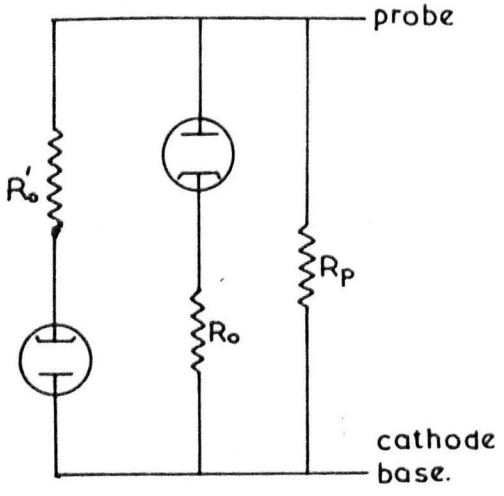

FIG. 4.5

Tomlinson (41) has subjected the results of Loosjes and Vink fig. (4.2) to a more rigorous analysis. A linear dependence of current upon voltage at high temperatures for the oxide rather than a parabolic one is suggested at higher applied voltages. This has been verified using probe tubes and applying up to 10 volts rms. for a short time during which the I-V characteristic was displayed and photographed. This has lead to the development of a new model applicable to probe tubes at high temperatures i.e. above 700°K. The low temperature mechanism is replaced by a resistance R_o and the high temperature mechanism (pore conduction) by a pair of diodes with series resistors as shown in fig. (4.5). This model accords with Tomlinsons measurements on several cathodes but further evidence will be required before it finds general acceptance.

A somewhat different method of conductivity measurements has been employed by Sparks and Philipp (48). Using a collector electrode behind the anode the retarding potential curve for the emitted electrons was plotted for different values of anode current, and the conductivity of the oxide determined by calculating the potential developed across the oxide. The conductivity vs. temperature curve gave two straight lines intersecting at about 700°K in agreement with results obtained by other methods. The advantage of this technique is that conductivity and emission can be measured simultaneously without the use of probes which might disturb the processes occuring in the cathode. Unfortunately since this method is dependent upon electron emission, the lower temperature measurements are restricted by the limits of current measuring devices. Moreover the method is only applicable to oxides with a

high conductivity to emission ratio. Some difficulty was encountered with BaO because of this and no doubt this would have been greater if measurements on SrO had been attempted.

Whereas it is generally agreed that conduction occurs through the electron gas in the pores of the coating above 800°K, there is not such good agreement about the nature of the low temperature conduction mechanism. Loosjes and Vink obtained values of 0.05 and 0.04eV for the activation energy in well activated samples of BaSrO. Similar values were obtained by Hughes and Coppola (49), but they stated that such low values were inconsistent with a semiconductor theory and instead favoured a mechanism of conduction over a monolayer of barium on the surface of the oxide. A similar low temperature mechanismwas favoured by Wright (50) who postulated conduction through a barium film on the surfaces of the crystal grains.

In support of the Loosjes Vink semiconductor hypothesis, Forman found that highly porous cathodes exhibited no bend in the conductivity curve, presumably because the area of contact between crystal grains was small.

The Japanese authors (46) cited above, employed an arrangement which permitted the pressure on the oxide to be studied as a parameter. It was found that those samples which were subjected to greater pressure exhibited the bend in the conductivity curve at higher temperatures. This indicated that when the area of contact was greater, the low temperatures process was predominant up to higher temperatures, which is consistent with a conduction mechanism dependent upon the areas of contact between the crystals.

Loosjes and Vink asserted that at temperatures below 800°K the conductivity was apparently low and that this might arise in serveral ways. The conductivity of the crystals might be high but the areas of contact between them small or barrier layers might exist between the crystals.

It is significant that there is a complete lack of agreement between work done on single crystals of barium oxide and that done on BaO cathodes. For example; Sproull (51) has made extensive measurements of the conductivity of single crystals of barium oxide over a wide range of temperature. The activation energy of the conduction process was in the region of 1.0eV. This may be compared with a value of 0.4 eV typical for oxide cathodes. A further anomaly arises in connection with the density of donor centres. It has been assumed that the density of donor centres in the oxide cathode is equal to the stoichiometric excess of barium metal, though this does not imply that the donor species is excess barium. Nergaard (37) in agreement with several other authors suggests a donor concentration of 10^{17} per cc. to account for the electrical behaviour of oxide cathodes. Recently the properties of single crystals containing this excess barium content have been studied by Dolloff (52) who found that such crystals exhibited blue colouration (colour centres) and gave a value of 2.0eV for the activation energy of conduction. Moreover, on heating in vacuum for several hours at 1000°K the crystals were bleached and the conductivity temperature dependence returned to a value associated with uncoloured crystals. Thus measurements of the properties

of oxide cathodes lead to calculated values of $n_b \approx 10^{17}$ and values of the activation energy of conduction ~ 0.4 eV which do not accord with the work on single crystals.

It is not improbable that this lack of agreement arises because authors have been too ready to identify the low temperature conduction with semiconduction in the crystal grains, without paying any attention to surface effects. Loosjes and Vink pointed out that conductivity through the crystallites could be limited by barrier layers at the surfaces of the crystals. The author suggests that a closer study of surface phenomena might lead to a better interpretation of the observed effects. Such a study will involve the introduction of some additional concepts and these are discussed in the next section.

Surface Electron Traps.

The simple equations given in Chapter 2 which describe the behaviour of N-type excess semi-conductors are all derived on the assumption of an infinite crystal lattice. Modifications to this more general theory are required to describe the energy states in the crystals at discontinuities in the lattice.

Now the work required to place an electron on a surface ion of the crystal lattice is less than that required to place an electron on an ion inside the lattice, since the Madelung term for the summation of the forces on an ion in a boundary plane is less than for the summation in an infinite solid. This gives rise to the possibility of surface energy states (Tamm Levels) which Shockley (53) suggests may or may not be occupied by electrons, but which lie close to the conduction band. Wright (54) states that in divalent oxides these extra

levels lie approximately at 0.3eV below the conduction band. In principal therefore, electronic conduction over the surfaces of oxide crystals by electrons in surface states is possible, though Seitz (44) points out that such conductivity would be impaired by surface cracks or adsorbed atoms and has as yet not been observed.

The oxide-coated cathode however is very porous and consists of very many small crystals ranging in size from 0.2 - 1 microns. The surface to volume ratio is thus quite high and it is possible therefore that conduction in Tamm levels might be greater than in the bulk of the crystals at low temperatures. Conductivity in such energy states would have a small temperature dependence and at quite low temperatures electrons would be excited into the conduction band of the oxide from these nearby levels. Such an explanation may account for the very low slopes of the log σ vs. $1/T$ curves (fig. 4.3) reported by Loosjes and Vink and other authors.

The problem of interpreting the changes in slope of the log σ vs. $1/T$ curves during activation must now be attempted. This kind of change is experienced in other N-type semiconducting compounds such as zinc oxide when the stoichiometric excess of zinc is gradually increased; Fritsch (56).

Mott and Gurney (57) have interpreted this phenomenon in terms of interaction between donor centres. This interaction will occur with a surprisingly small donor concentration and can give rise to a number of donor levels instead of one. The energy diagram is modified to include an impurity band which widens as the number of donors is increased.

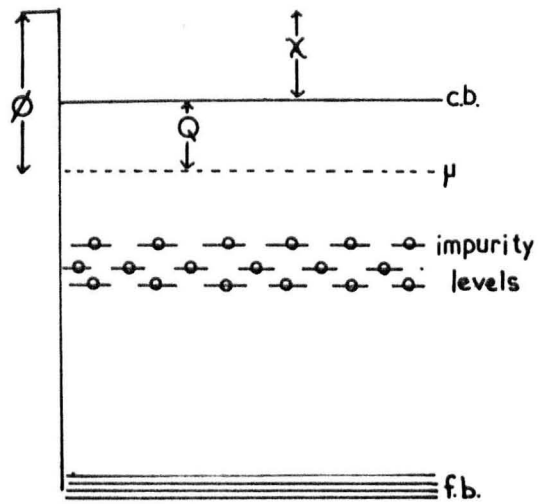

FIG. 4.6

The Fermi level thus rises to a level nearer the conduction band and so the slope of the log. σ vs. $1/T$ curve which gives μ directly (fig. 4.6) decreases as activation proceeds.

This however is not the only possible explanation of the observed decrease in Q during activation. It must be emphasised that the activation procedure is performed at quite high temperatures in a vacuum, a process which cannot fail to modify the surfaces of the crystal grains. In particular this process would gradually remove electron traps from the surface leading to enhanced conductivity by increasing the mean free path of surface electrons. This, in turn, would diminish the observed activation energy of the conduction process.

An explanation in these terms is more in accordance with the main thesis that surface conduction over the crystal grains is important at low temperatures. It merely remains to suggest the particular type of electron trap most likely to impede the movement of electrons. This is, of course, oxygen. It is well established that oxygen both charged and in the molecular state is evolved from the cathode during the activation procedure. Much of this oxygen arises from the interaction of reducing impurities in the nickel base with the oxide layer. It is not impossible that such oxygen could become adsorbed at crystal interfaces where it would form deep electron traps and seriously impair the conduction of electrons between the oxide grains.

The following chapters of Sections 2 and 3 describe experimental investigations into the behaviour of oxide-coated cathodes during thermal and emission activation and during deactivation by oxygen and sulphur.

It is clear from the above discussion that a better understanding of the conduction process at low temperatures is required. Accordingly, in the investigations described below attention is focussed on behaviour of cathodes in the temperature region below 700°K.

CHAPTER 5

PRELIMINARY EXPERIMENTS

Introduction

This Chapter describes some of the preliminary measurements of coating conductivity made on barium oxide and barium-strontium oxide cathodes. Some of the general effects noted are discussed briefly before passing on to more recent work.

The Conductivity of Oxide Coatings.

The coating conductivity is measured by noting the current flowing between the core and the probe when positive and negative potentials are applied. The alternative method of drawing emission current and measuring the potential fall between core and probe is not used, for this method would not indicate if any rectification effect were present at the interface, since currents would be drawn through the oxide in only one direction.

The potentials applied to the probe are kept low that is, fractions of a volt, and the currents drawn are correspondingly small. In this way as far as possible, the equilibrium conditions given by semiconductor theory are preserved.

The conductivity measured in this manner may also include a contribution from the interface at either, or at both, the core and the probe. The rectifying effect of the interfaces should oppose each other, but the large difference in current density should cause any rectifying action at the probe to be clearly seen in the probe current-voltage characteristics.

In the absence of any interface resistance, the measured conductivity $\frac{1}{R}$ may be related to the specific conductivity σ' of the specimen by the relation:-

$$\sigma' = \frac{1}{R} \frac{\cosh^{-1} t/a}{2\pi l}$$

where a and l are radius and length of the probe wire and t is the coating thickness between the probe and the core. This equation is true provided $t \gg a$. In the experimental tubes the probe has a radius of 6.3 u and the coating thickness is about 50 u. when applied as carbonate.

The effect of the correction term is to add a constant value to the logarithm of the measured conductivity. This does not affect the gradient of the log σ' vs. $^{1}/T$ graph from which the inner work function is calculated nor does it alter the relative changes of conductivity during activation.

The specific conductivity σ' measured in this way bears only an indirect relation to the specific conductivity of barium oxide crystals for it is also a function of the grain size the density of packing and the degree of sintering.

Measurements on BaO coatings.

Tube Bal.

This cathode was sprayed with a barium carbonate suspension supplied by G.E.C. which contained ethyl and butyl acetates and resulted in a cathode with a fluffy appearance due to the rapid evaporation of the solvent during the spraying process. The probe consisted of

six turns of wire at a distance of 55 microns from the core. The assembled tube was baked for five hours at 420°C and the carbonates decomposed by raising the temperature of the cathode to 900°C over a period of 30 hours. Frequent checks during this period showed that the pressure during breakdown was not higher than 10^{-4} mm.Hg. The anode was eddy current heated, and the cathode flashed at 1050°C for 2 minutes. On reducing the temperature to 900°C and applying 100 volts D.C. to the anode an emission current of 1 m/a was noted which increased to 2 m/a during a 15 minute period. The tube was then disconnected from the supplies, the cathode cooled to room temperature and after preheating, the getters were fired and the tube sealed off from the pump.

The cathode was allowed to age at 850°C at V_a = 100 volts. At intervals during the ageing process, when the anode current under these conditions was 10, 35, 80 and 130 m/a, complete conductivity versus temperature measurements were made by applying up to 100 mV positive and negative between the probe wire and the core and noting the probe current. Fig. 5.1 shows a number of the probe current voltage characteristics taken at various cathode temperatures at activation stage No. 2 when the anode current was 35 m/a. The curvature of the lines at all temperatures is quite distinct, and was at first thought to be due to polarisation of the coating, for the potentials were applied continuously to the probe while the measurements were being made. However, when the cathode was fully activated, the curvature had disappeared in all but the highest temperature

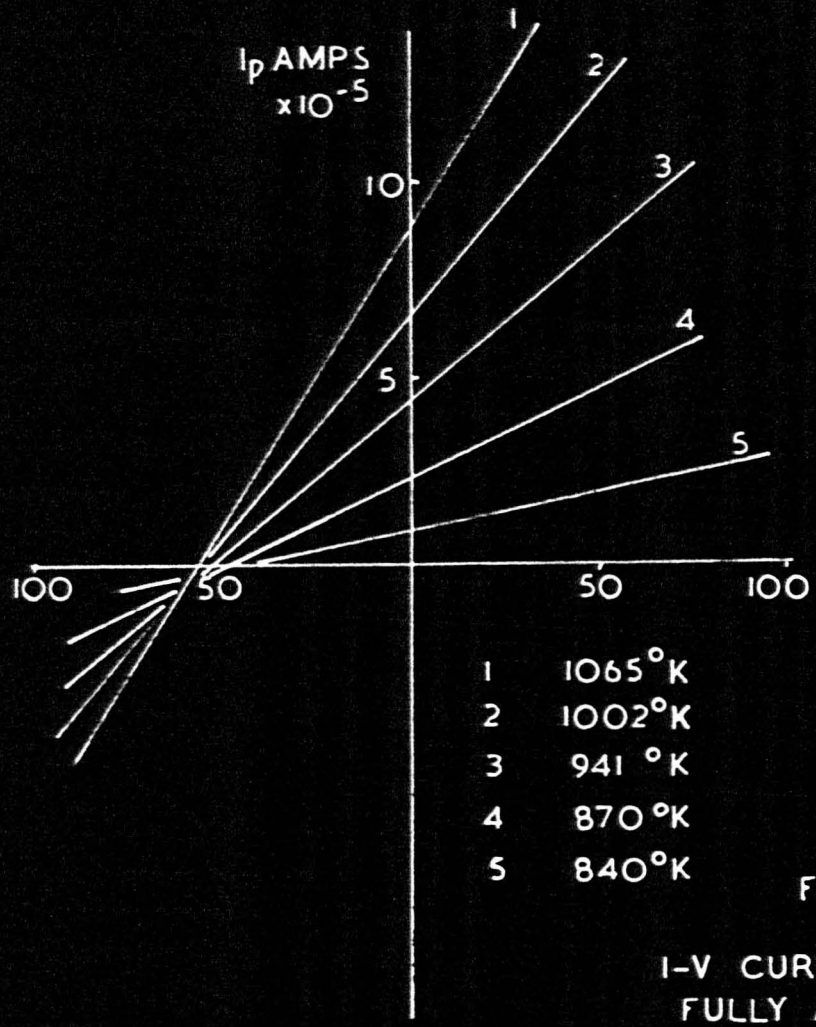

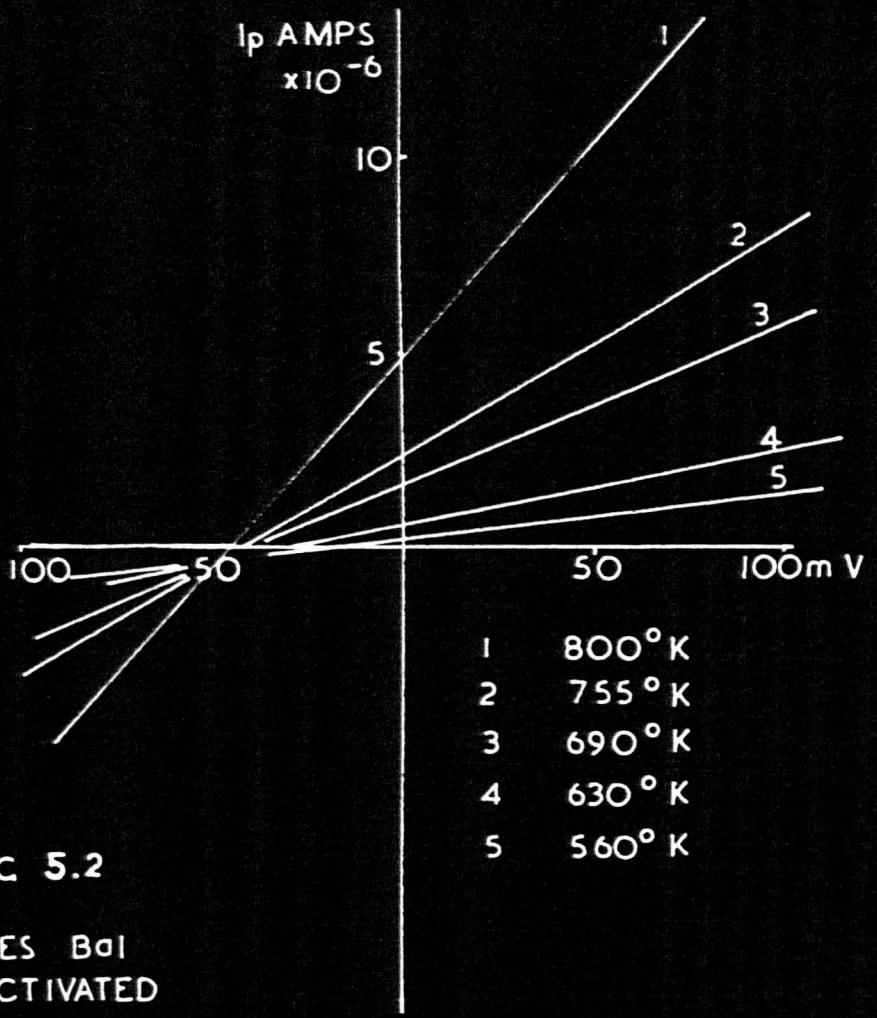

FIG 5.2

I-V CURVES Ba1
FULLY ACTIVATED

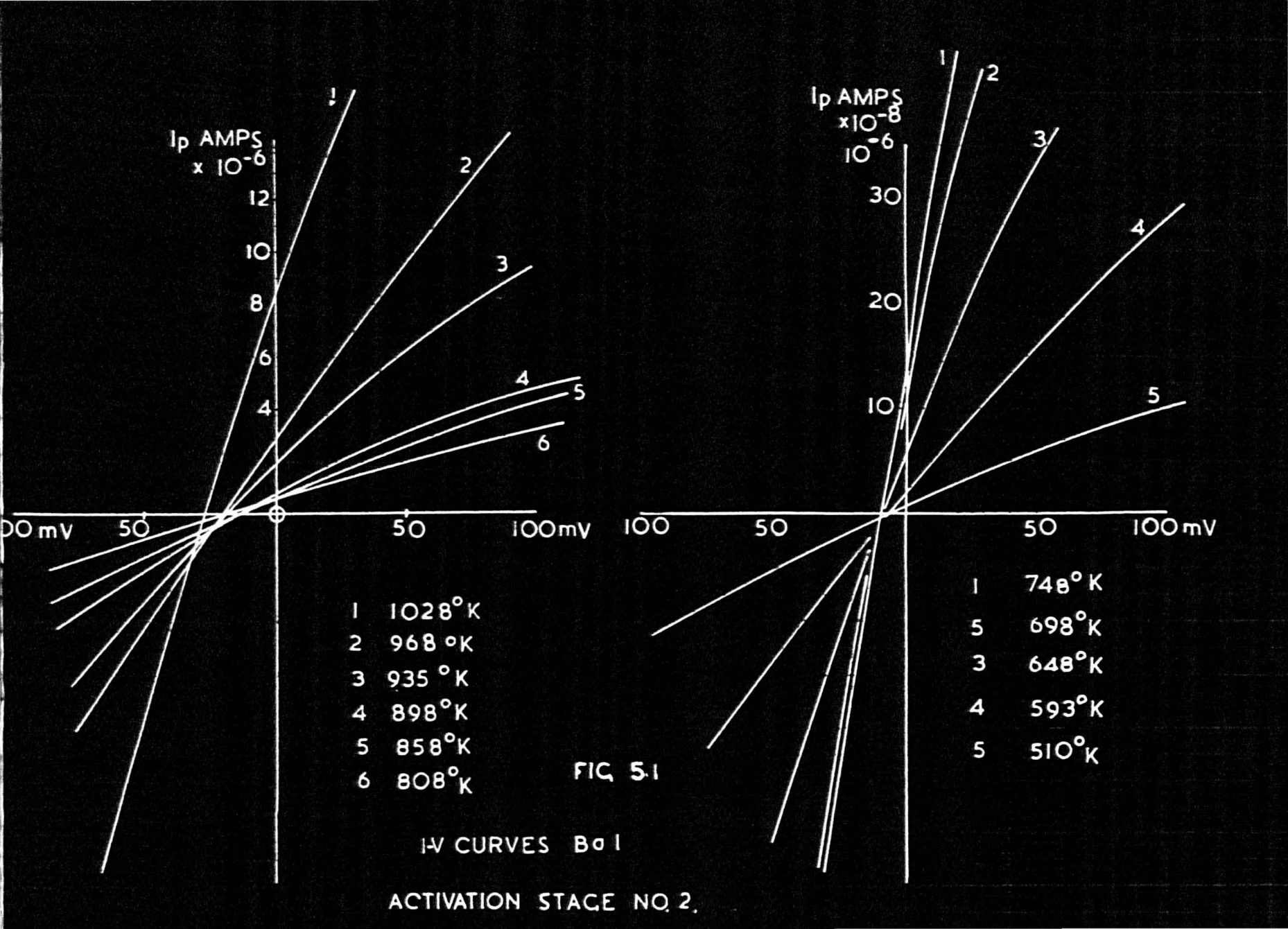

FIG. 5.1

I-V CURVES Bo 1

ACTIVATION STAGE NO 2.

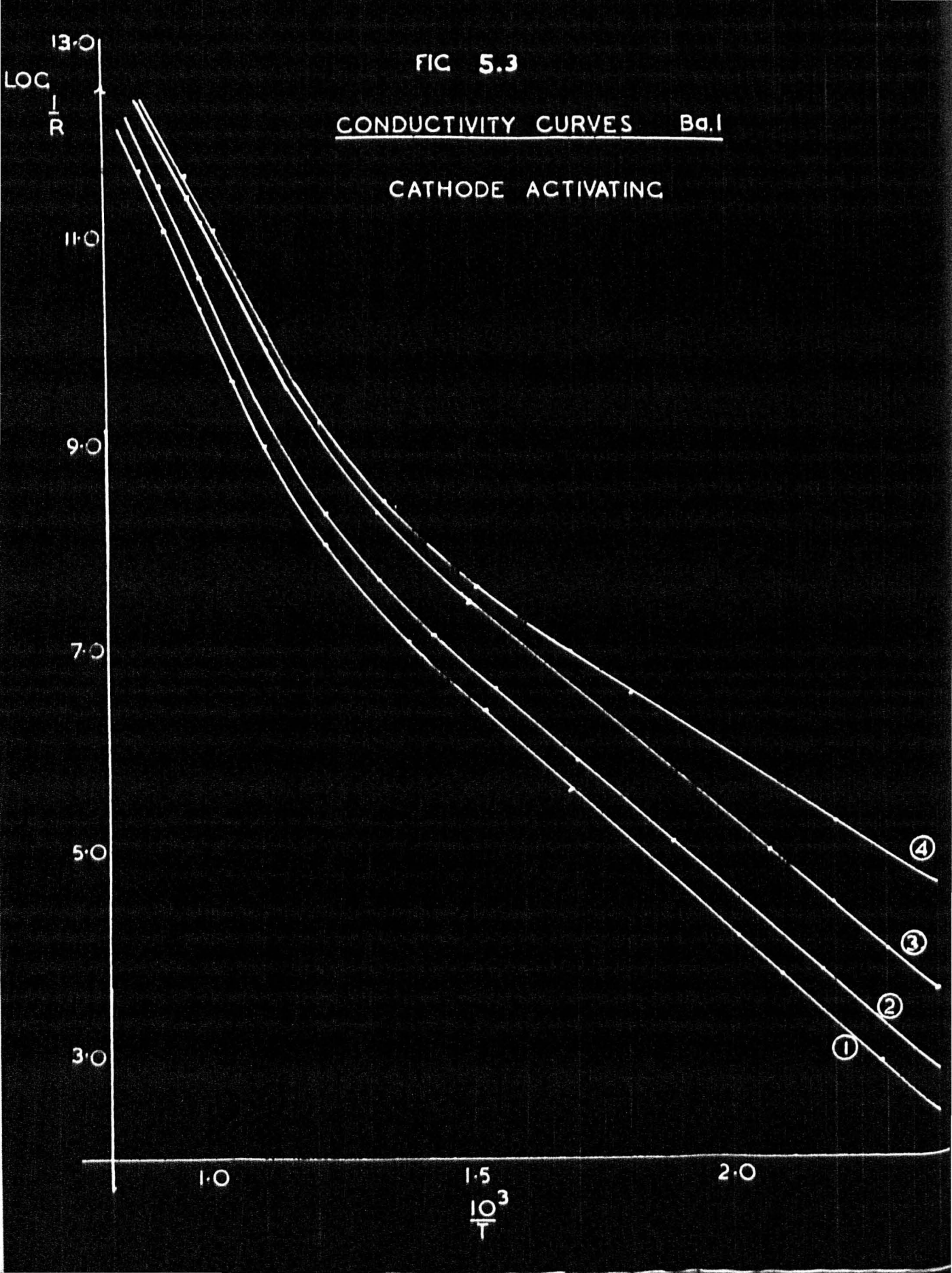
FIG 5.3
CONDUCTIVITY CURVES Ba.I
CATHODE ACTIVATING
LOG 1/R
13·0
11·0
9·0
7·0
5·0
3·0
1·0
1·5
2·0
10³/T
①
②
③
④

lines (Fig. 5.2). The curves do not pass through the origin, but intersect the ordinate axis above zero. This current is caused by the thermoelectric e.m.f. due to the temperature drop between the core and the probe. Assuming a thermo-electric power of 1 mV/°C for the fully activated cathode, Fig. 5.2 indicates that the temperature drop between core and probe increases from 15° to 55° as the core temperature increases from 560°K to 1065°K. This temperature drop is probably greater than in the case of a normal cathode of equivalent thickness, due to the cooling effect of the probe wire.

The gradient of the curves gives the conductivity at that particular temperature. In the case of the curves of Fig. 5.1 the gradient near to the origin was used, for the curves exhibit marked departure from linearity in the positive region. The values obtained were used to plot Fig. 5.3 which shows graph of Log. $^{1}/R$ versus the reciprocal of the absolute temperature, at each stage during the activation of the cathode.

It is convenient when discussing Fig. 5.3 to refer to the gradient of any line in terms of the associated energy expressed in electron-volts. The relation between conductivity and temperature

$$\sigma = \sigma_0 \exp\left(\frac{-Q}{kT}\right)$$

is approximately correct. Fig. 5.3 shows that the conductivity cannot be expressed simply in terms of this formula. Each curve has two different gradients. Curve (4) taken at the highest state of activation, has gradients of 0.81eV at high temperatures and 0.25eV at

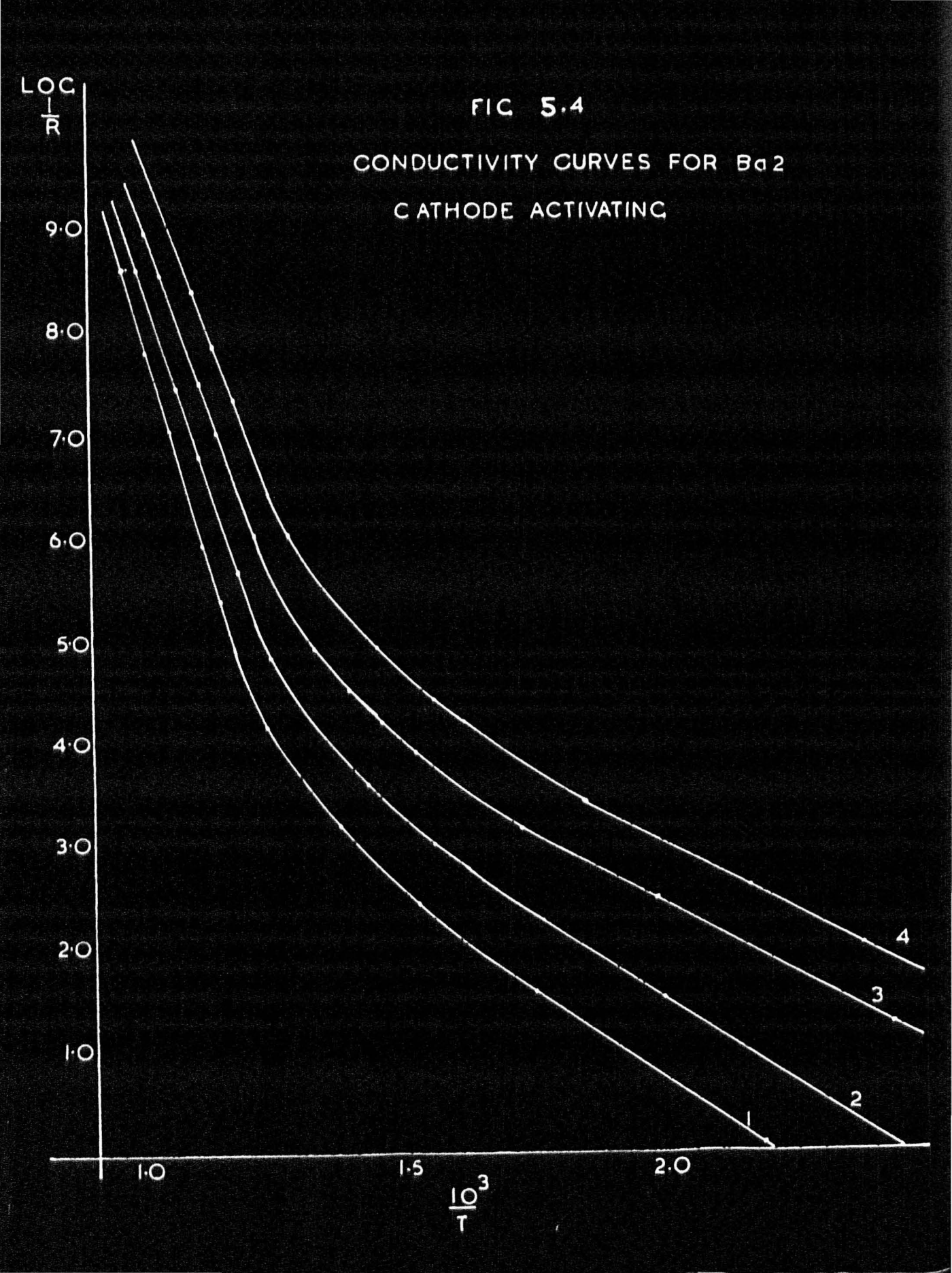

FIG 5.4

CONDUCTIVITY CURVES FOR Ba 2

CATHODE ACTIVATING

lower temperatures; the transition occurring at about 700°K. In all respects Fig. 5.3 is similar to the results of Loosjes and Vink shown in Fig. 4.3.

Tube Ba2.

The cathode of this tube was sprayed with the G.E.C. suspension in the same way as Ba1, in an attempt to reproduce as nearly as possible the same conditions in the cathode. A six turn probe wire was again employed and the processing schedule was identical with that for Ba1.

Conductivity measurements were made at four stages during the ageing of the cathode. Precisely similar behaviour to Ba1 was observed. At low stages of activation the current voltage characteristics were curved but exhibited linearity when the emission from the cathode was saturated at 850°C. Fig. 5.4 shows the family of conductivity curves obtained; in good agreement with those of Fig. 5.3 except that the transition temperature is slightly higher, in this case about 800°K. The high temperature activation energy is 1.1eV and the low temperature value is 0.21eV.

Tube Ba5.

The cathode of this tube was sprayed with B.D.H. barium carbonate suspension so as to give uniformly smooth coatings. The coating thickness was 50 μ between the six turn probe and the core. After baking for 4 hours at 450°C the temperature of the cathode was raised to 850°C over a period of 30 hours. The anode was then outgassed and the getters preheated by eddy-current heating. After an activation flash at 1100°C the getters were fired and the tube sealed off.

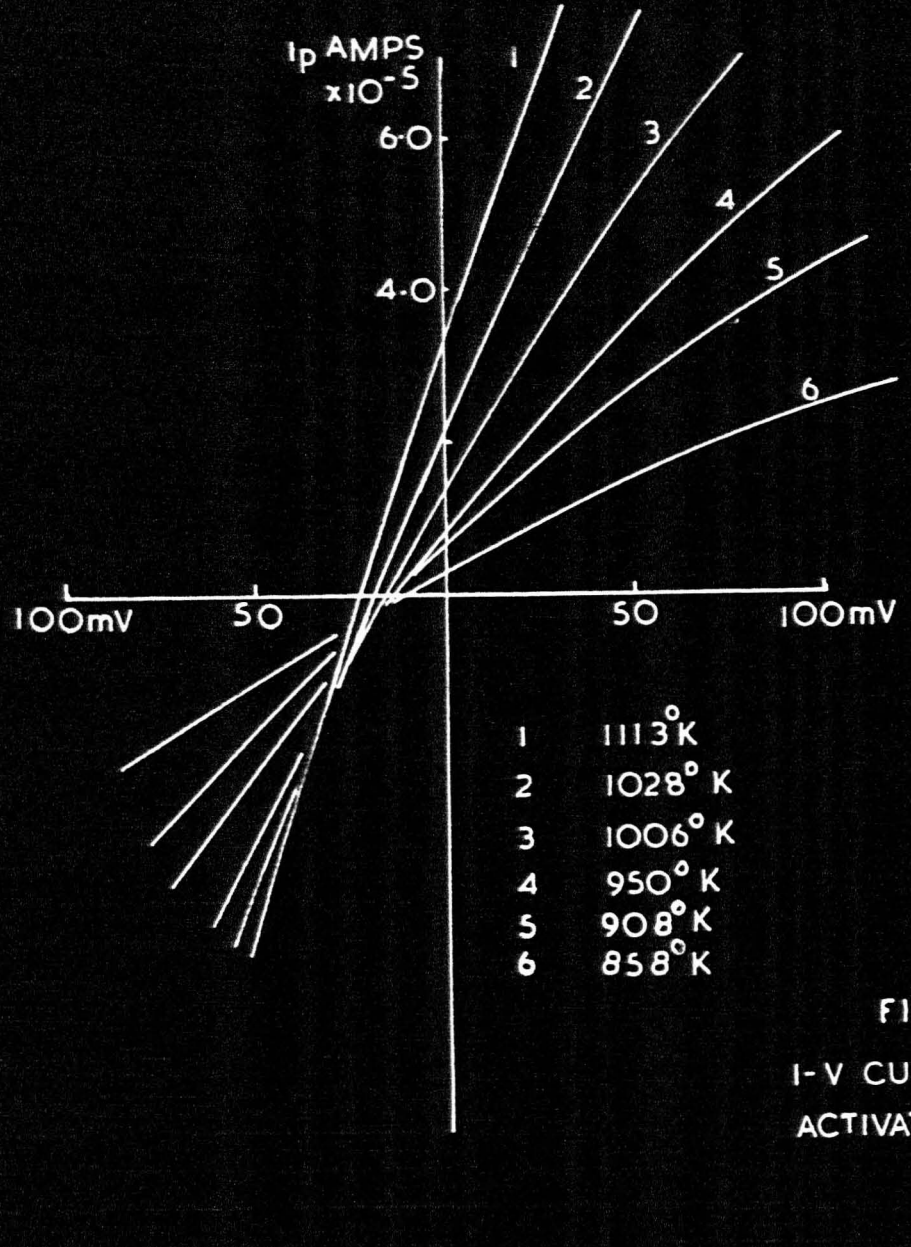

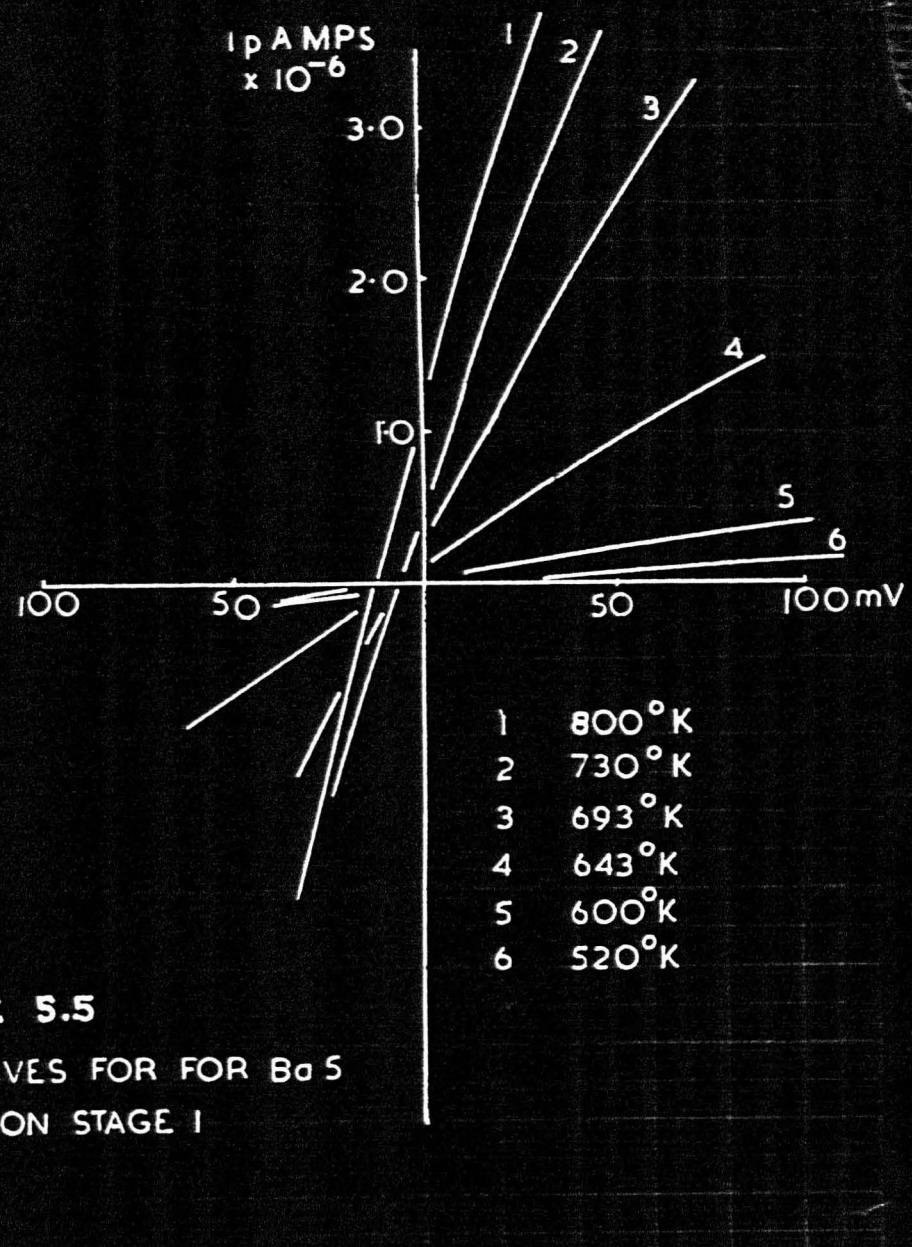

FIG 5.5

I-V CURVES FOR FOR Ba S
ACTIVATION STAGE I

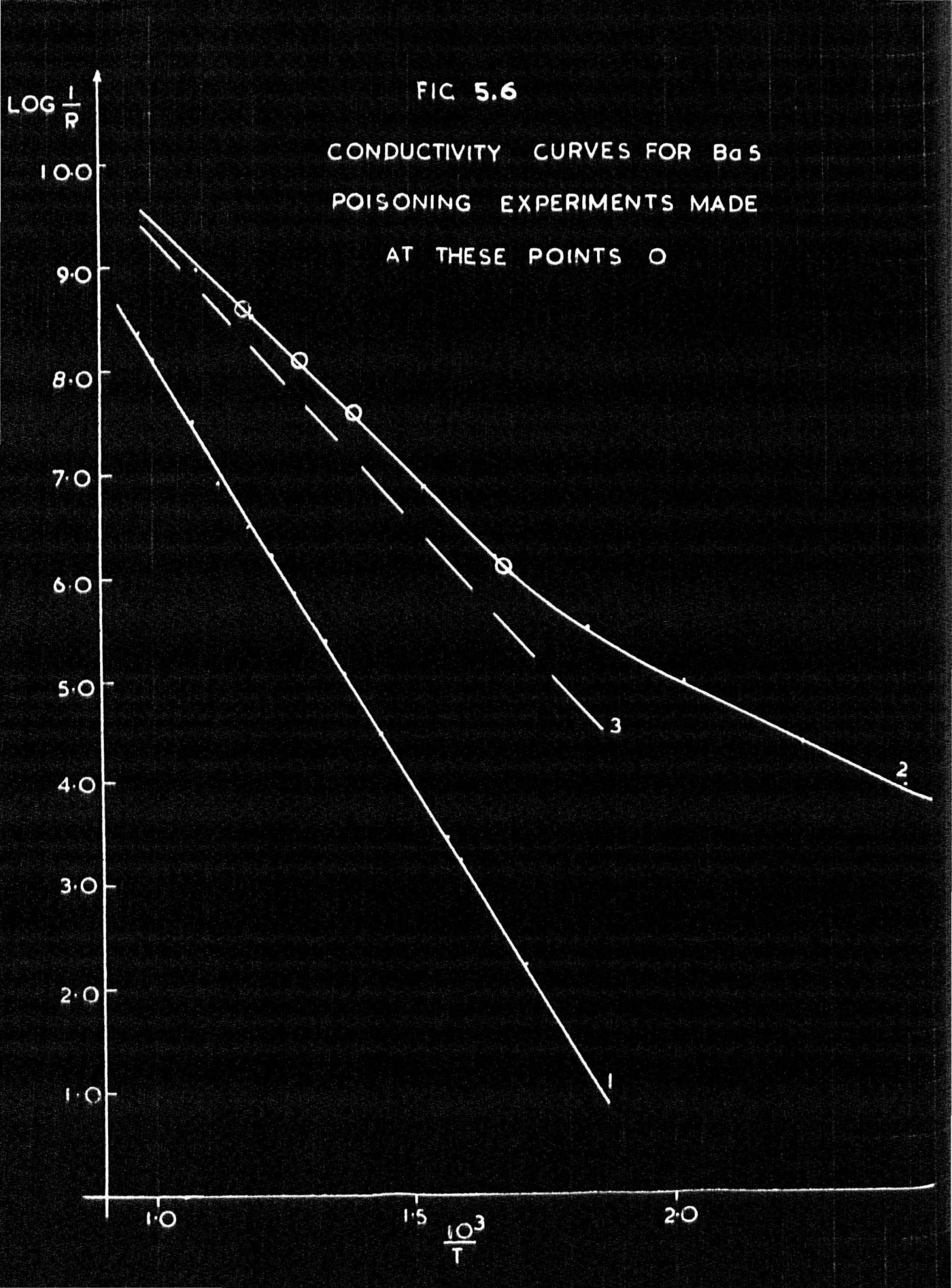
FIC 5.6
CONDUCTIVITY CURVES FOR BaS
POISONING EXPERIMENTS MADE
AT THESE POINTS O
LOG 1/R
10·0
9·0
8·0
7·0
6·0
5·0
4·0
3·0
2·0
1·0
1
2
3
1·0
1·5
2·0
10³/T

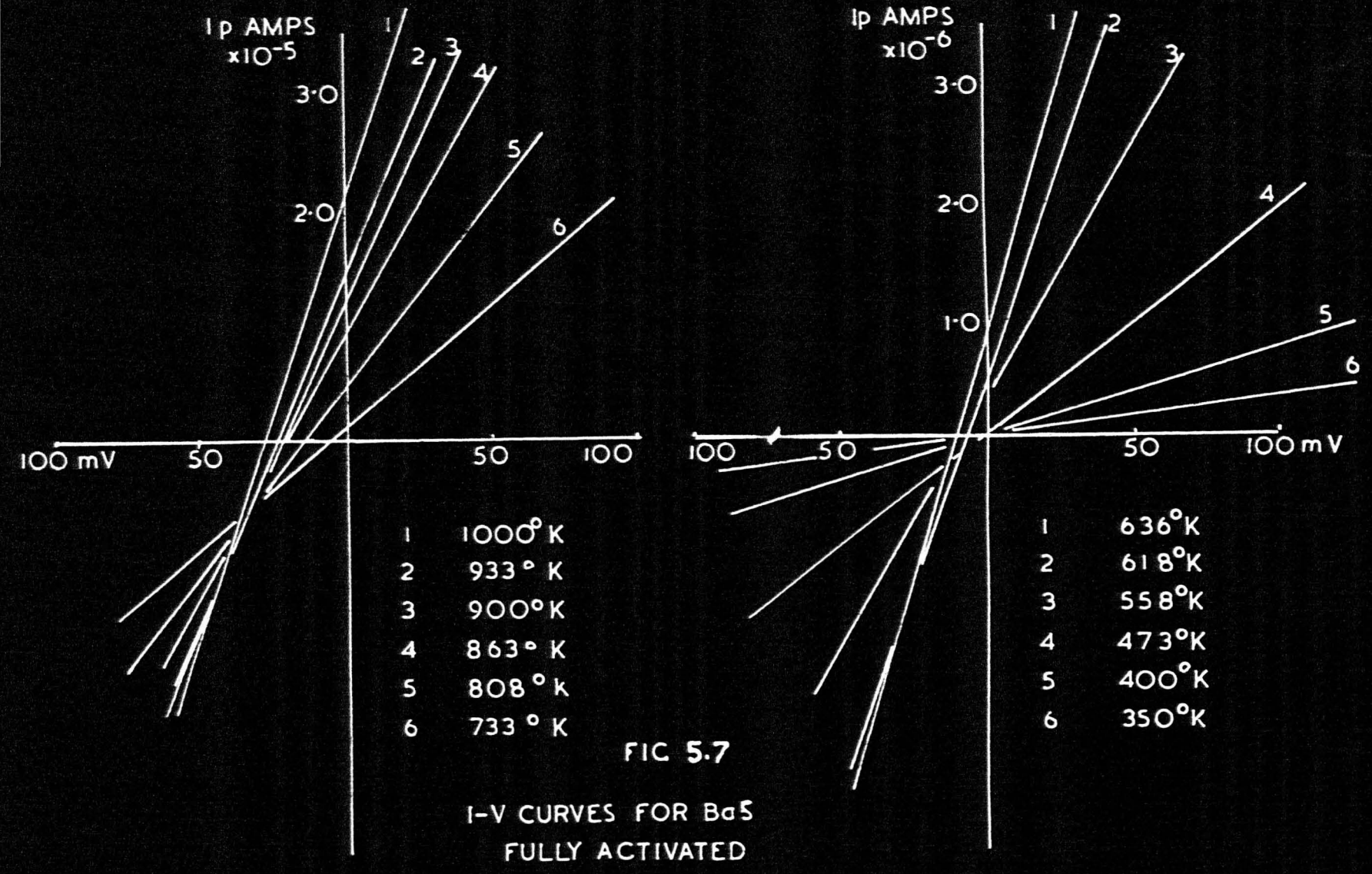

FIG 5.7

I-V CURVES FOR BaS
FULLY ACTIVATED

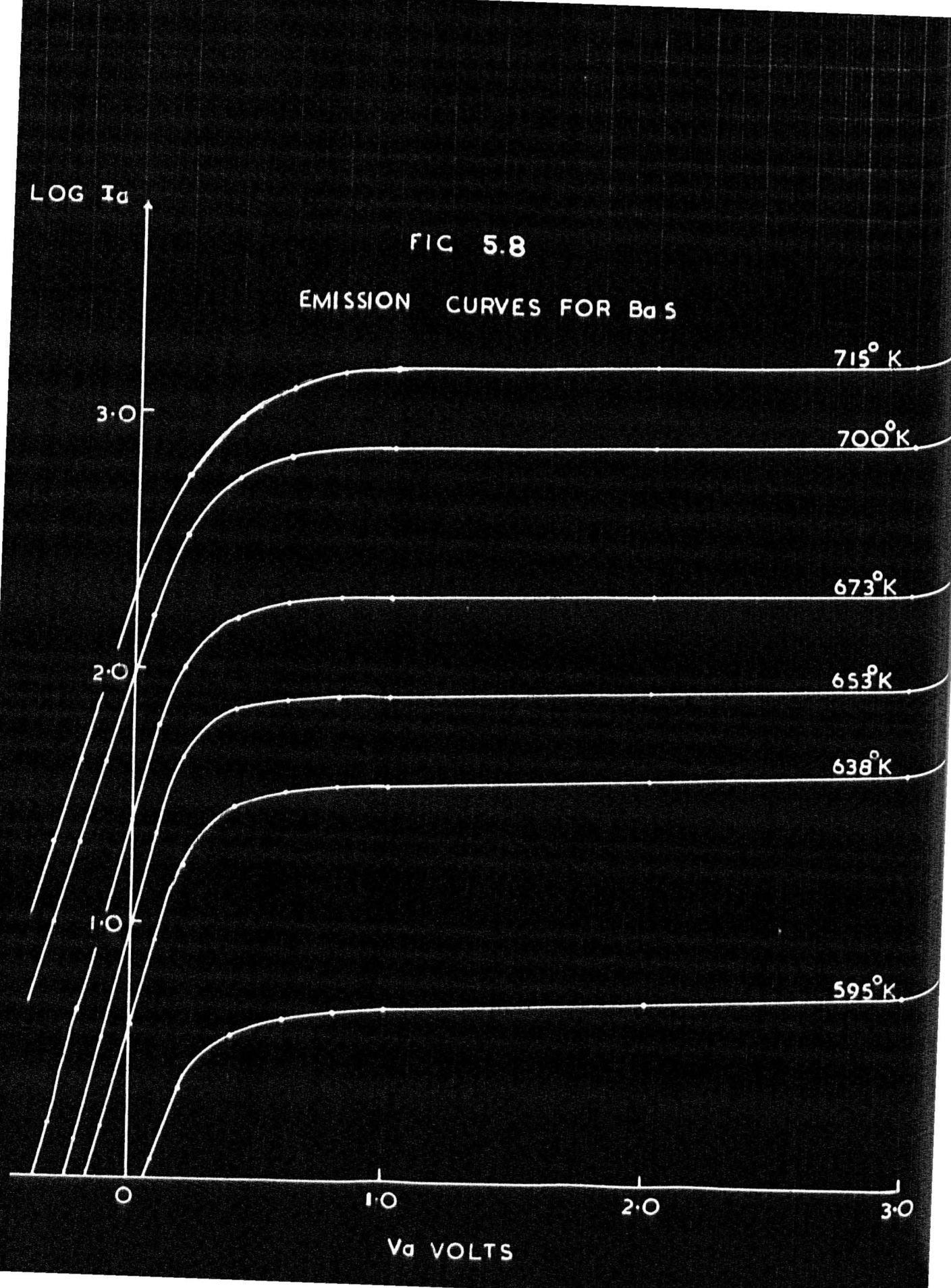
LOG Ia
FIC 5.8
EMISSION CURVES FOR BaS
715° K
700°K
673°K
653°K
638°K
595°K
3·0
2·0
1·0
0
1·0
2·0
3·0
Va VOLTS

A complete set of probe current-voltage curves were then taken (Fig. 5.5). Again the bending of these lines was observed. The conductivity versus reciprocal of temperature curve was then plotted (Fig. 5.6 curve 1). The curve does not exhibit any bend in the temperature range over which measurements were made. This effect has been reported by Loosjes and Vink for poorly activated cathodes (Fig. 4.3 curve 1).

In order that poisoning experiments might be made the cathode was aged in the usual way by applying 100 volts to the anode; cathode temperature 850°C. the emission saturated at 120 m/a. A further set of probe characteristics were obtained (Fig. 5.7). The current-voltage lines are again quite linear in this the fully activated state of the cathode. The conductivity versus temperature curve is shown in Fig. 5.6 curve 2, and the activation energies are 0.43eV in the high temperature region and 0.19eV at lower temperatures.

In order that the high temperature activation energy might be compared with the thermionic work function obtained from a Richardson plot, a number of emission measurements were made. The characteristics are shown in Fig. 5.8.

A Richardson plot was constructed from the saturation current values at zero applied field and gave a value of 0.78 eV for the thermionic work function. This kind of discrepancy between the two activation energies (0.43eV and 0.78eV) has been found by several previous workers.

A correction was applied to the high temperature slope of curve 2 in Fig. 5.6 in order to eliminate the parallel low temperature

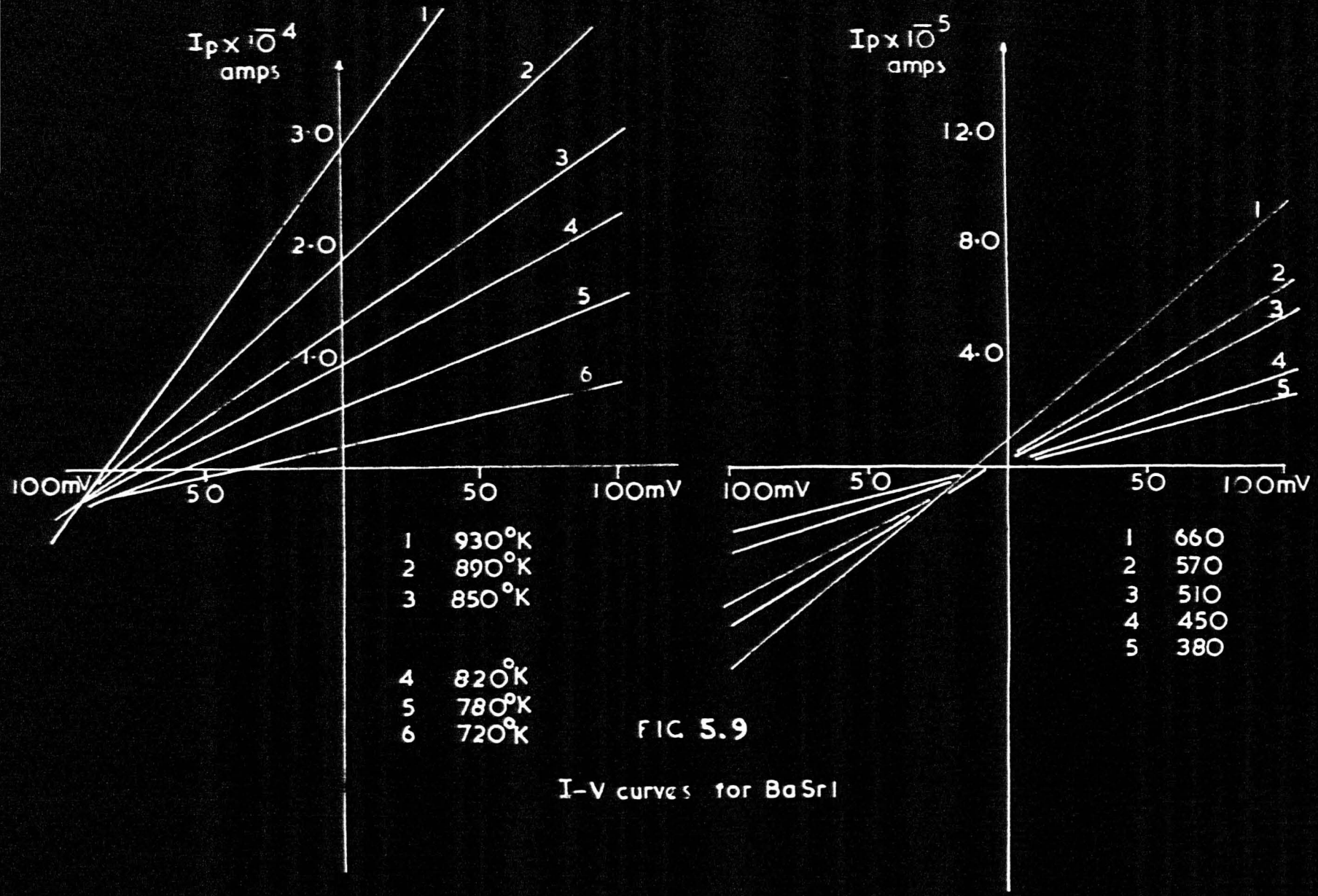

FIG 5.9

I-V curves for BaSrI

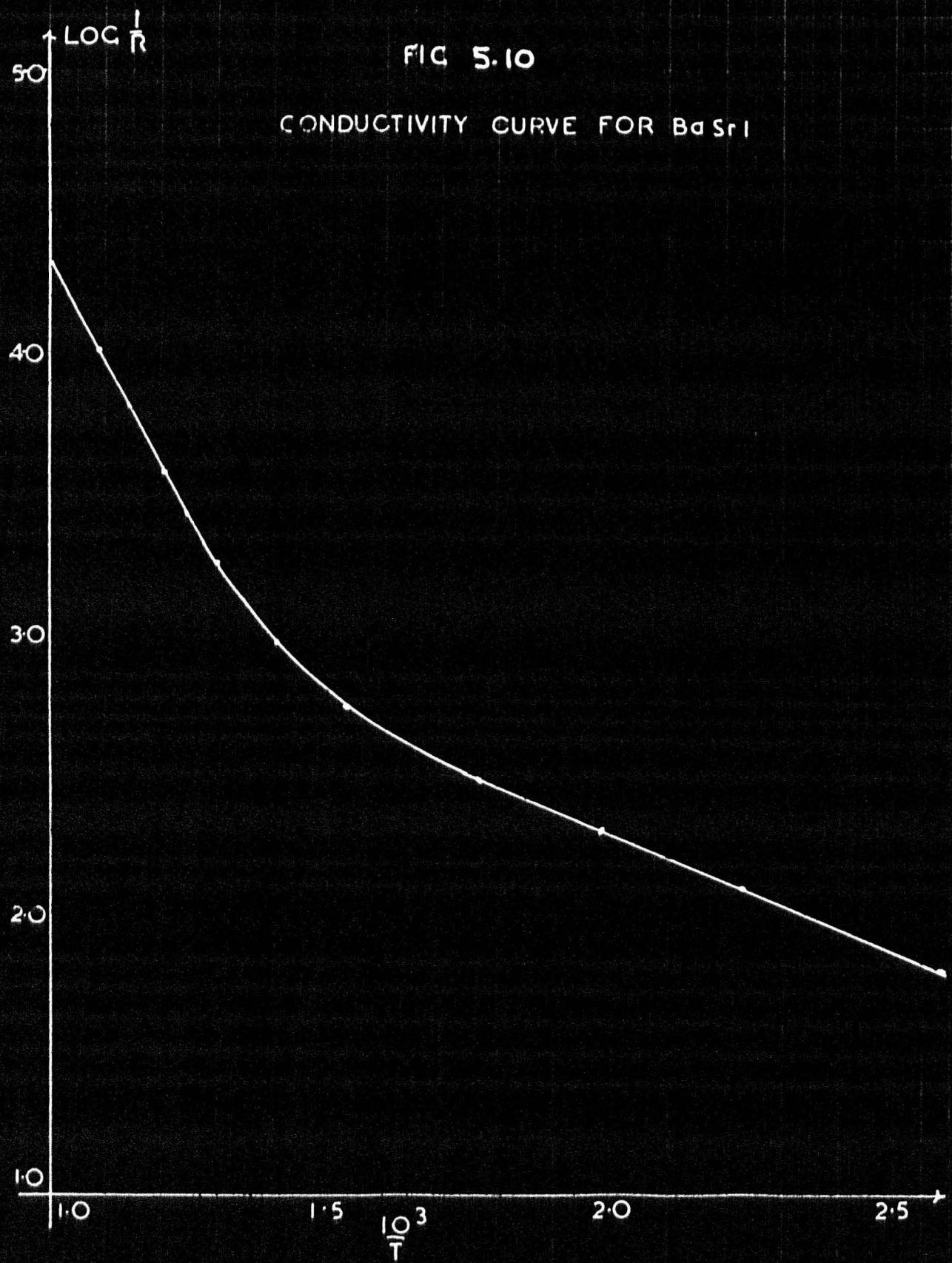

FIG 5.10

CONDUCTIVITY CURVE FOR BaSrI

contribution. This was done as follows:-

By producing the low temperature line towards the ordinate axis, the values of $^{I}/_{R}$ corresponding to the extrapolated section were found and subtracted from those given by the high temperature line. A new line (curve 3) was drawn using the resulting values, giving an activation energy of 0.49eV. While it must be pointed out that this is only an approximate correction, the true activation energy of the high temperature conduction process, which may be found by successive approximation of this type, cannot in this case be greater than 0.49eV.

Measurements on mixed oxide (BaSr)O coatings.

Cathode BaSr1.

This cathode was sprayed with B.D.H. barium strontium carbonate suspension. The spray gun was held some distance (50cm.) from the cathode so that a fairly dry coating resulted. A five turn probe wire was employed at a distance of 50 microns from the core. After assembly and baking for four hours the carbonates were decomposed over a period of 2 hours. This resulted in a coating which exhibited many cracks over its surface, no doubt due to the too rapid evolution of carbon dioxide. When breakdown had been accomplished, the anode and getters were outgassed by eddy-current heating. A two minute activation flash at 1100°C was then given, the getters fired and the tube sealed off.

The tube was aged at 900°C, Va = 100 v. until the emission became saturated at 180 m/a. (The anode was red hot under these conditions). Conductivity measurements were made in the usual way on the fully

FIG 5.11

I-V CURVES Ba Sr 2

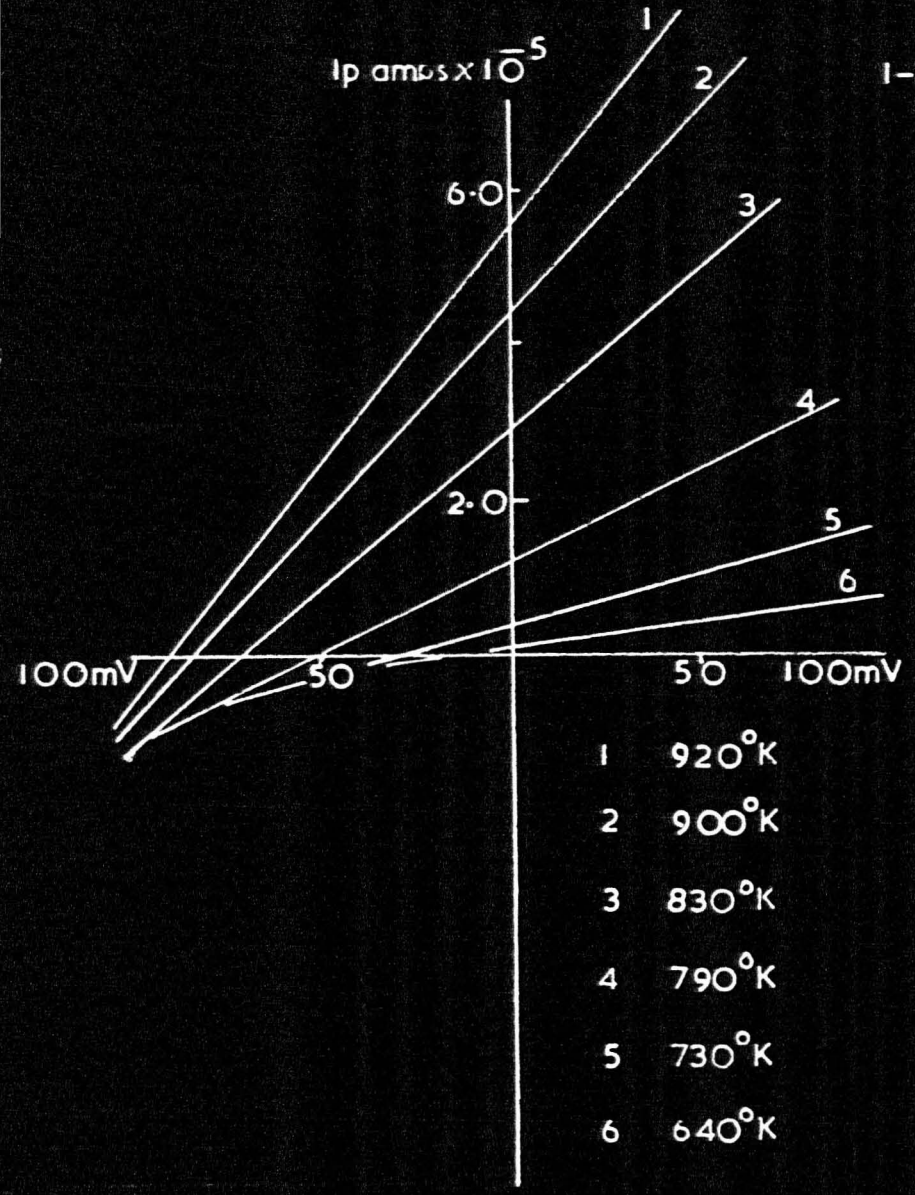

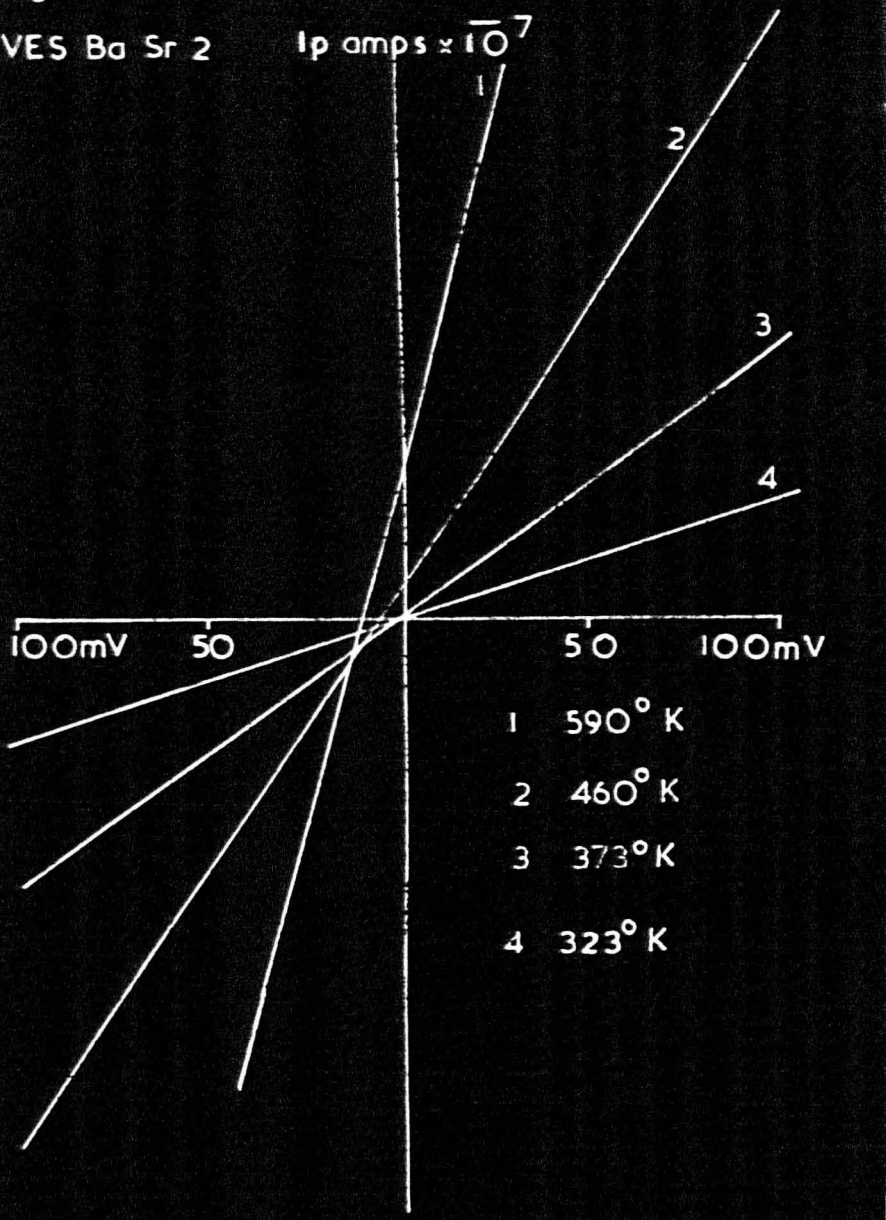

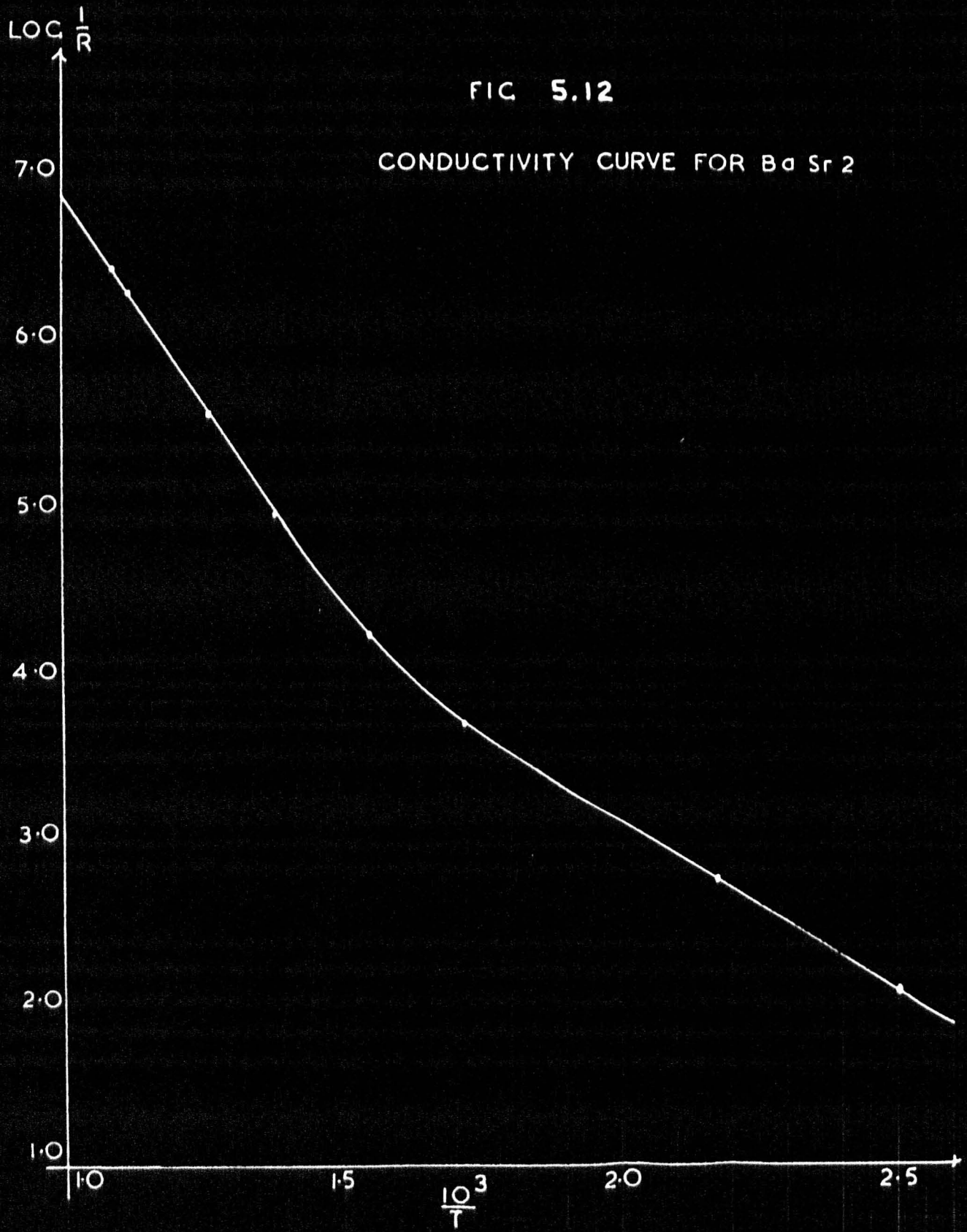

FIG 5.12

CONDUCTIVITY CURVE FOR Ba Sr 2

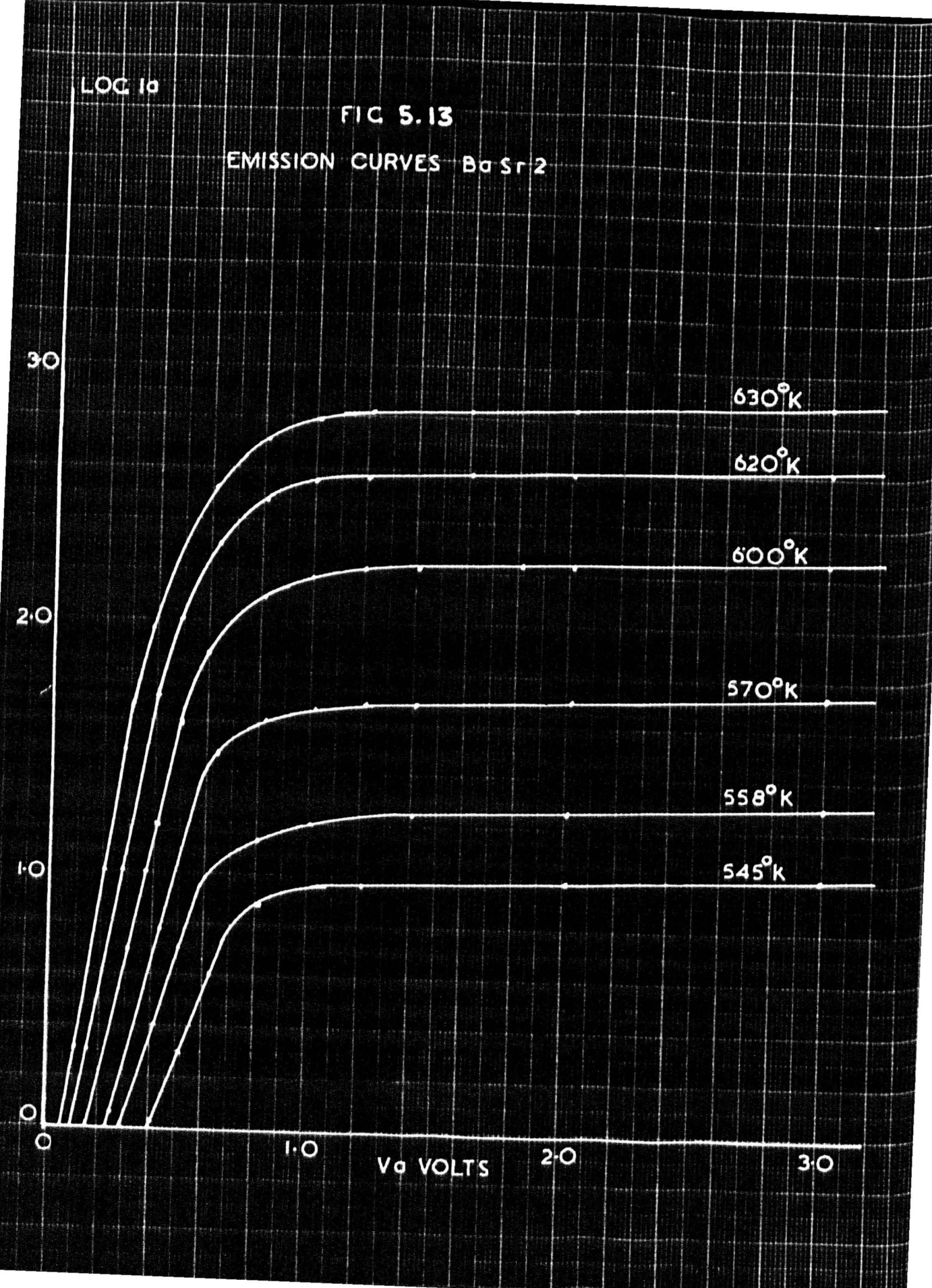
LOG Ia
FIG 5.13
EMISSION CURVES Ba Sr 2
3·0
2·0
1·0
0
0
1·0
2·0
3·0
Va VOLTS
630°K
620°K
600°K
570°K
558°K
545°k

FIG. 5.14

RICHARDSON LINE FOR $BaSr_2$.

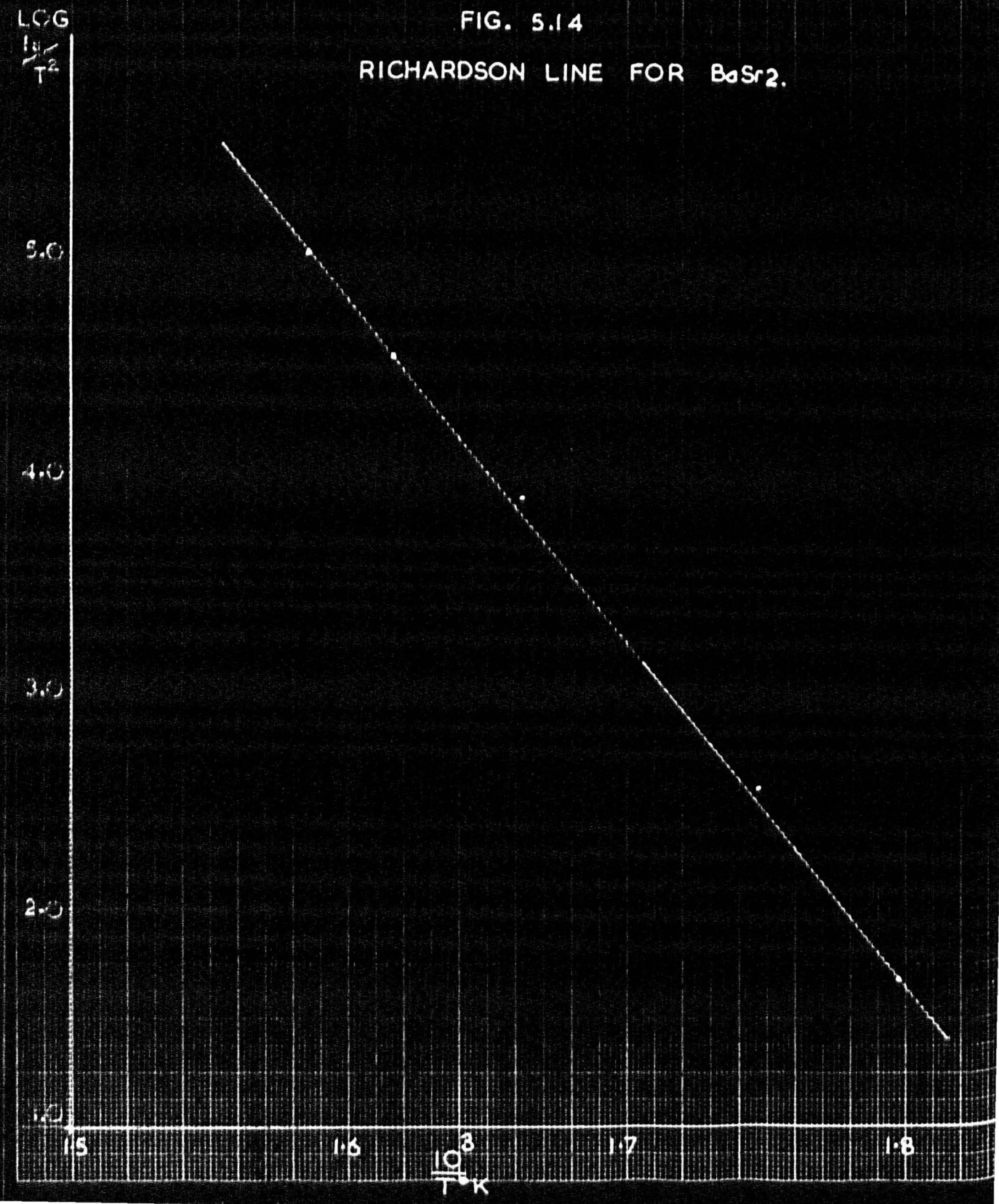

activated cathode. The probe current-voltage characteristics were quite linear (Fig. 5.9) and the log. conductivity vs. $^{1}/_{T}$ curve (Fig. 5.10) exhibits two straight line portions, the transition temperature being about 760°K. The high temperature activation energy was found to be 0.9eV and the low temperature activation energy 0.17eV.

During subsequent operations the heater of this tube burned out and further measurements were rendered impossible.

Cathode BaSr2.

The cathode of this tube was sprayed to a depth of 50 u and a 5 turn probe wire was used. The suspension used was one supplied by the English Electric Valve Co. Ltd., and contained a small quantity of calcium carbonate in addition to equal proportions of barium and strontium carbonates. The breakdown of the cathode was accomplished over a period of thirty hours and a smooth cathode exhibiting no cracks or mosaic-like appearance resulted. Ageing was carried out at 850°C at an anode potential of 100 volts. The emission stabilised at 150 m/a.

Conductivity measurements were made; 100 mV being applied to the probe in either direction. Fig. 5.11 shows the probe characteristics which were linear, and Fig. 5.12 the conductivity curve. The activation energies from the latter are 1.0eV at high temperature and 0.17eV at lower temperatures.

Emission characteristics over a limited temperature range were also obtained for this tube (Fig. 5.13), enabling a Richardson plot

FIG 5.15

I-V CURVES BaSr3.

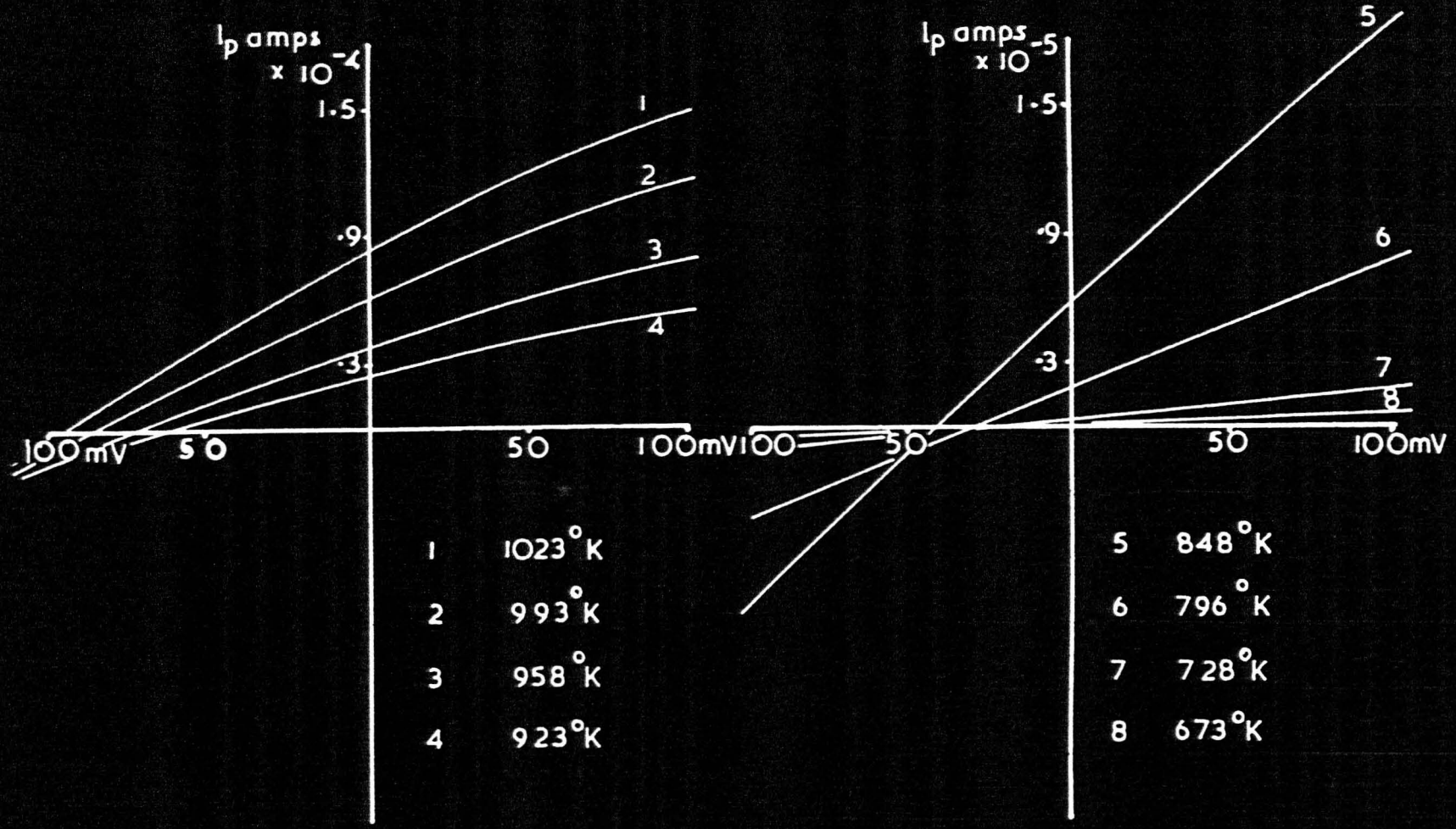

1	1023°K
2	993°K
3	958°K
4	923°K

5	848°K
6	796°K
7	728°K
8	673°K

FIG 5·16

CONDUCTIVITY CURVES BaSr3

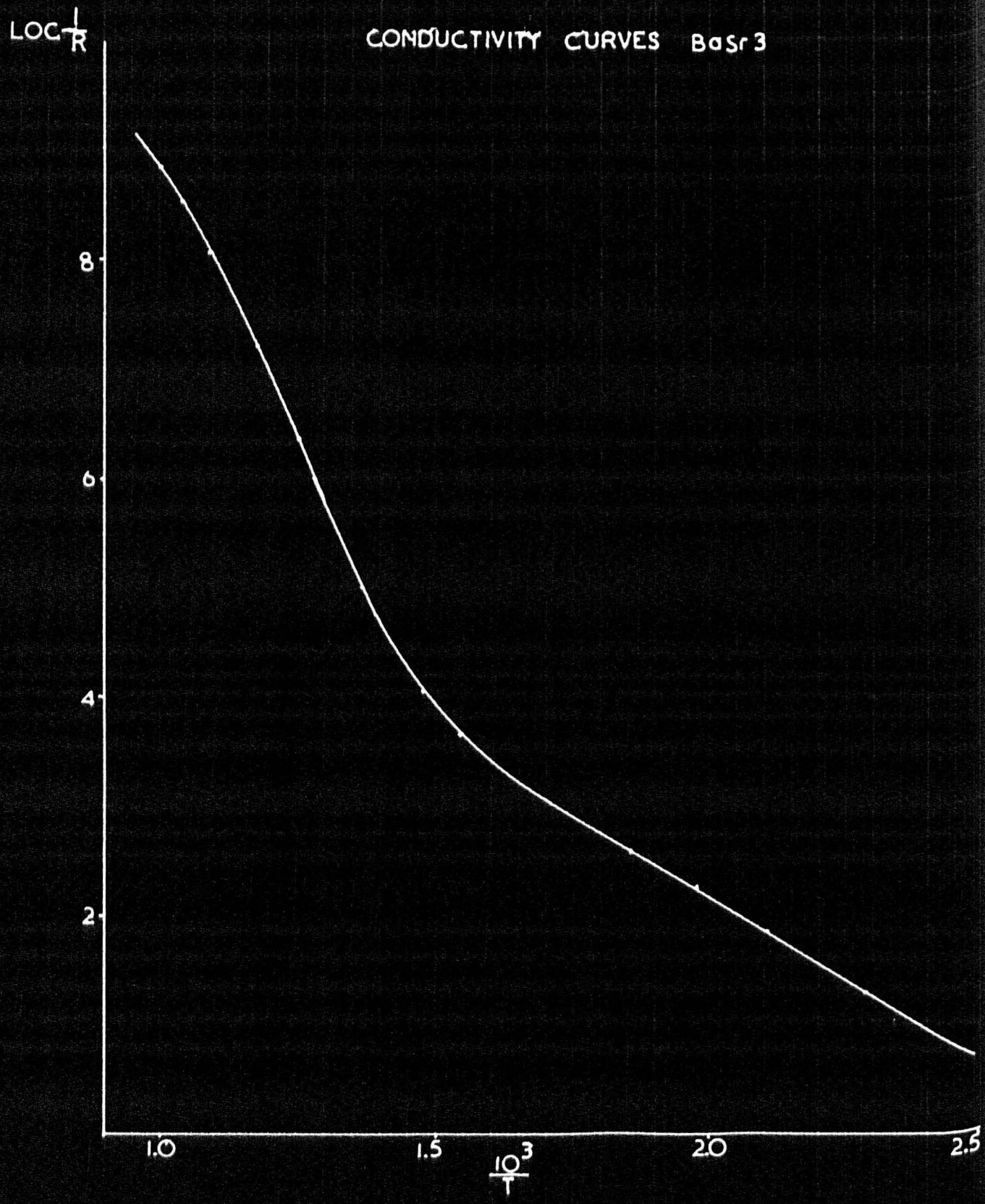

to be made (Fig. 5.14). The thermionic work function from this line is 1.28eV, which again does not agree with the high temperature activation energy.

Cathode $BaSr_3$.

This cathode was sprayed with B.D.H. mixed carbonate suspension to a depth of 50 u before the six turn probe was wound on. A 'wet' spray was used, resulting in a cathode of smooth appearance. The assembled tube was baked for 4 hours and the carbonates decomposed over a period of 30 hours at the end of which the cathode temperature was 900°C. After eddy-current heating the anode, 100 volts was applied and a small emission current (2m/a) was noted. This increased to 5m/a after 1 hour. Accordingly it was decided to proceed with conductivity measurements before an activation flash, while the tube was still on the pump. The probe characteristics are shown in Fig.5.15 and are seen to exhibit the bending experienced with other cathodes at low levels of activation. The conductivity versus temperature curve is shown in Fig. 5.16. It exhibits the bend at about 700°K usually found for cathodes in sealed-off tubes. This curve also shows curvature towards the ordinate axis in the high temperature region which may be due to the onset of saturation of the emission in the pores of the coating, in view of the low state of activation of this cathode.

The high temperature activation energy is 1.0eV and at lower temperatures 0.26eV.

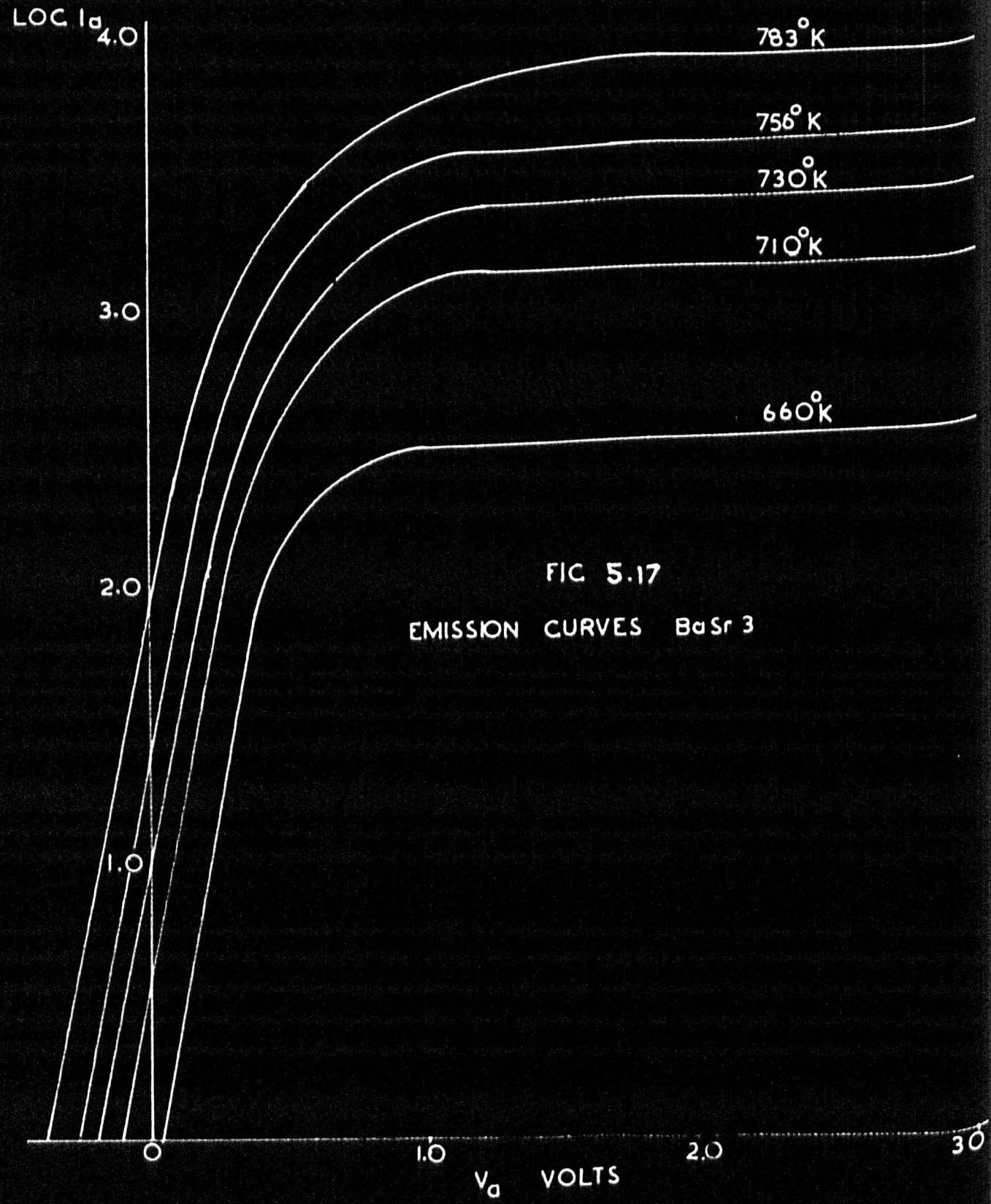

FIG 5.17

EMISSION CURVES BaSr 3

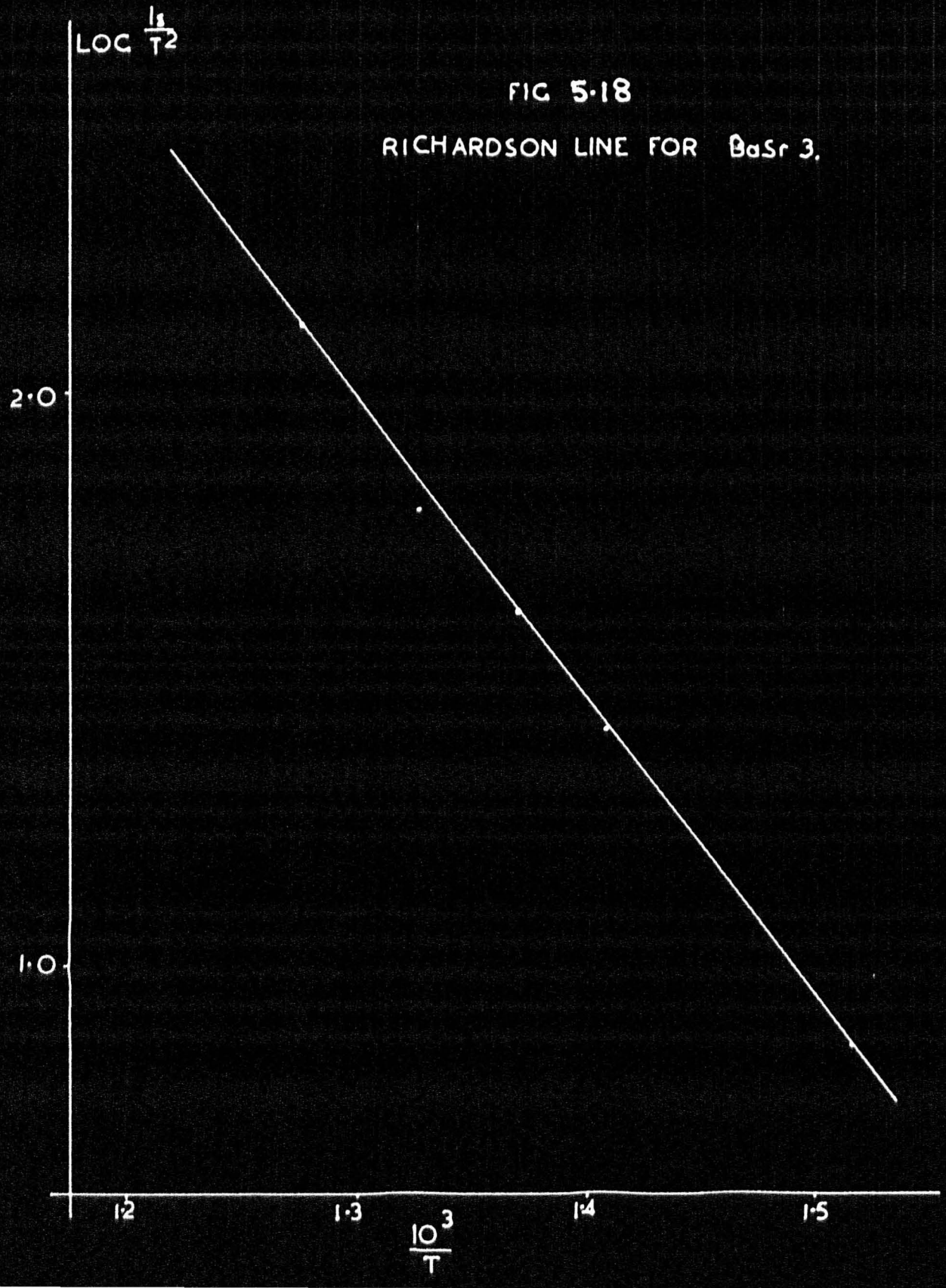

FIG 5·18

RICHARDSON LINE FOR BaSr 3.

Under the same conditions emission measurements were made (Fig. 5.17) and a Richardson line plotted (Fig. 5.18). This gave a value of 1.06eV for the work function of the cathode. All these measurements were made with the tube on the pump. The pressure was monitored with the Penning gauge and was always less than 10^{-6} mm.Hg.

An attempt was made to activate the cathode in the normal way by flashing at 1100°C. During this operation the probe wire became discontinuous and the conductivity of the oxide measured from one end of the probe was found to be a factor of 10 less than previously. Since comparative data could not be obtained under such conditions, further measurements were discontinued.

The results shown in the conductivity plot (Fig. 5.17) are significant in so far that Hannay et al (58) and Hughes and Coppola (49) reported that the bend and low temperature slope could not be obtained on the pump and adjudged this to be evidence in favour of conductivity in a barium film at low temperatures, which would be readily oxidised while pumping. It is unfortunate that comparable measurements could not be made with the tube in the sealed-off and gettered state.

Summary Table of Activation Energies.

The following table gives a summary of the activation energies obtained from conductivity and emission measurements.

Cathode	High Temp conductivity eV	Low Temp. conductivity eV	Richardson plot slope eV
Ba1	0.81	0.25	-
Ba2	1.1	0.21	-
Ba5	0.49	0.19	0.78

Summary Table of Activation Energies (Contd....)

Cathode	High Temp. conductivity eV	Low Temp. conductivity eV	Richardson plot slope eV
BaSr1	0.9	0.17	-
BaSr2	1.0	0.17	1.28
BaSr3	1.0	0.26	1.06

Discussion of Results.

Two points of interest have emerged during the course of these preliminary experiments. The first to claim attention was the marked departure from linearity of the probe voltage-current characteristics when the cathode was only partially activated. This does not appear to have been noted in previous work although departure from linearity at higher applied voltages has been discussed by Loosjes and Vink and more recently by Tomlinson (41) in terms of saturation of the emission in the pores of the coating. It is not improbable that the curvature noted here arises from the same cause. Emission from the partially active grains would become saturated fairly readily at low probe potentials. Application of larger potentials to the probe may cause heating and possibly disrupt the coating. An a.c. technique which overcomes this difficulty is described in Appendix I and a more extensive investigation of probe I-V characteristics is reported there.

A further point arising from these experiments is the marked disagreement between the activation energy of the high temperature conduction mechanism and the work function obtained from a Richardson Plot. This disagreement has been reported by several authors. Possibly

it arises from the presence of contaminating materials on the outer surface of the cathode. Evidence for an oxygen film on the outer surface of the cathode has been advanced by Duckworth (59). This would vary with temperature and could lead to the disagreement observed here and elsewhere.

Sufficient experience has been gained in performing these preliminary experiments to enable a more carefully conducted investigation to be made of the changes occurring in an oxide cathode during activation. These measurements are described in the next Chapter.

CHAPTER 6

FURTHER CONDUCTIVITY MEASUREMENTS

Introduction.

This Chapter is concerned with an investigation of the differences between cathodes which have been activated thermally and those which have been activated by drawing an emission current. The former process is termed 'thermal activation' and occurs when the temperature of the cathode is maintained at 800°C or higher. The latter process termed 'emission activation' requires a potential to be applied to the anode of the diode assembly. This is usually 50 or 100 volts positive with respect to the cathode.

All the work described in this Chapter is confined to barium-strontium oxide cathodes, but experience gained from preliminary experiments suggests that the behaviour of barium oxide cathodes would be similar in many respects.

Cathode BaSr4.

This cathode was processed in a manner similar to that described previously (Chapter 3). After finally outgassing the anode and getters by eddy current heating the tube was not sealed off from the pumping system. The cathode was maintained at 850°C for 12 hours; then after cooling to 1000°K and allowing time for the temperature to stabilise throughout the coating, conductivity measurements were made in the temperature range 1000° - 400°K. At each temperature setting complete probe I-V characteristics were obtained. These were only slightly curved and the conductivity line, (Fig. 6.1 curve 1) indicated an

Fig. 6·1

Conductivity lines for BaSr4

$\text{Log}\frac{1}{R}$ vs. $\frac{1}{T}$

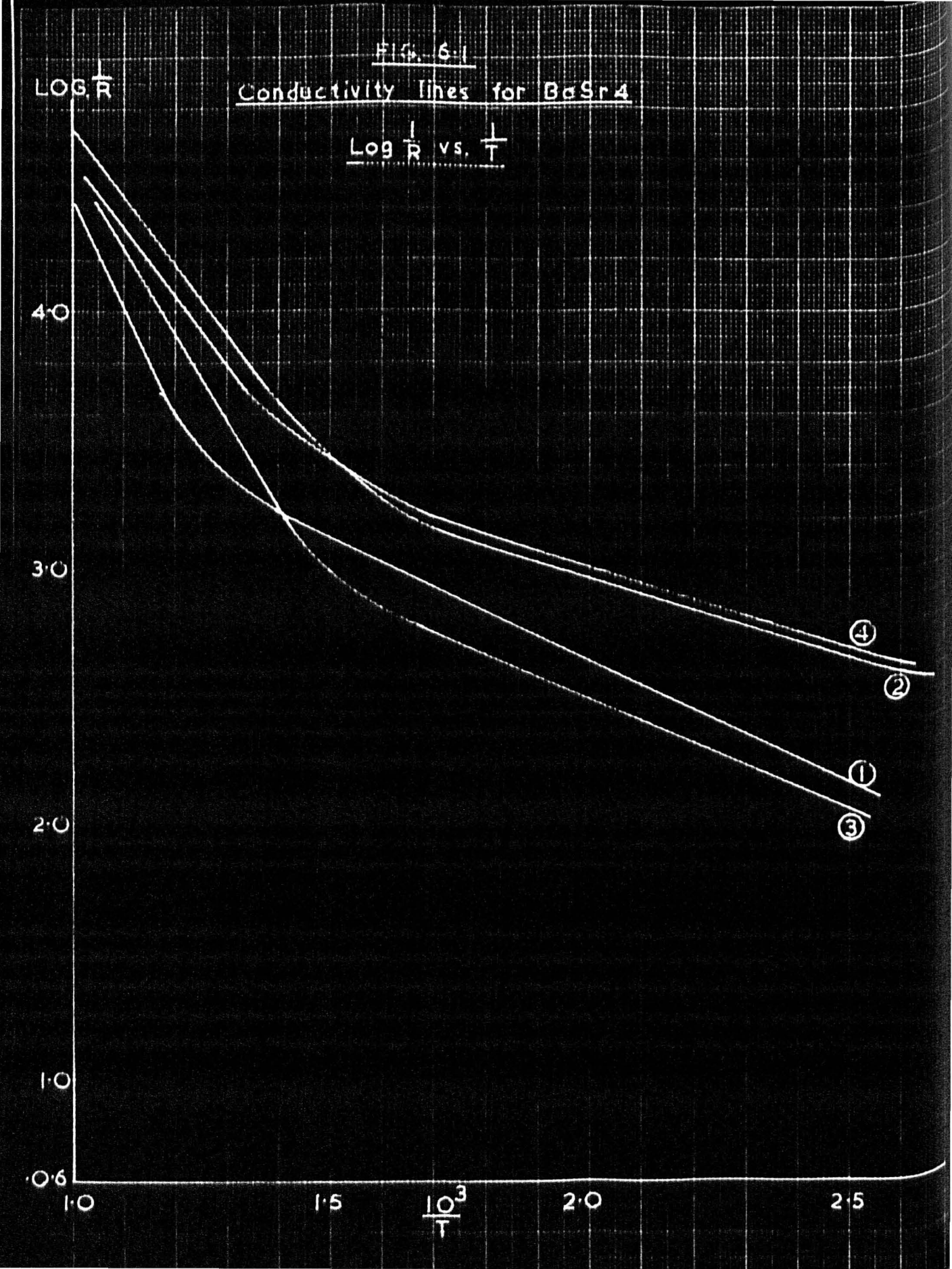

advanced state of activation. Further thermal activation for 24 hours and subsequent conductivity measurements gave curve 2. The slopes of the upper sections of these curves were corrected in the manner described previously in Chapter 5. The activation energies are listed in table 1.

Table 1.

curve	Q	Ø	
1	0.19	1.10 eV	Low temperature slope = Q
2	0.12	0.59 eV	Corrected High Temp.slope = Ø

The corrected high temperature slope in this and subsequent tables is represented by the symbol Ø since, on the basis of the Loosjes-Vink theory, this is the work function of the internal crystal surfaces. The change in Q, which in terms of semiconductor theory (page 13) reflects a movement of the Fermi level, is much smaller than the change in Ø. This may be explained by a reduction in χ the electron affinity of the oxide due to the removal of surface electron traps e.g. oxygen.

In order to ascertain whether the degree of activation indicated by curve 2 could be improved emission activation was attempted. A potential of 100 volts (E_a 100v) was applied to the anode. The initial anode current (Ia_i) was 120 m/a, which experience had shown was indicative of a well activated cathode. However an immediate decay in Ia occurred and the Philips Gauge indicated a rise in pressure. When Ia had decreased to 40 m/a the anode potential was removed and the cathode allowed to operate at 850°C for two hours. At the end of this

period application of Ea 100v. gave an initial current of 40 m/a which rose to 56 m/a in 30 seconds. This was accompanied by a further release of gas, the Philip's gauge recording an increase in pressure from 10^{-6} mm.Hg. to 3×10^{-6} mm.Hg. in 2 minutes. Conductivity measurements were made at this stage. These gave curve 3 fig. 6.1, which exhibited an unusual effect in that the high temperature section of the conductivity line was above that of curve 1, while the low temperature section was below that of curve 1. The whole of curve 3 in the range plotted lay below curve 2, indicating that deactivation had occurred. It is reasonable to attribute this deactivation to the decomposition of material on the anode by the electron beam; some or all of the products of the decomposition attacking the cathode. Such poisoning effects have been described in the literature and are discussed in Chapter 2.

The anode potential was reduced to 50 volts in an effort to overcome poisoning by reducing the intensity of the electron beam. The initial current was 56 m/a, which after a decay to 55 m/a over a period of five minutes, gradually increased in an hour to 71 m/a and over a further 3 hour period to 74 m/a. This gradual increase in emission suggested that the material on the anode was removed by the electron beam or its effect reduced to negligible proportions. Reapplication of Ea 100v. did not produce any poisoning effect but the anode current, initially 170 m/a, decreased to 160 m/a as the anode became red hot. Under these conditions a blue discharge was observed in the anode-cathode space and the Philips Gauge indicated

FIG 6-2

BaSr4 Conductivity lines

$\log \frac{1}{R}$ vs $\frac{1}{T}$

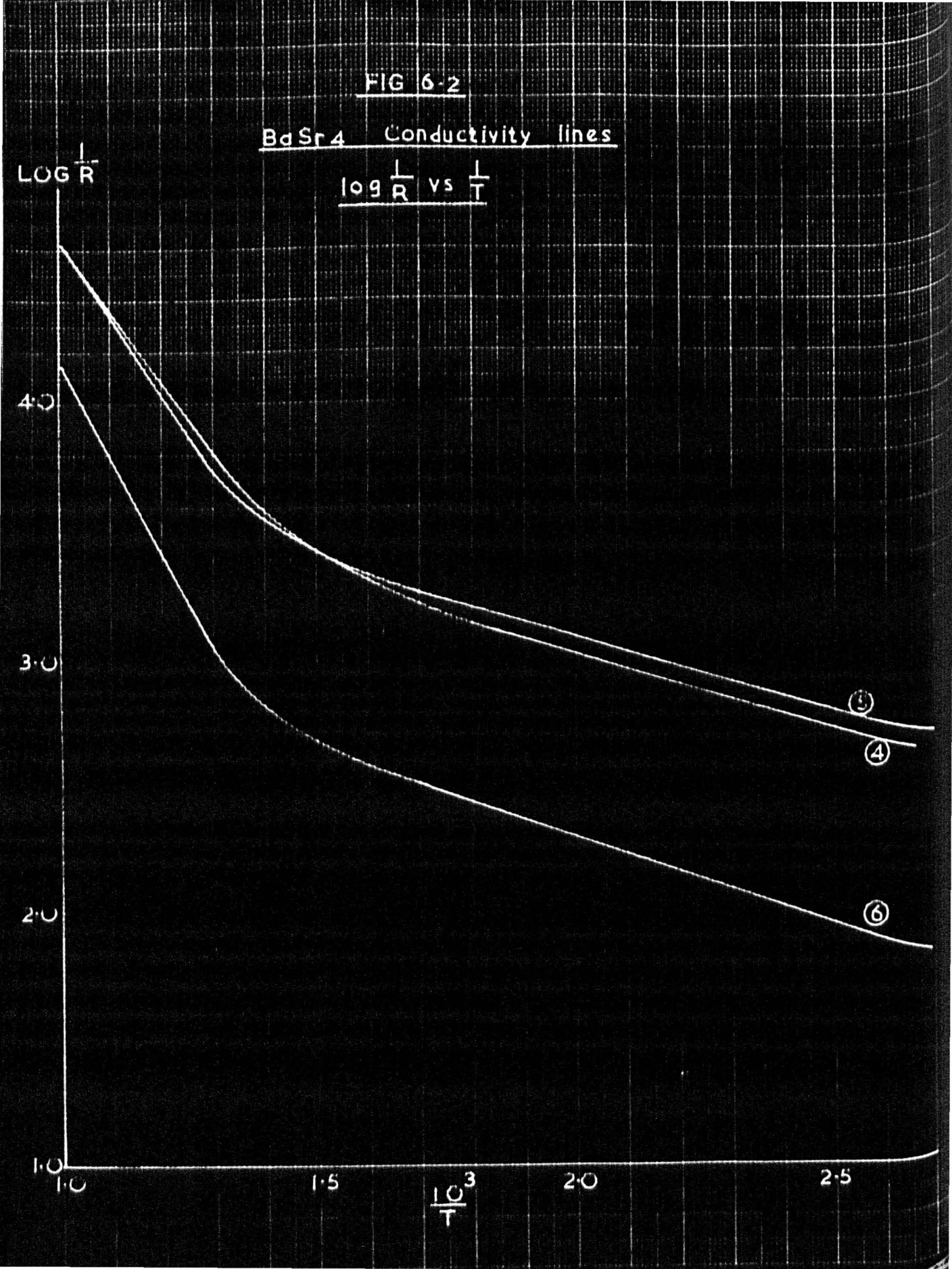

a slight increase in pressure. After 20 secs. the blue discharge gave place to a bright green discharge and at this stage the anode potential was removed. Subsequent measurements of the conductivity gave curve 4 fig. 6.1.

Table 2 gives the activation energies obtained from curves 3 and 4.

Table 2

Curve	Q	ϕ	χ
3	0.17	0.73	0.56 eV
4	0.12	0.68	0.56 eV

On this occasion the value of $\chi = (\phi - Q)$ did not change during the reactivation procedure. This result is at variance with that obtained in the thermal activation experiment (curves 1 and 2).

At a later stage a number of controlled oxygen poisoning experiments were performed on this cathode as described in Section 3. Recovery from poisoning was accelerated by increasing the cathode temperature to 900°C and applying a potential to the anode. In order not to overheat the anode, 50 volts was always applied during these recovery operations. After several poisoning-recovery experiments, a further conductivity measurements were made which gave curve (5) Fig. 6.2. The two curves (4) and (5) indicate a similar degree of activation but it is interesting to note that the corrected high temperature slope of curve (4) gives a higher value of ϕ than curve (5) whereas the low temperature sections give similar values for Q.

Table 3 shows that χ has increased during the poisoning experiments, indicating an increase in surface contamination of the crytal grains possibly by residual oxygen not removed by the recovery procedure.

Table 3

Curve	Q	ϕ	χ
4	0.12	0.68	0.56 eV
5	0.11	0.73	0.62 eV

All the measurements described in the preceeding paragraphs were performed with the vacuum tube continuously pumped. The pressure was maintained at $< 10^{-6}$ mm.Hg. except where noted in the text. Many poisoning experiments had been performed on this cathode involving the liberation of small quantities of oxygen gas inside the tube envelope and so it was decided to bake the glassware at 450°C before gettering and sealing off the tube.

The glass was baked at this temperature for 4 hours, the cathode reheated to 900°C and 100 volts applied to the anode. The anode current was 1 m/a indicating excessive poisoning of the cathode, presumably by gas desorbed from the glass. Over a one hour period the anode current increased to 40 m/a. Two barium getters were fired and the tube sealed off from the pump. The cathode was then aged at 900°C, anode voltage 100v. until the emission stabalised at 120 m/a with the anode at a dull red-heat. This was a lower value of emission than had been obtained before the tube was sealed off but under these conditions the anode would be outgassing slightly and so the cathode

would be partially poisoned. Conductivity measurements (Fig. 6.2 curve 6) confirmed this. Table 4 gives the activation energies obtained from the curve.

Table 4

Curve	Q	ø	χ
4	0.12	0.68	0.56 eV
5	0.11	0.73	0.62 eV
6	0.14	0.88	0.74 eV

Again the value of χ c.f. curve 2 and 4 is quite large implying contamination of the surfaces of the crystal grains.

Several poisoning experiments were performed in this sealed off tube. Recovery at 900°C, Ea 50v. gave a conductivity line shown in fig. 10 chapter 10 which lay slightly below curve 4 fig. (6.2).

These results show that a cathode may be activated thermally to a high degree if operated at 850°C for about 30 hours. Subsequent application of an anode potential however is liable to produce deactivation. This is thought to arise in the decomposition of material adsorbed on the anode by the electron stream; the products of this reaction returning to poison the cathode. This in turn reduces the emission from the cathode and the conductivity in the high temperature region. The activation energy of the low temperature conduction mechanism is increased, but not to the same extent as the surface work function.

Material may be evaporated from the cathode onto the anode either during the breakdown of the carbonates to oxide or during the sub-

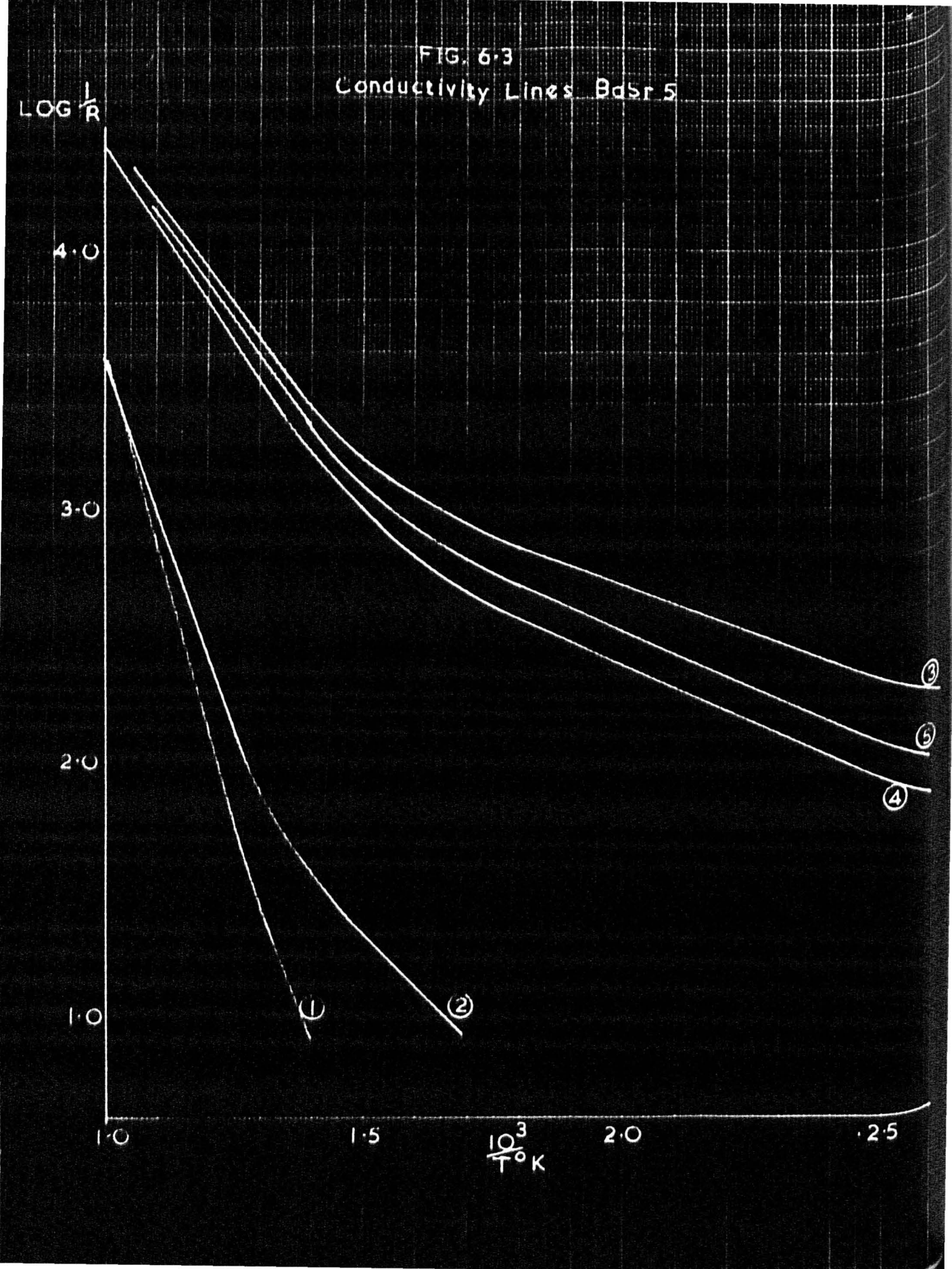
FIG. 6·3
Conductivity Lines Bdsr 5
LOG 1/R
4·0
3·0
2·0
1·0
1·0
1·5
10³/T°K
2·0
2·5
①
②
③
④
⑤

sequent thermal activation when the temperature of the cathode is maintained at a high value for a lengthy period. An anode which had not been carefully cleaned before assembly might well lead to poisoning effects which would be confused with either of these two processes. Some experiments are described in the ensuing paragraphs which enable these three processes to be studied separately.

Cathode BaSr5.

This cathode was required for preliminary sulphur poisoning experiments and so an MoS_2 filament was enclosed in the tube envelope. This meant that baking of the glassware hadto be carried out at a lower temperature (250°C). Baking was therefore continued for 14 hours at this temperature. The carbonates were decomposed over a period of 36 hours by raising the cathode temperature slowly to 900°C. The anode and getters were outgassed, the cathode cooled and the tube pumped down to $< 10^{-6}$ mm.Hg. This processing schedule had avoided operation at high temperatures except during the carbonate-oxide conversion, and so very little thermal activation should have occurred.

Conductivity measurements were attempted at this stage. The probe current-voltage characteristics were very curved and measurements could only be obtained at elevated temperatures. Curve 1 fig. 6.3 shows the curve obtained. The activation energy from the slope was 1.56 eV.

Emission activation was then attempted, at 900°C with Ea 100v. The initial anode current was 10 m/a showing that the cathode was potentially activated. This decayed to 5 m/a indicating some poisoning probably by decomposition of material on the anode. Over a two

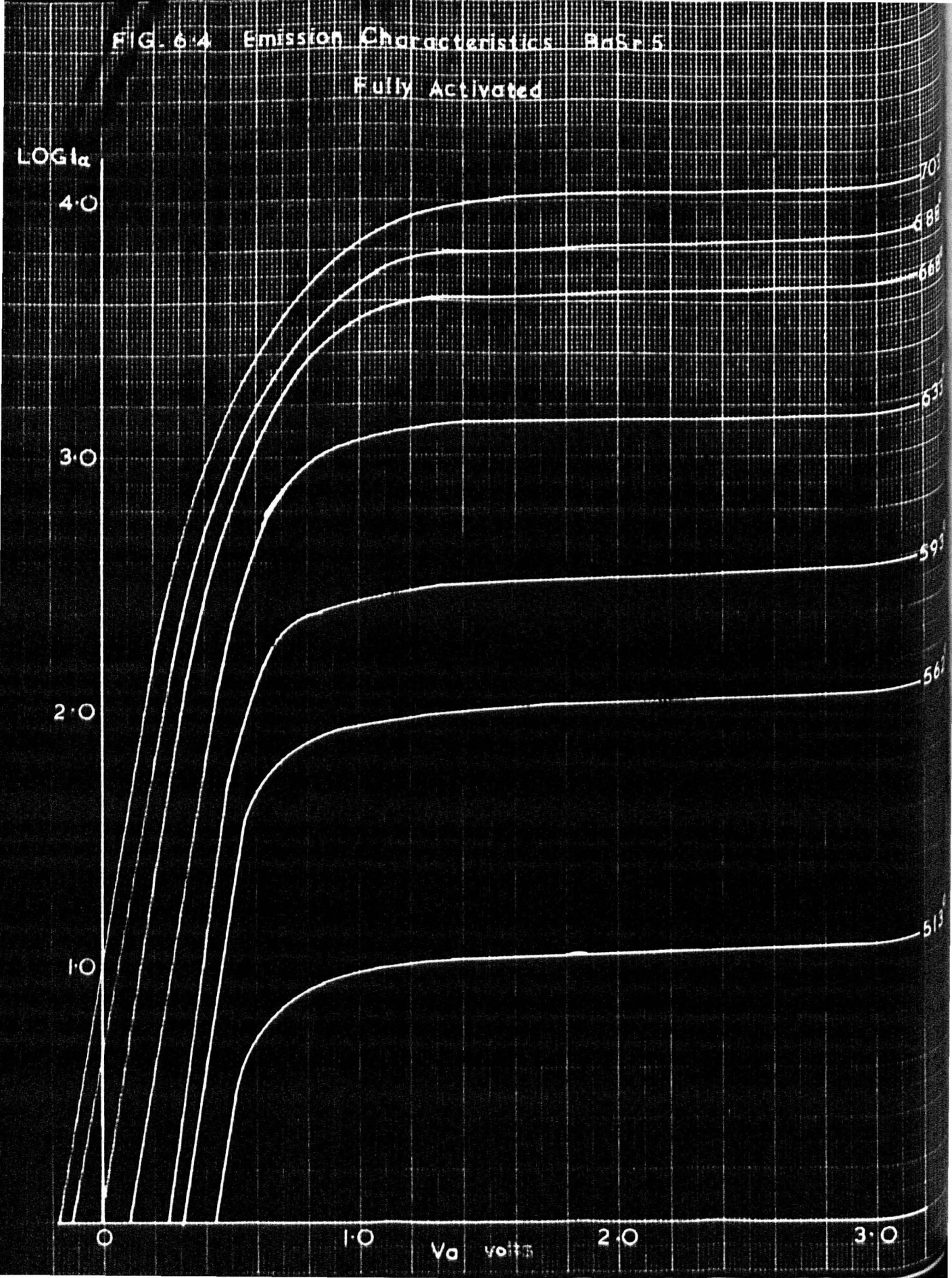
FIG. 6·4 Emission Characteristics BaSr 5
Fully Activated
LOG Ia
4·0
3·0
2·0
1·0
0
1·0
2·0
3·0
Va volts
70
68
66
63
59
56
51

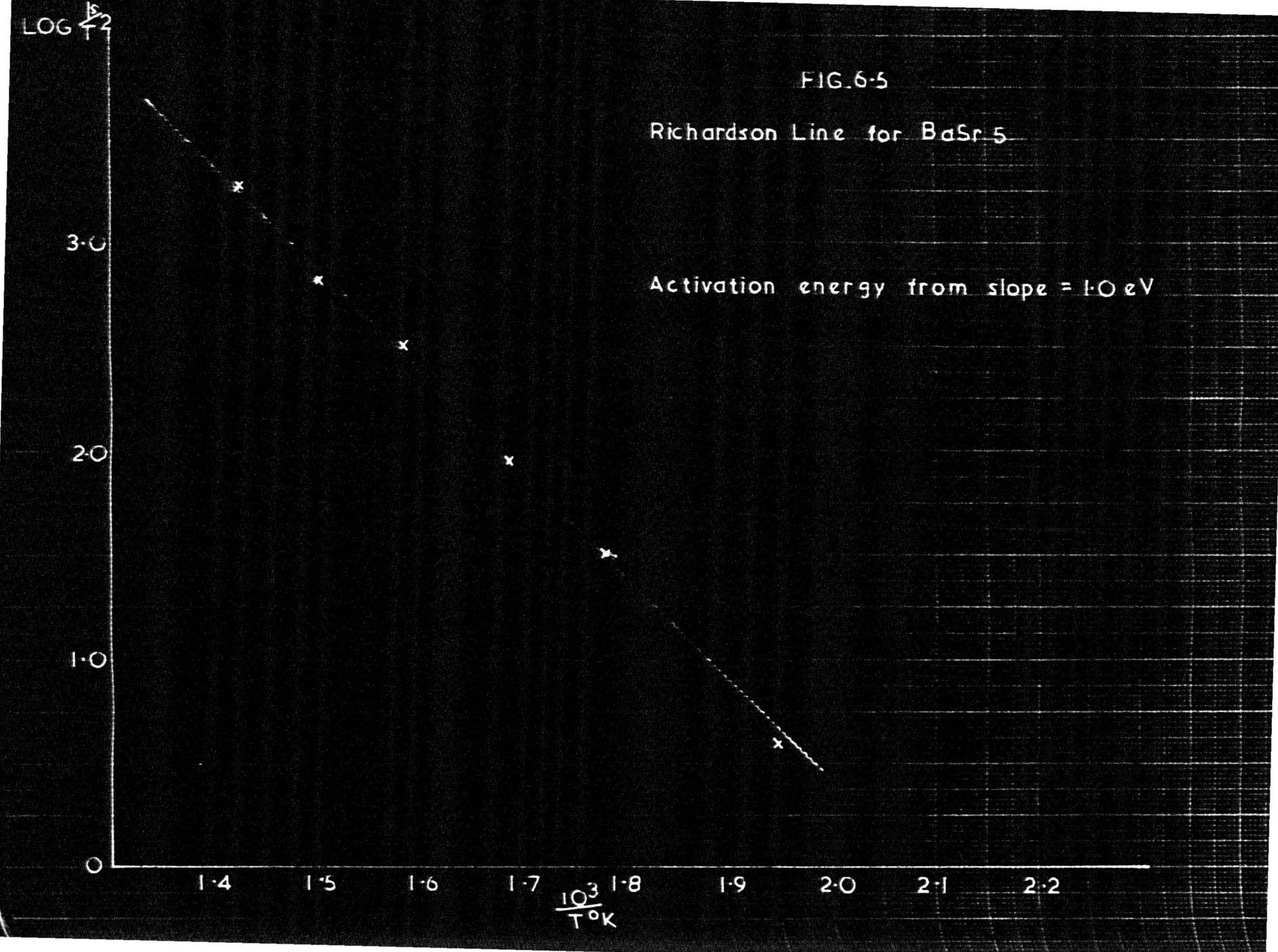

FIG. 6·5

Richardson Line for BaSr 5

Activation energy from slope = 1·0 eV

hour period the current increased to 36 m/a. Conductivity measurements were then made which gave curve 2 fig. 6.3.

Further emission activation for 30 minutes gave an anode current of 72 m/a. The anode potential was reduced to 50v. and activation continued until the emission saturated at 80 m/a. Reapplication of 100 volts for a short interval gave an emission of 180 m/a. This was a higher value than had been previously attained and so both emission and conductivity measurements were made. From the emission measurements fig. 6.4 a Richardson line fig. 6.5 was constructed. The conductivity curve (line 3 on fig. 6.3) indicated a well activated cathode. The activation energies are given in Table 5

Table 5

Curve	Q	ϕ	Richardson ϕ	
1	-	1.56	-	eV
2	0.40	1.35	-	eV
3	0.12	0.64	1.0	eV

Correspondence between the corrected high temperature activation energy ϕ and the work function given by the Richardson plot is not obtained, a point which was noted several times in the preliminary experiments. The decrease in ϕ during activation is much greater than the change in Q, again suggesting the removal of surface contaminants from the internal crystal grains.

Curve 3 represents a state of the cathode attained after emission activation at 900°C Ea 50v. Application of 100 volts would give 180 m/a anode current which in a short time would heat the anode

to redness. This would probably release a further quantity of material adsorbed on the surface of the anode.

In order to investigate this effect the anode potential was increased to 100 volts and the anode current and pressure indicated by the Philips gauge were noted over a 10 minute period. The Philips gauge has an approximately linear calibration, 1μa ≈ 10^{-6} mm.Hg. The results are shown in the accompanying table

Table 6

Time min.	0	1.0	2.0	4.0	5.0	8.0	10.0
I_a m/a	170	165	160	148	140	130	130
P/G μa	0.2	1.2	1.0	0.9	0.8	0.6	0.6
			Anode red-hot green/ blue glow observed		Anode not red-hot		

The table shows that application of 100 volts was accompanied by a release of gas. This probably came from the anode, since the cathode had been well activated, and suggests that the higher energy electrons desorbed or decomposed further anode contaminants. These in turn would poison the cathode and reduce the emission to the level indicated at the right of the table. Conductivity measurements (curve 4, fig. 6.3) indicated a less active cathode.

Emission activation was attempted at 900°C Ea50v, but over a period of one hour the emission remained constant at 74 m/a. This suggested that some permanent poisoning effect had occurred which could not be removed by normal emission activation procedures.

Thermal activation was then attempted; the cathode temperature being raised to 1000°C for 2 minutes. On returning to 900°C Ea 100v. the anode current was 170 m/a indicating some recovery. Conductivity measurements gave curve (5).

Table 7.

Curve	Q	ø	χ
3	0.12	0.64	0.52 eV
4	0.18	0.72	0.54 eV
5	0.18	0.67	0.49 eV

Table 7 shows that no change occurred in Q as a result of the high temperature operation for 2 mins. The value of χ decreased and this can best be explained as before in terms of removal of material from the internal crystal surfaces.

In subsequent experiments it was found impossible to reproduce the state of conductivity represented by curve 3 even after operation under emission activation conditions for almost 200 hours.

Cathode BaSr6.

The temperature of this cathode was increased to 900°C over a period of 30 hours and maintained at that temperature for a period of 14 hours. Conductivity measurements were made and these are shown in figs. 6.6 curve 1. The long term operation at 900°C resulted in a cathode that was well activated. Emission measurements were also made and used to construct a Richardson line. The activation energies obtained from these curves are shown in Table 8.

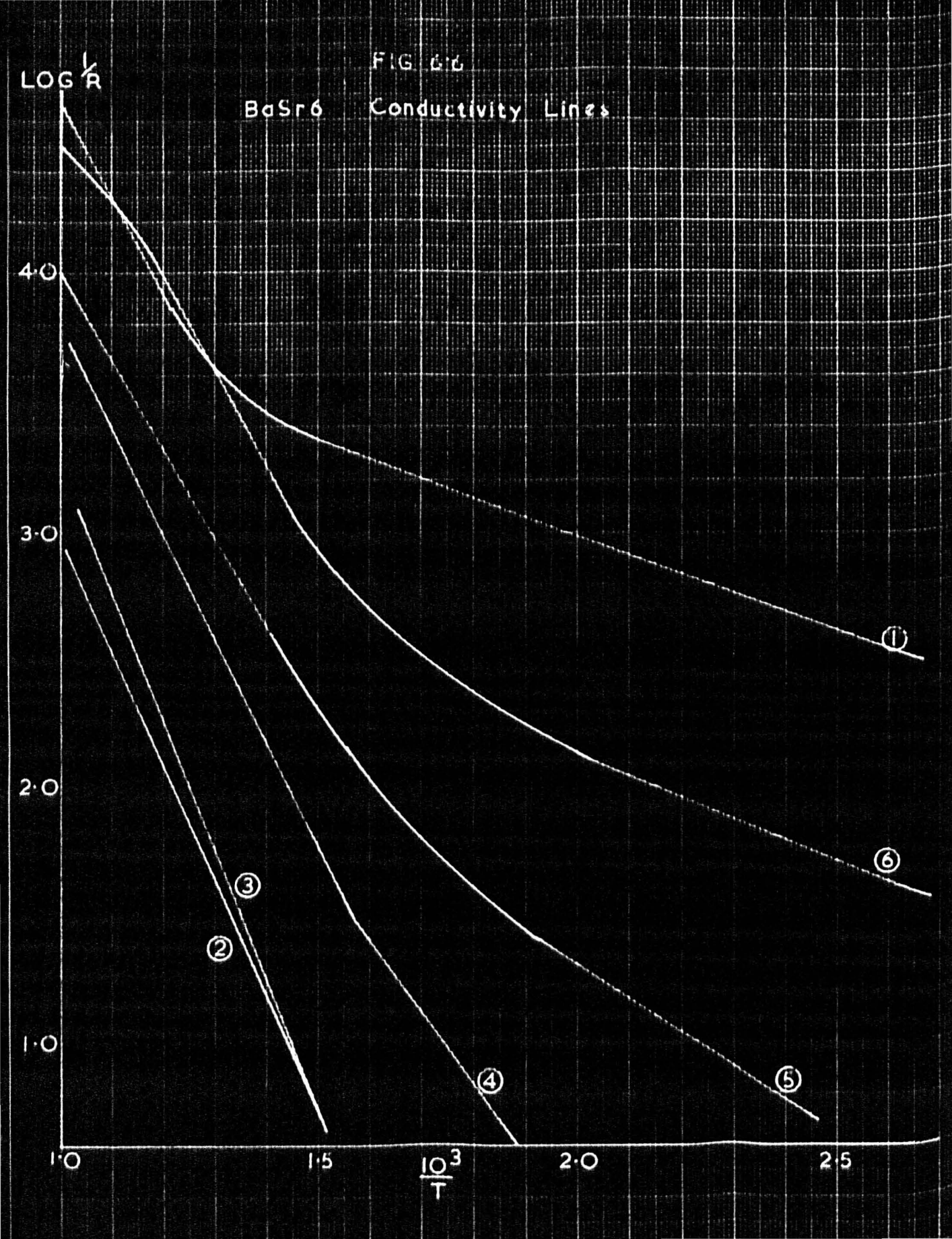
FIG. 6.6
BaSr6 Conductivity Lines
LOG 1/R
4·0
3·0
2·0
1·0
1·0
1·5
2·0
2·5
10³/T
①
②
③
④
⑤
⑥

FIG 6-7

BaSr6 Emission Activation

Application of Ea50v cathode temp 900°C

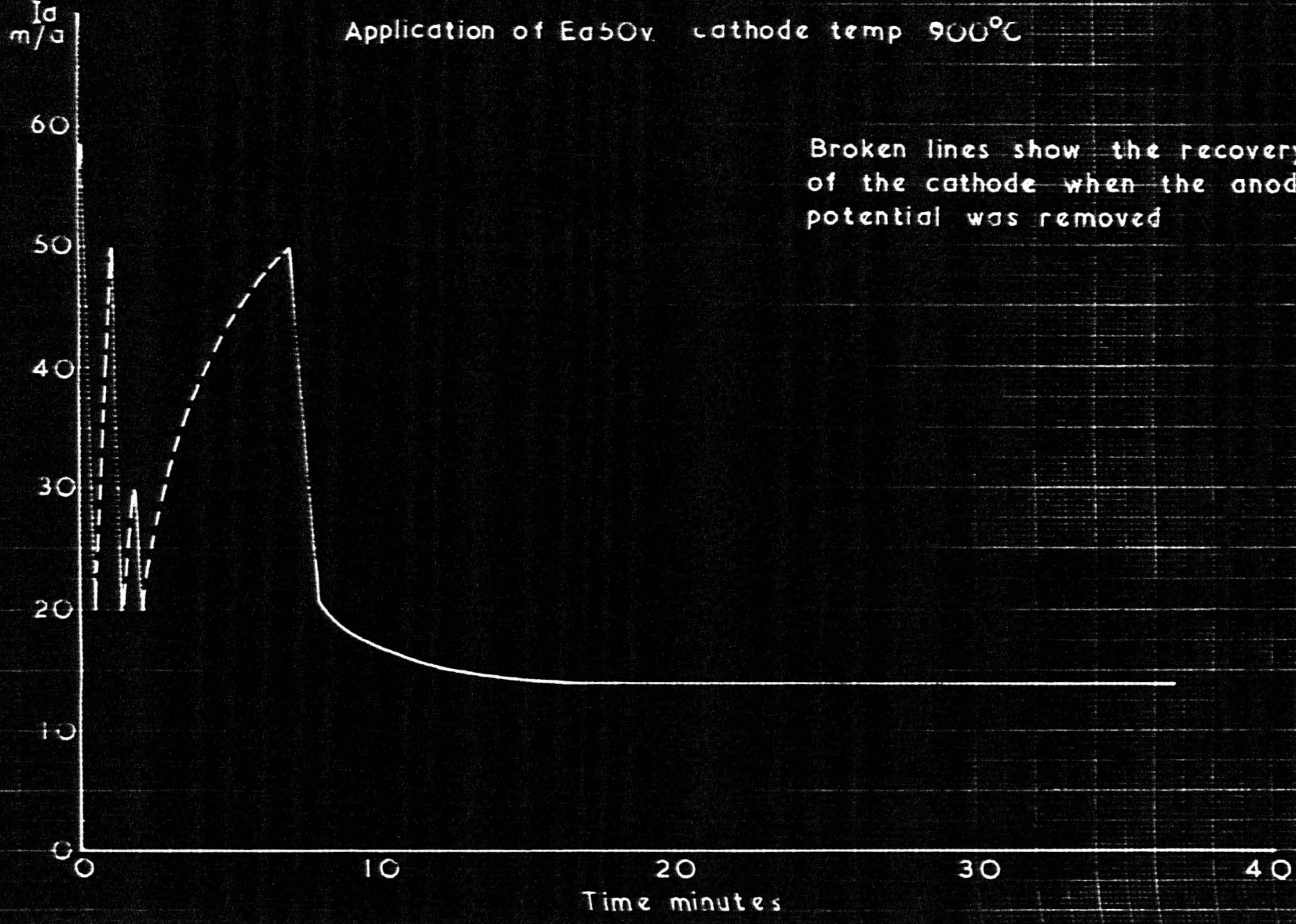

Table 8

Curve	Q	ϕ	Richardson ϕ
1	0.15	0.92	1.24 eV

Application of an anode potential of 50 volts with the cathode at 900°C resulted in a decay of anode current from 60 to 20 m/a. Fig. 6.7 shows the effect of applying and removing the 50 volts anode potential at successive intervals in time, the cathode temperature being maintained at 900°C. The graph shows that recovery from the poisoning effect occurs during the 'off' periods presumably due to thermal reactivation. Reapplication of the anode potential produces further decay and the curve gradually flattens out to a low level of anode current. This (level) presumably represents an equilibrium state between the rate of recovery of the cathode from poisoning and the rate of release of further poisoning material from the anode. Experiments on BaSr4 and 5 have shown that the cathode will recover from this state if it is allowed to operate under emission activation conditions. This means that the recovery of the cathode depends on the removal of the contaminating material from the anode. Conductivity measurements made in this poisoned state gave curve 2 fig. 6.6. The activation energy from the slope gave $\phi = 0.90$ eV.

In order to facilitate more rapid recovery 100v. was applied to the anode. The initial anode current was 24 m/a which after 80 minutes had increased to 30 minutes. Conductivity measurements were made at this point, (curve 3) giving a value of ϕ of 1.0 eV. It is difficult to account for this larger value of ϕ.

Recovery at Ea 100 volts was continued for a period of one hour during which the anode current increased to 70 m/a. Conductivity measurements at this stage gave curve 4, fig. 6.6. This curve was found to have a steeply sloped low temperature section. The activation energies are given in Table 9 below.

A further 30 minutes under emission activation conditions resulted in a value of 115 m/a for the anode current. Conductivity measurements gave curve 5 fig. 6.6.

The emission activation process was continued. On applying 100 volts after raising the temperature to 900°C the initial current 120 m/a decayed slightly to 115 m/a then increased to 150 m/a in one minute. As the anode became red hot slight decay of current was observed and so the anode potential was removed to allow the cathode to recover thermally. After 1 minute reapplication of 100 volts to the anode gave an anode current at 150 m/a. Before decay could occur due to the anode temperature increasing the anode potential was removed, the cathode cooled to 1000°K and conductivity and emission measurements made. Curve 6, fig. 6.6 was obtained.

Table 9

Curve	Q	ϕ	Richardson ϕ	$\chi = (\phi - Q)$
1	0.15	0.92	1.24	0.77 eV
2	-	0.90	-	- eV
3	-	1.0	-	- eV
4	0.53	0.89	1.15	0.36 eV
5	0.26	0.73	-	0.47 eV
6	0.17	0.82	1.0	0.65 eV

Table 9 shows the activation energies obtained from curves 1-6 of fig. 6.6. The value of χ obtained from Q-ϕ appears to increase as the cathode becomes more active. This does not accord with the previous interpretation, on the basis of semiconductor theory, that χ is decreased as surface contaminants are removed by the activation process. It is difficult to see how χ could increase in this way. In addition curve 6 on fig. 6.6 does not show the bend displaced to the left as in curve 1 where χ has a fairly high value. This would suggest that an interpretation of the changes in ϕ and Q on a semiconductor basis must be subject to a closer scrutiny. This is discussed more fully in the Conclusions to this chapter.

Cathode BaSr7.

It was decided to eliminate the possibility of poisoning the cathode through anode contaminants arising from handling the anode during assembly. Accordingly the anode of this tube and all the metal parts were washed in hot distilled water before sealing onto the tube envelope. This should remove any deposits of sodium chloride, chlorine being a notable poisoning agent (34). The carbonate-oxide conversion was performed slowly in the usual way but operation at 900°C was avoided. The anode and getters were outgassed before and after breakdown by eddy-current heating. Conductivity measurements curve 1, fig. 6.8 revealed a very poorly active cathode. Thermal activation at 900°C for 3 hours and subsequent conductivity measurements gave curve 2 which exhibited a low slope section at temperatures below 700°K.

FIG. 6·8

Bo5r 7 Conductivity Lines

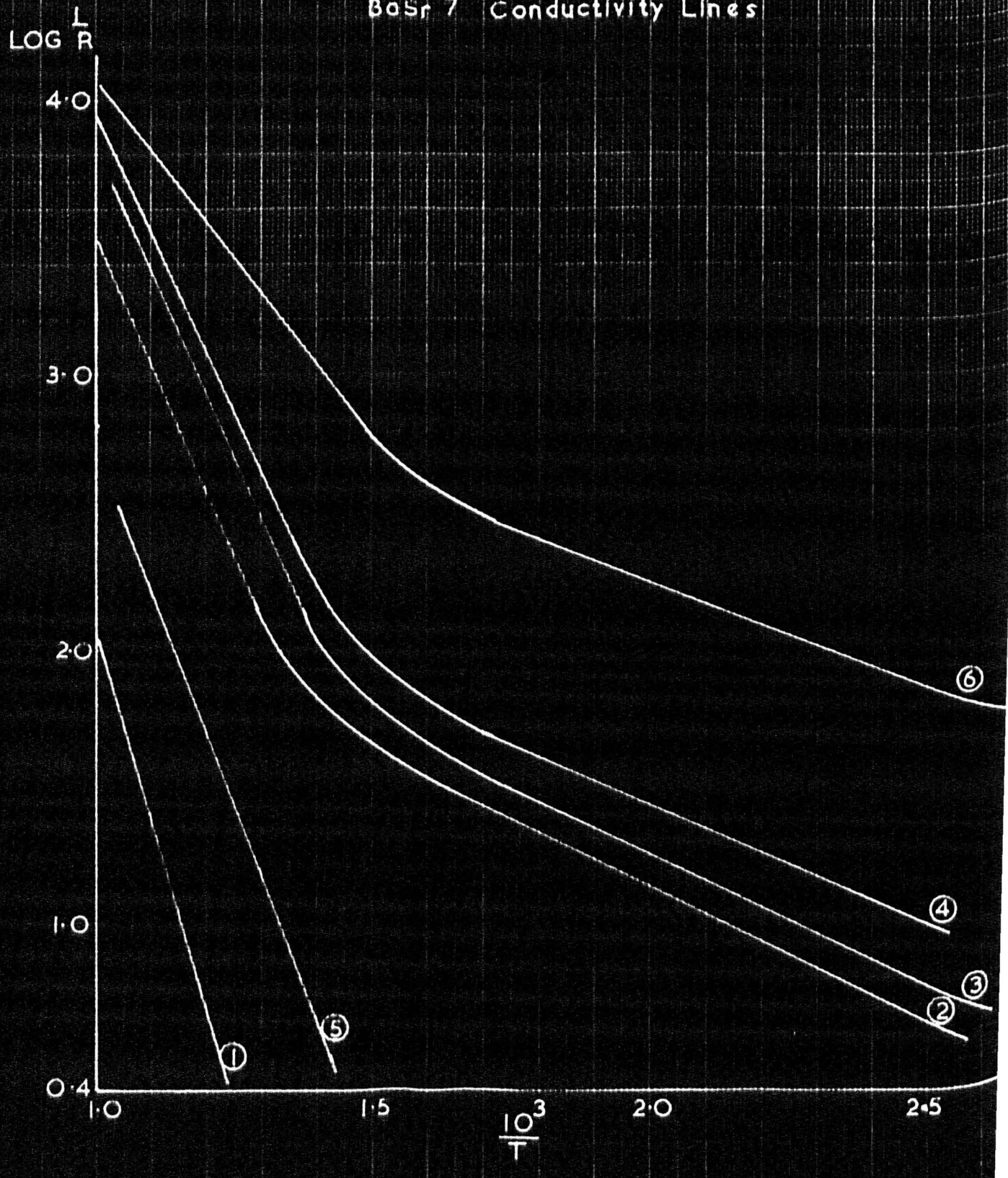

A power failure occurred at this stage which necessitated leaving the tube at backing pump pressure for 3 hours. After switch on the pressure fell to 2×10^{-6} mm.Hg. but on raising the cathode temperature to 900°C the pressure increased to 8×10^{-5} mm. Hg. This indicated that quite a large quantity of gas had been taken up by the cathode. Over a one hour period the pressure decreased to $< 10^{-6}$ mm.Hg. The cathode was thermally activated for a period of 6 hours after which conductivity measurements were made. Curve 3, fig. 6.8 was obtained. No appreciable differences in slopes between curves 2 and 3 were noted but nothing may be deduced from this since the poisoning-recovery cycle intervened and a controlled experiment was impossible. Thermal activation was continued for 12 hours at 900°C and curve 4 finally obtained. Table 10 gives the activation energies obtained from the slopes of curves 1-4.

Table 10

Curve	Q	ϕ	$\chi = (\phi - Q)$
1	-	1.37	-
2	0.20	1.03	0.83 eV
3	0.20	1.03	0.83 eV
4	0.17	0.93	0.76 eV

This time χ decreases as activation proceeds from state 3 to 4.

The cathode, now in an active state, could be used to investigate the poisoning effect previously described. Accordingly, anode potentials from 0 to 7.0 volts were applied in steps of 0.5 volts. After

each increase in potential, time was allowed for any decay in anode current to be observed (1 minute).

No decay occurred at potentials less than 7.0 volts but at 7.5 volts, decay from 6.7 to 6.2 m/a in 5 mins. was observed. Several poisoning effects at different anode potentials in the range 0-10 volts have been reported in the literature and Deb (23) has attributed these to decomposition of such materials as BaO, SrO, $BaCO_3$ etc. which are evaporated onto the anode probably during breakdown or activation.

Attempts to remove the poisoning species from the cathode by raising the cathode temperature were not effective. Application of 100 volts gave an initial current of 85 m/a which decayed rapidly to 5 m/a. After 12 hours the cathode recovered so that the anode current at Ea 100 v. was 40 m/a. Conductivity measurements gave curve 5 indicating extensive deactivation.

After a further 6 hours emission activation the anode current was 110 m/a and the anode became red hot. To prevent the onset of the green discharge previously noted under these conditions emission activation was continued at Ea 50v. The emission increased from 40 to 80 m/a over a four hour period. Conductivity measurements gave curve 6 fig. 6.8. This emission activation appeared to have produced a very active cathode. Table 11 compares this state of the cathode with that shown by curve 4.

Table 11

Curve	Q	ϕ	χ	
4	0.17	0.93	0.76	eV
6	0.15	0.59	0.44	eV

The change in χ is quite large here and in view of the high state of activation of the cathode shown by curve 6 on interpretation of this change as the removal of contaminants from the crystal grains is quite reasonable.

Cathode BaSr8.

The anode of this tube was washed in distilled water and carbon tetrachloride before hydrogen furnacing in the usual way. Subsequently it was not handled. During the construction of this tube information became available in a paper by Stoll (70) which suggested that contamination of the anode during the carbonate-oxide conversion could be avoided by maintaining the anode at a temperature 100°C higher than the cathode by eddy-current heating. This practice is simple to apply in commercial cathodes but more difficult in the case of probe tubes in view of the long breakdown schedule necessary to prevent to coating cracking. However, eddy current heating for 2 minute periods several times during the breakdown operation was possible and this was done. Very little outgassing of the anode occurred when heated to redness at the end of the breakdown schedule.

To ascertain if the anode was clean the cathode had to be activated thermally at 900°C for 2 hours so that some anode current could be drawn. The anode potential was then increased in 0.1 volt steps to

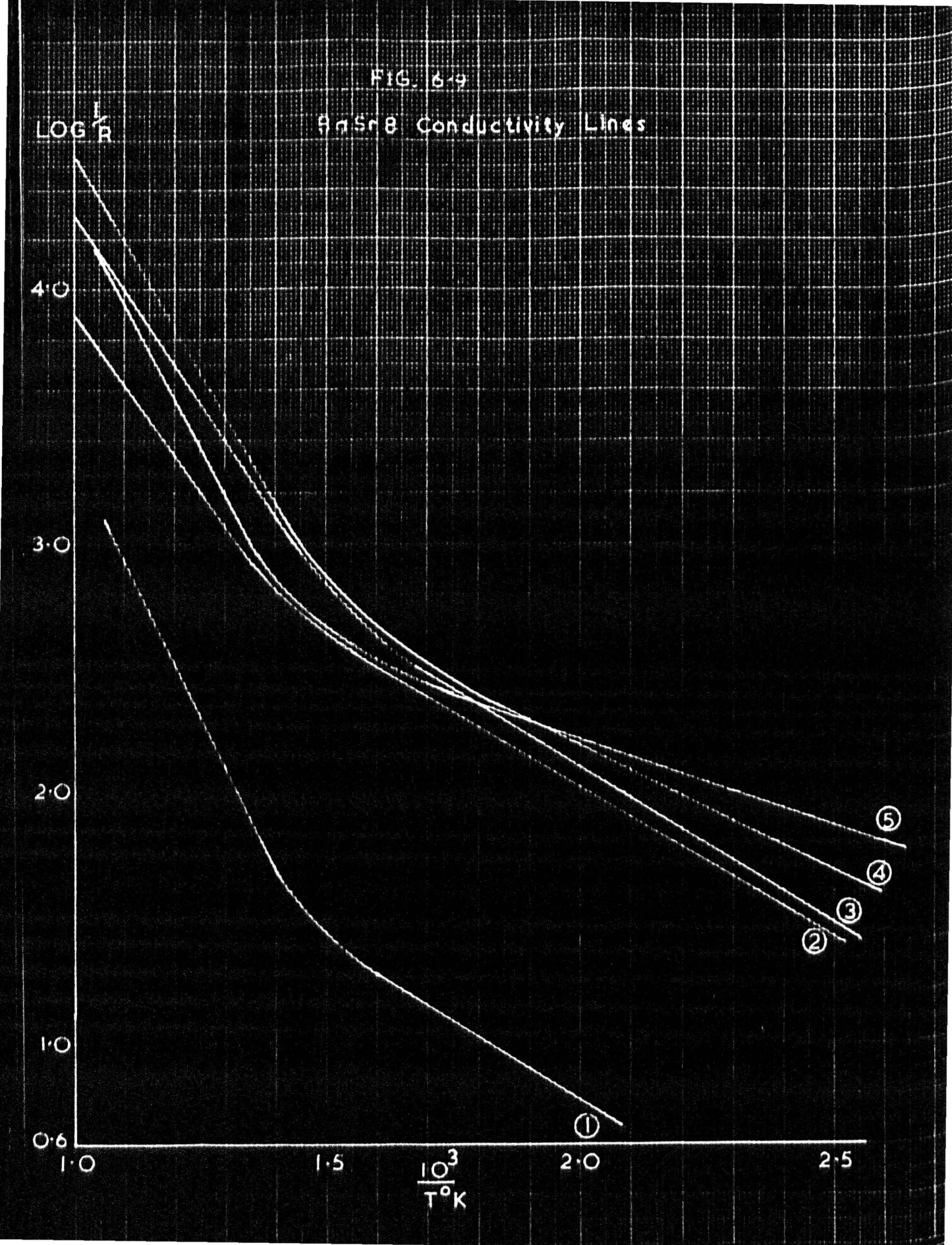
FIG. 6-9
BaSrB Conductivity Lines
LOG 1/R
4·0
3·0
2·0
1·0
0·6
1·0
1·5
2·0
2·5
10³/T°K
①
②
③
④
⑤

ascertain at what voltage decay in emission occurred. No decay was observed up to 25 volts suggesting that the anode was in a clean condition, as a result of the washing and subsequent heating during breakdown.

Thermal activation at 800°C was continued for 12 hours and a re-examination for poisoning effects was made. A slight poisoning effect was noted at E_a 28 volts.

Conductivity measurements in this state were made, (curve 1, fig. 6.9). This curve shows that the cathode is fairly active. After these measurements the cathode temperature was raised to 900°C and 50 volts applied to the anode. A decay in anode current from 32 m/a to 28 m/a occurred and then the current began to increase.

This type of behaviour had not been noted previously. Usually a thermally activated cathode was poisoned extensively when an anode potential was applied e.g. BaSr5 fig. (6.7). The effect was attributed initially to the well cleaned anode but subsequent experiments showed that this was not a fully active cathode.

The anode potential was increased to 100 volts in order to ascertain whether the poisoning-recovery effect could be reproduced - the higher potential decomposing more material on the anode. No decay was observed however and the current increased rapidly from 54 to 64 m/a. At this point a rapid decay of current occurred. In 30 seconds the emission decreased to 40 m/a and then began to recover. Re-application of 50 volts revealed that the anode current was 28 m/a i.e. the original poisoned state had been reproduced.

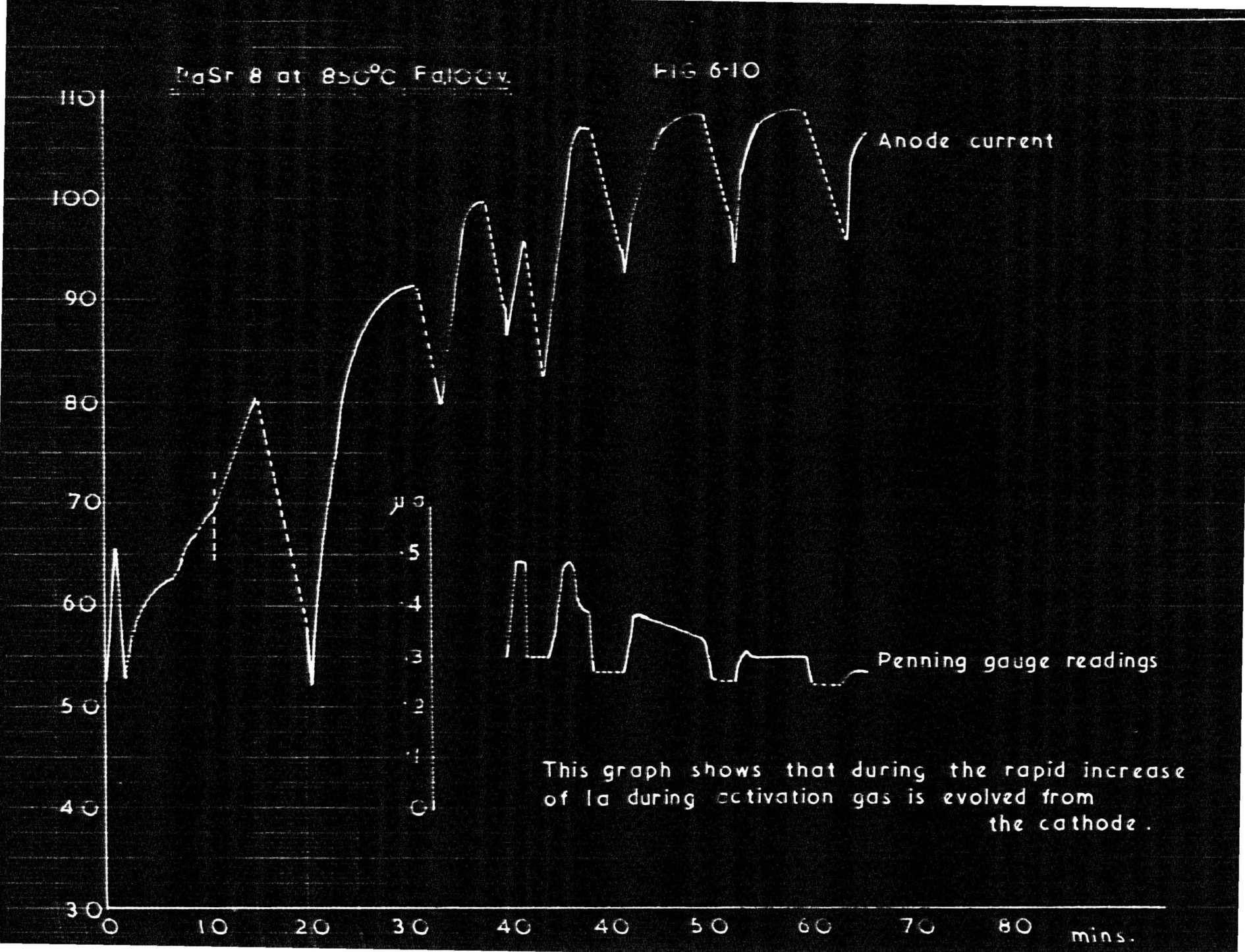
BaSr 8 at 850°C Fa100v.
FIG 6-10
110
100
90
80
70
60
50
40
30
0
10
20
30
40
40
50
60
70
80
mins.
μa
·5
·4
·3
·2
·1
0
Anode current
Penning gauge readings
This graph shows that during the rapid increase of Ia during activation gas is evolved from the cathode.

The cathode was allowed to operate with anode potential of 50 volts for 9 minutes during which the emission increased to 35 m/a. The application of E_a 100 volts at this point produced a precisely similar effect as that observed previously: the anode current increase to 66 m/a then decayed to 53 m/a after which it proceeded to increase. Fig. 6.10 shows the sequence of events thereafter. At times, during the recovery, the anode potential was removed with the unusual effect noted. The cathode appeared to be poisoned during the 'off' periods. After several operations it was noted that the Philips gauge indicated a change in pressure and so simultaneous recordings of gauge reading and anode current were made.

It is apparent from the curves fig. 6.10 that application of anode potential results firstly in poisoning then secondly in recovery. Moreover, this application is accompanied by an increase in pressure. It is also clear that during the 'off' periods the cathode is poisoned in some way in complete contrast with the results shown in fig. 6.7 where the cathode is seen to recover from poisoning when the anode potential was not applied.

However, the important difference between this cathode BaSr8 and cathode BaSr5 is that the latter was fully activated whereas BaSr8 was only partially activated as subsequent experiments showed. The strange effects shown in fig. 6.10 may then be explained in the following way.

Application of 100 volts E_a produces rapid activation, drawing oxygen from the cathode and giving increased emission. The oxygen produced in this way is not pumped away sufficiently quickly.

During the time when no anode potential is applied this oxygen is readsorbed by the cathode and some is adsorbed by the anode. On applying anode potential that which is present on the anode is desorbed and poisons the cathode; hence the slight initial decrease before reactivation occurs. Pumping action continues during these operations so that the general level of pressure gradually dinishes as the Philips gauge readings indicate. This leads to less rapid poisoning as time goes on so that the general effect is one of activation, the level of emission being gradually raised. The rapid recovery from poisoning by oxygen which these experiments suggest is confirmed by experiments described in Section III.

The last section of fig. 6.10 indicates that activation is not complete so that some poisoning of the cathode probably occurred when the anode potential was removed. Conductivity measurements were made which gave curve 2, fig. 6.9.

After these measurements the tube was sealed off from the vacuum system after preheating and firing two barium getters. Potentials up to 50v. were applied to the anode to see if any deposit on the anode due to firing the getter could be detected. No decay effects were observed.

A number of sulphur and oxygen poisoning experiments were performed on this cathode and in the course of performing these curves 3 and 4 (fig. 6.9) were obtained. The general level of conductivity indicated by these curves is higher than curve (2) but they do not represent true stages in the activation of the cathode since the

surfaces of the crystallites may be modified by residual sulphur or oxygen.

Curve (5) (fig. 6.9) was obtained after 170 hours operation under emission activation conditions (Chapter 7). The increase in slope of the high temperature section is mott noticeable. Table 12 gives the activation energies obtained from the slopes of the curves

Table 12

Curve	Q	ø	χ
2	0.23	0.72	0.49
3	0.25	0.72	0.47
4	0.20	0.76	0.56
5	0.14	0.88	0.74

Again an increase in χ on the basis of semiconductor theory is indicated by these results for curves 4 and 5. This implies an increase in surface contamination during the 170 hours operation which is difficult to account for.

Cathode BaSr9.

The anode of this tube had been washed in the same way as that of BaSr8 but during the carbonate-oxide conversion process the anode of this tube was not eddy current heated. When breakdown of the carbonates was complete, eddy current heating the anode liberated a large volume of gas.

The cathode was thermally activated at 800°C for 12 hours, after which anode potentials up to 30 volts were applied. No decay in emission was noted.

FIG. 6·11

BaSr9 Conduction Lines

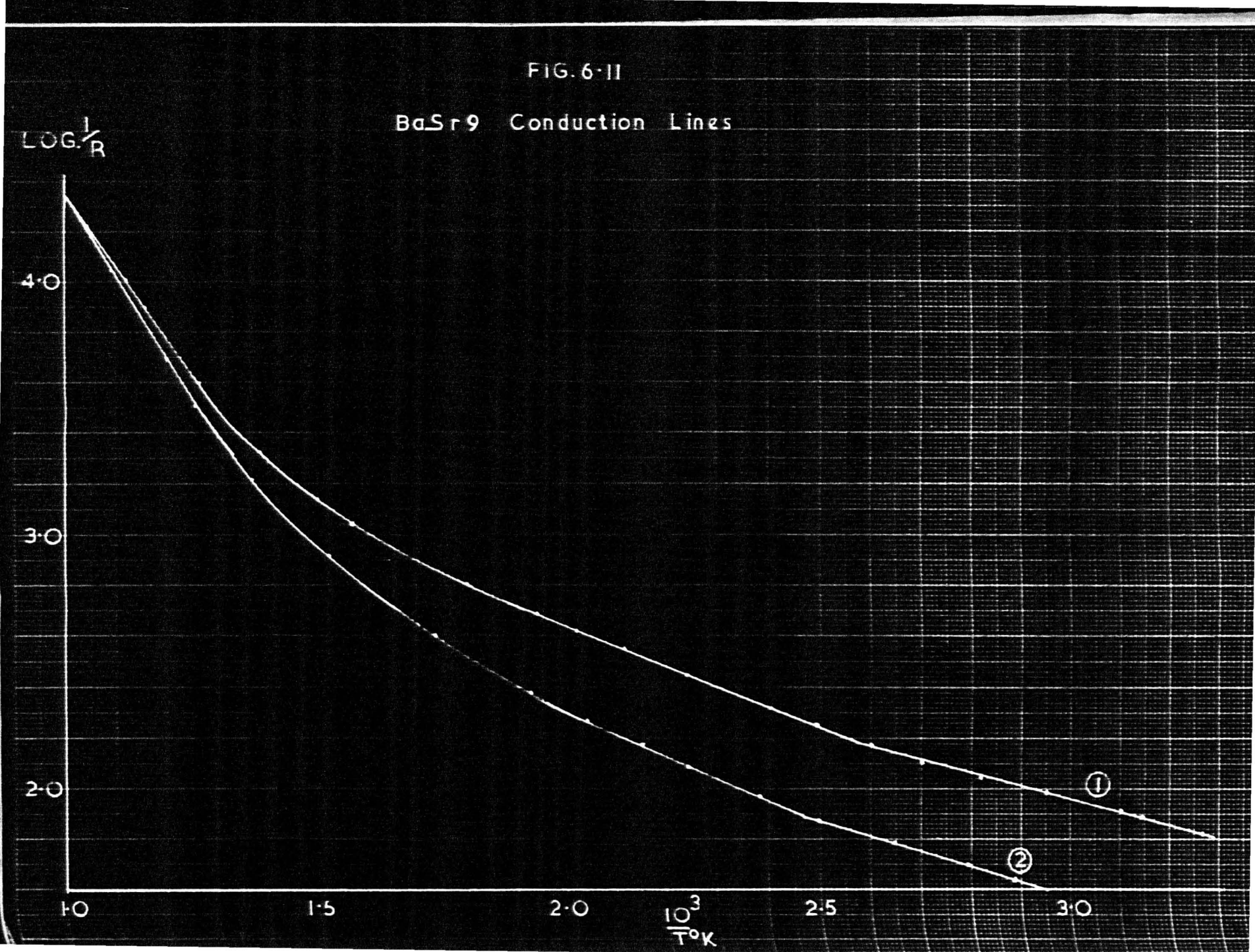

Activation at Ea 24 volts was then attempted. The initial current of 19 m/a gradually increased to 26 m/a.

On applying 100v. to the anode a rapid decay of emission from 140 to 30 m/a occurred. This type of decay had been observed previously when an emission was drawn from a cathode after thermal activation. Continued operation at 900°C, Ea 100 volts for 12 hours overcame this poisoning and after firing the getters the tube was sealed off. Activation was continued and after an hour at Ea 50 volts, the anode current was 80 m/a.

This cathode was required for poisoning experiments in which it was desired to measure the conductivity in the low temperature region in the poisoned state. Consequently, very careful measurements were made at small temperature intervals down to laboratory temperature. The curve obtained is shown in fig. 6.11 curve (1).

It was found impossible to draw a continuous straight line through the plotted points at temperatures below 600°K and so the final conductivity curve was represented by two straight line sections in this temperature range within the limits of experimental accuracy. The two straight lines intersected at a value of $1/T$ corresponding to about 400°K.

This effect was one which had never been encountered before, either during previous measurements or in the literature and so re-measurement of the conductivity vs temperature was made.

The temperature of the cathode was raised to 900°C and 50 volts applied to the anode. The original value of the emission, 80 m/a, was obtained again. The temperature was then reduced and the con-

ductivity measured both with temperature decreasing and increasing, allowing 15 minutes at each setting for the temperature to achieve uniformity throughout the coating. A conductivity curve identical with curve (1) was obtained.

A further investigation of this extra-low temperature conductivity is described in the next section.

Subsequently this cathode was operated at 900°C, E_a 50v. for 170 hours. Conductivity measurements gave curve 2 (fig. 6.11). The activation energies obtained from the two curves are given in the table.

Table 13

Curve	Q	ø	χ
1	0.15	0.65	0.50 eV
2	0.17	0.71	0.54 eV

Curve 2 corresponds to a lower state of activation of the cathode and therefore the increase in χ shown by this table is not inconsistent with a semiconductor interpretation.

Discussion of Results.

In this Chapter an attempt has been made to investigate some of the changes which occur in an oxide-coated cathode during the process of activation. This investigation has been complicated by poisoning effects but the source of this poisoning was eventually located.

The general form of the conductivity curves is similar to that obtained by Loosjes and Vink. The high temperature section of each curve has a high slope similar to, but not identical with, the slope

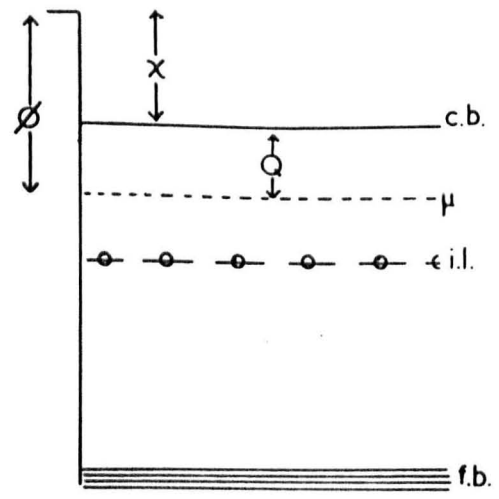

FIG. 6·12

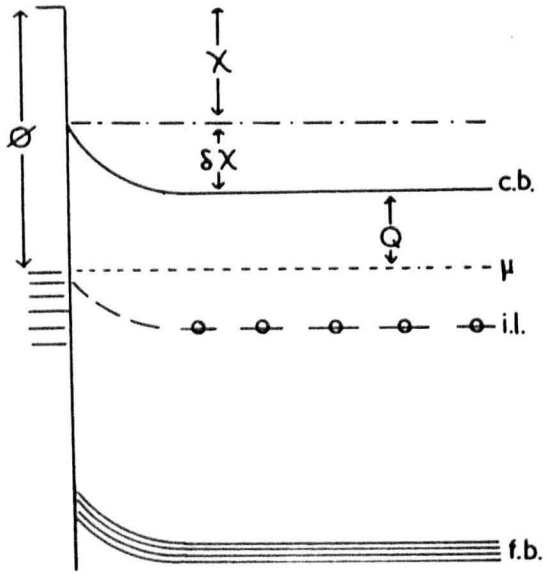

FIG. 6.13

of a Richardson plot for the cathode. Following Loosjes and Vink the upper section of this curve is interpreted as evidence for an electron emission process in the pores of the coating. The slope of the curve is probably closely related to the thermionic work function ϕ of the internal crystal surfaces.

The lower section of the conductivity curve is assumed to represent the bulk conductivity of the crystallites. Assuming that this is purely semiconduction then the slope of this lower section (Q) should give the separation of the Fermi level from the conduction band. Fig. 6.12 shows the energy diagram with ϕ and Q marked. The difference ϕ-Q is then the depth of the conduction band χ .

One of the facts emerging from the experimental investigation is that χ appears to change during the activation of the cathode. This is in addition to a gradual diminution in Q during activation. Such a change is difficult to explain on the basis of energy levels as depicted in fig. 6.12. However fig. 6.13 illustrates the way in which the effective value of χ viz $(\chi+\delta\chi)$ may be modified due to the presence on the surface of the crystals of electron accepting elements. Oxygen is an example of this category for it will accept electrons and form a dipole layer on the surfaces of the crystallites. This increases the work function ϕ since the Fermi level adjusts itself so that the free energy of electrons in the crystal and the surface states is the same. The increase in χ i.e. $\delta\chi$ may be found if ϕ and Q can be measured. In practice only changes in χ may be determined by noting the changes in ϕ and Q. As oxygen is adsorbed

the value of $\delta\chi$ should increase and during desorption of oxygen, e.g. during activation, a decrease in $\delta\chi$ would be expected.

These sorts of changes are not obtained consistently in the experiments described. For example the change from state (3) to (4) in BaSr4 is not accompanied by a change in χ and in states 4, 5 and 6 in BaSr6 a pronounced increase in χ occurs in that order although the curves show that activation has occurred. It must be emphasised, however, that true changes in $(\chi+\delta\chi)$ are obtained in this way only if semiconductor theory is applicable. Several considerations suggest that this is not the case. Firstly, there is some doubt whether the function ϕ is the work function of the crystallite surfaces. In any case it can only represent an average value for all the crystallites. Secondly, the condition that semiconductor theory is applicable to the conduction process i.e. that $\Delta E > 0.5eV$ is not suggested by the values of Q obtained from the curves. However, the results on cathode BaSr9 indicate that the values of Q do not represent the true slope of this conduction process but that the slope of the curve in this temperature regions requires correction in much the same way as the higher slope section is corrected to obtain a value of ϕ.

The position, then, is rather unsatisfactory with regard to placing a semiconductor interpretation on the results reported in this chapter.

Several other conclusions do emerge however in connection with the poisoning phenomena encountered in these experiments. It is clear

that a cathode may be activated by either operation at temperatures above 800°C for several hours or by drawing an emission with 50 or 100 volts anode potential, again for several hours. During the thermal activation procedure, much oxygen is liberated from the cathode and some of this is adsorbed on the relatively cold anode. This oxygen is produced in the reduction of the oxide at the core-coating interface by reducing impurities, e.g. silicon and magnesium, in the '0' nickel core metal. This leads to the production of a stoichiometric excess of barium and strontium in the lattice, giving the requisite conditions for N-type semiconduction. The application of a high anode potential (> 30v) after thermal activation results in the removal of this oxygen on the anode by the energy of the incident electrons and some of it returns to, and poisons, the cathode. It is impossible to avoid high temperatures when completing the carbonate-oxide conversion process and so even at this stage some thermal activation has occurred and a poisoning effect is observed on applying an anode potential.

Conductivity curves in such poisoned states exhibit very little difference from those during stages of a thermal activation procedure; e.g. figs. 6.1 and 6.8. In the light of the reversible nature of the poisoning phenomena indicated by fig. 6.7 and in a slightly different way by fig. 6.10, it may be concluded that no significant difference exists between a thermally activated cathode and an emission activated one. This is true provided the anode is free from other contaminants and this is difficult to achieve unless elaborate precautions are

taken. Such precautions must include careful cleaning of the anode to remove all traces of sodium chloride and the prevention of anode contamination during breakdown of the carbonates. If such precautions are not observed then non-reversible poisoning may occur. This is probably the explanation of the large difference between the initial thermally activated state curve 1, fig. 6.6 for BaSr6 and the final emission activated state curve 6. Non-reversible poisoning of this kind could arise from chlorine forming chloride ions in the oxide. These are removed over a lengthy period of time but their immediate effect is deleterious to cathode operation.

The enhanced conductivity at temperatures below 400°K experienced in cathode BaSr9 is subjected to a more rigorous investigation in the next Chapter. It suggests however, that the present theory of N-type semiconduction only, in the low temperature region will have to be revised.

CHAPTER 7

AN INVESTIGATION OF THE LOW TEMPERATURE CONDUCTIVITY EFFECT

Conductivity vs. temperature measurements on cathode BaSr9 in the temperature range 600° - 300°K revealed a break in the conductivity line at about 400°K with a lower slope section attemperatures below that value. It was not surprising that this effect had not been encountered previously, for measurements of the conductance of the cathodes, described in Chapter 6 had not been extended below 400°K.

The measurement of $\log.\sigma(\frac{1}{R})$ vs. $1/T$ in this temperature range was dependent upon fairly precise measurement of temperature and this was first suspected to be unreliable at such low temperatures. Extrapolation of the higher slope section revealed that an error of several degrees in temperature measurement would be necessary to account for the observed results in terms of a faulty temperature measuring technique. Reference to previous work by other members of this research group revealed that a careful investigation of the reliability of the tungsten-nickel thermocouple of precisely the same dimensions and materials as those used in the tubes described here had been made by Duckworth (59) and this was in agreement with that given in the literature by Fan (27) who claimed a precision of better than 1°C (but see last paragraph on page 31). It was concluded that the temperature measuring technique did not introduce a source of error of sufficient dimensions to account for the non-linearity of the $\log 1/R$ vs. $1/T$ curves below 600°K.

FIG. 7-1

Ba6 LOW TEMPERATURE CONDUCTIVITY

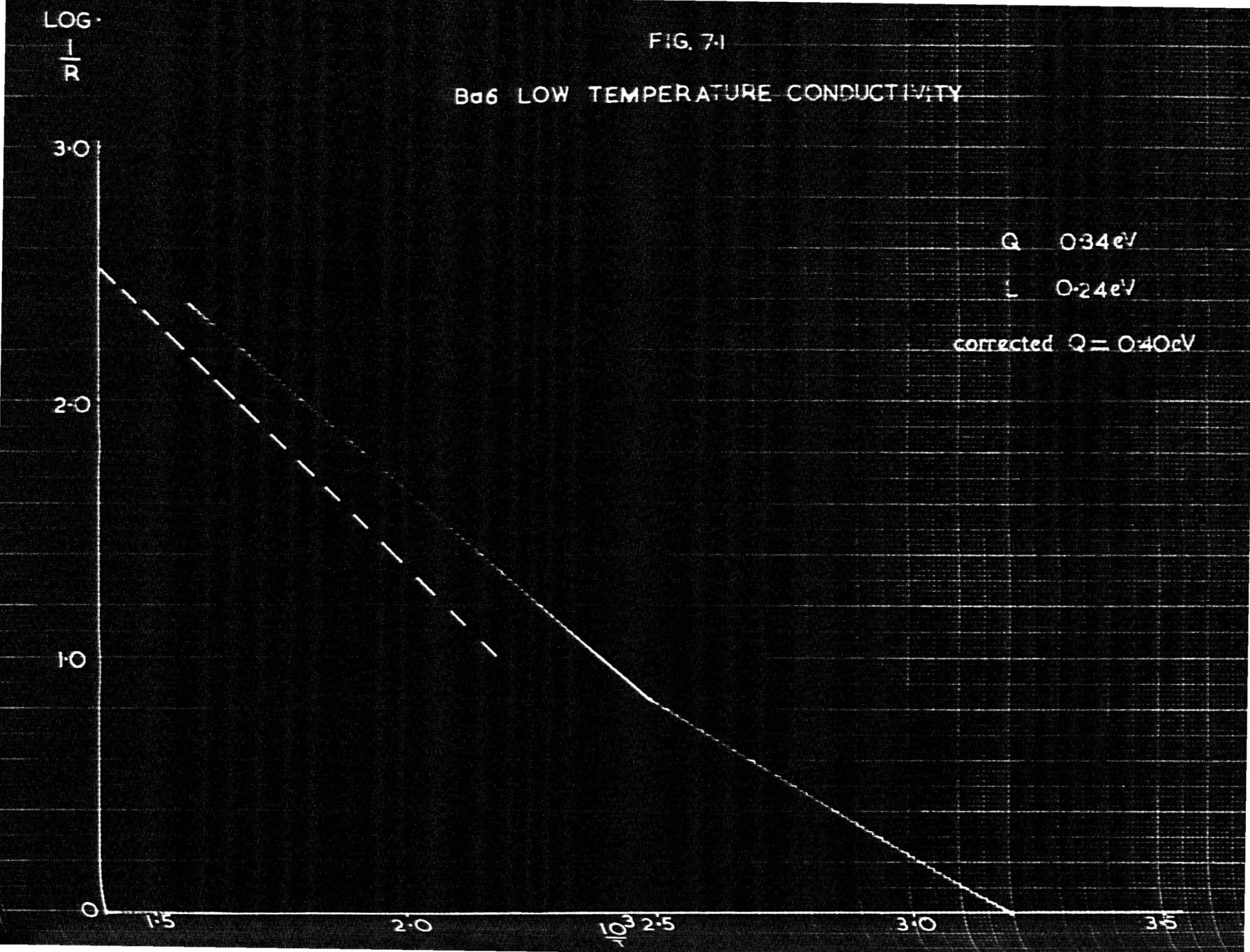

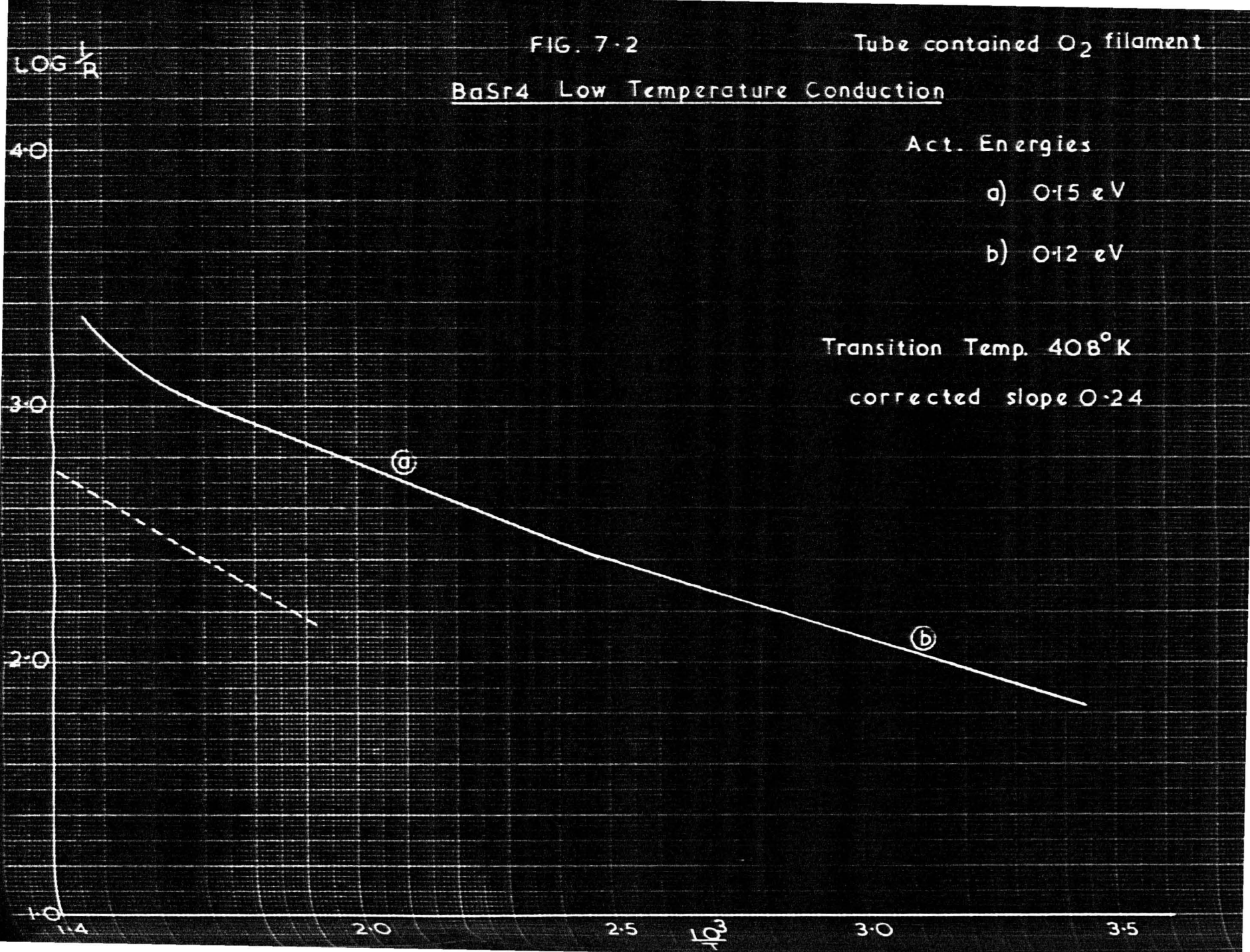
FIG. 7·2
Tube contained O_2 filament
BaSr4 Low Temperature Conduction
Act. Energies
a) 0·15 eV
b) 0·12 eV
Transition Temp. 408°K
corrected slope 0·24
LOG $\frac{1}{R}$
4·0
3·0
2·0
1·0
a
b
1·4
2·0
2·5
$\frac{10^3}{T}$
3·0
3·5

FIG. 7·3

BaSr5 CONDUCTION LINES

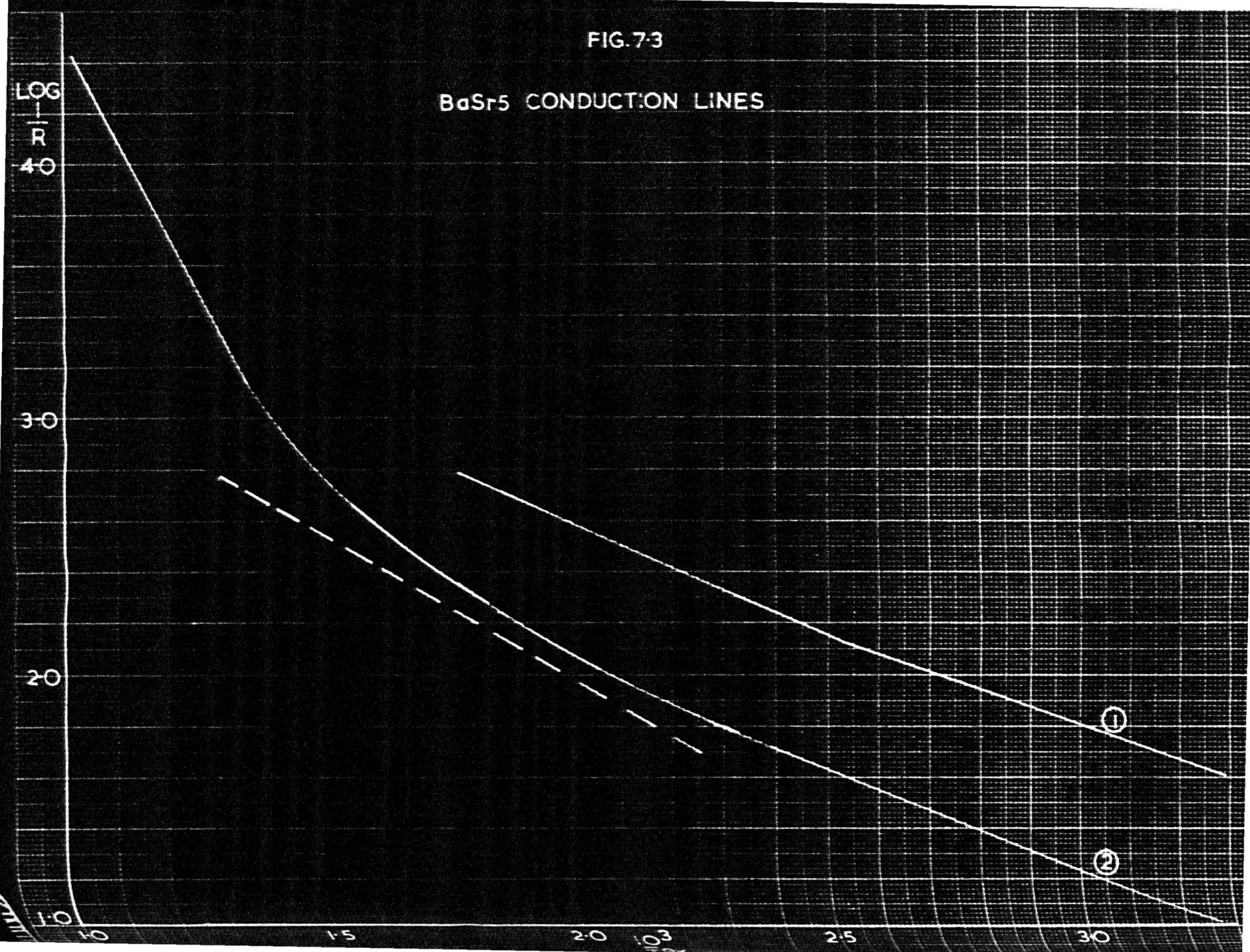

FIG. 7.4

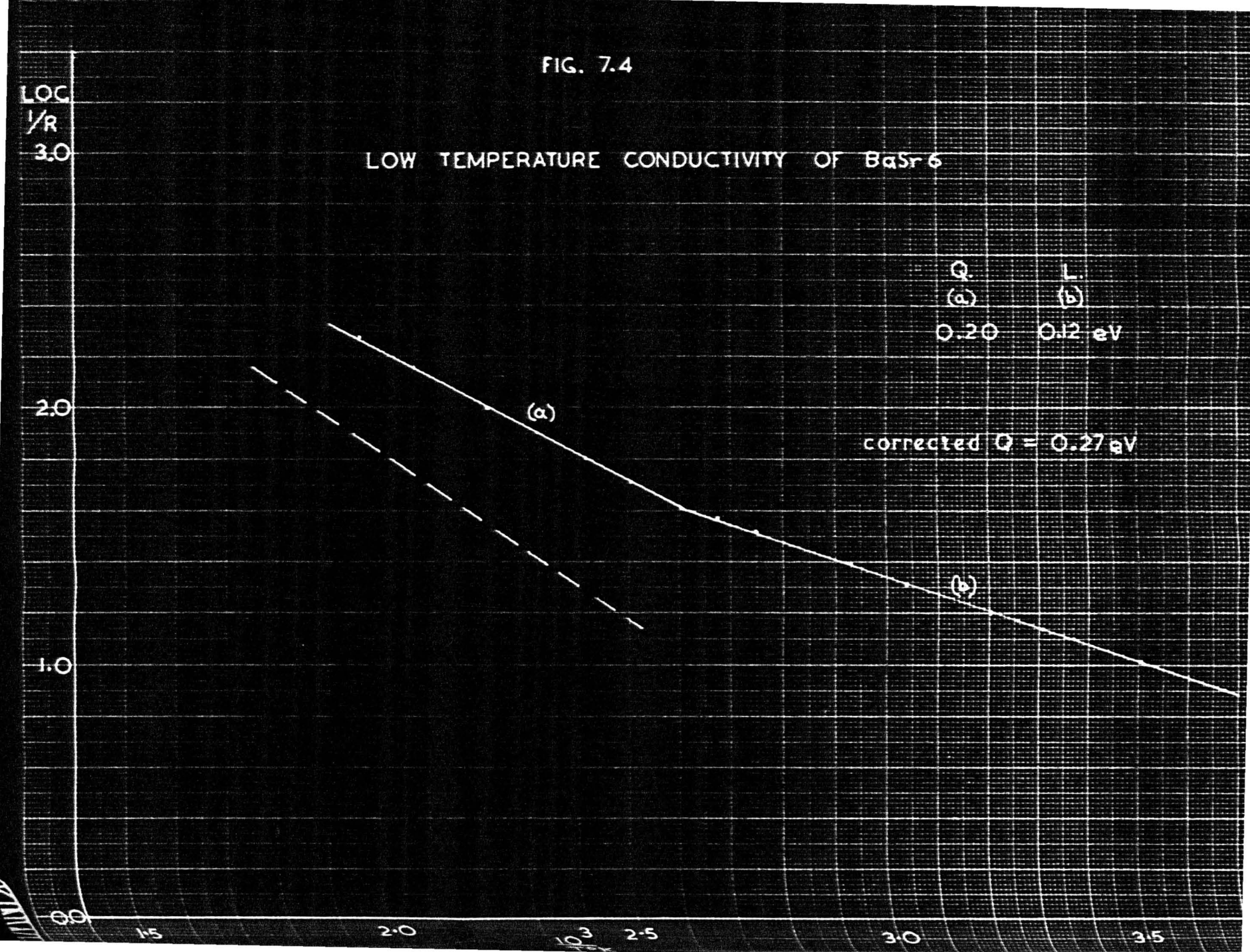
LOG 1/R
3.0
2.0
1.0
0.0
LOW TEMPERATURE CONDUCTIVITY OF BaSr6
Q. (a) 0.20
L. (b) 0.12 eV
(a)
(b)
corrected Q = 0.27 eV
1.5
2.0
10^3
2.5
3.0
3.5

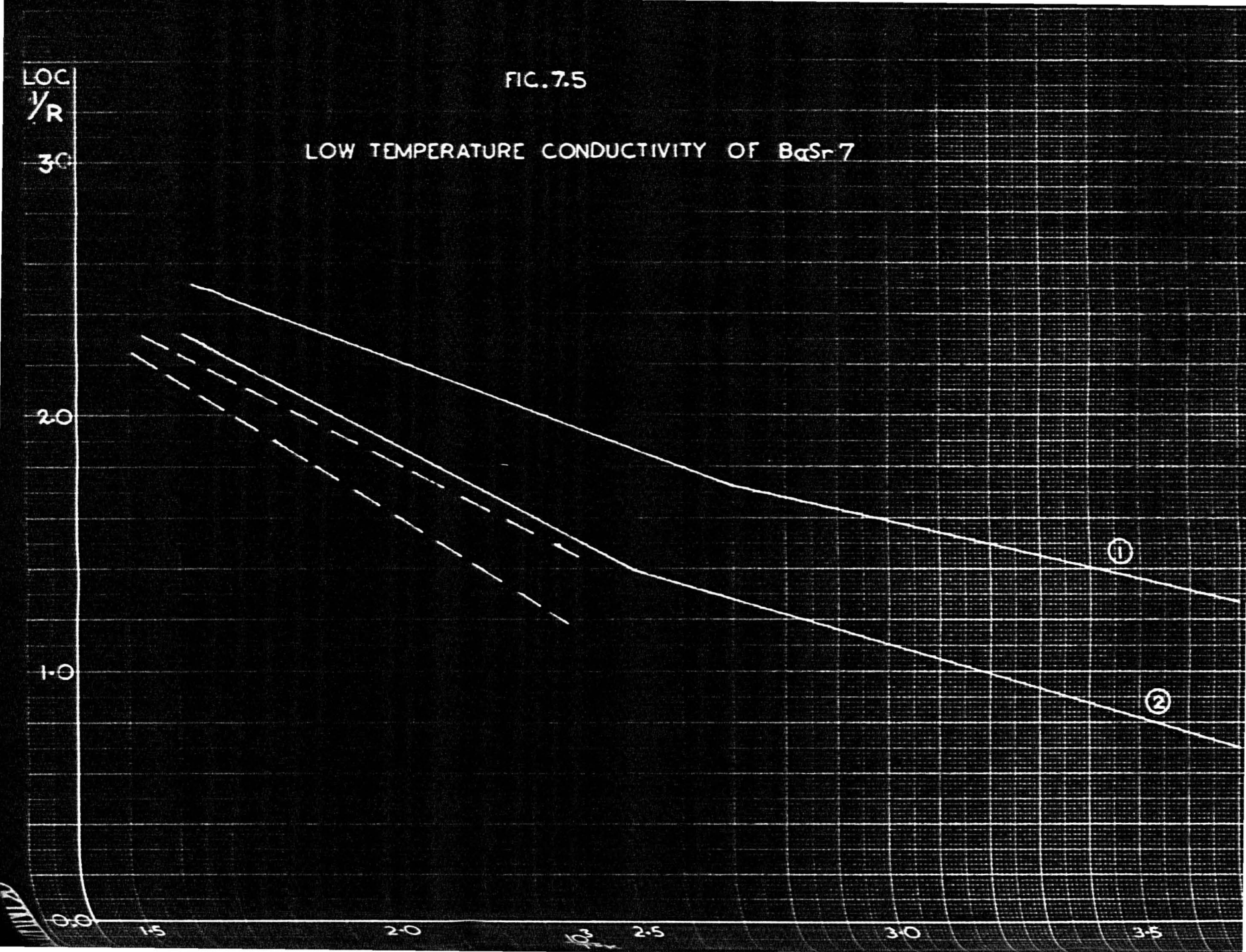
FIC. 7.5
LOW TEMPERATURE CONDUCTIVITY OF BaSr 7
LOG 1/R
3·0
2·0
1·0
0·0
1·5
2·0
2·5
3·0
3·5
10³
1
2

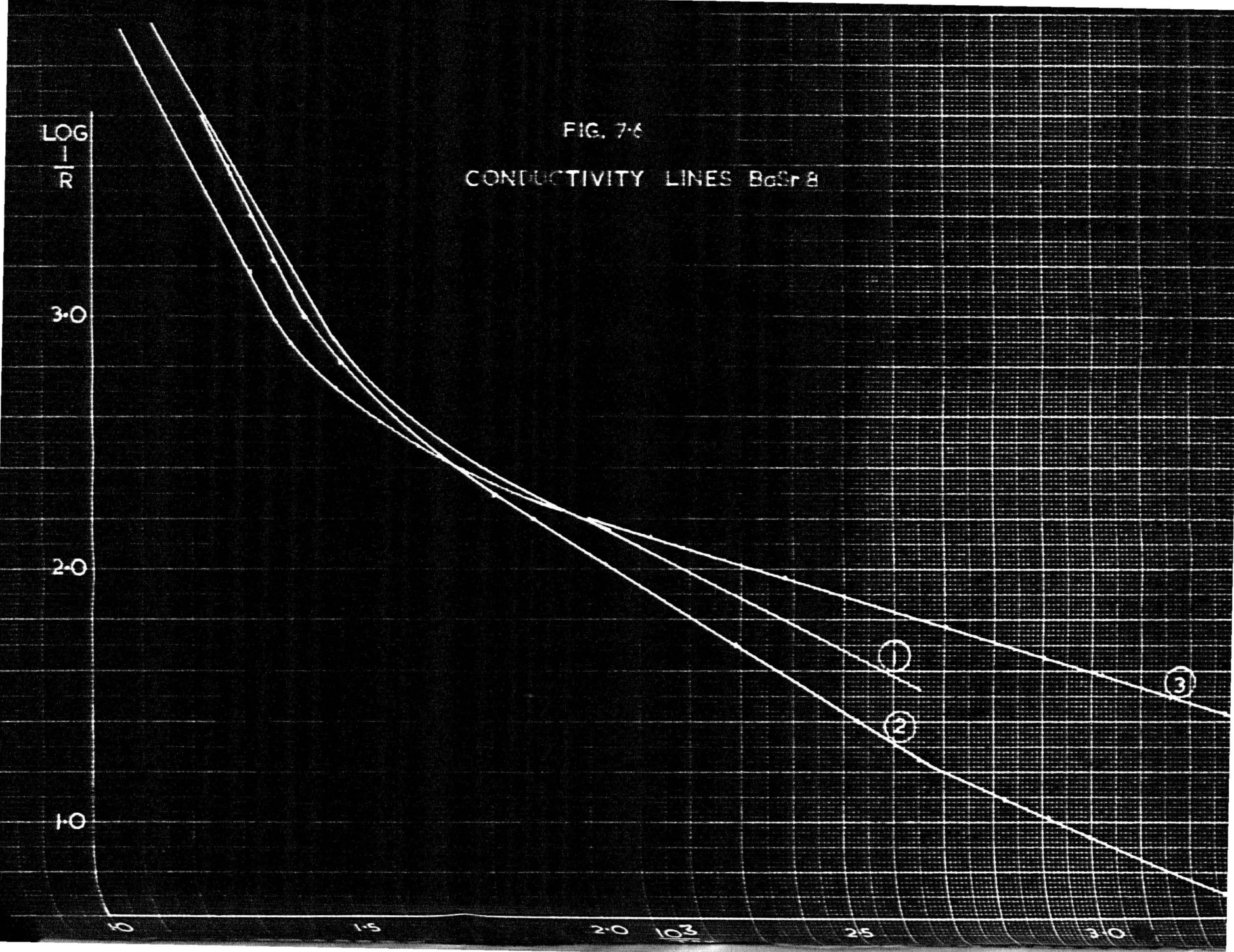
FIG. 7·6
CONDUCTIVITY LINES BaSr 8
LOG 1/R
3·0
2·0
1·0
1·5
2·0
10³/T
2·5
3·0
1
2
3

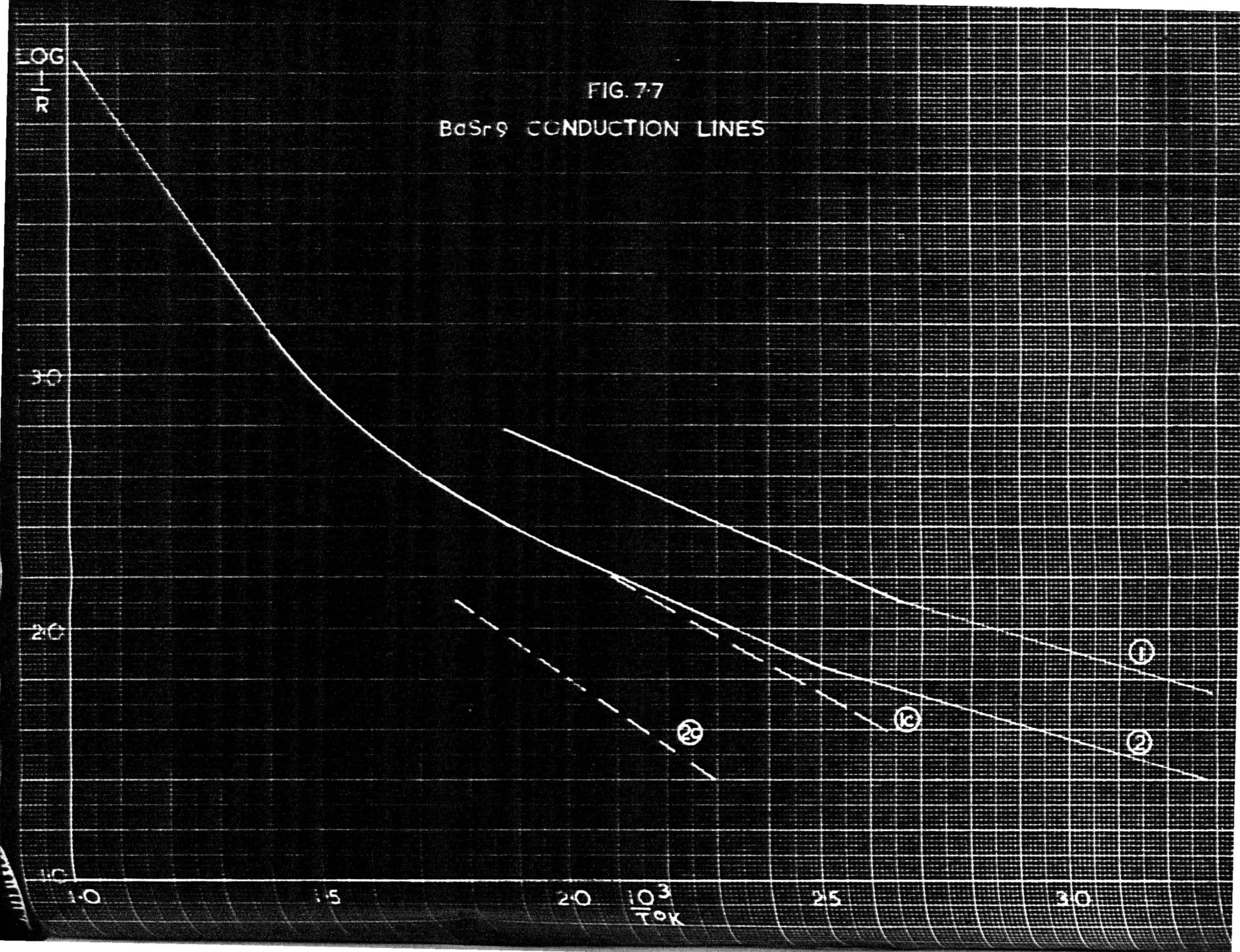
FIG. 7·7
BaSr9 CONDUCTION LINES
LOG 1/R
3·0
2·0
1·0
1·0
1·5
2·0
10³/T°K
2·5
3·0
1
1c
2
2c

Attention was then directed to the possibility of electrical leakage over the ceramic end pieces of the electrode assembly which might shunt the probe-base conductance at low temperatures. This effect could not be investigated immediately in BaSr9 and so measurements were made in the low temperature region on as many cathodes as possible. Figs. 7.1 to 7.7 show the results obtained. In each case careful measurement revealed a break in the conductivity curve. In the case of Ba6 (a discarded barium oxide cathode) the extra-low temperature section lay below the range of measurement of the galvanometer usually employed. A more sensitive instrument was used for measurements on this cathode. All the tubes had identical electrode construction yet the extra low temperature section was observed at different levels in conductivity but always below 400°K. This seemed to rule out the possibility of conduction over the ceramic end pieces.

It was also noted that these measurements were performed on tubes which contained oxygen and sulphur filaments and some which contained both of these, so that the effect did not appear to be associated with a particular type of poisoning filament.

This effect was observed in all the cathodes which could be tested which suggested that it might in fact be a new phenomenon and not an extraneous effect produced by faulty measuring technique.

A survey of the literature since 1949 revealed that no work had been reported which included careful measurements of low temperature conductivity. Following the report of Loosjes and Vink (45) several

authors extended conductivity measurements down to room temperature but in every case only a few points in the low temperature region were plotted and consequently the effect reported here, if it existed, was not observed.

Theoretical Curves.

The log $1/R$ vs. $1/T$ curves obtained in the last section revealed that a correction must be applied to the experimental curve in the range 500° to 1100°K in order to obtain the activation energy of the conduction process. Both the low temperature and extra-low temperature conduction lines were linear to within experimental error and so by analogy with the bend in the log $1/R$ vs. $1/T$ curves at higher temperatures (following Loosjes and Vink), it was assumed that two conduction processes were operating in parallel in the low temperature region.

The conductivity would then be given by a relation of the form:-

$$\frac{1}{R} = A \exp\left(\frac{-Q}{kT}\right) + B \exp\left(\frac{-L}{kT}\right)$$

Some theoretical curves based on this relation were constructed by plotting

$$\text{Log}_{10}\left[{}^{A}/_{B} \exp\left(\frac{-\phi_1}{kT}\right) + \exp\left(\frac{-\phi_2}{kT}\right)\right] \text{ vs. } 1/T$$

Values were allotted to ϕ_1, ϕ_2 and $^{A}/_{B}$, and by trial and error curves very similar to those obtained by measurement were produced. Some of these are shown in figs. (7.8 - 7.11). In each case the values of ϕ_1, ϕ_2 and $^{A}/_{B}$ are given together with the activation energies obtained

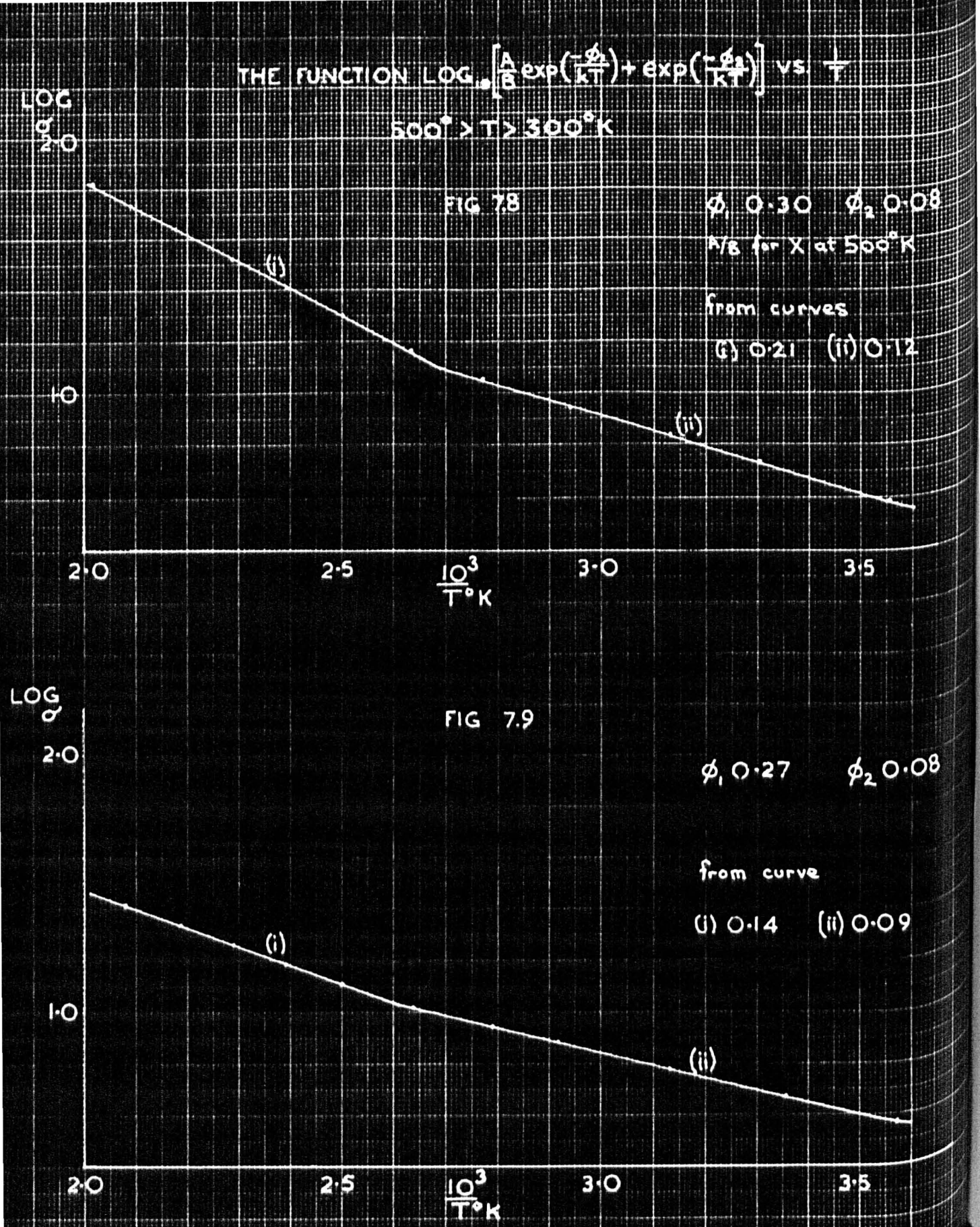
THE FUNCTION LOG$_e$ $\left[\frac{A}{B}\exp\left(\frac{-\phi_1}{kT}\right)+\exp\left(\frac{-\phi_2}{kT}\right)\right]$ vs. $\frac{1}{T}$
500° > T > 300°K
LOG σ
2·0
1·0
FIG 7.8
ϕ_1 0·30 ϕ_2 0·08
A/B for X at 500°K
from curves
(i) 0·21 (ii) 0·12
(i)
(ii)
2·0
2·5
3·0
3·5
$\frac{10^3}{T°K}$
LOG σ
FIG 7.9
2·0
ϕ_1 0·27 ϕ_2 0·08
from curve
(i) 0·14 (ii) 0·09
(i)
(ii)
1·0
2·0
2·5
3·0
3·5
$\frac{10^3}{T°K}$

THE FUNCTION $\log_{10}\left[\frac{A}{B}\exp\left(\frac{-\phi_1}{kT}\right)+\exp\left(\frac{-\phi_2}{kT}\right)\right]$ VS. $\frac{1}{T}$

$500^{\circ} > T > 300^{\circ}K$

FIG 7.10

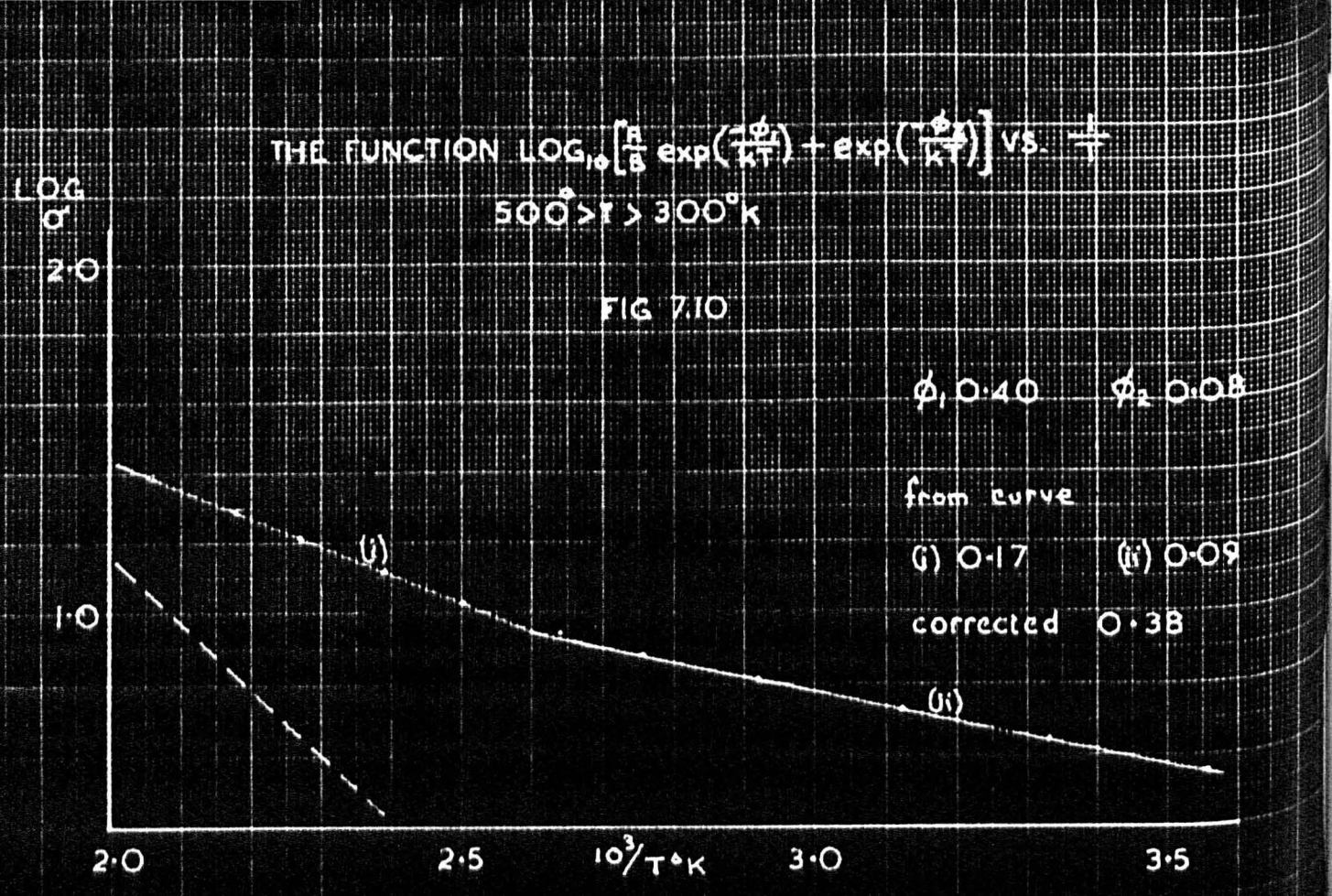

FIG. 7.11

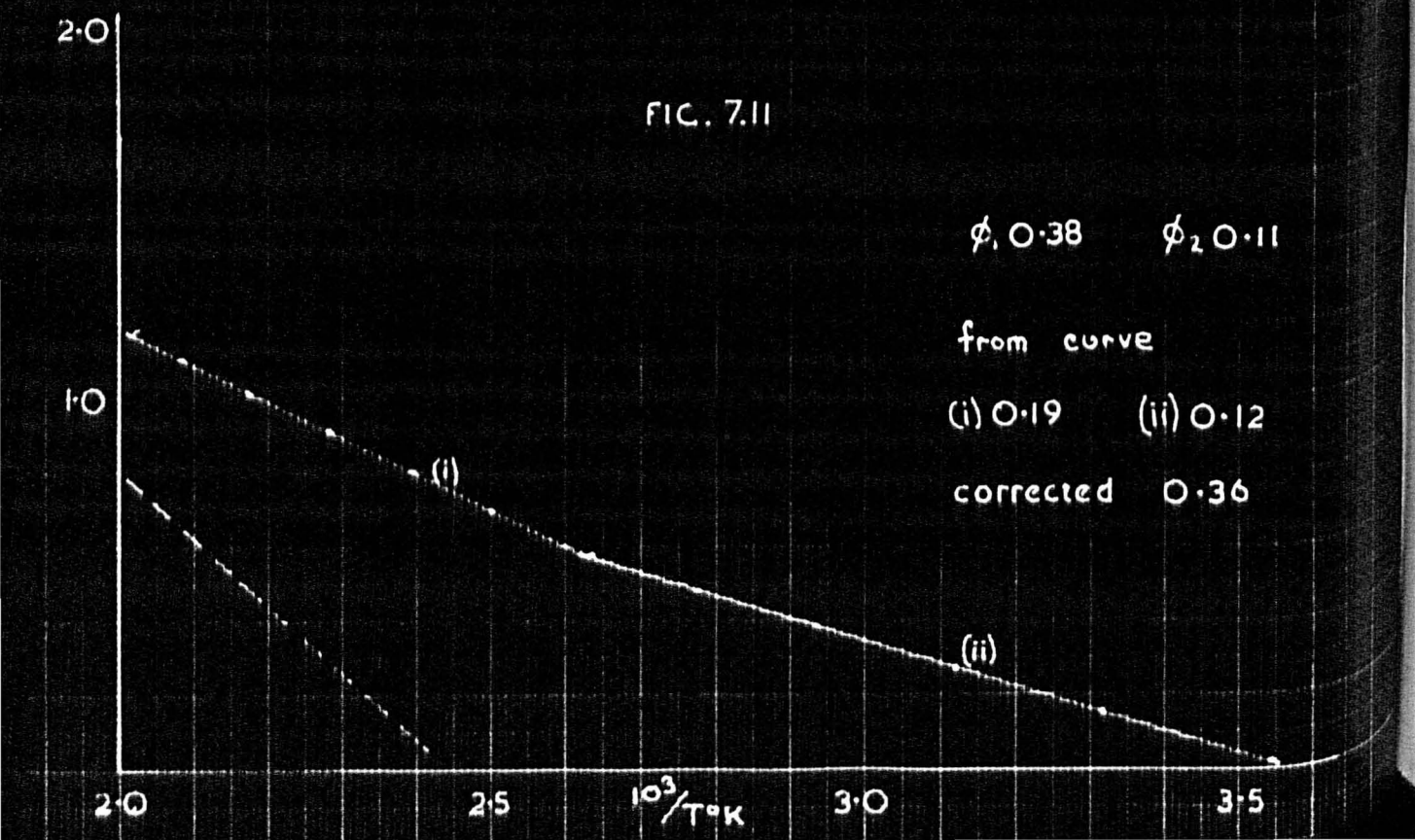

FIG. 7.12

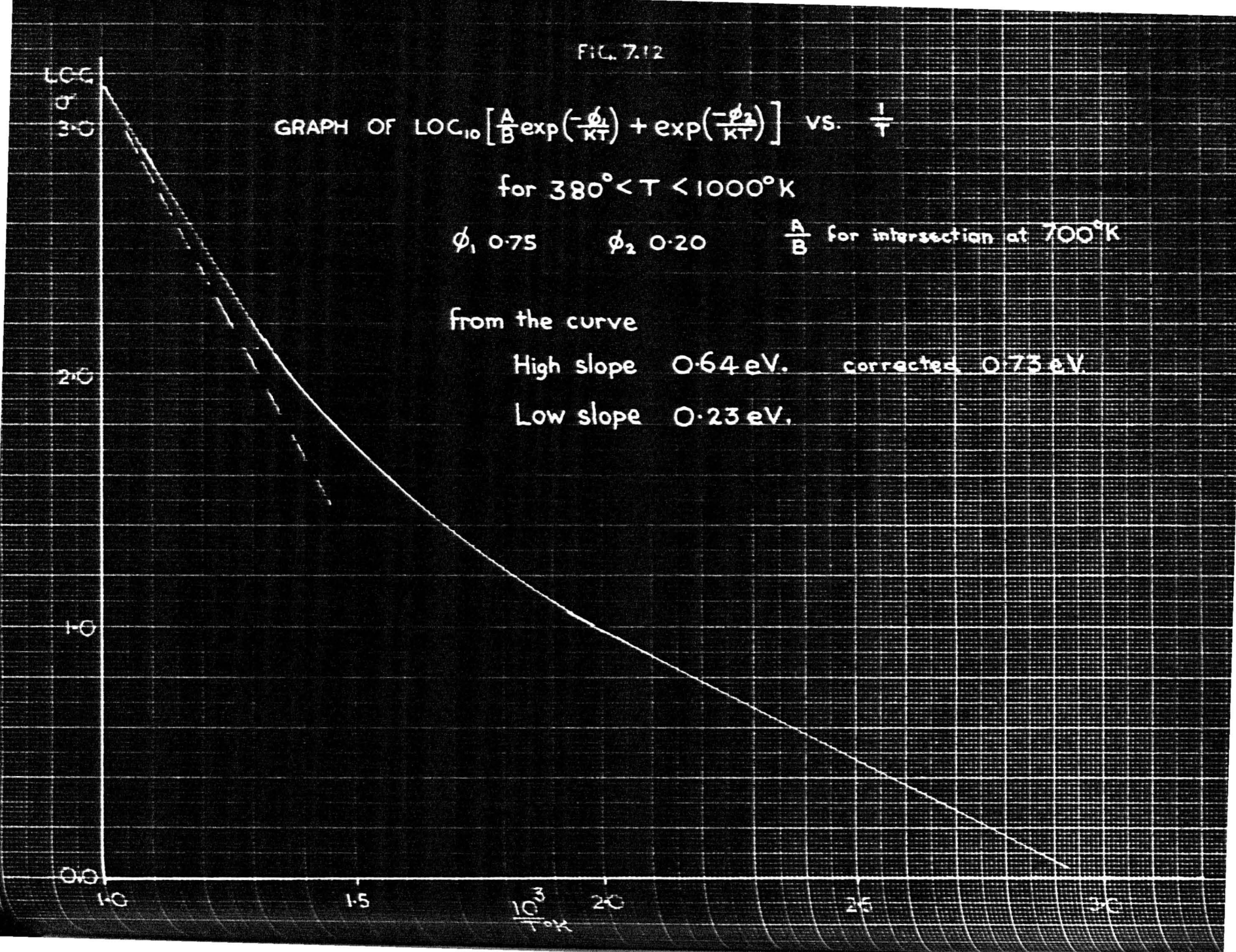

GRAPH OF $LOG_{10}\left[\frac{A}{B}\exp\left(\frac{-\phi_1}{KT}\right) + \exp\left(\frac{-\phi_2}{KT}\right)\right]$ VS. $\frac{1}{T}$

for $380° < T < 1000°K$

ϕ_1 0·75 ϕ_2 0·20 $\frac{A}{B}$ for intersection at 700°K

From the curve

High slope 0·64 eV. corrected 0·73 eV.

Low slope 0·23 eV.

directly from the curves.

The sum of two exponential functions of this kind produces a curve and not two linear sections. However, within the limits imposed by the scale and the range of temperature concerned, two straight lines could be drawn which in most cases gave a satisfactory fit to the points. It is interesting to note the extent to which the gradients of these lines differ from the values of ϕ_1 and ϕ_2 used to construct them. This difference is most noticeable in the higher temperature section. For example in fig. 7.10, ϕ_1 was 0.40 whereas the value obtained from the graph was 0.17.

This observation is applicable to the experimental situation and implies that the measured value of the slope of the conductivity curve in the temperature range 500° to 400°K must be converted so as to allow for the parallel extra low temperature mechanism.

A method of applying a similar correction at higher temperatures had been used extensively to obtain corrected values of ϕ in Chapter 5 and 6. In order to ascertain the extent of the inaccuracy produced by this method (described on page 48) theoretical curves, based on the above relationship, but with values of ϕ_1 and ϕ_2 similar to those obtained in Chapters 5 and 6 were constructed. One of these is shown in fig. 7.12. It was found to be very similar in shape to many of the conductivity curves obtained by measurement. The upper slope of this curve was connected and found to agree to within 3% of the value of ϕ_1. This seemed to justify this particular form of correction.

Accordingly the same method was employed to correct the theoretical curves in the lower temperature region. The corrected curve is

shown as a broken line on figs. 7.10 and 7.11 and was found to agree with ϕ_1 to within 5%.

Employing this method the experimental results shown in figs. (7.1 to 7.7) were corrected. The broken line on these graphs indicates the corrected value of Q. The following table lists the values of Q and L and the corrected values of Q for all the cathodes upon which measurements were made.

Table 1

Cathode	Q	Corrected Q	L
BaSr4	0.15	0.24	0.12 eV
5	0.17	0.23	0.14 eV
6	0.20	0.27	0.12 eV
7	0.15	0.20	0.09 eV
9	0.18	0.22	0.12 eV

The average value of Q is 0.23 eV and of L, 0.12 eV although it is doubtful if these average values have any real significance.

Long Term Activation Experiments.

The measurements reported in the last section were made upon fully activated cathodes. Measurements were also made on cathode BaSr8 which had undergone a large number of poisoning-recovery cycles resulting in the cathode exhibiting a lower state of activity. Curve (1) in fig. 7.6 shows the fully activated state reported as curve 4 in fig. 6.9. Curve (2) indicates the partially deactivated condition of the cathode as a result of the poisoning experiments. This curve exhibits a much steeper slope in the low temperature region but the

extra low temperature section of slope L is clearly evident. The measured and corrected values of the slopes are given in the following table:-

Table 2

State	ø Corrected	Q	Corrected Q	L
1	0.76	0.20		eV
2	0.90	0.25	0.32	0.17 eV

The values of Q = 0.32 and L = 0.17 are larger than those listed in table 1 and represent a cathode in a slightly deactivated condition.

This cathode had been reactivated for short periods after poisoning experiments and so in an attempt to improve cathode activity it was subjected to a long period of operation under activating conditions. A period of 170 hours at 900°C, Ea 50v. was allowed before further conductivity measurements were made. At the end of this period curve (3) (fig. 7.6) was obtained.

This curve showed a surprising effect in that it was quite linear below the Loosjes-Vink bend. The slope, 0.12 eV, of the low temperature section corresponded with the value of L from the measurements on other cathodes previously described. This result suggested that the long term activation procedure had so increased the effective cross-section of the extra-low temperature conduction process that this had become the predominant conduction mechanism below 700°K.

It was decided to investigate the possibility for such changes occurring in other cathodes. Accordingly cathodes BaSr5, 6, 7 and 9

were subjected to activation treatment for 170 hour periods. Conductivity measurements were then made which gave curve 2 oneach graph (fig. 7.1 - 7.7). The results for each tube are discussed below under separate headings.

BaSr5.

Continuous operation of the cathode under activating conditions for 170 hours resulted in a state of lower conductivity. Again no bend in the conductivity curve was noted. The activation energy of the low temperature section was found to be 0.16 eV a value somewhat higher than that previously obtained for the lowermost part of the curve. It is possible that a similar change had occurred to that which took place in cathode BaSr8. Long term activation had increased the cross section of the extra-low temperature conduction process so that it became the predominant mechanism below 700°K.

BaSr6.

This cathode did not appear to have been affected by the long term activation procedure. The two conductivity lines (1) and (2) coincided.

Corrected Q = 0.27 eV L = 0.12 eV

BaSr7.

Again continuous operation resulted in a lower level of conductivity, but this time the two sections of the curve were still evident. The changes in activation energymay be seen from the table

Curve	Q	Corrected Q	L
1	0.15	0.20	0.09 eV
2	0.21	0.25	0.12 eV

The change to larger values of Q and L possibly indicates that state (1) represented an enhanced state of conductivity. The value 0.12 eV is the average value of L in several cathodes.

BaSr9

A reduction in conductivity occurred in this cathode after 170 hours operation under activating conditions. The changes in activation energy were found to be slight and are recorded in the following table.

Curve	Q	Corrected Q	L
1	0.17	0.22	0.12 eV
2	0.18	0.23	0.12 eV

It may be concluded from the long term activation experiments that the non linearity of the conductivity line below 700°K is a function of the cathode itself, since this may disappear and the log. conductivity v. reciprocal temperature become linear under certain conditions. This change may be explained in terms of the variation of the effective cross-section of one conduction process so that the extra-low temperature conduction mechanism becomes the predominant conduction process in the low temperature region.

Summary of Results.

Measurement of the variation of conductivity with temperature of

describes the behaviour of the conductivity of an oxide cathode in the temperature range 500° – 290°K. This equation implies the presence of two conduction mechanisms operating in parallel.

It was pointed out at the end of Chapter 4 that an N-type semiconduction mechanism alone was not an adequate interpretation of the conductivity v. temperature curves below the knee or Loosjes-Vink bend in the curve. This is particularly true when the observed activation energy Q has a value less than 0.25 eV (Chapter 2 page 16) which is the case in all the measurements on fully activated cathodes described in Chapter 6.

An explanation of these low observed values of Q and the extra low temperature section of slope L must be sought in terms of another conduction mechanism. It is not improbable that ionic conduction might play some part in the conduction process at such low temperatures. Conductivity measurements would not distinguish such a process from one of electronic conduction. Very little information is available with regard to ionic mobilities in the oxide cathode but some work has been done on the diffusion of barium in single crystals of barium oxide by Reddington (68). He found that a charge transporting diffusion process of activation energy 0.3 ± 0.05 eV was present but more important still the surface diffusion constant for barium on barium oxide was found to have a temperature dependence of 0.16 ± 0.03 eV. The porous multi-crystalline oxide cathode has a large surface to volume ratio and hence the cross section for a surface

barium-strontium oxide cathodes in the range 600° – 300°K has revealed that a simple relation of the form

$$\sigma = \sigma_0 \exp\left(\frac{-Q}{kT}\right)$$

does not describe the variations observed.

A curve of $\log 1/R$ vs. $1/T$ exhibits two linear sections intersecting at approximately 400°K.

Theoretical curves based on the relation

$$\frac{1}{R} = A \exp\left(\frac{-Q}{kT}\right) + B \exp\left(\frac{-L}{kT}\right)$$

were obtained by plotting

$$\text{Log}_{10}\left[A/B \exp\left(\frac{-\phi_1}{kT}\right) + \exp\left(\frac{-\phi_2}{kT}\right)\right] \text{ vs. } 1/T$$

in the range $500 > T > 300$°K, choosing values of ϕ_1 and ϕ_2 similar to the values of Q and L observed experimentally. Curves very similar to the experimental ones were obtained. A method of correcting the upper section of the curve so as to obtain the true value of ϕ_1 gave values in fairly good agreement (10%) with the value used in constructing the curves. The same method was employed to correct the experimental curves. The activation energy Q at higher temperatures was found to be in the range 0.22 – 0.27 eV. The activation energy at temperatures below 400°K (L) was found to be in the range 0.09 – 0.14 eV.

Conclusions.

The agreement obtained between the theoretically constructed curves for $\log 1/R$ vs. $1/T$ and the observed temperature dependence of the conductivity suggest that the equation

$$\sigma = A \exp\left(\frac{-Q}{kT}\right) + B \exp\left(\frac{-L}{kT}\right)$$

charge transporting mechanism is high. This implies that conductivity over the surfaces of the crystal grains by the movement of barium ions is highly probable. The results obtained indicate that this process becomes the predominant conductivity mechanism at temperatures below $400^{\circ}K$.

In order to test the hypothesis that surface donduction over the total grains by movement of barium ions was important in the low temperature region some experiments were performed in which barium was deposited onto the cathode. These are described in the next Chapter.

FIG.84

BaSr II CONDUCTIVITY LINES

Barium deposition experiment

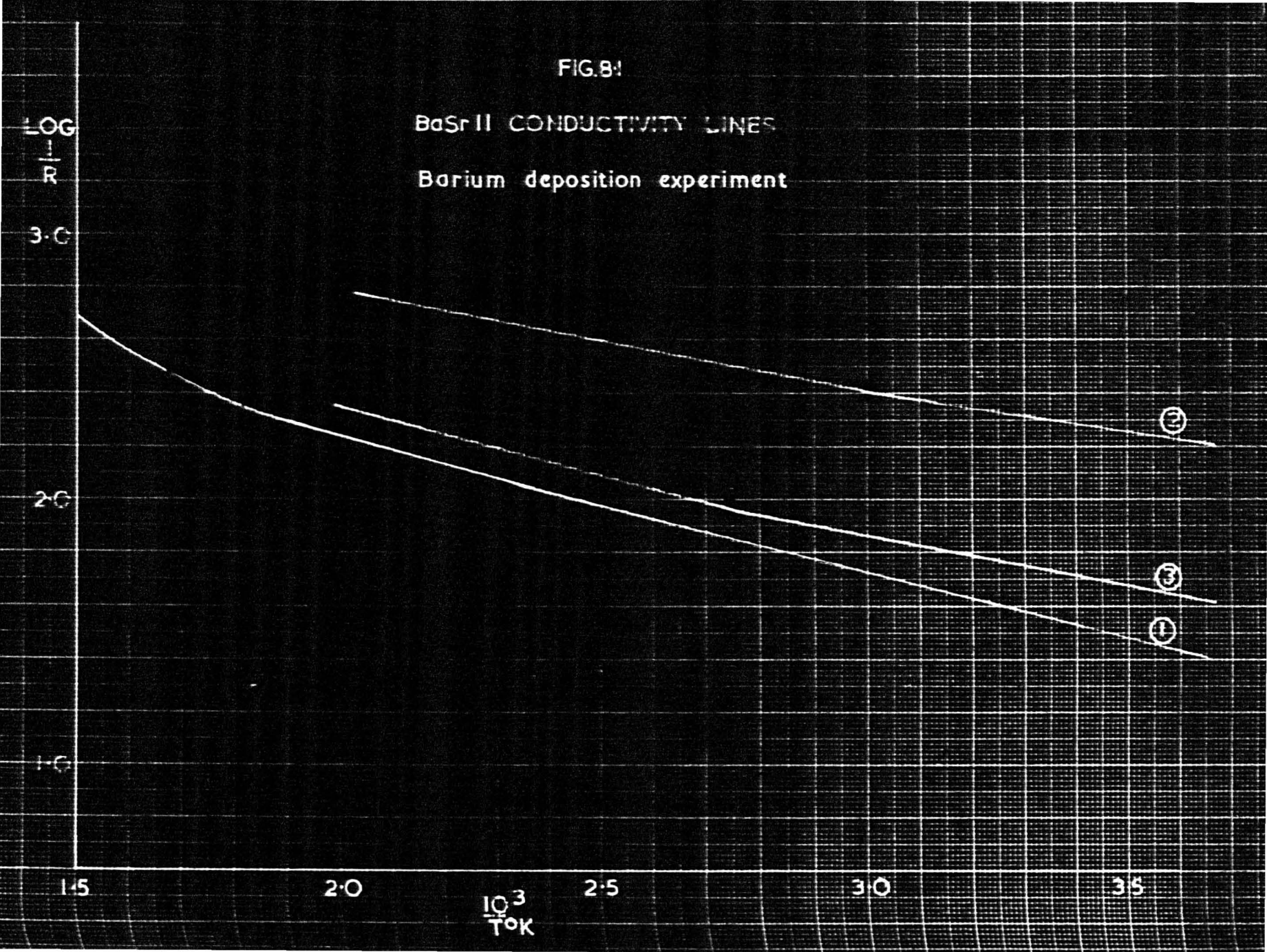

CHAPTER 8

BARIUM DEPOSITION EXPERIMENTS

During the course of activating some of the cathodes described in the preceeding Chapters by applying an anode potential of 100 volts when the cathode temperature was 900°C a green glow in the anode-cathode space was noted. This occurred only when an anode had become red hot under the influence of the bombarding electrons.

This green glow was associated with the ionisation of barium which is known to be evaporated from the cathode during normal operation. Doubtless under the conditions stated this barium was vapourised from the anode. The question arose as to whether this barium would have an effect on the cathode and accordingly the phenomenon was investigated. Tube BaSr11 was selected for this purpose. The cathode of this tube had been emission activated at 150 volts until anode current of 150 m/a was obtained. The anode potential was then reduced to 50 volts to prevent overheating until emission saturated at 70 m/a . Emission and conductivity were then measured.

The conductivity v. temperature curve is shown in fig. 8.1 curve (1). This was found to have very low slopes in the low temperature region. It was difficult to distinguish between the two sections of this curve and so no correction was applied to the upper part. A Richardson plot from emission measurements gave curve A in fig. (8.2). The cathode temperature was raised to 800°C and 50 volts applied. I_a was 60 m/a. 100 volts was then applied. The initial current was

FIG 8.2

RICHARDSON LINES

BaSrII.

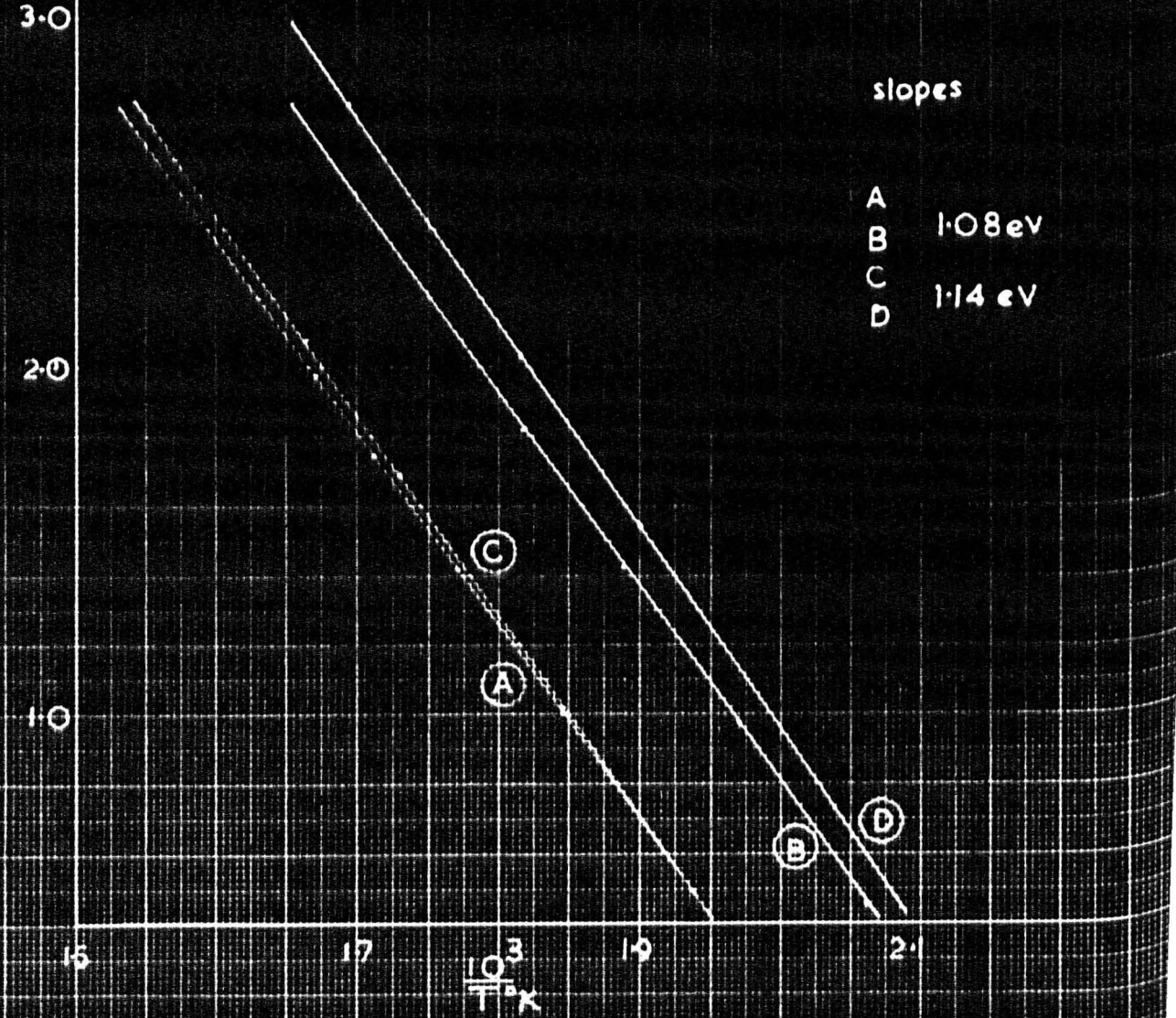

160 m/a increasing slightly - 165 m/a as the anode became red hot (20 seconds). When the anode had attained a red heat the green discharge occurred. This was allowed to continue for 40 seconds. The anode potential was then removed and the cathode coded over a period of 15 minutes by gradually reducing the heater current until the temperature was about 500°K. Conductivity and emission measurements were then made. Curve (2) fig. (8.1) was obtained showing a considerable increase in the overall level of the conductivity and each section of the curve exhibiting a lower slope than curve (1). The emission characteristics were used to plot a Richardson line - curve (B) of fig. (8.2). This was found to have a slope of the same value as curve (A). However, the curve indicated a higher level of emission than curve (A) suggesting that the work function ϕ of the cathode had not changed appreciably, but that the number of donors n_o had increased.

At the conclusion of these measurements the temperature of the cathode was raised to 900° for 15 minutes without the application of an anode potential. Subsequent conductivity measurements gave curve (3) and a Richardson plot from emission measurements gave curve (C) fig. (8.2). These curves lay below those obtained previously and showed that the cathode had been reduced to a lower state of activity by re-evaporation of the barium deposited initially.

The barium deposition was repeated by again operating the cathode at 800°C with 100 volts anode potential for 60 seconds. A conductivity curve almost identical with curve (2) fig. (8.1) was obtained and a Richardson plot (curve D, fig. 8.2) showed that again the emission had

FIG. 8·3

Ba&r9 CONDUCTIVITY LINES

Barium deposition experiment

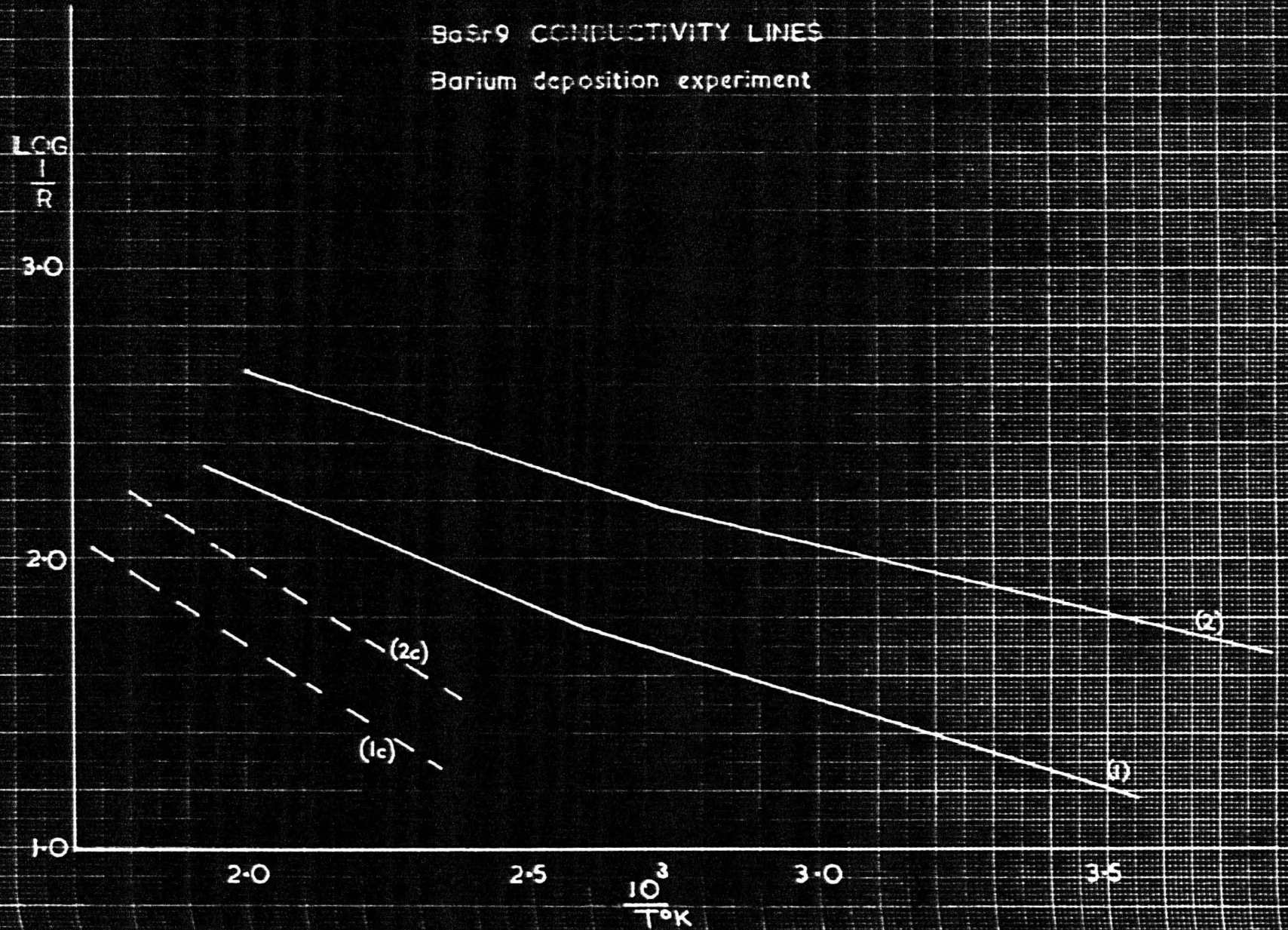

increased without a change in work function.

It was decided to extend this barium deposition technique to a cathode in which the two sections of the low temperature conductivity curve were more distinguishable. BaSr9 was selected for this purpose. Precisely the same technique was used; the green discharge being passed for 1.0 minute. Fig. (8.3) shows the change in conductivity and Fig. (8.4) the change in emission. In this instance the change in emission was quite small whereas the change in conductivity was appreciable. However, it was possible to correct the conduction curves to account for the extra-low temperature conductivity. The broken lines on fig. (8.3) give the slopes of the corrected lines and these were found to be almost identical. This is significant since it suggests that the barium deposition affects the extra low temperature mechanism predominantly.

The activation energies obtained are

	Low Temp Q	Corrected Q	Extra Low	Ø Richardson
Before Ba dep.	0.17	0.25	0.13	1.1 eV
After Ba dep.	0.14	0.24	0.10	1.1 eV

Discussion of Results.

The increase in emission evidenced from the Richardson lines fig. (8.4) is very small. This suggests that if the number of donor centres has been increased then this increase is quite small. This would explain the almost negligible difference in the corrected values of Q.

The increase in conductivity exhibited by the curves must then be accounted for by the decrease in the slope of the lower temperature

FIG. 8·4

BaSr·9 RICHARDSON LINES

Barium deposition experiment

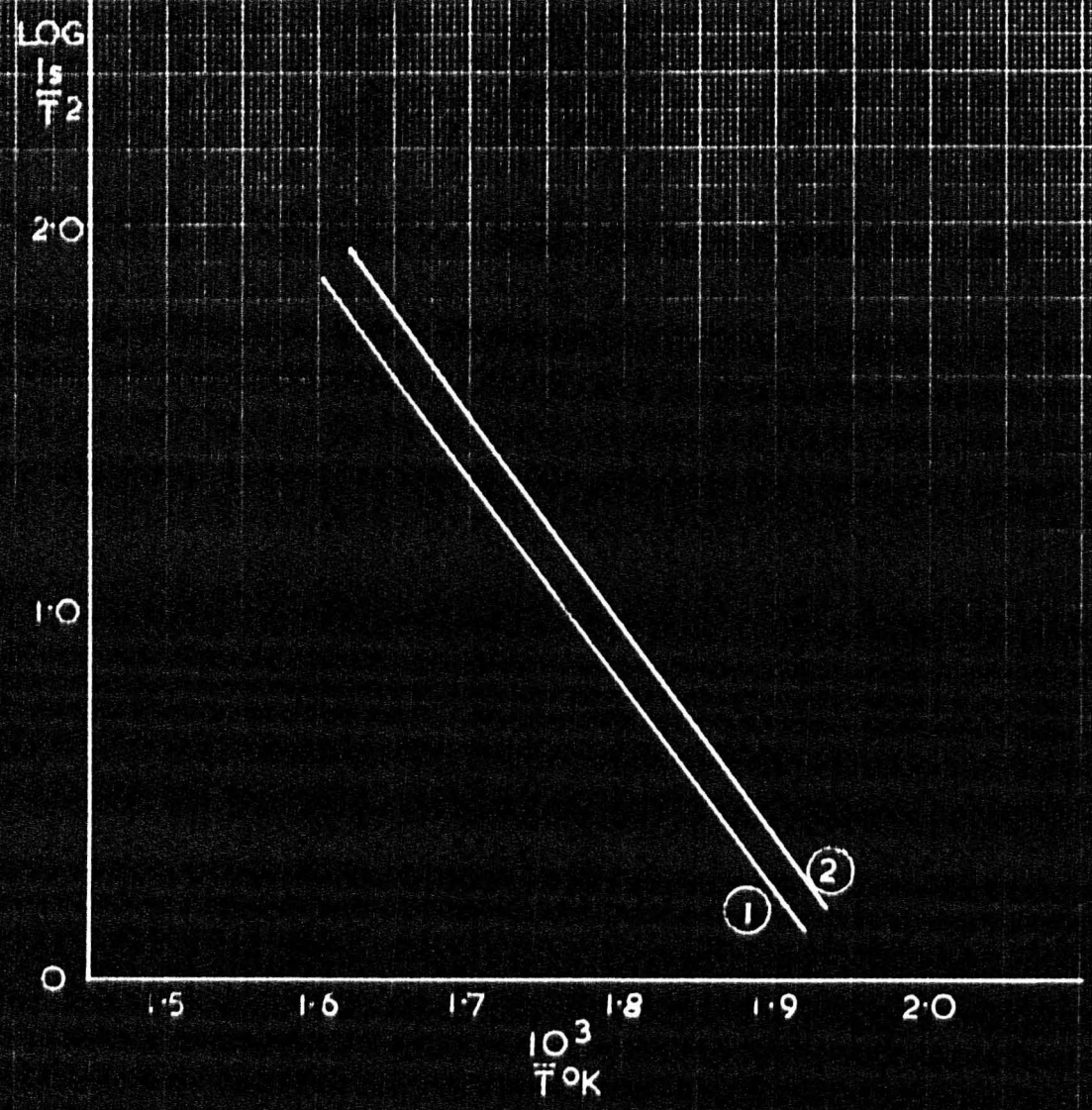

section.

On the basis of a change of slope from 0.13 to 0.10 eV the calculated change in log. $^{1}/R$ assuming a simple exponential relationship is 0.5 at 300°K. The actual change in $^{1}/R$ at 300°K is 0.58. The difference might be explained by an increase in the value of A in the expression

$$\frac{1}{R} = A \exp\left(\frac{-L}{kT}\right)$$

for the conductivity in this region.

It would seem therefore that the deposition of barium from the anode onto the cathode under the influence of the electron stream affects the cathode in two ways. The number of donor centres is increased slightly, giving slightly increased emission without change in the work function, but the larger change occurs in the extra low temperature conduction mechanism. If the extra-low temperature conduction were due to some kind of movement of barium ions on the surfaces of the internal crystal grains then additional barium should assist such a conduction mechanism. A decrease in the measured activation energy for this surface mechanism would be expected since with additional barium present more current would be carried by the surface ions. This slight reduction in L does in fact occur and so the barium deposition experiments constitute evidence for conduction over the crystal surfaces by ion movement. If sufficient barium were evaporated onto the cathode, conduction in a film of barium as postulated from time to time (49) might actually occur. However, experiments on BaSrll indicate that an excess of barium is rapidly evaporated, and the cathode

returns to its initial level of conductivity when allowed to operate at 900°C fpr a time.

The experimental evidence suggests, therefore, that the extra-low temperature mechanism is one of movement of barium ions over the surfaces of the internal grains of the oxide in parallel with whatever 'bulk' conductivity there may happen to be.

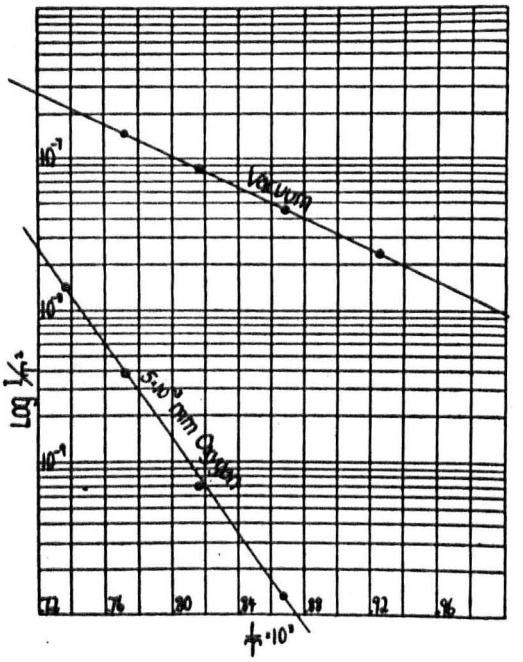

Log (i/T^2) as a function of $10^3/T$.

Fig. 9.1

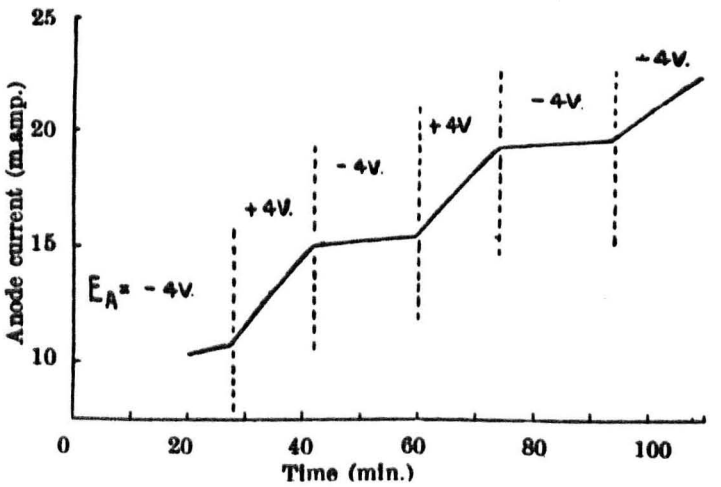

Fig. 9.2

SECTION 3

AN INVESTIGATION OF THE EFFECT OF OXYGEN AND SULPHUR ON THE OXIDE-COATED CATHODE

CHAPTER 9

PREVIOUS WORK

The Effect of Oxygen on Electron Emission

The deleterious effect of oxygen on the emission from fully activated oxide cathodes has been studied by many workers. Fig.(9.1) shows the change in Richardson line obtained by Koller (60) after admitting oxygen at 10^{-3} mm.Hg. It was also noted that the cathode could be reactivated by pumping away the gas evolved as the cathode was operated at normal temperatures (near 1000°K).

Kawamura (61) from the results of oxygen poisoning deduced the following empirical relationship between the partial pressure of oxygen p and the saturation current i

$$i = K p^{-\frac{1}{m}}$$

K and m are constants.

This relationship was verified by Arizumi and Narita (62) who also studied the recovery of the cathode from attack by oxygen. It was concluded that only the surface was poisoned and that during recovery excess barium diffused from the body of the coating to the surface layers and so increased the number of donors.

Metson (63) has made an extensive study of the reversible nature of oxygen poisoning. A heater wire coated with barium peroxide was used as an oxygen source placed close to the cathode in the experimental tube.

A well activated cathode was poisoned to 10% of its initial emission by admitting oxygen and the recovery was recorded continuously. Even after several repetitions, complete recovery was obtained.

In a further experiment the anode voltage was applied in the reverse direction for periods during the recovery operation. Fig. (9.2) shows the result obtained. While current was drawn, recovery was rapid but became much slower during the time when the anode was negative with respect to the cathode. This was explained by assuming that oxygen atoms or molecules have entered the coating where they become negatively ionised. The presence of an emission current assists the ejection of these ions. Metson pointed out that such assistance is not essential for a cathode will recover by heat treatment alone.

Shepherd (64) has confirmed the complete reversibility of oxygen poisoning observed by previous authors and has shown conclusively that oxygen ions O^-_{16} are evolved during recovery which was suggested by Metson's experiments. A mass spectrometer was employed which enabled the energy distribution of the emitted ions to be measured. This showed that oxygen poisoning was not only a surface phenomenon since some of the ions possessed energies which indicated that they were evolved from the interior of the coating.

The Effect of Oxygen on the Conductivity.

Hannay and his coworkers (58) found that when a cathode at a temperature of 1100°K was deactivated by oxygen, a linear relationship was maintained during poisoning between the emission and the conduc-

tivity, suggesting that the body of the coating, and not merely the surface, was affected. The method consisted of introducing oxygen into the tube at a pressure of 2×10^{-2} mm.Hg. for 1-2 minutes. When a similar procedure was adopted at room temperature, and the temperature of the cathode quickly raised to 1000°K for measurement, it was found that the emission was poisoned, without a corresponding reduction in conductivity. It was concluded that at high temperatures oxygen could diffuse into the coating, reducing both conductivity and emission, but at low temperature little diffusion occurred resulting in a reduction of emission only, due to a lowering of the Fermi level near the surface.

Shepherd has also studied the effect of oxygen on the conductivity and electron emission, using probe diodes. Unlike the work of Hannay et al, measurements were made over a wide temperature range 500-1000°K. It was found that at temperatures below 700°K the conductivity was poisoned and underwent recovery in the same way as did the thermionic emission. This observation lends additional support to the pore conduction theory of Loosjes and Vink.

The method used by Hannay et al was later employed by Young (42) in an attempt to decide between the two current theories for the low temperature conduction mechanism. Oxygen was admitted to the cathode at room temperature and the change in conductivity was noted. The temperature of the cathode was then raised gradually and the conductivity noted at intervals. At approximately 800°K the conductivity decreased rapidly and on returning to room temperature a considerable

decrease in conductivity was found to have occurred. It was concluded that the low temperature conductivity could not be mainly in a surface barium film since if it were the considerable decrease in conductivity would occur at room temperature. This experiment thus supports the Loosjes Vink hypothesis of semiconductor conduction below 500°K.

Both Shepherd and Young report that some poisoning of conductivity occurs in the low temperature region. Shepherd found that this was to a small extent -80% of initial value at 500°K while Young found that 66% poisoning occurred at room temperature at only 10^{-7} mm.Hg. pressure of oxygen. Since oxygen is not thought to diffuse very rapidly into the lattice at low temperatures, causing a reduction in conductivity by occupying donor sites; the possibility of conduction over crystal surfaces cannot be entirely neglected. Further poisoning experiments in the low temperature region may help to show to what extent each mechanism plays a part in the conduction process.

The Effect of Sulphur on the Electrical Properties of Oxide Cathodes.

There is little published work concerned with the effect of sulphur on the oxide-coated cathode. In principle it is to be expected that an electron accepting element such as sulphur would diminish the emission from a cathode if adsorbed on its surface in much the same way as oxygen does.

Stahl (65) has investigated the effect of leaving cathodes in the carbonate state in the atmosphere for varying periods. After the carbonate-oxide conversion such cathodes had poor emission properties

This was attributed to the presence of sulphur in the oxide lattice surface subsequently detected by X-Ray diffraction techniques.

Plumlee (66) mentions that Matheson has studied the effect of sulphur vapour at pressures $\approx 10^{-8}$ mm.Hg. on the emission from oxide cathodes. He found that the effect was slight, but that the effects produced by impurities in the sulphur were large and 'varied from beneficial to deleterious'. The precise method employed by Matheson is not described.

Nothing is known of the effect of sulphur on the conductivity of oxide cathodes. Comparative measurements employing sulphur and oxygen as alternate poisoning agents might be a useful way of distinguishing between a surface as opposed to a 'bulk' conduction process in the low temperature region. Sulphur has a larger ion size than oxygen and hence if the poisoning ions diffuse through the lattice to occupy donor sites and so reduce the conductivity; sulphur, diffusing less rapidly than oxygen, should reduce the conductivity more slowly.

A source of ambiguity arises however in that sulphur may, under certain conditions, react with the barium oxide lattice, displacing oxygen and giving rise to a permanent poisoning effect such as that observed by Stahl. Plumlee in discussing the impurity concentrations in the oxide cathode gives thermodynamical data for the reaction

$$BaO + \tfrac{1}{2}S_2 \rightarrow BaS + \tfrac{1}{2}O_2$$

at 1000°K ΔG_o for this reaction is +7.7 K cals./mole

This gives a value of -1.7 for the logarith of the equilibrium constant. Calculation then shows that the partial pressure of sulphur must be at least 1000 x that of oxygen for this reaction to proceed at 1000°K. At lower temperatures the reaction will be even less likely to occur.

In the following Chapters a simple technique is described which was used to produce sulphur within the vacuum tube. This introduced limitations in that the amount of sulphur admitted to the cathode could not be measured. The results obtained could thus only be qualitative but this was not thought to be a disadvantage at this preliminary stage of investigation.

CHAPTER 10

EXPERIMENTAL RESULTS

Introduction.

In this Chapter some preliminary measurements of the effect of oxygen on the conductivity and emission of barium oxide cathodes are first described. Attention is then directed to poisoning experiments on (BaSr)O cathodes in the low temperature region. Later sulphur and oxygen poisoning is introduced as a means of investigating the low temperature conduction process; some results are described and general conclusions drawn.

Preliminary Experiments.

In all the poisoning experiments described below, oxygen was produced in the immediate vicinity of the anode by heating a tungsten wire coated with barium peroxide. A longitudinal slit of dimensions 0.2 x 2.0 cms. was provided in the anode in line with the cathode and the oxygen filament in order that oxygen could be admitted rapidly to the cathode. The procedure employed in the poisoning experiments was as follows:- The cathode temperature was set and with +4 volts applied to the anode the saturated anode current was noted. The initial conductivity was measured by applying $\pm$ 100mV between the probe and the cathode base and noting the current which flowed. The emission was then reduced to 10% of its initial value by heating the oxygen producing filament and, after cut-off of the gas flow, both the emission and conductivity were recorded over a period of 10 minutes. After each poisoning experiment recovery was accelerated by raising the

FIG 10·1

CONDUCTIVITY LINES

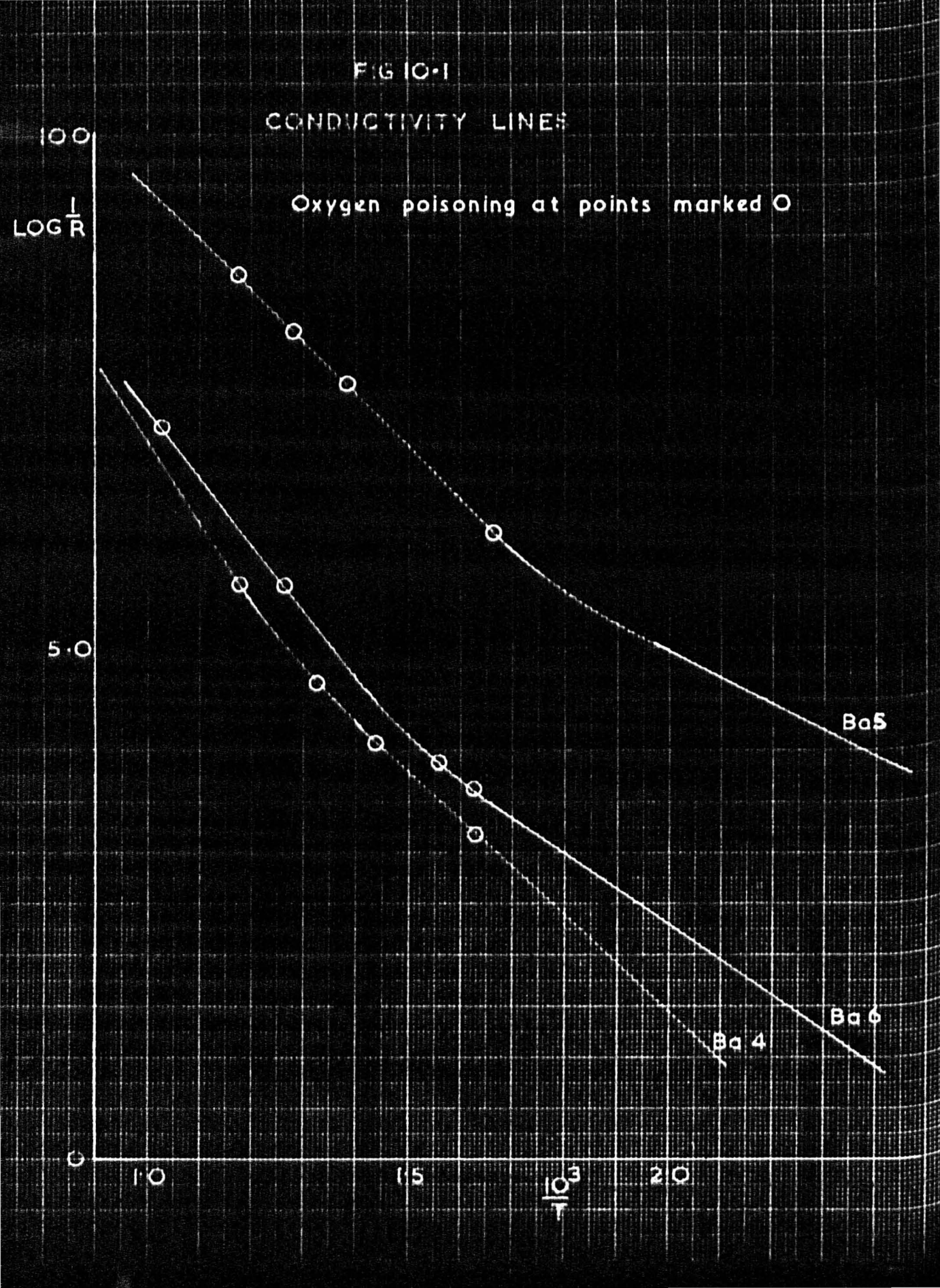

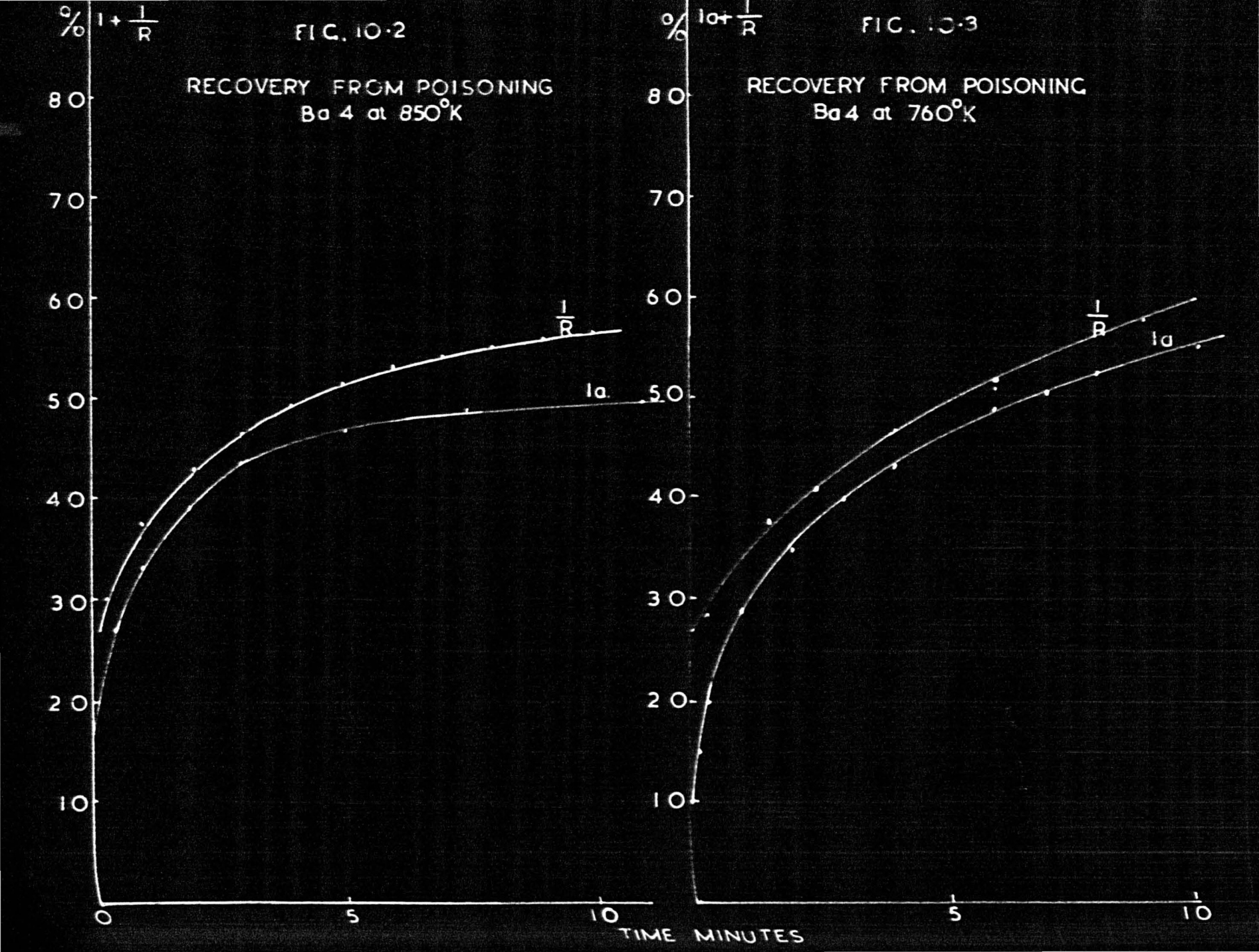

FIG. 10·2

RECOVERY FROM POISONING
Ba 4 at 850°K

FIG. 10·3

RECOVERY FROM POISONING
Ba 4 at 760°K

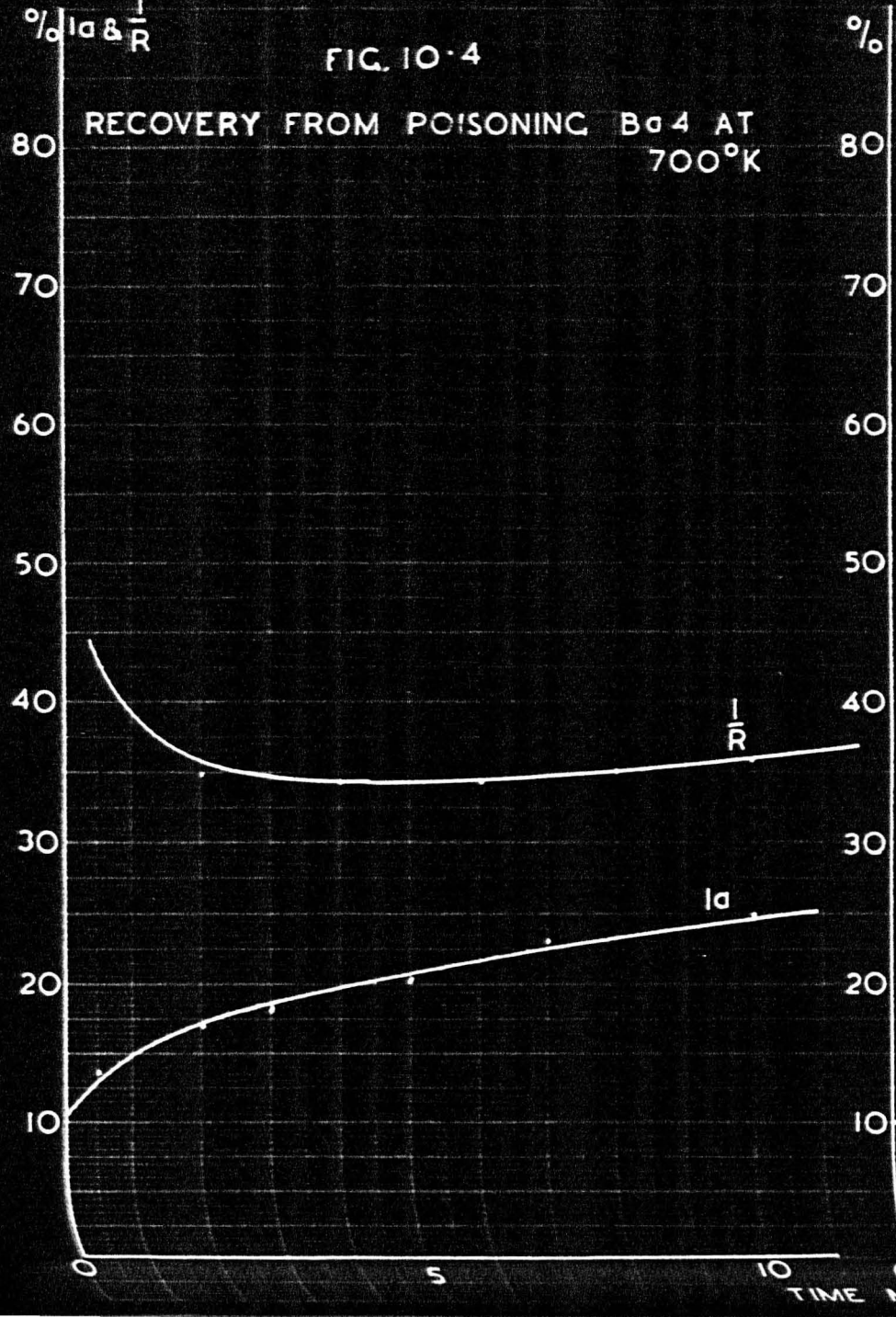

FIG. 10·4

RECOVERY FROM POISONING Ba 4 AT 700°K

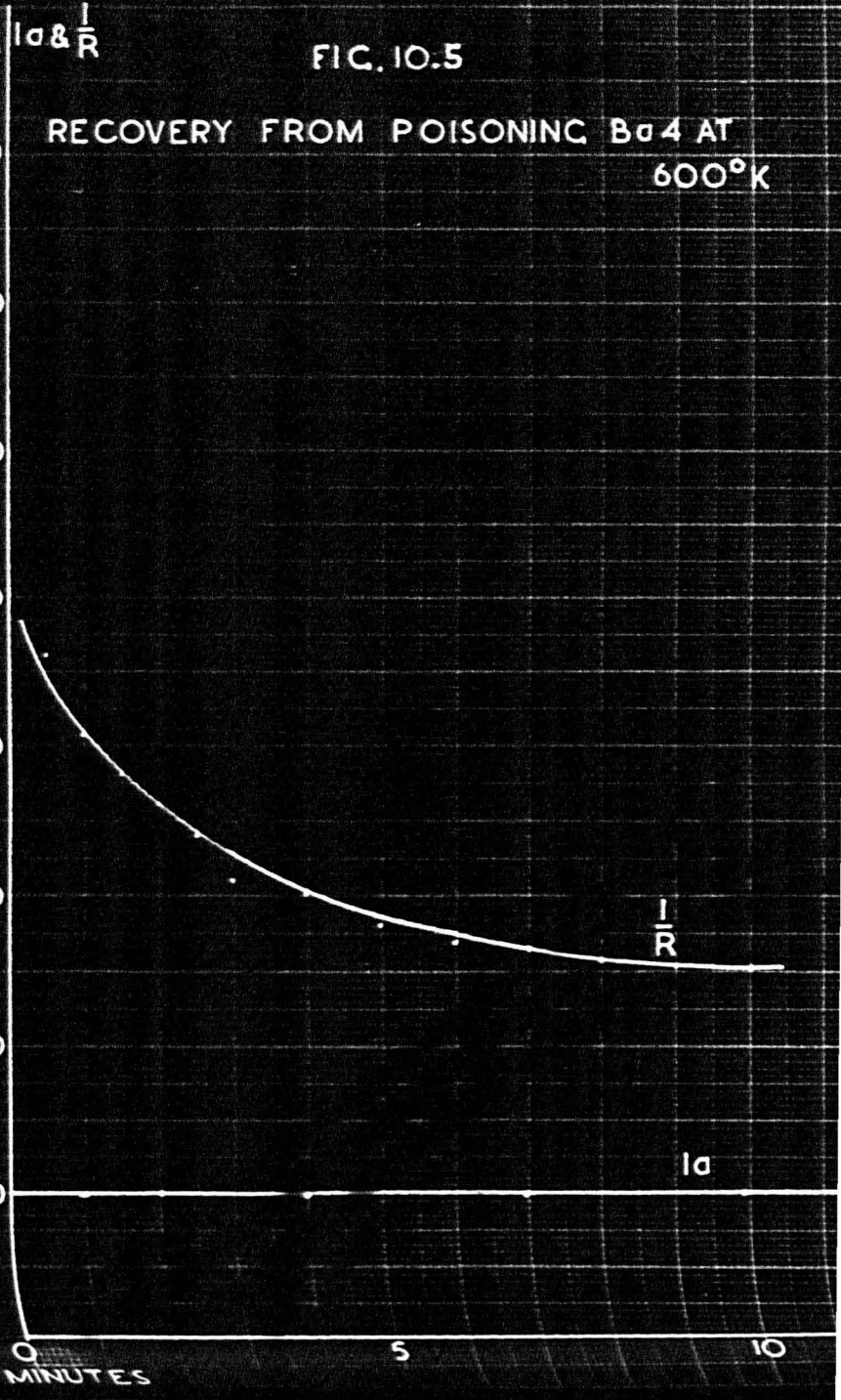

FIG. 10.5

RECOVERY FROM POISONING Ba 4 AT 600°K

temperature of the cathode to 900°C and applying 50 volts to the anode, until the emission attained a steady value, usually in 10-15 minutes.

Cathode Ba4.

The points on the conductivity line at which poisoning experiments were made are indicated in fig. 10.1. The recovery characteristics at 850°K and 760°K are shown in figs. 10.2 and 10.3. The conductivity is found to recover in a way very similar to the emission (I_a) and both emission and conductivity are poisoned to a similar extent. This kind of behaviour in the high temperature region was reported by Shepherd (64) who employed mixed oxide (BaSr)O cathodes. It was accounted to be additional evidence in f vour of the Loosjes and Vink theory of pore conduction, for, if the high temperature conduction process is due to electron emission in the pores of the coating it should behave in a manner closely analogous to the emission from the cathode surface, when oxygen is admitted.

Fig. 10.4 shows the recovery of conductivity and emission at 700°K on the bend of the conductivity v. temperature curve. Recovery is much less rapid at this temperature and the conductivity is not poisoned to the same extent as the emission. At 600°K fig. 10.5 the emission does not recover appreciably, implying that at this temperature oxygen is not ejected from the coating. The conductivity gradually decreases from 50 to 25% of its initial value suggesting that the low temperature conductivity process is poisoned more slowly than the emission process or that oxygen gradually diffuses into the coating.

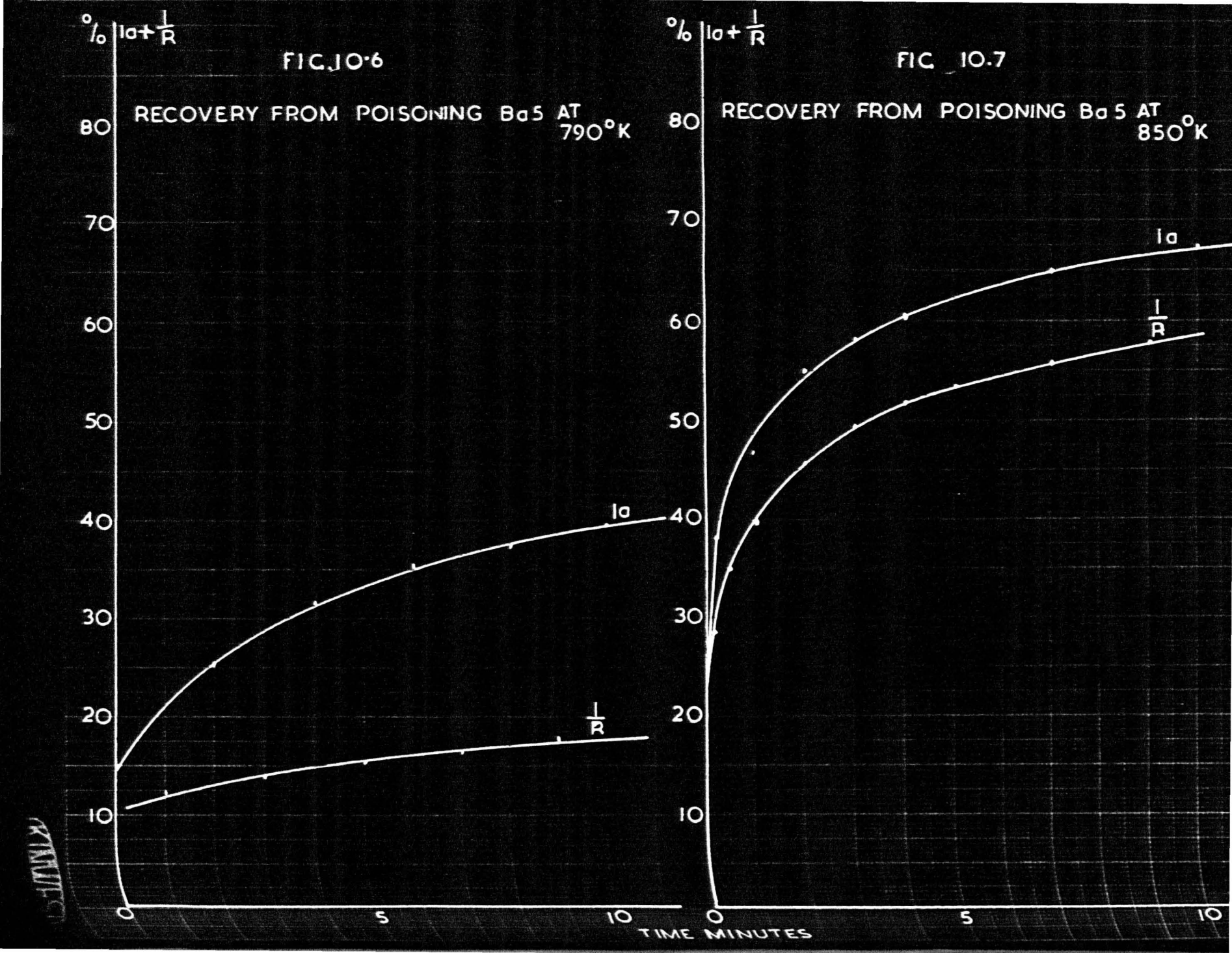
%
Ia + 1/R
FIG. 10·6
RECOVERY FROM POISONING Ba 5 AT 790°K
80
70
60
50
40
30
20
10
Ia
1/R
0
5
10
%
Ia + 1/R
FIG. 10.7
RECOVERY FROM POISONING Ba 5 AT 850°K
80
70
60
50
40
30
20
10
Ia
1/R
0
5
10
TIME MINUTES

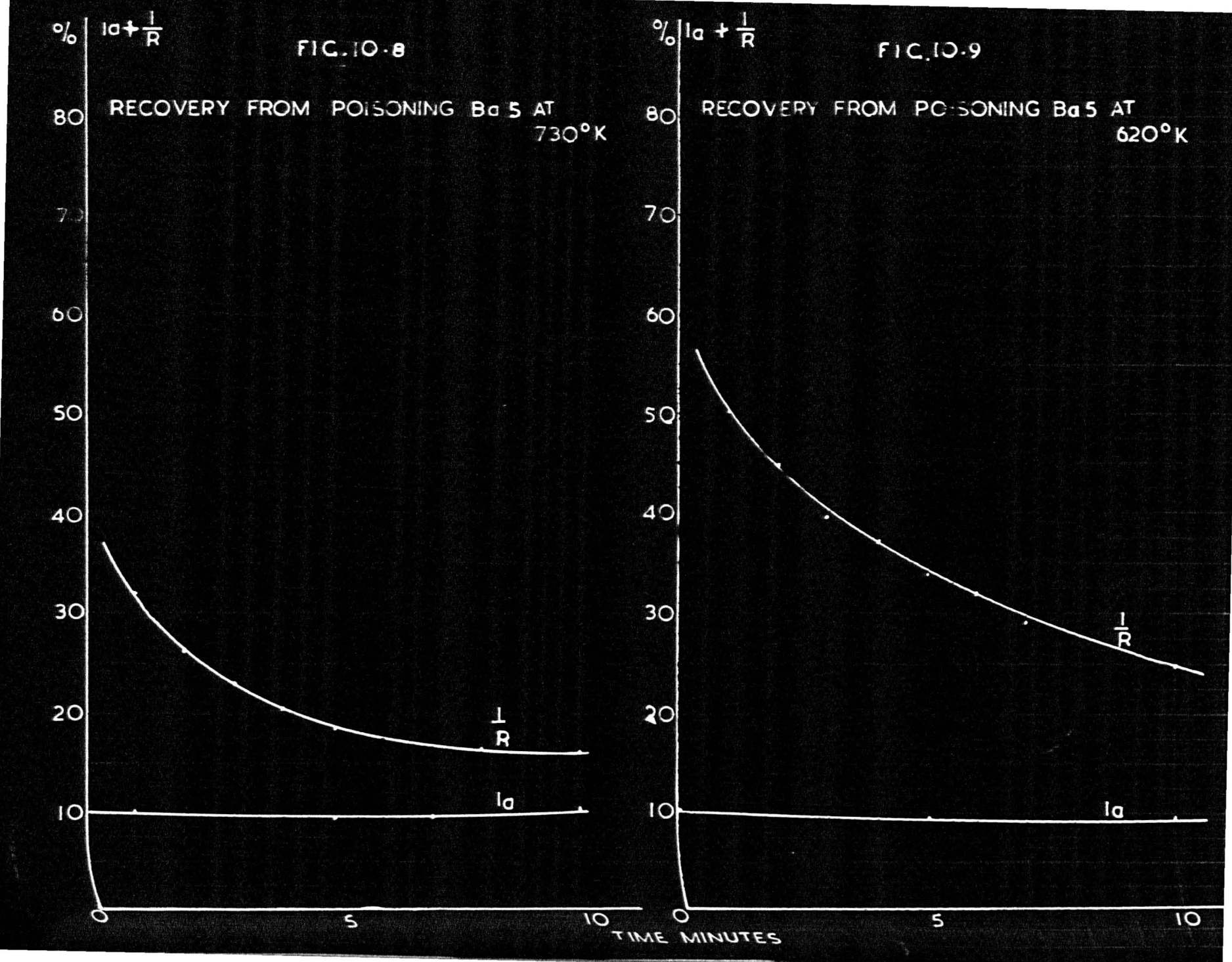
%
Ia + 1/R
FIG. 10-8
RECOVERY FROM POISONING Ba 5 AT 730°K
80
70
60
50
40
30
20
10
1/R
Ia
0
5
10
%
Ia + 1/R
FIG. 10-9
RECOVERY FROM POISONING Ba 5 AT 620°K
80
70
60
50
40
30
20
10
1/R
Ia
0
5
10
TIME MINUTES

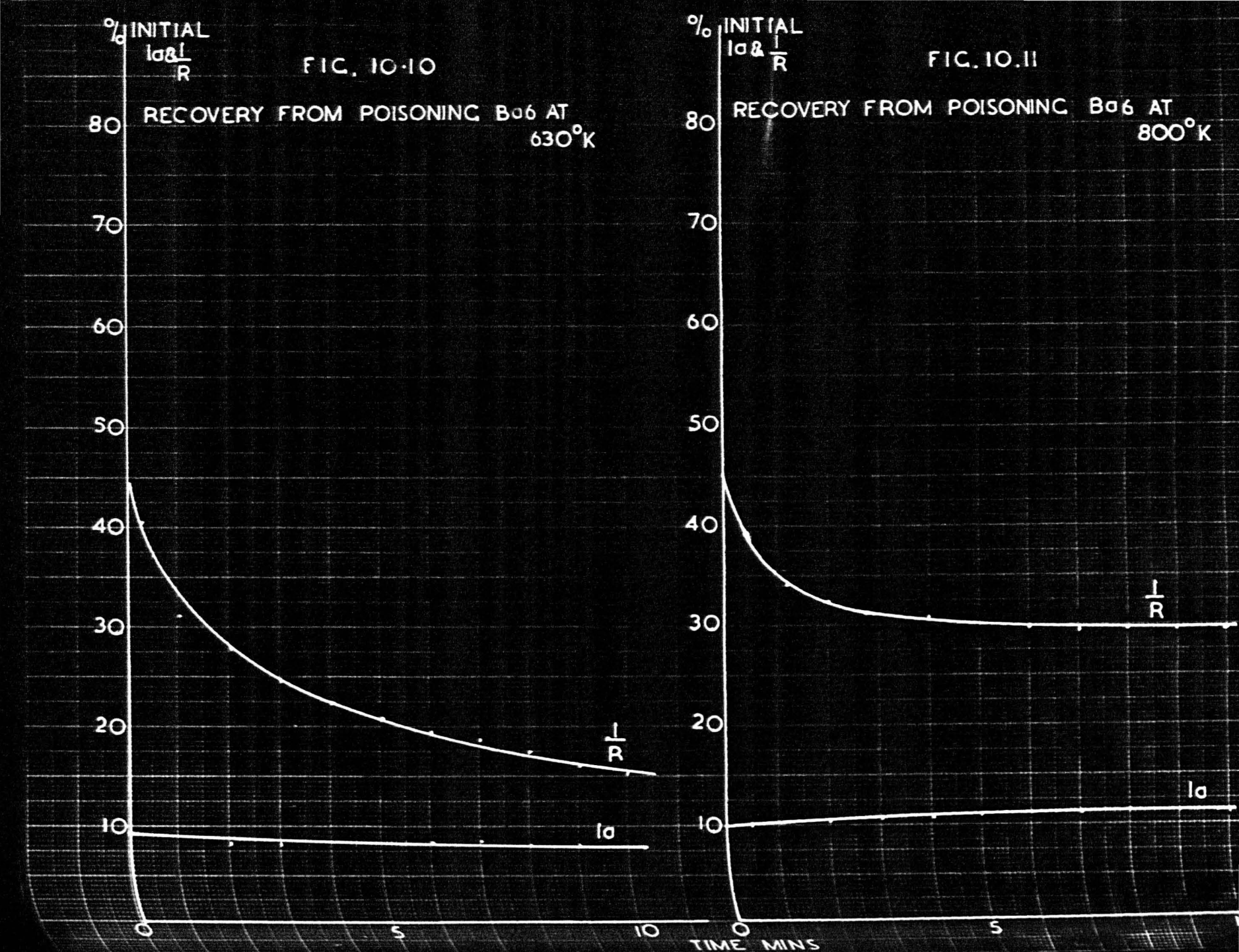
% INITIAL Ia & 1/R
FIG. 10·10
RECOVERY FROM POISONING Ba6 AT 630°K
80
70
60
50
40
30
20
10
1/R
Ia
0
5
10
% INITIAL Ia & 1/R
FIG. 10.11
RECOVERY FROM POISONING Ba6 AT 800°K
80
70
60
50
40
30
20
10
1/R
Ia
0
5
TIME MINS

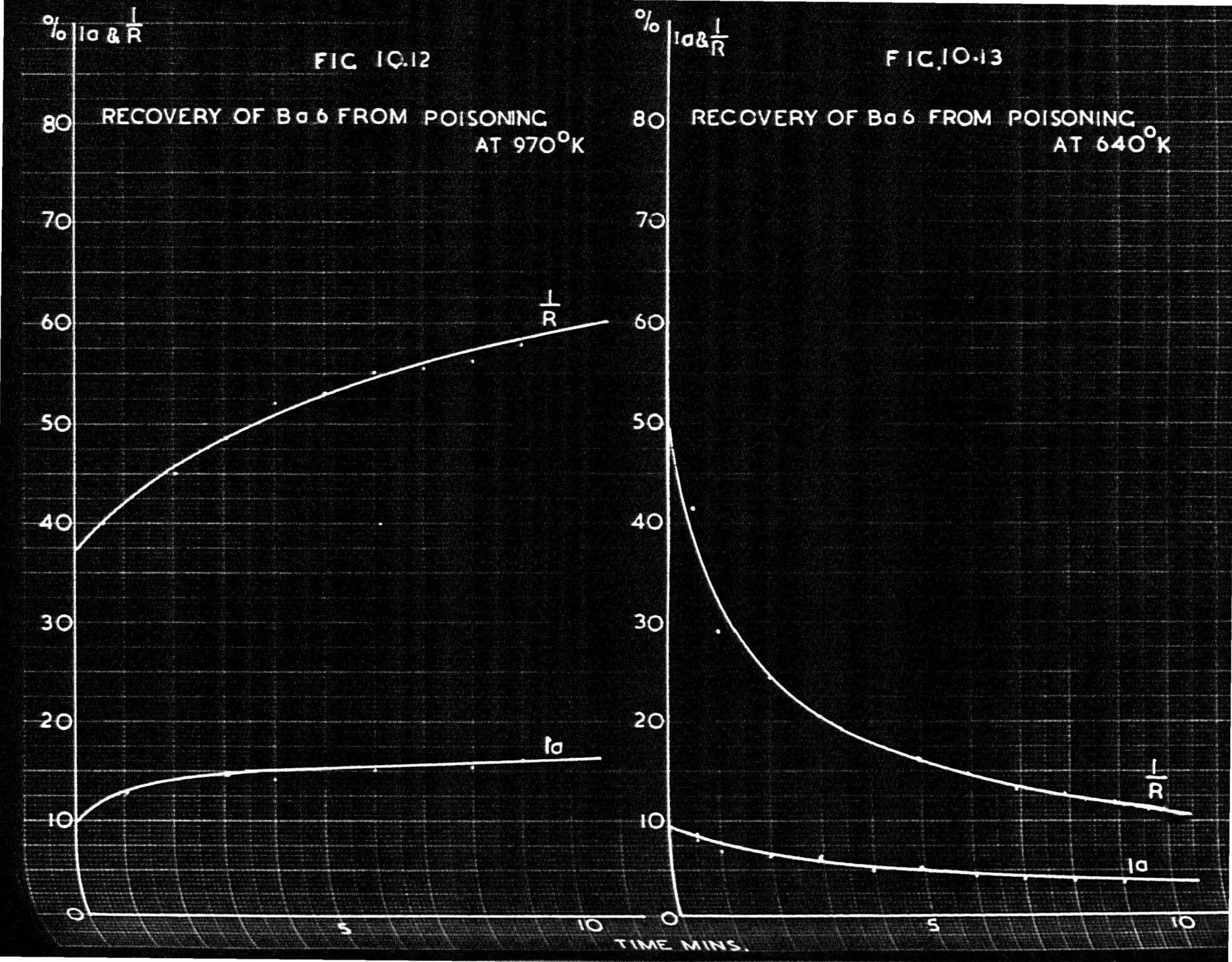
%
Ia & 1/R
FIC 10.12
RECOVERY OF Ba 6 FROM POISONING
AT 970°K
80
70
60
50
40
30
20
10
0
1/R
Ia
5
10
%
Ia & 1/R
FIC. 10.13
RECOVERY OF Ba 6 FROM POISONING
AT 640°K
80
70
60
50
40
30
20
10
0
1/R
Ia
5
10
TIME MINS.

Cathode Ba5.

At higher temperatures this cathode shows behaviour similar to Ba4 (figs. 10.6 and 10.7). At lower temperatures the emission does not recover and the conductivity continues to decrease after the oxygen supply has been cut off (figs. 10.8 and 10.9). The points at which poisoning experiments were made all lie on the high temperature section of the curve (fig. 10.1) and so it is difficult to draw conclusions about the low temperature conduction process from these experiments. However, in the case of the poisoning experiment at 620°K (fig. 10.9) the low temperature conductivity contributes about 50% to the total conductivity and hence the curve fig. 10.9 is fairly indicative of low temperature behaviour.

Cathode Ba6.

Oxygen poisoning experiments were made on a third barium oxide cathode at the points shown in fig. 10.1. No recovery was observed after poisoning at 800°K (fig. 10.11) which is surprising in view of the results previously obtained. At present this cannot be explained. At lower temperatures 630°K, fig. 10.10 and 640°K, fig. 10.12 the behaviour is very similar to that reported for Ba4, a gradual decrease in conductivity occurring and no recovery in emission being observed.

Discussion of Preliminary Results.

The results obtained at temperature above the bend in the conductivity vs. temperature curves, with one exception, are in complete agreement with those reported by Shepherd (64) and Metson (32). The latter was the first to show that oxygen poisoning was a reversible phenomena at higher temperatures. The results reported here support

this since recovery could always be obtained if the cathode temperature was raised to 900°C and an anode potential of 50 volts applied. Shepherd extended the poisoning technique to a study of the behaviour of cathode conductivity. Similar results to those reported were obtained at high temperatures and were adjudged to be evidence in favour of the Loosjes and Vink theory of pore conduction. At lower temperatures Shepherd did not observe the kind of behaviour reported here. Usually in his measurements the conductivity was poisoned to about 67% of its initial value and the characteristic showed a steady level of conductance after a slight initial decrease.

The poisoning characteristics obtained indicate a gradual reduction of the conductivity at lower temperatures due to the presence of oxygen in the coating. There is insufficient evidence from these preliminary experiments to account for this gradual reduction. However, it is a phenomenon worthy of further investigation for it may lead to an explanation of the way in which oxygen impairs the low temperature conduction process and subsequently to a better understanding of the nature of that process.

Further experiments are described below in which the effect of oxygen on the low temperature conduction process is investigated more closely. One of the difficulties encountered in the preliminary measurements was the inability to perform poisoning experiments at sufficiently low temperatures to ensure that only the low temperature process was operating. The limit was set by the sensitivity of the galvanometer employed to measure the emission. An attempt was made to

FIG. 10·14

CONDUCTIVITY LINE Ba_2Sr_4

Oxygen poisoning at points marked O

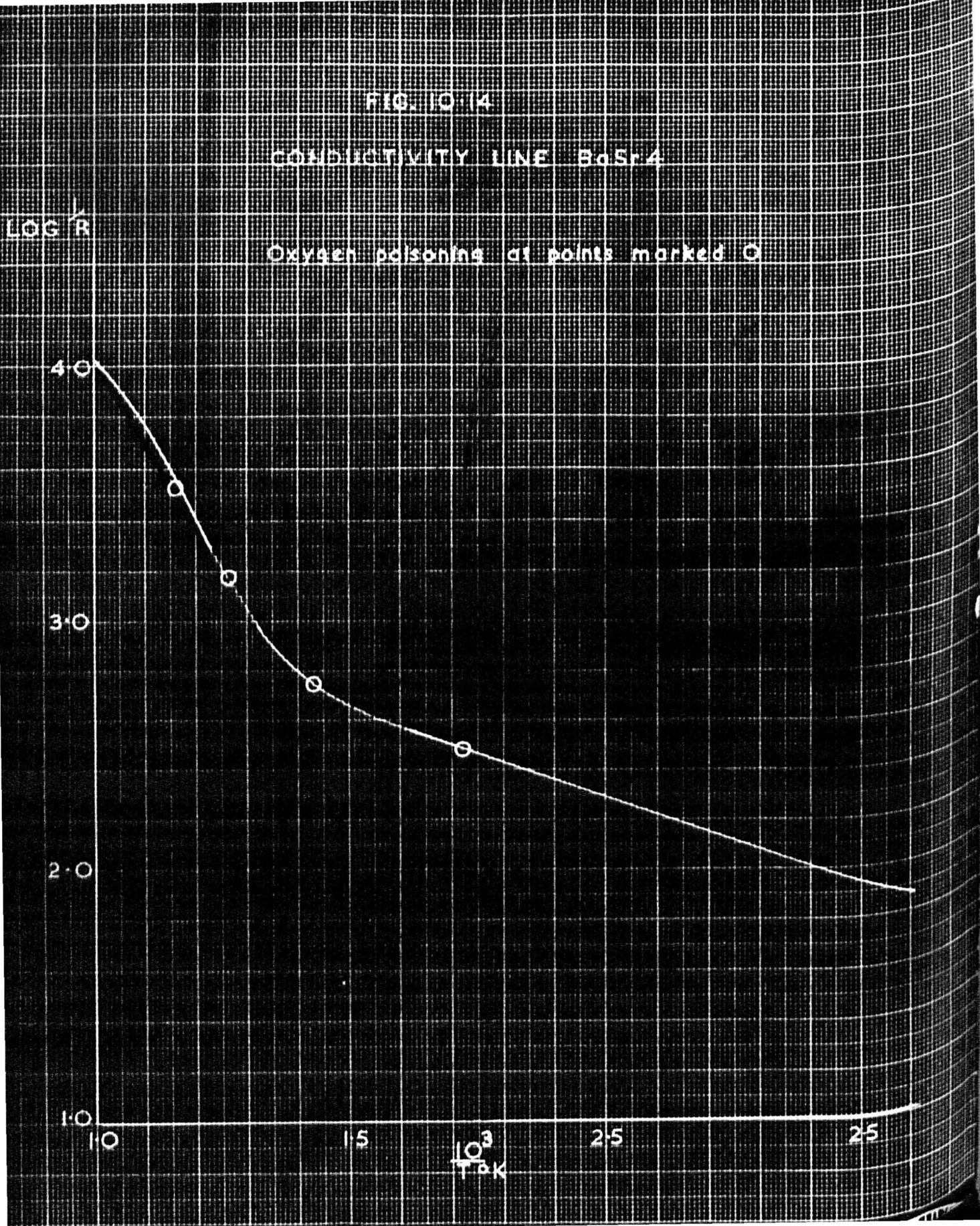

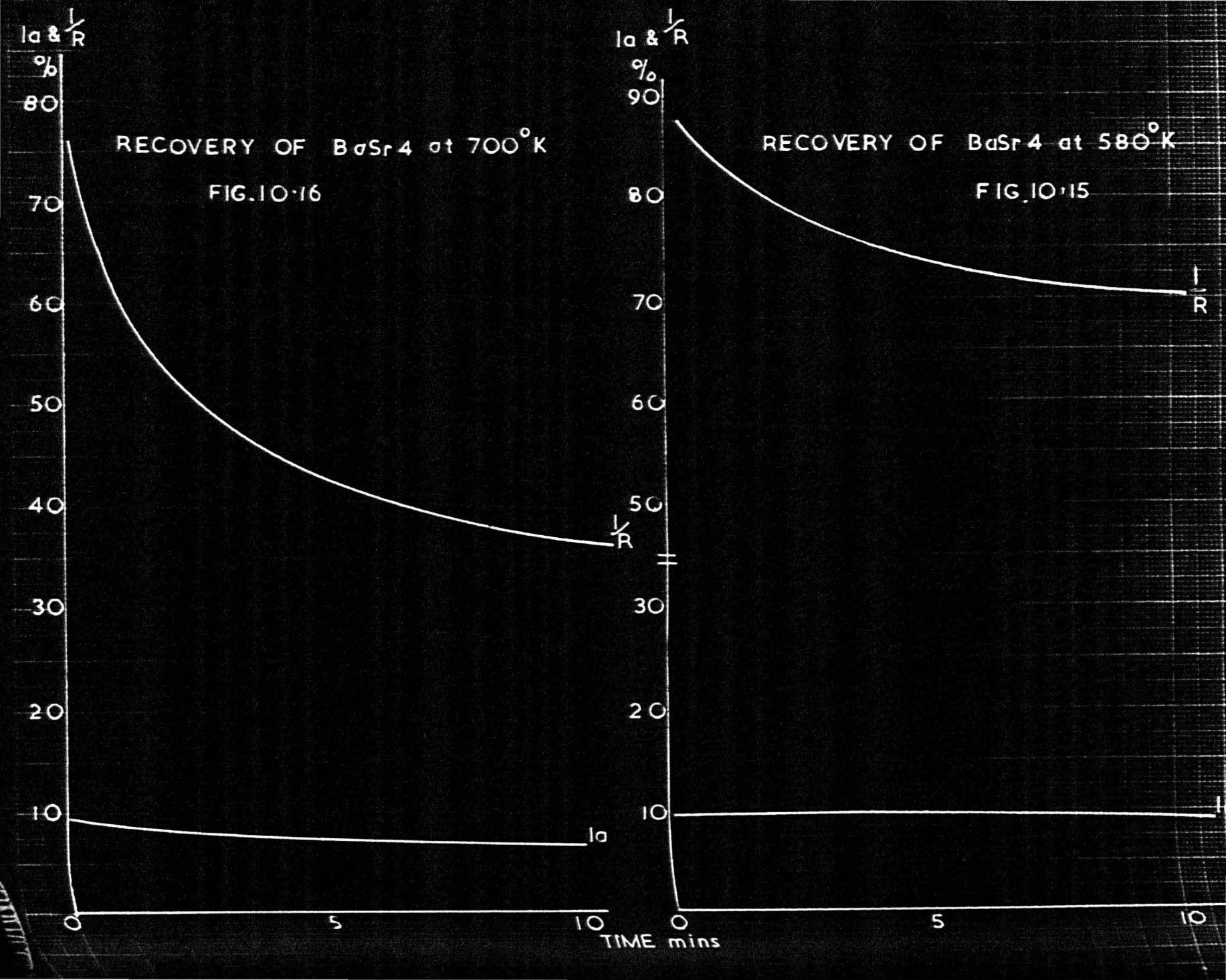
Ia & 1/R
%
80
70
60
50
40
30
20
10
0
5
10
1/R
Ia
RECOVERY OF BaSr4 at 700°K
FIG. 10·16
Ia & 1/R
%
90
80
70
60
50
30
20
10
0
5
10
1/R
I
RECOVERY OF BaSr4 at 580°K
FIG. 10·15
TIME mins

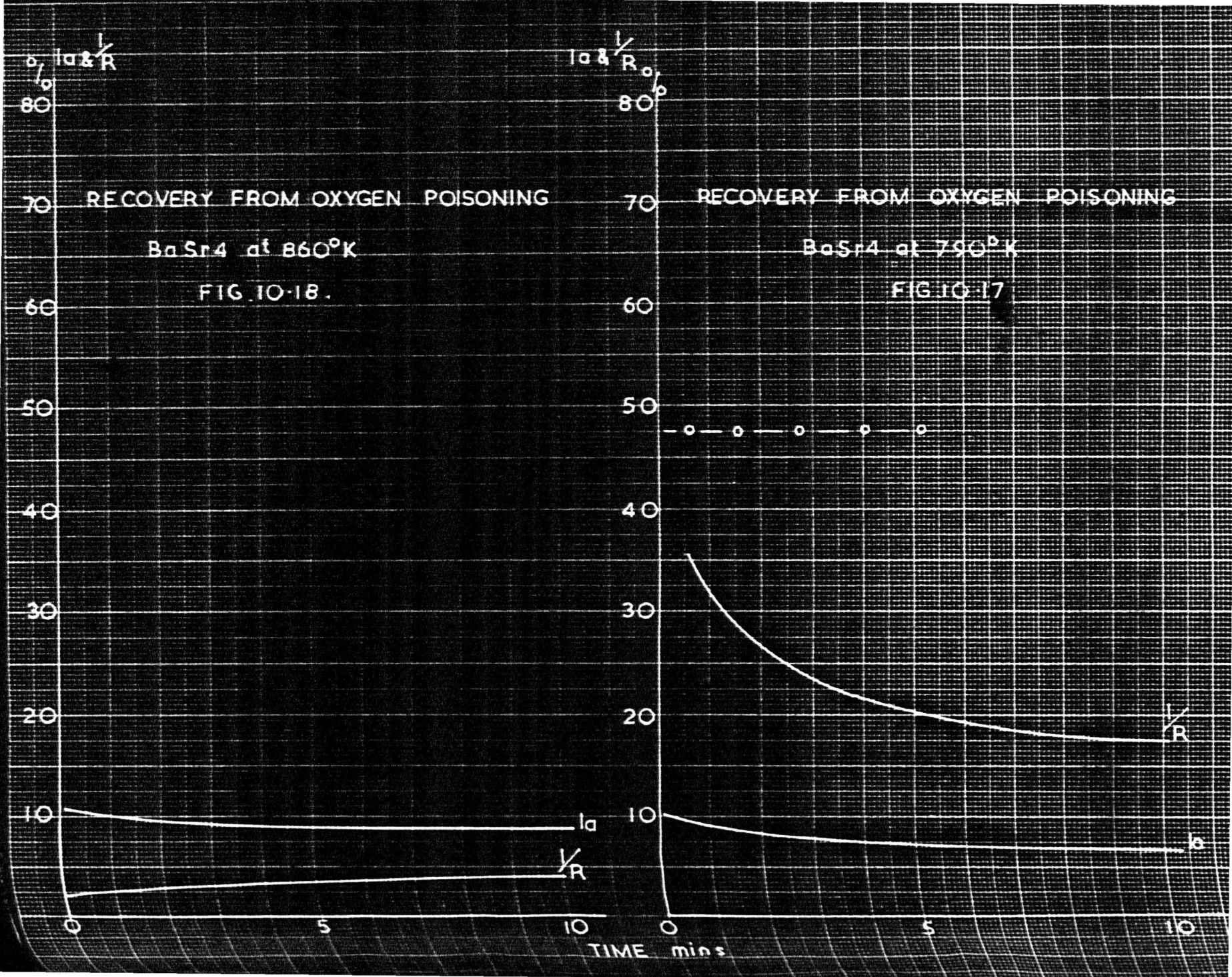
Ia & 1/R
%
80
70
60
50
40
30
20
10
0
5
10
TIME mins
RECOVERY FROM OXYGEN POISONING
BaSr4 at 860°K
FIG 10-18.
Ia
1/R
Ia & 1/R
%
80
70
60
50
40
30
20
10
0
5
10
RECOVERY FROM OXYGEN POISONING
BaSr4 at 790°K
FIG 10-17
1/R
Ia

overcome this by employing mixed oxide cathodes in subsequent measurements since these have better emission properties than BaO cathodes and hence give a measurable emission at lower temperatures.

Further Oxygen Poisoning Experiments.

Cathode BaSr4.

Fig. 10.14 gives the conductivity line for BaSr4 and indicates the points at which poisoning experiments were made. The improved emission properties of this mixed oxide cathode over those of barium oxide cathodes enable measurements to be made at a temperature where the contribution from the high temperature conduction process was negligable.

Fig. 10.15 shows the poisoning characteristic at 580°K well below the bend on the conductivity line. No recovery in emission was observed and the conductivity continued to decrease over a period of ten minutes after the poisoning source had been cut-off.

Similar behaviour was observed at 700°K and 790°K. (figs. 10.16 and 10.17) although the extent of poisoning was greater in each case. These measurements tended to confirm the effect noted in the preliminary experiments; that the conductivity at low temperatures is slowly poisoned by oxygen. This slow rate of poisoning may arise in several ways depending upon the precise nature of the conductivity mechanism in that temperature range. For example if the conductivity is mainly a surface effect on the internal crystal grains, then the rate at which oxygen will diffuse into the interstices of the oxide layer will determine the rate of reduction of the conductivity. If, however, N-type semiconduction is the predominant conduction process, oxygen could

reduce the conductivity by diffusing into the crystal lattice and so depleting the number of donor centres. Under these circumstances the rate at which oxygen could diffuse into the oxide lattice would limit the rate of reduction of the conductivity. Yet one further possibility exists, for oxygen could diffuse into the gaps between crystals in addition to diffusion over the surfaces. This could lead to a deepening of electron traps between the crystals and hence a reduction in low temperature conductivity.

The gradual reduction in conductivity after the poisoning source has been cut-off suggests that oxygen diffuses into the interior of the coating and, in one of the ways outlined above, reduces the conductivity. The diffusion of oxygen into the crystal lattice may be one of these ways although the characteristics indicate a rather rapid initial decay in conductivity not indicative of a bulk diffusion process. One method of ascertaining whether a bulk diffusion process occurs is to employ a larger poisoning species, which might be expected to diffuse less radily. Sulphur was chosen for this purpose since chemically it is very like oxygen and possesses a larger ion size.

Sulphur Poisoning Experiments.

In addition to the reason outlined in the preceeding paragraph, sulphur was chosen as a second poisoning species because it could be generated in situ in a similar manner to oxygen by warming a filament coated with molybdenum disulphide (MoS_2)

The best quality molybdenum disulphide, supplied by Messrs. Hopkin and Williams Ltd., was employed. This was mixed to a paste with amyl acetate and a little collodion and applied to an alumina coated tungsten

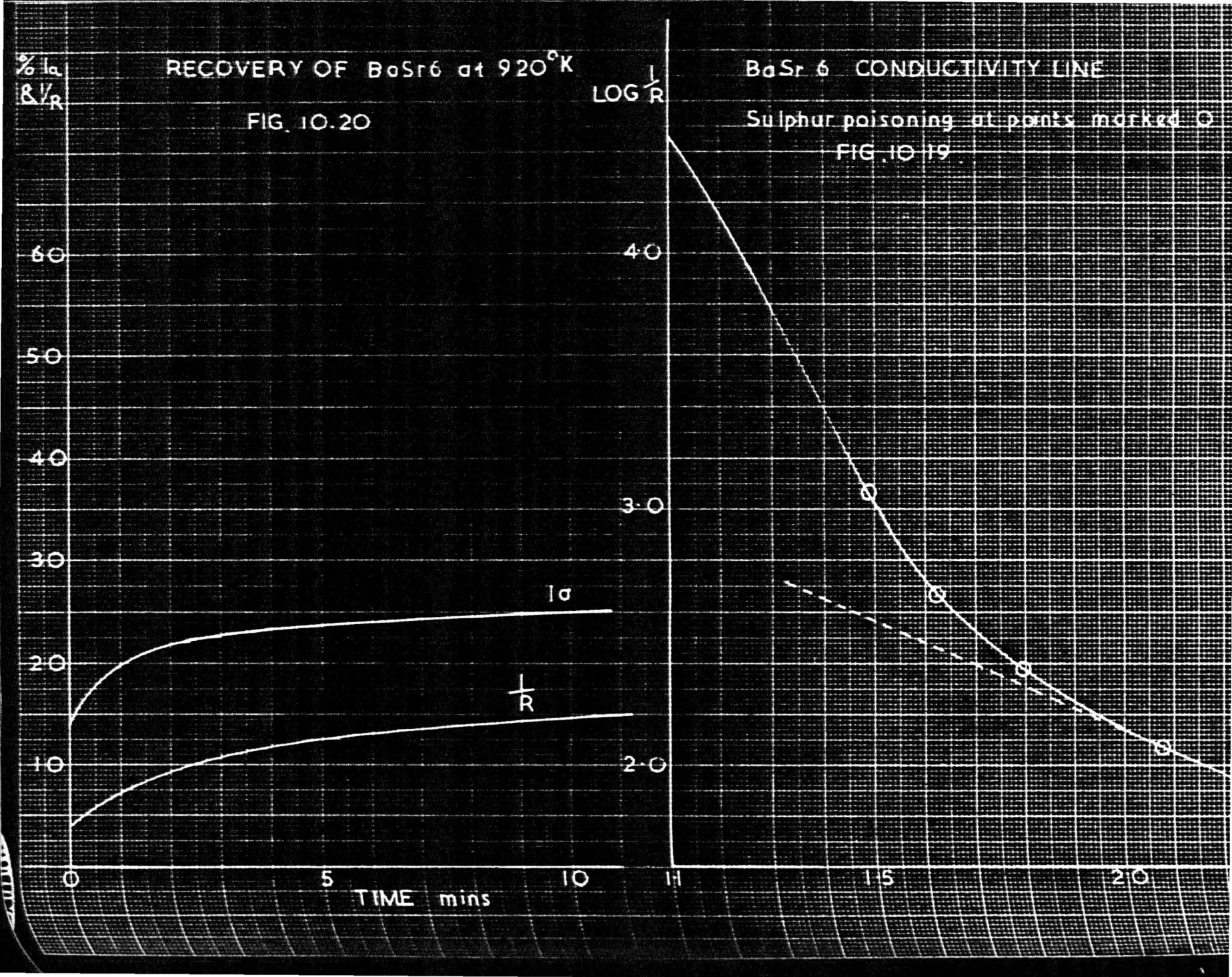
% Iσ & 1/R
RECOVERY OF BaSr6 at 920°K
FIG. 10.20
60
50
40
30
20
10
0
5
10
TIME mins
Iσ
1/R
1/R LOG
4·0
3·0
2·0
1·1
1·5
2·0
BaSr 6 CONDUCTIVITY LINE
Sulphur poisoning at points marked O
FIG. 10 119

wire mounted in the vacuum tube in just the same manner as the oxygen filament described above. A preliminary experiment was made to ascertain at what temperature the filament would produce small quantities of sulphur vapour. This was found to be 350°C and accordingly the baking schedule of vacuum tubes containing sulphur poisoning filaments was adjusted so that baking at 250°C for at least 24 hours could be arranged in order to ensure adequate degassing of the glass.

A further preliminary experiment was arranged to ascertain if the emission would recover after admitting sulphur vapour to the cathode. Recovery at an elevated temperature -900°C was found to occur after poisoning the emission to 10% of its initial value. On applying 50v. to the anode during this recovery a deep blue glow was observed in the anode-cathode space which was interpreted to be due to the ionisation of the liberated sulphur. This glow diminished and disappeared as the activity of the cathode increased, presumably due to the action of the barium getter deposit within the tube. Several weeks after seal-off and gettering and a score of poisoning experiments the tube was still quite 'hard' indicating that the low temperature bake at 250°C was satisfactory.

Cathode BaSr6.

The effect of admitting sulphur to the cathode was investigated in precisely the same manner as that recorded above for oxygen. At 920°K (fig. 10.20) the conductivity was extensively poisoned by sulphur but both emission and conductivity recovered once the poisoning source

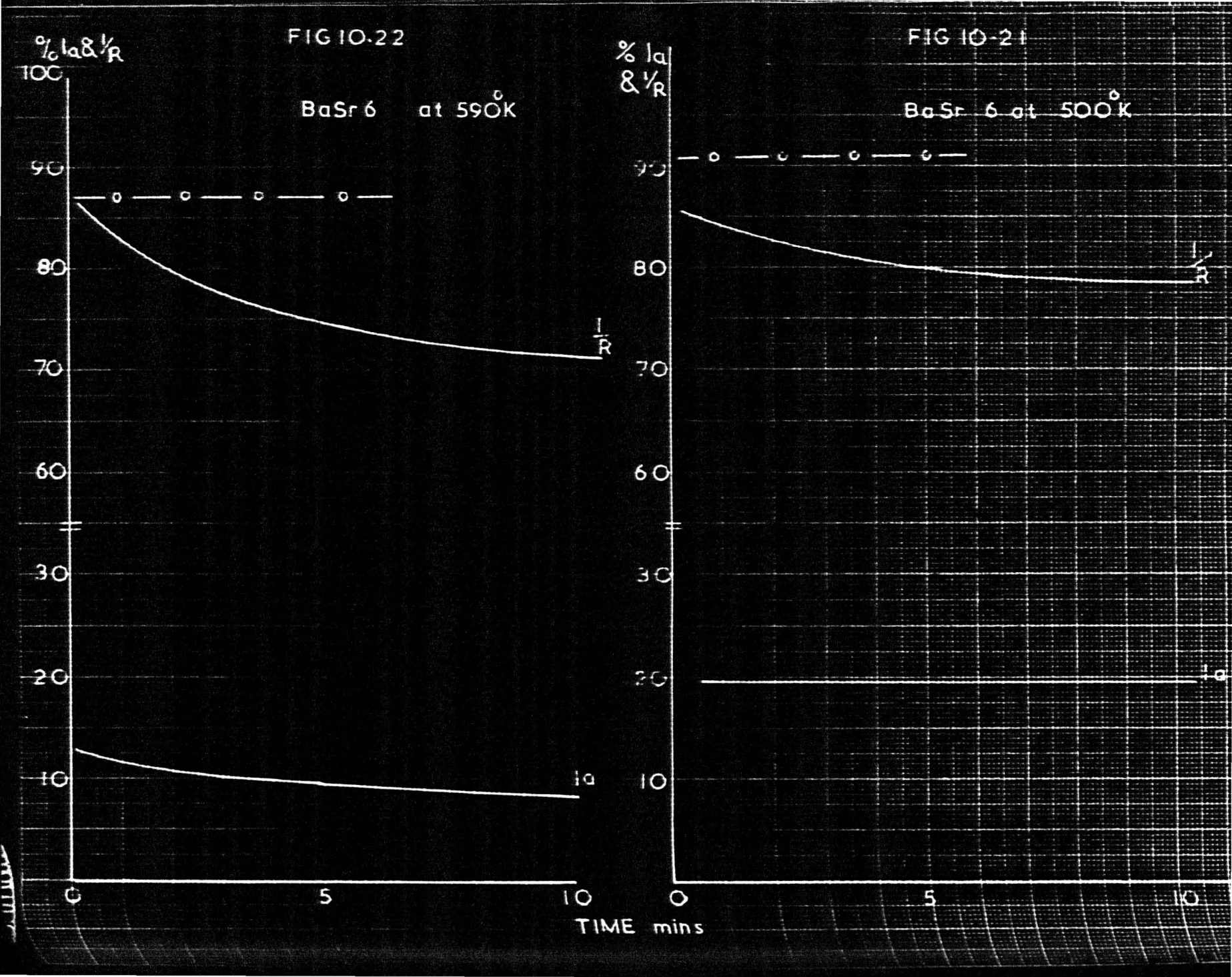
FIG 10.22
% Ia & 1/R
100
90
80
70
60
30
20
10
0
5
10
BaSr 6 at 590°K
1/R
Ia
FIG 10-21
% Ia & 1/R
90
80
70
60
30
20
10
0
5
10
BaSr 6 at 500°K
1/R
Ia
TIME mins

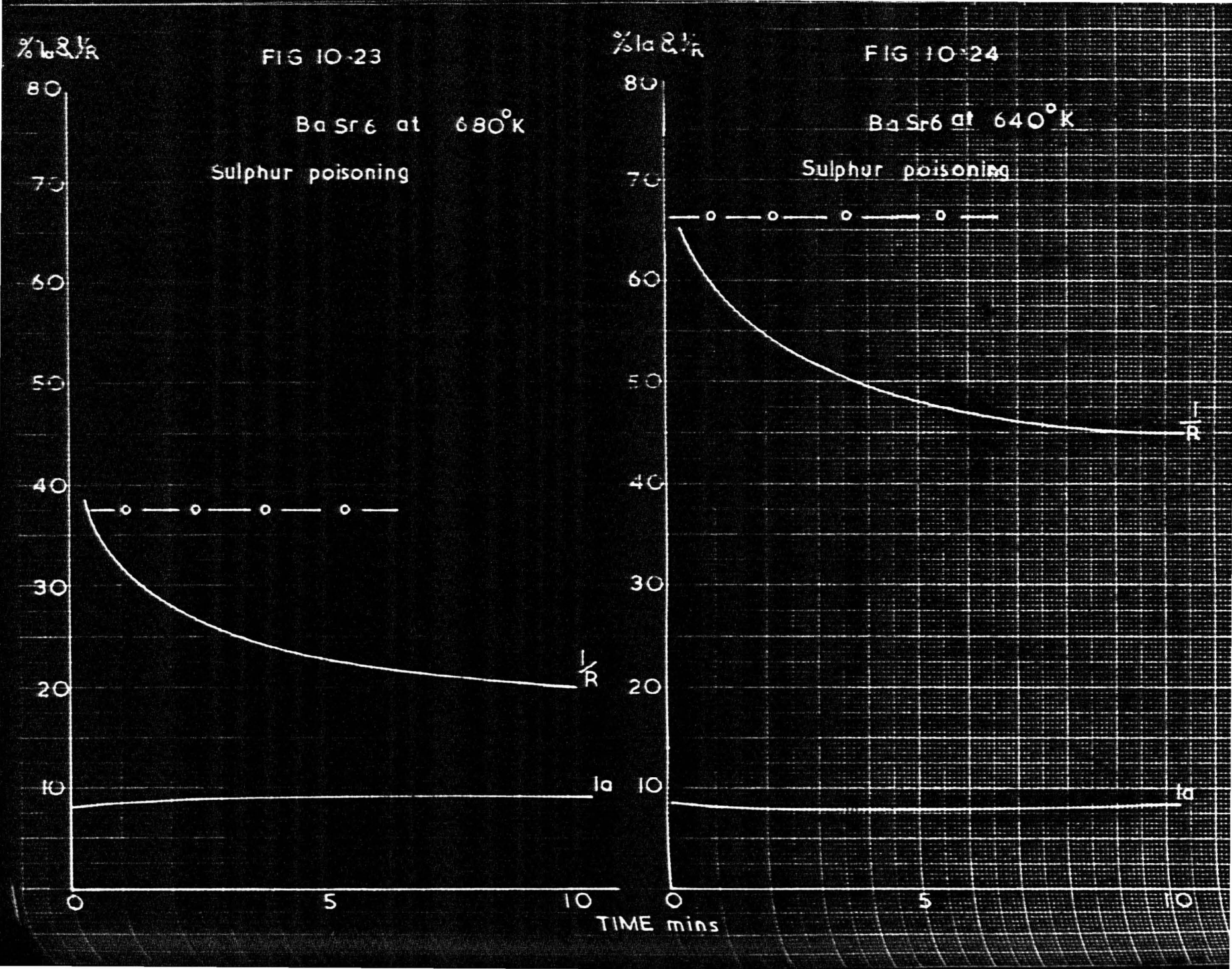
%Ia & I/R
FIG 10-23
Ba Sr6 at 680°K
Sulphur poisoning
80
70
60
50
40
30
20
10
I/R
Ia
0
5
10
%Ia & I/R
FIG 10-24
Ba Sr6 at 640°K
Sulphur poisoning
80
70
60
50
40
30
20
10
I/R
Ia
0
5
10
TIME mins

was cut-off. Four poisoning experiments were made at lower temperatures as indicated in fig. 10.19. Only one of these (at 500°K) was actually on the low temperature section of the conductivity v. temperature line. However the contribution from the low temperature process to the total conductivity is recorded by a broken line on each poisoning characteristic. This is obtained from fig. 10.19 by producing low temperature section of the curve towards the ordinate axis (shown as a broken line). The contribution of the low temperature process may then be obtained at each temperature at which a poisoning experiment was performed.

The results obtained are shown in figs. 10.21 - 24. Behaviour very similar to that exhibited by a cathode poisoned by oxygen was observed. Again a gradual decrease of conductivity after poisoning was noted. These results were encouraging in that no pronounced difference from oxygen poisoning-like behaviour was observed indicating that sulphur behaved in a similar way to oxygen when admitted to a cathode. Complete recovery from each poisoning experiment was obtained by increasing the cathode temperature to 900°C and applying 50v. to the anode, suggesting that no permanent change in the emitting surface of the cathode had occurred.

Sulphur and Oxygen Poisoning Comparative Measurements.

In this section the results of oxygen and sulphur poisoning experiments on three cathodes are described. The experimental tubes each contained an oxygen and a sulphur producing filament, mounted so that

FIG. 10.26

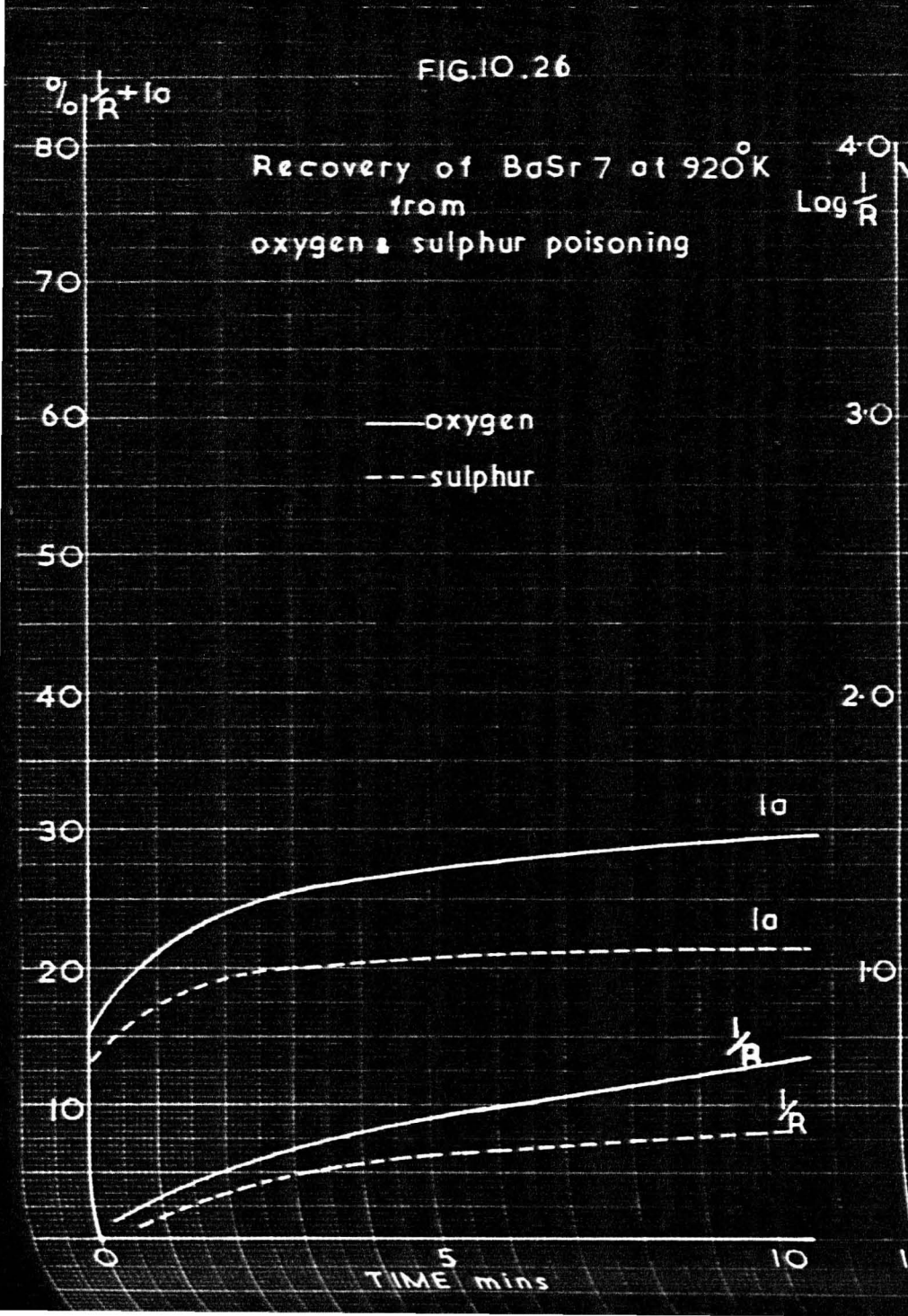

FIG 10.25

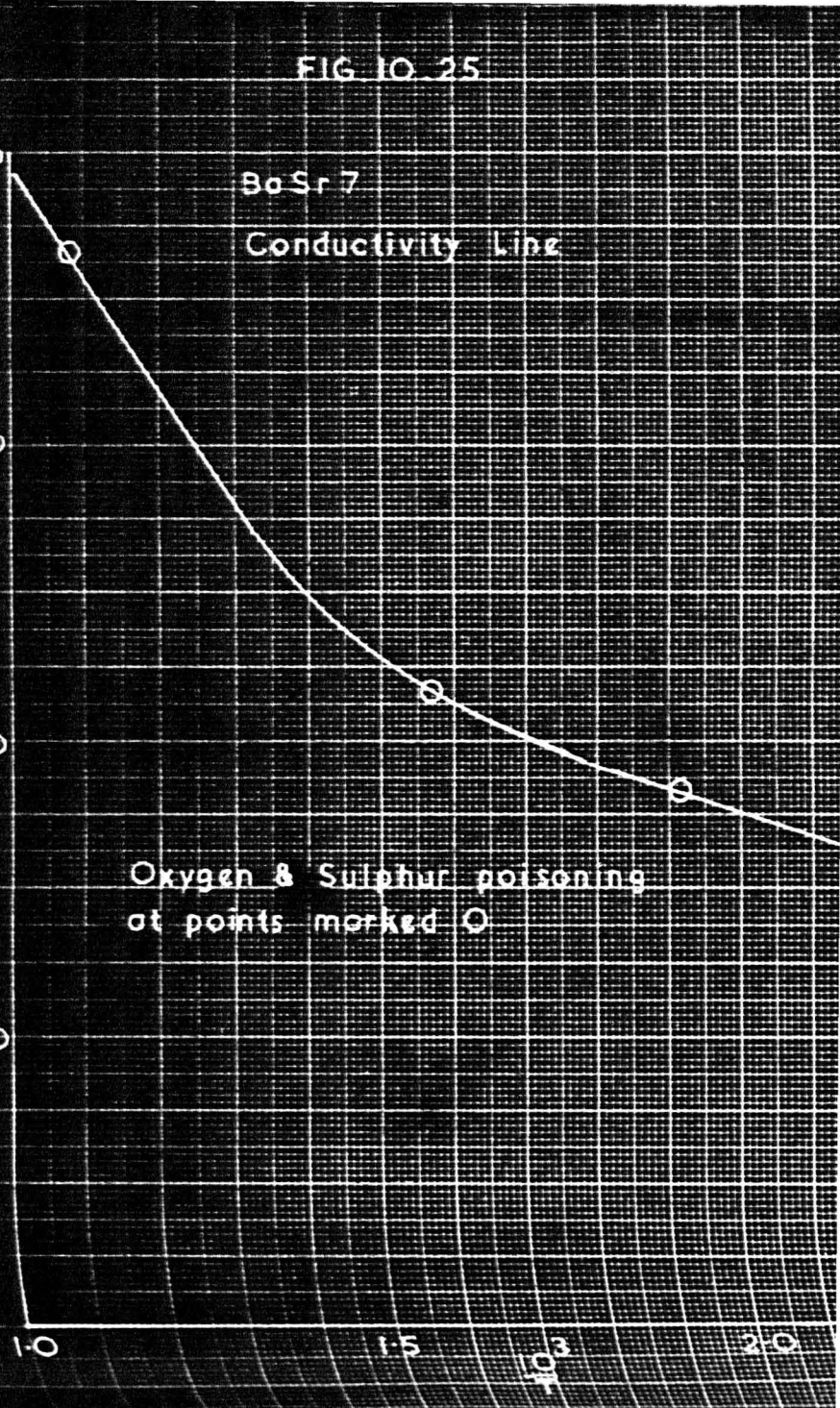

FIG. 10-27

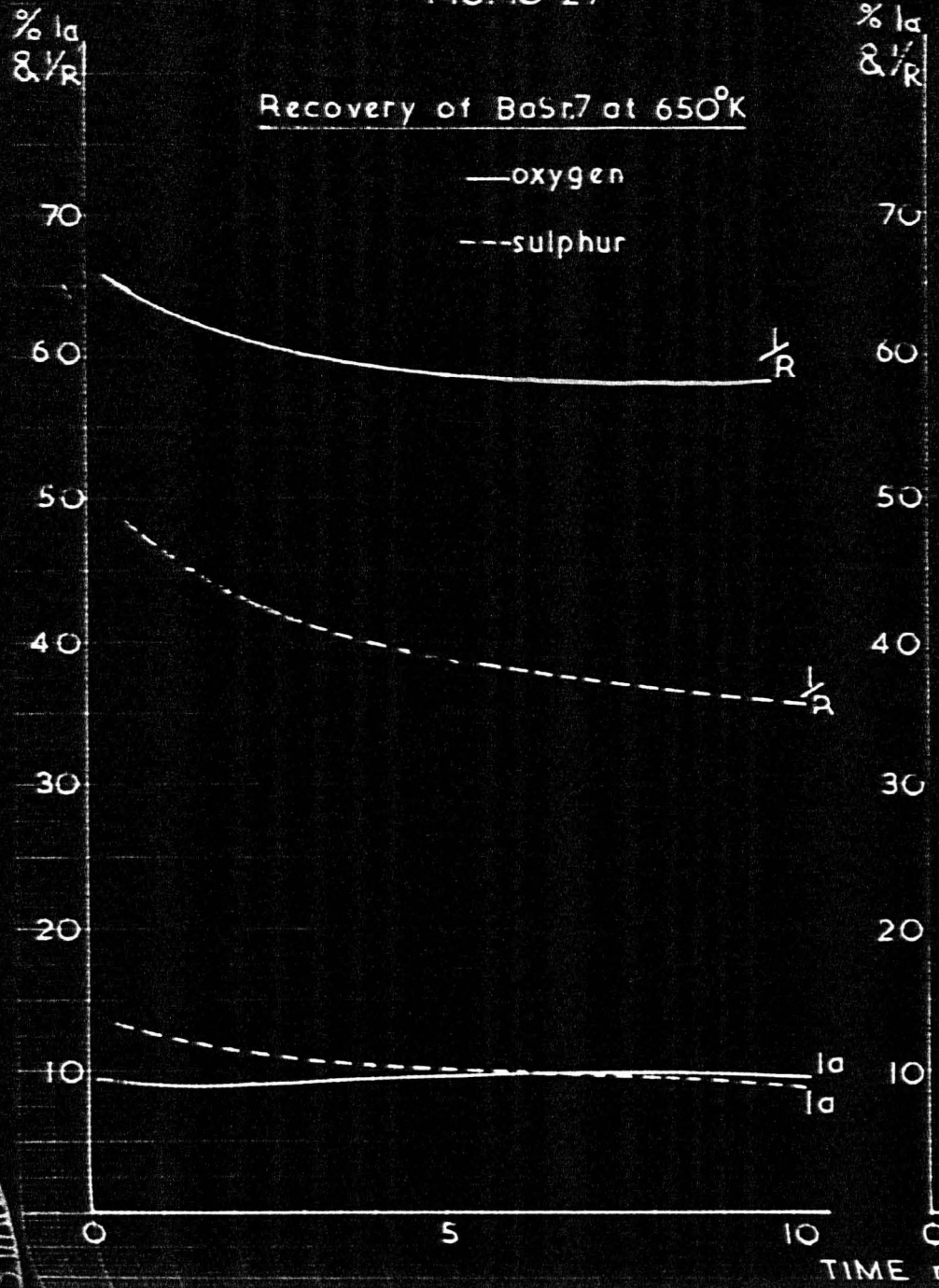

FIG. 10-28

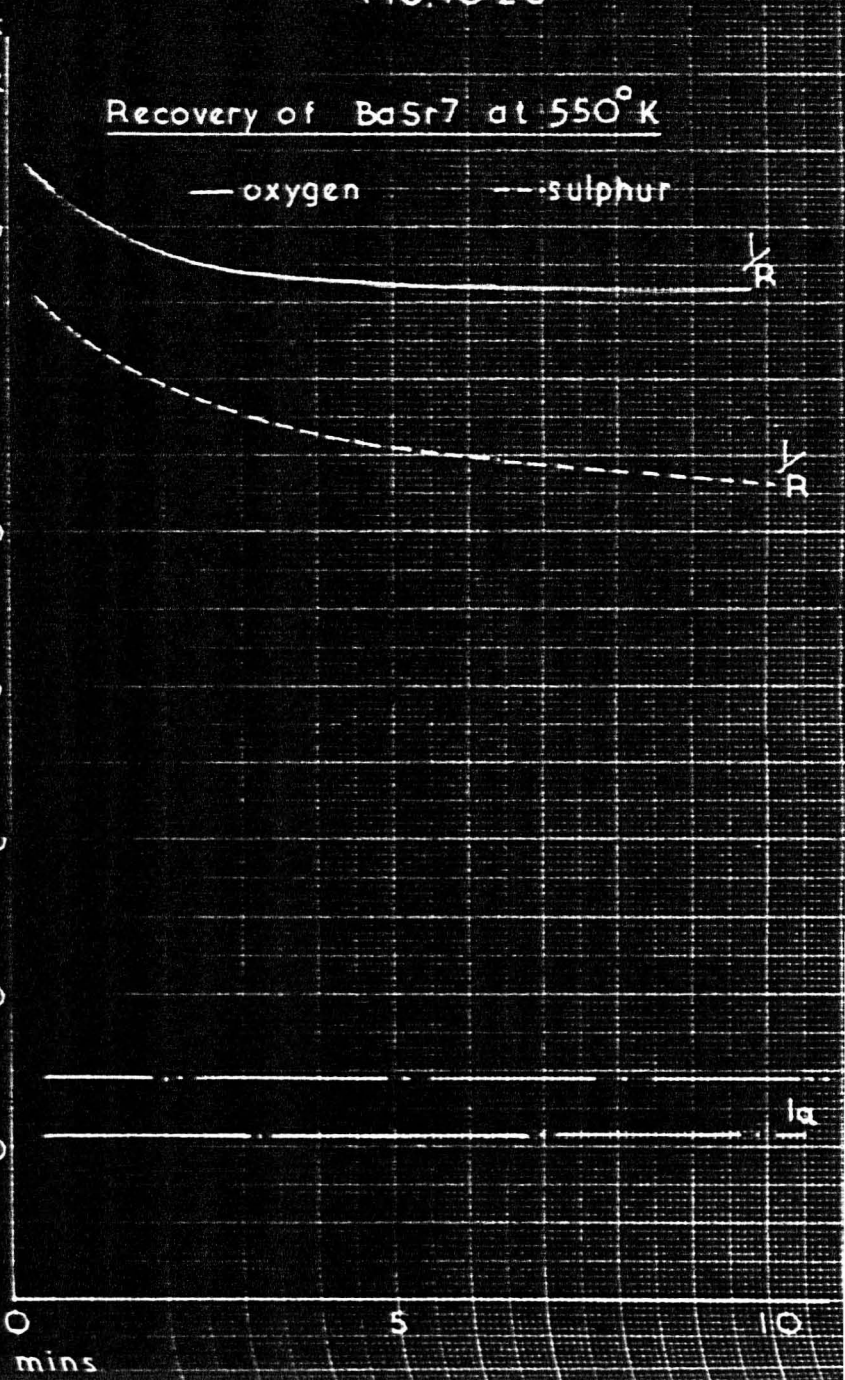

both "viewed" the cathode through the anode slit but did not view each other. This was to prevent material from being evaporated from one filament to the other.

Cathode BaSr7.

Fig. 10.25 shows the conductivity line and the points at which oxygen and sulphur poisoning attacks were made. At high temperatures fig. 10.26 recovery of both emission and conductivity occurs in agreement with previous results. Sulphur appears to poison the cathode to a greater extent than oxygen and is not liberated so rapidly during recovery.

In the low temperature region figs. 10.27 and .28 an initial decrease during poisoning occurs so that in the case of oxygen poisoning the characteristics become horizontal after a few minutes. The sulphur poisoning characteristics however indicate a continued poisoning effect after the initial decrease in conductivity during poisoning. These results seemed to indicate that most of the poisoning occurred during the time in which the emission was reduced to 10% as oxygen or sulphur was admitted. Conductivity measurements could not be made during the actual poisoning period (usually a minute or so).

Cathode BaSr8.

Oxygen and sulphur poisoning measurements were made on this cathode as before but the technique was varied slightly. Instead of admitting oxygen or sulphur slowly to the cathode, the emission was reduced very rapidly to 10% of its initial value. This enabled the initial portion of the poisoning characteristic to be observed, howbeit

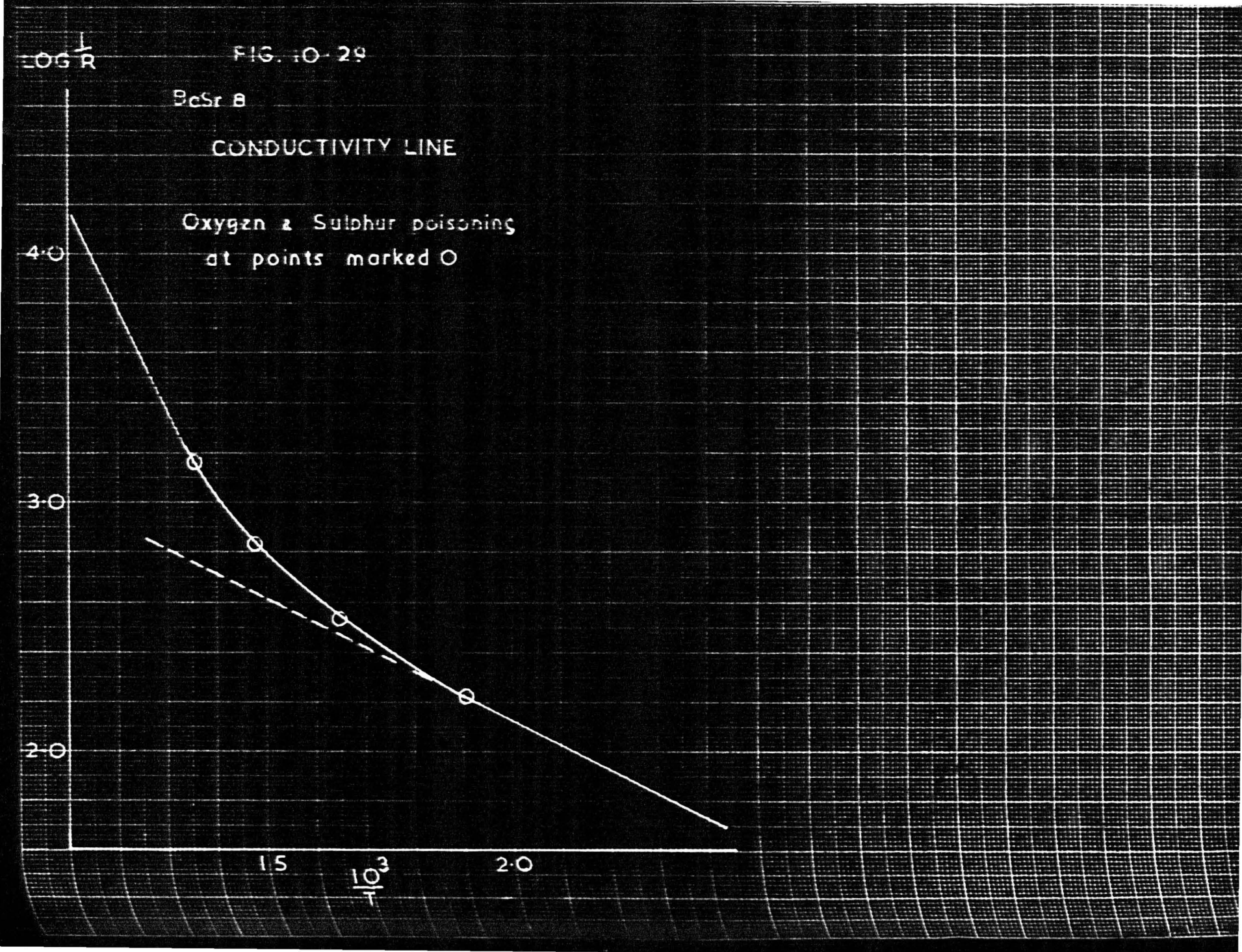
LOG 1/R
FIG. 10-29
BeSr B
CONDUCTIVITY LINE
Oxygen & Sulphur poisoning
at points marked O
4·0
3·0
2·0
1·5
2·0
10³/T

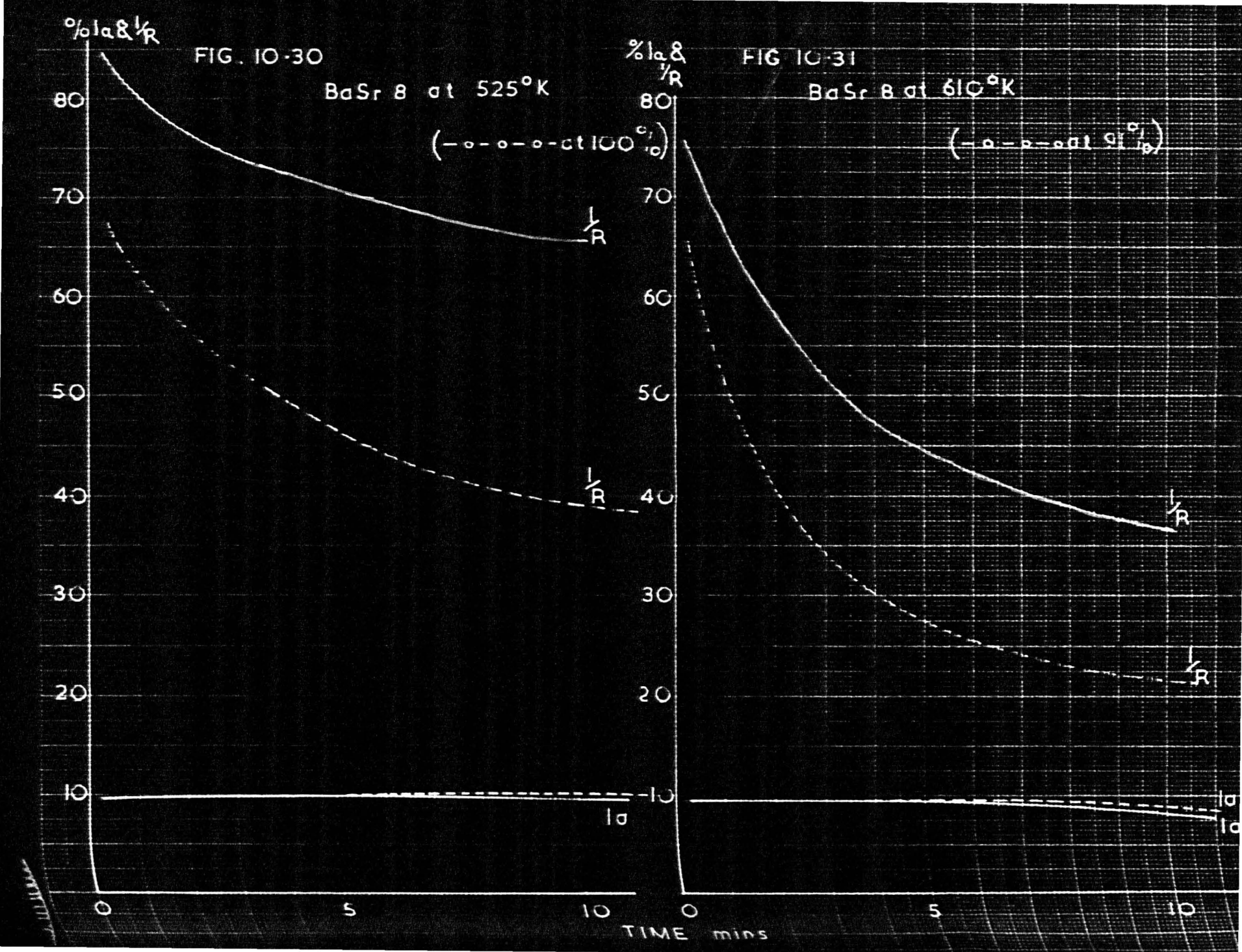
%Ia & 1/R
FIG. 10-30
BaSr 8 at 525°K
(-o-o-o-at 100°C)
80
70
60
50
40
30
20
10
1/R
1/R
Ia
0
5
10
%Ia & 1/R
FIG 10-31
BaSr 8 at 610°K
(-o-o-o-at 91°C)
80
70
60
50
40
30
20
10
1/R
1/R
Ia
Ia
0
5
10
TIME mins

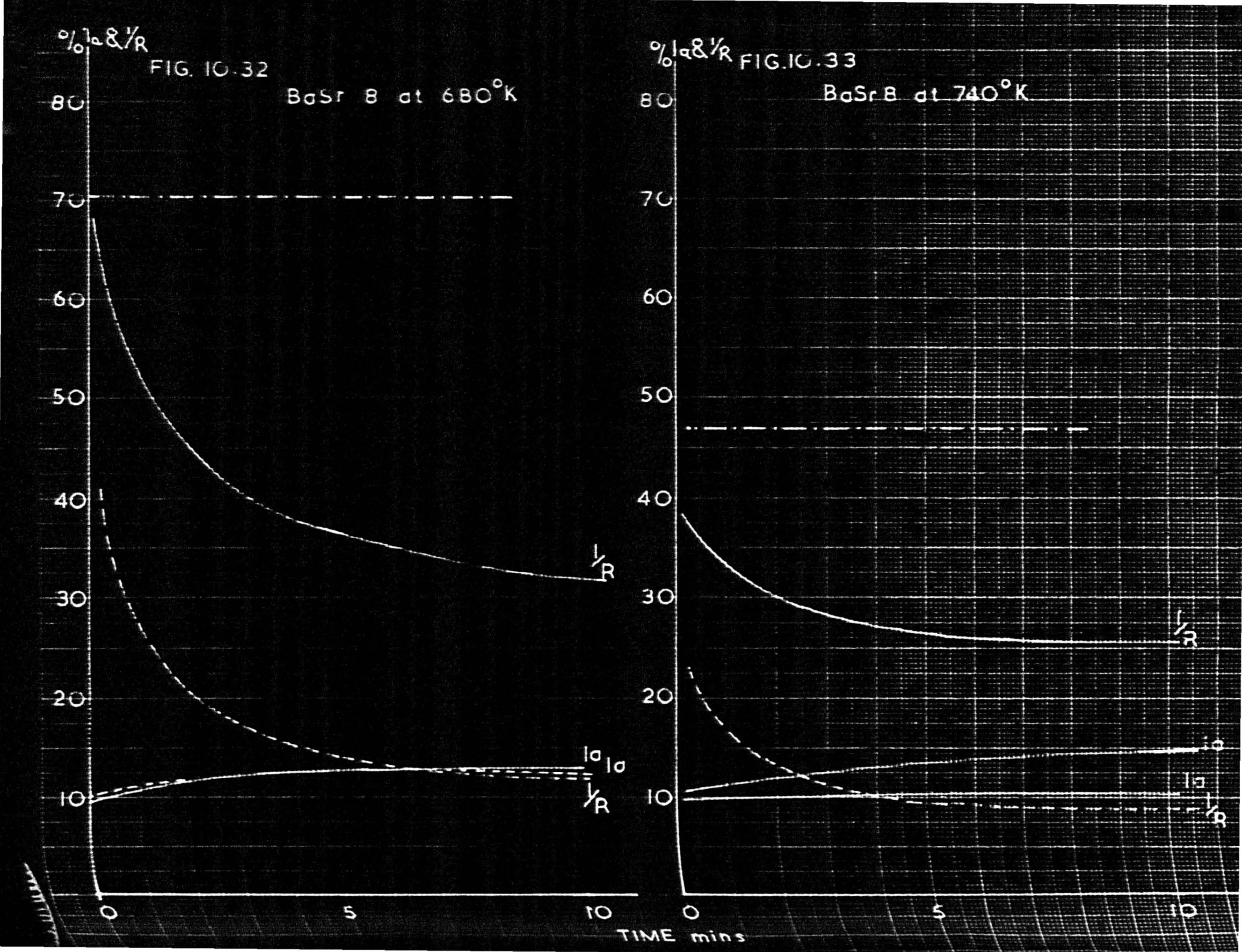
%Ia&1/R
FIG. 10.32
BaSr 8 at 680°K
80
70
60
50
40
30
20
10
1/R
Ia
Ia
1/R
0
5
10
%Ia&1/R
FIG.10.33
BaSr 8 at 740°K
80
70
60
50
40
30
20
10
1/R
Ia
Ia
1/R
0
5
10
TIME mins

under slightly different conditions of oxygen or sulphur pressure than hitherto.

Fig. 10.29 shows the conductivity line and Figs. 10.30 - .33 the poisoning characteristics. It is interesting to note that the extent of reduction in conductivity is much greater than at corresponding temperatures for cathode BaSr7. Again sulphur appears to have a greater effect upon the conductivity than does oxygen. The rapid initial decrease in conductivity observed does not argue for a bulk diffusion process but rather suggests that a surface conductivity process is impaired by admission of oxygen or sulphur.

Cathode BaSr9.

Oxygen and sulphur poisoning experiments made on this cathode gave results which, in general, were in agreement with those obtained previously. Poisoning at a fairly slow rate was employed; the emission being reduced to 10% of its initial value in approximately 1 minute by the controlled admission of oxygen or sulphur to the cathode. Fig. 10.34 shows the conductivity line and the points at which poisoning experiments were made. At 910°K (fig. 10.35) the conductivity was excessively poisoned by both oxygen and sulphur and recovery was very slow. However the emission showed a rapid recovery characteristic. At lower temperatures (figs. 10.36 - 10.39) the greater poisong effect of sulphur is clearly evident. Again there are indications in all these curves of a rapid initial poisoning of the low temperature conductivity, the initial level of which is indicated on the curves by the borken (-.-.) line. This was obtained by extrapolating the low temper-

FIG. 10-35

BaSrS at 9.0 °K

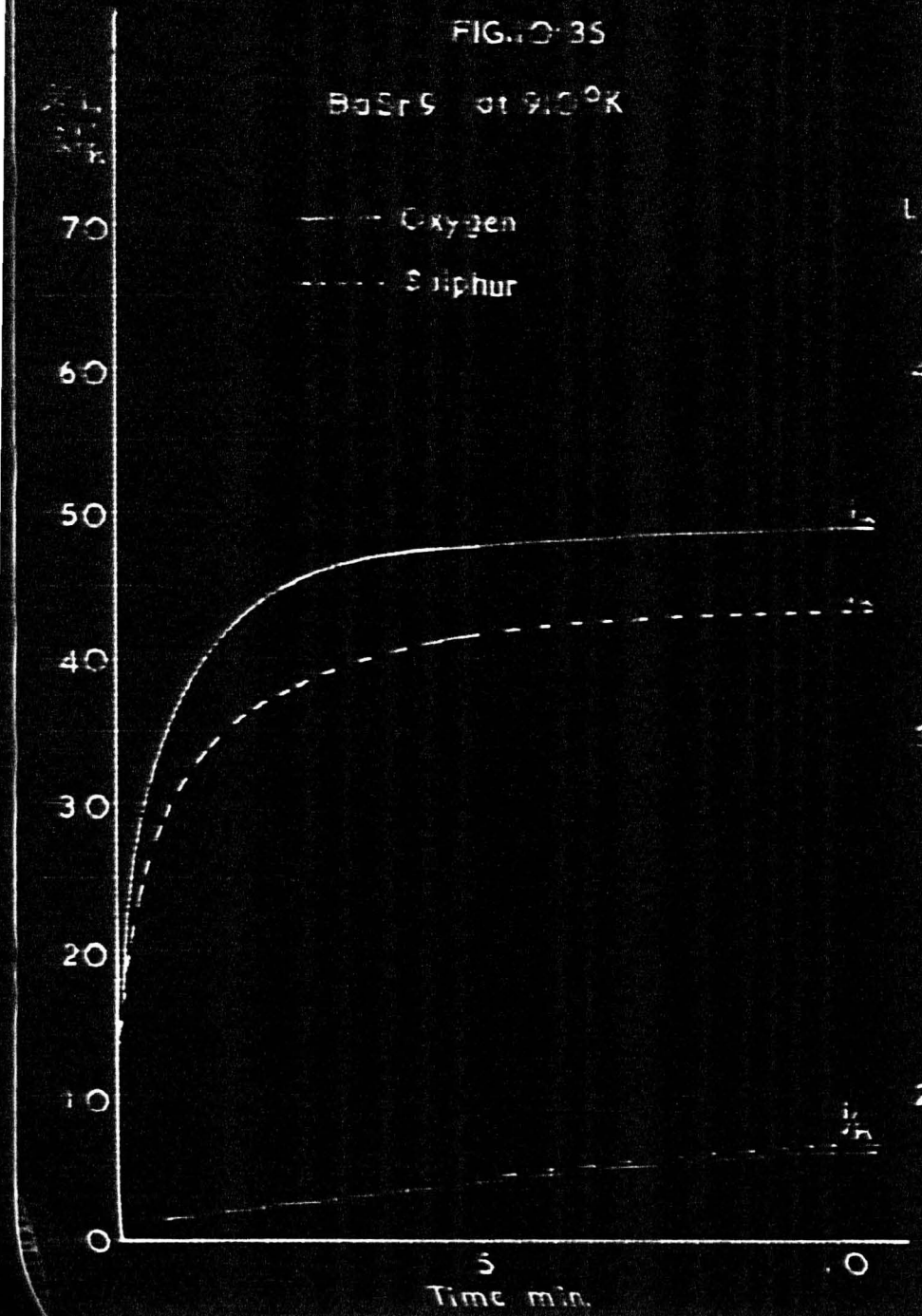

FIG. 10-34

BaSr9 CONDUCTIVITY LINE

Sulphur & Oxygen poisoning at points marked C

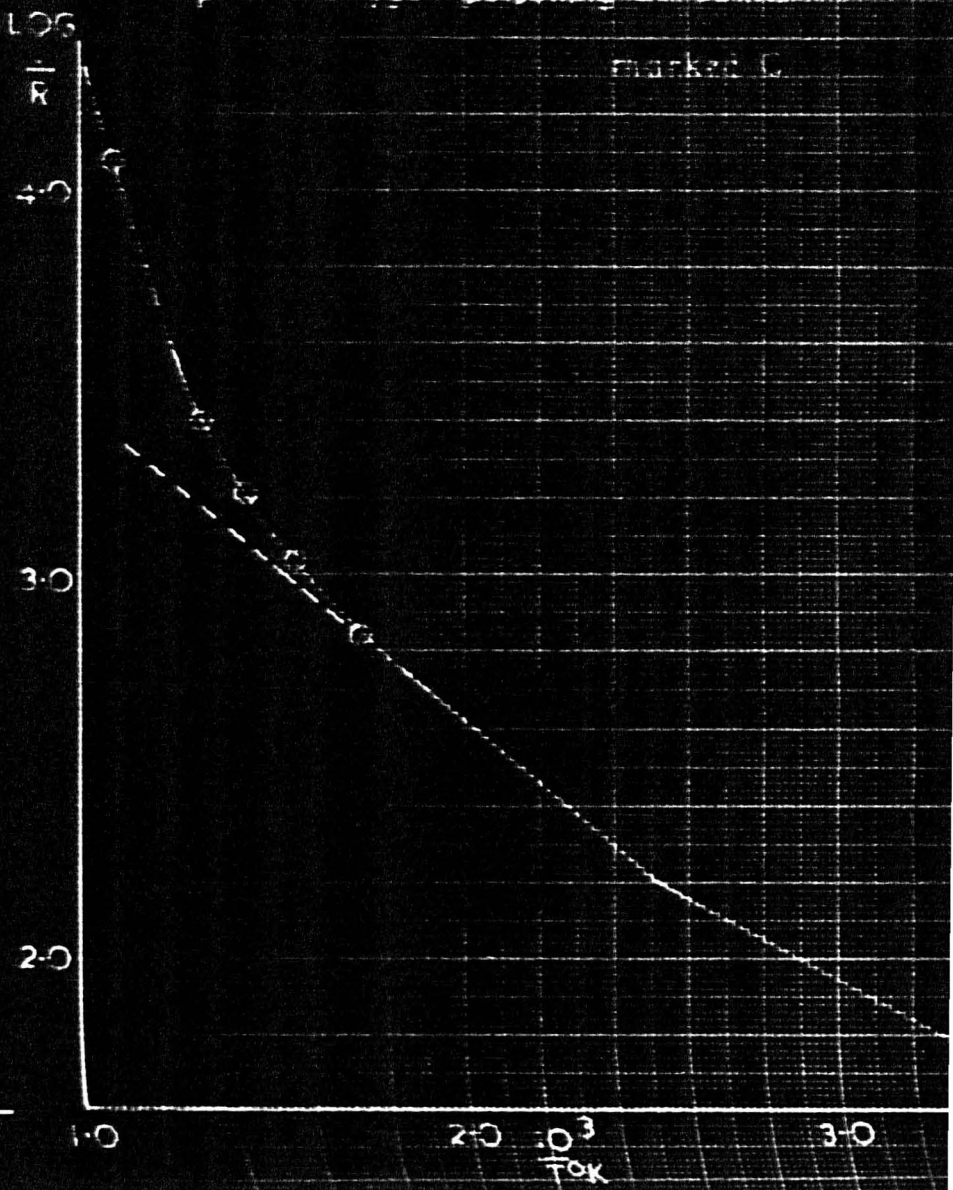

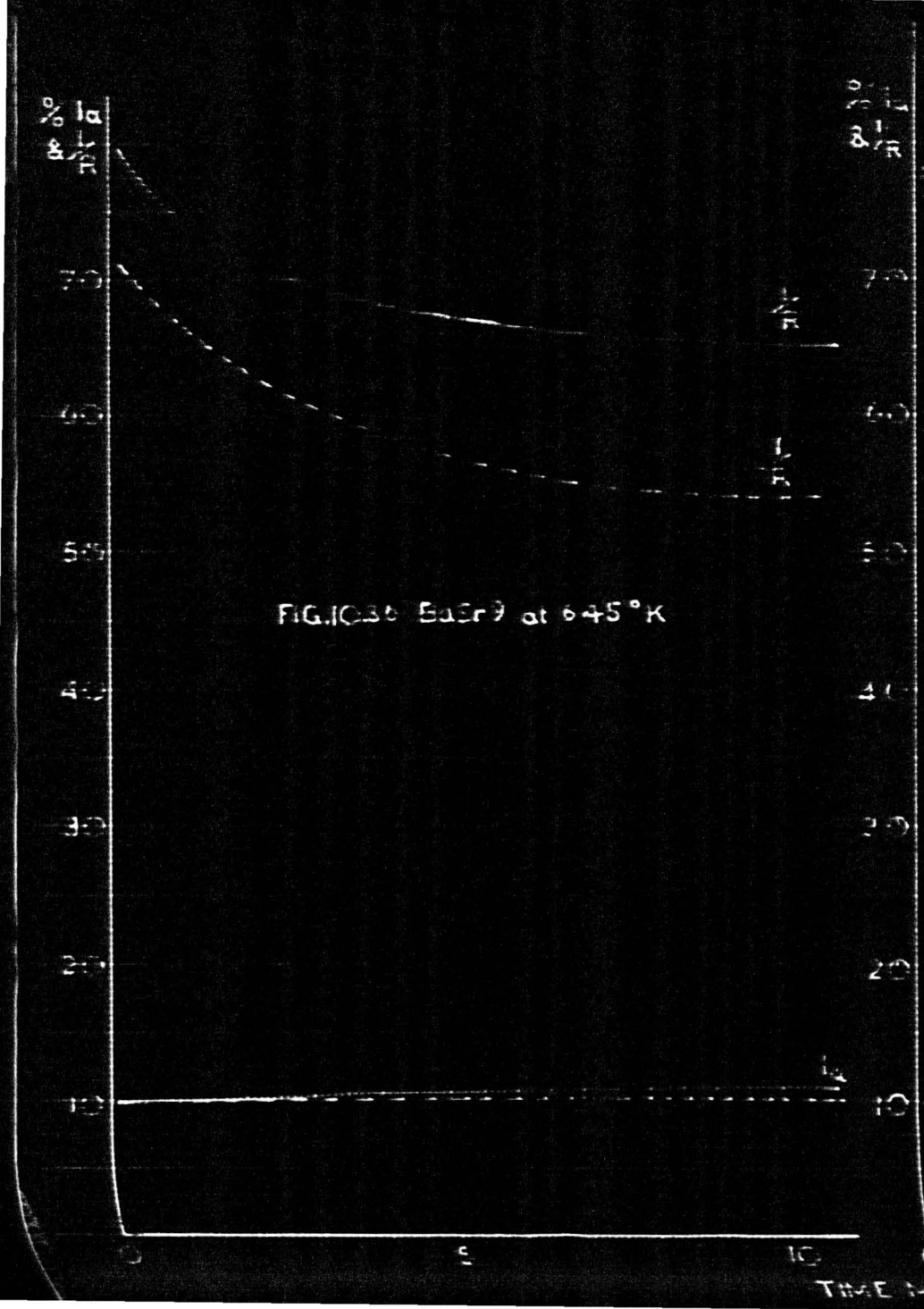

FIG.(C36 BaBr) at 645°K

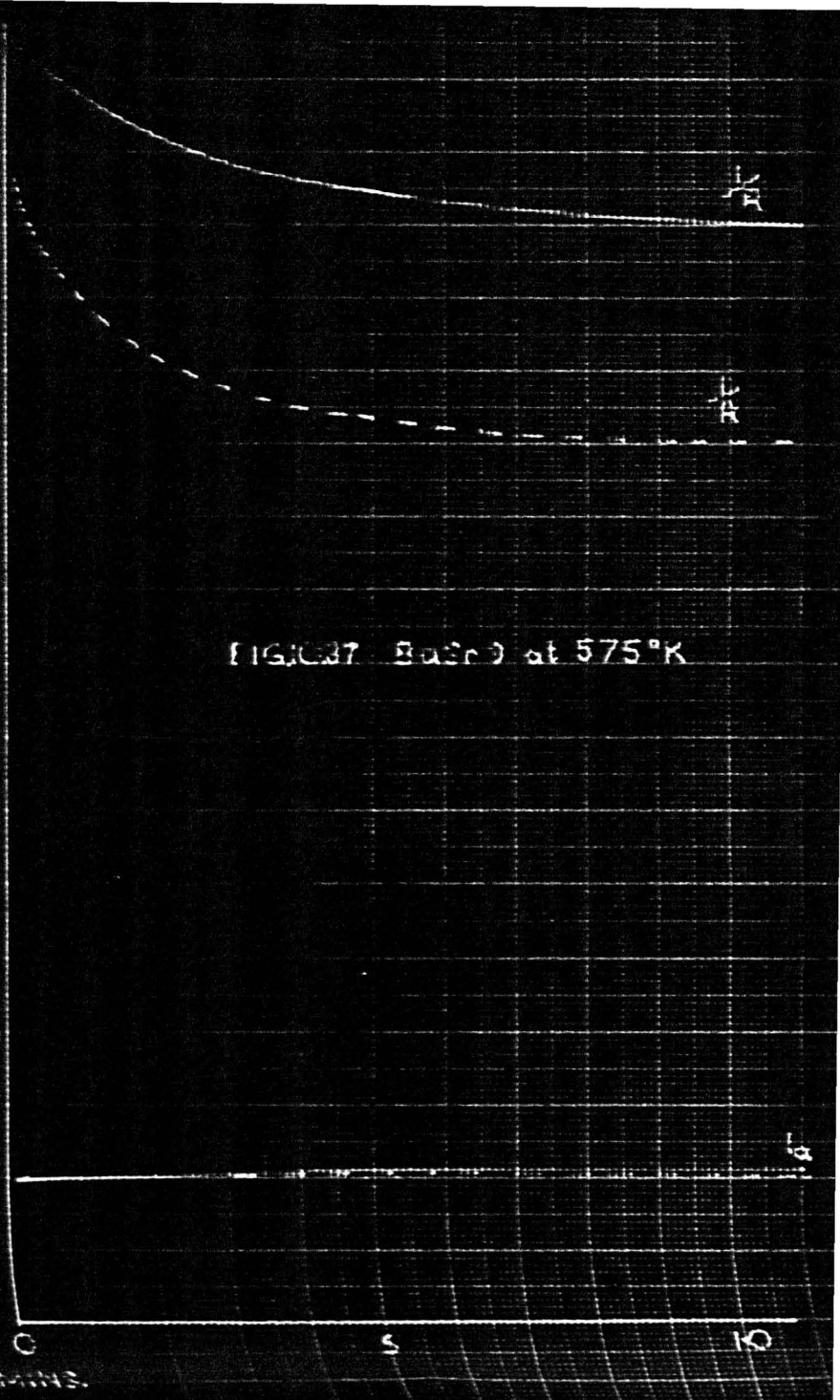

FIG.(C37 BaBr) at 575°K

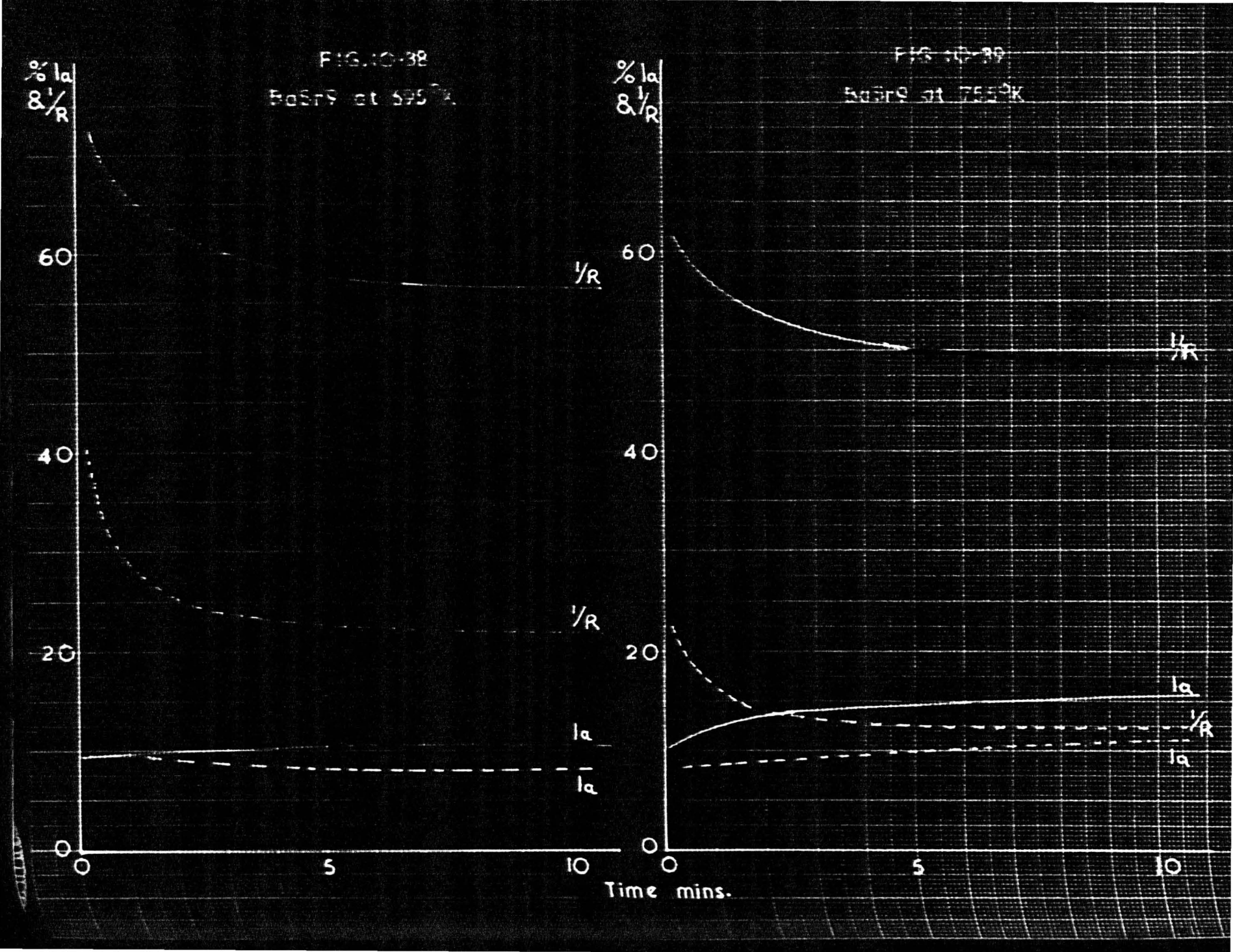
FIG. 10-38
BaSr9 at 595°K.
% Ia & 1/R
60
40
20
0
1/R
1/R
Ia
Ia
0
5
10
FIG. 10-39
BaSr9 at 755°K
% Ia & 1/R
60
40
20
0
1/R
Ia
1/R
Ia
0
5
10
Time mins.

ature section of the conductivity line as explained above.

Discussion of Results of Oxygen-Sulphur Poisoning Experiments.

The results obtained from measurements on tubes BaSr7 - BaSr9 are not sufficiently reproducible to warrant further experiments of this kind. However some qualitative evidence is afforded by these experiments and this is discussed below.

The general effect noted in nearly all the poisoning experiments made in or near to the low temperature region of the conductivity line is the rapid decrease in conductivity at the onset of poisoning. This is most readily interpreted in terms of the reduction of a surface conductivity process over the crystallites by oxygen or sulphur. Such an interpretation is in agreement with the results reported in Section 2 of this work which suggested that the movement of barium ions over the crystallite surfaces might be a contributory low temperature conduction process.

No obvious difference emerges from these results between the conductivity characteristics for sulphur and oxygen poisoning. If a bulk diffusion process does occur and the conductivity is due to a depletion of the number of donor centres by the poisoning species, this is not indicated by the shape of the characteristics. The difference in ion sizes: O^{-}_{16} 1.34 Å S^{-}_{32} 1.72 amounting to 28% of the oxygen ion size might be expected to show up in a slower rate of diffusion of sulphur. Yet all the evidence points to a more rapid initial diffusion of sulphur if the conductivity characteristics are interpreted on a diffusion basis.

In all the poisoning experiments sulphur appears to poison the cathode to a greater extent than oxygen. This is explained by the fact that more sulphur is present in the region of the cathode in sulphur poisoning than oxygen in the case of oxygen poisoning. Poisoning the emission to 10% by either sulphur or oxygen involves increasing the average work function of the cathode by a definite amount, given by the equation:-

$$\Delta\phi = 4\pi M\zeta$$

where M is the average dipole moment of the adsorbed ions

ζ is the surface density of the ions

The dipole moment of the ion will be proportional to its electron attracting power. Pauling (67) lists the relative attracting powers of oxygen and sulphur as 3.5 and 2.5 respectively. On this basis more sulphur than oxygen will be required to change ϕ by the same amount. In the poisoning experiments this implies that a larger quantity of sulphur is evaporated from the filament than oxygen from the oxygen filament. Supposing that the same fraction attacks the surface of the cathode in each kind of poisoning then a larger number of sulphur molecules than oxygen molecules should penetrate into the oxide layer.

In conclusion, therefore, the results of oxygen and sulphur poisoning experiments indicate the complete reversibility of sulphur and oxygen poisoning in the high temperature region. In addition the poisoning characteristics strongly suggest that a surface conduction mechanism is operating which is impaired on admitting oxygen or sulphur

to the cathode. No evidence has been found to suggest that during poisoning oxygen or sulphur diffuses into the crystallites of the oxide layer.

FIG. II-1

OXYGEN POISONING EXPERIMENT BaSrII

Conductivity lines

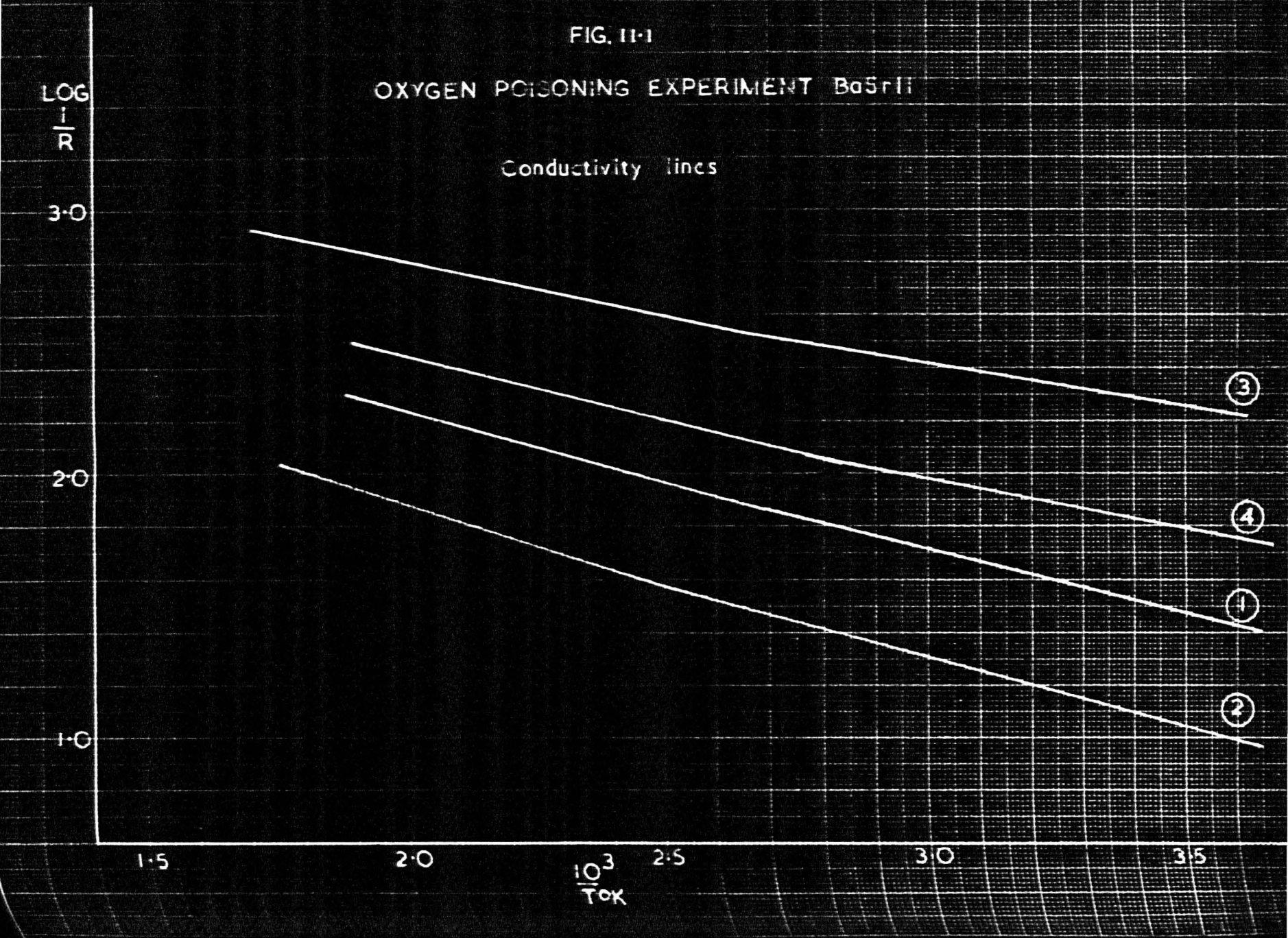

CHAPTER 11

Introduction.

The experiments described in the last Chapter suggest that the poisoning of the low temperature conduction process is a surface as opposed to a bulk phenomenon. The measurements described in Section II of this thesis revealed that the conduction process at temperatures below 600°K consisted of two mechanisms operating in parallel. Evidence was provided which suggested that the movement of barium ions over the surfaces of the internal crystal grains of the oxide layer was one of these processes and was the predominant conduction process at the lowermost temperatures. The movement of barium ions might well be impeded by the presence of oxygen on the cathode surface, and so lead to a diminution in conductivity.

In this chapter some oxygen poisoning experiments are described which enable the temperature dependence of the cathode conductivity to be measured in the poisoned state.

Experiments on Cathode BaSr11.

Two oxygen poisoning experiments were performed on this cathode in order to observe the general effect of poisoning on the conductance line. Fig. 11.1 curve 1 represents the state of the cathode before poisoning. Oxygen was admitted to the cathode, maintained at 500°K in the manner described in Chapter 10, until the emission was reduced to 10% of its initial value. When the conductivity had decreased to a constant value, after a period of 15 minutes, the temperature was reduced and conductivity vs. temperature measurements made down to

laboratory temperature. The curve obtained is shown as curve 2, fig. 11.1.

The changes in the activation energies of the two sections of the curves are given in table 1. The slope of the upper portion of the curve Q was corrected in the manner described in Chapter 7. However, the slopes Q and L were found to be very similar in each case and so the corrected values are only approximate.

Table 1

Curve	State	Q corrected eV	L eV
1	Unpoisoned	0.14	0.097
2	Poisoned with O_2	0.15(5)	0.107

This cathode was later subjected to a barium deposition experiment as described in Chapter 8 at the conclusion of which the cathode exhibited an enhanced conductivity shown by curve 3 fig. 11.1. Another oxygen poisoning experiment was performed at 500°K as described above. The conductivity in the poisoned state is represented by curve 4. Table 2 gives the values of the activation energies obtained from the slopes of the curves.

Table 2

Curve	State	Q corrected eV	L eV
3	Unpoisoned	0.12(5)	0.066
4	Poisoned	0.13	0.075

These two experiments do not lead to any significant results but do show that both L and Q are increased as a result of poisoning.

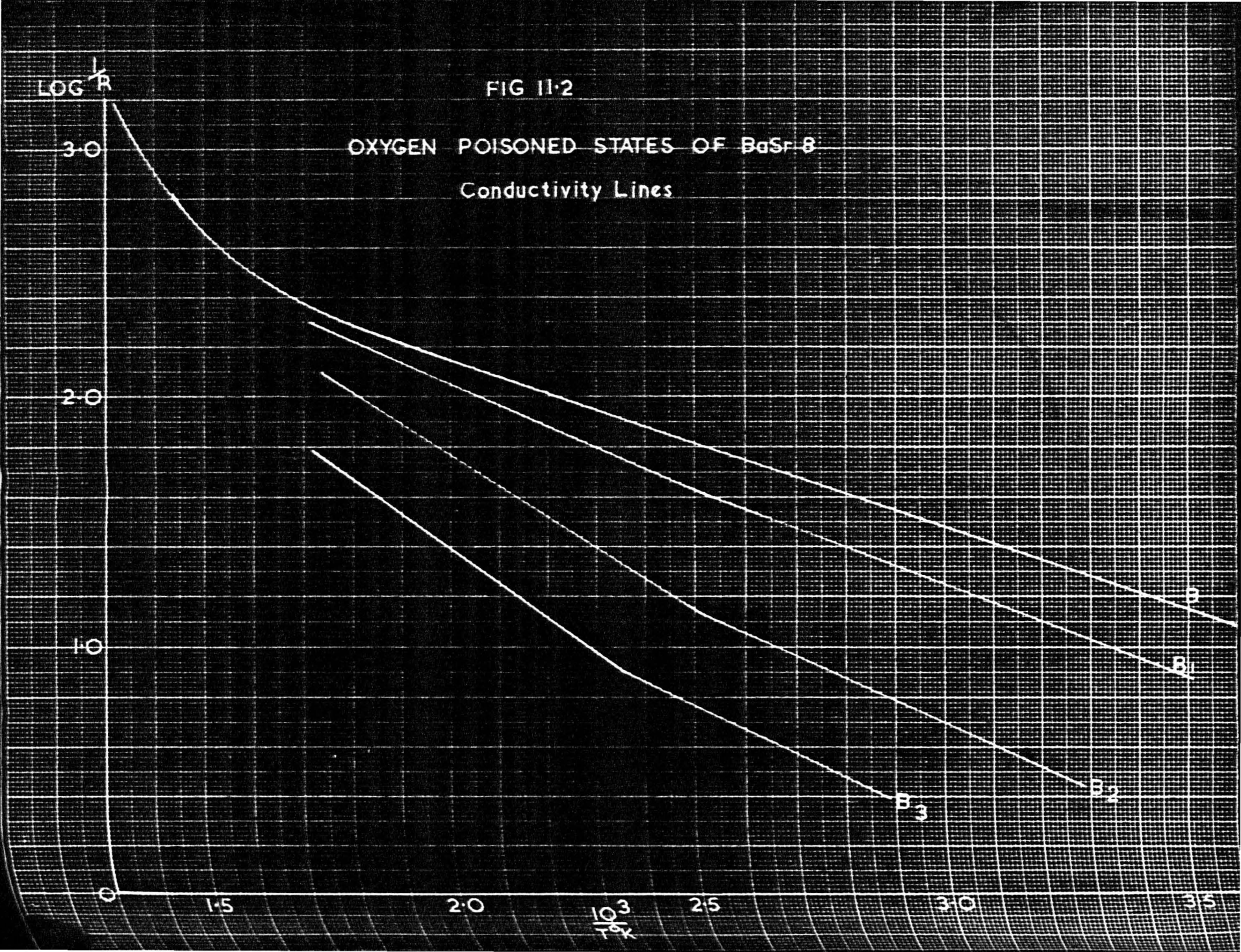
FIG 11·2
OXYGEN POISONED STATES OF BaSr·8
Conductivity Lines
LOG 1/R
3·0
2·0
1·0
0
1·5
2·0
2·5
3·0
3·5
10³/T°K
B
B1
B2
B3

Unfortunately the slopes of the two sections of each curve were very similar and so no conlusions may be drawn from the magnitude of the changes involved.

Experiments on Cathode BaSr8.

BaSr8 was chosen for these further experiments since it exhibited the unusual effects noted in Chapter 7 page 84 and shown in fig. 11.2 curve B. The conductivity curve at temperatures below 600°K failed to show two linear sections. This was assumed to be due to the predominance of the extra-low temperature conduction mechanism at all temperatures in this range.

Three oxygen poisoning experiments were performed with this cathode. The emission was poisoned to a different extent in each case, but the temperature and the initial values of the conductivity and emission were the same in each experiment. On the basis of the theory outlined on page 112 Chapter 10 this implied that different quantities of oxygen were admitted to the cathode in each experiment although it cannot be maintained that the amount was exactly proportional to the change in emission.

The three curves B_1 B_2 and B_3 obtained in these experiments are shown in fig. 11.2 and table 3 gives the values of the activation energies.

Table 3

Expt.	Poisoned to % initial I_a	Activation Energies	
		L	Corrected Q
B	Activated -	0.12	- eV
B_1	66	0.15	0.26 eV
B_2	30	0.18	0.27 eV
B_3	10	0.19	0.34 eV

In these experiments the changes were more obvious than in the case of the experiments with BaSr11. Moreover, due to the greater difference in the slopes of each section, greater reliability in the corrected values of Q was ensured.

Two important indications may be found in this table. Firstly, the extra-low temperature conduction mechanism is affected by small quantities of oxygen, but additional quantities do not produce correspondingly larger increases in the value of L. Secondly, the low temperature process with temperature dependence Q, is not affected by small quantities of oxygen. This is deduced from the fact that Q undergoes only a slight change from 0.26 to 0.27 when the quantity of oxygen added is approximately doubled. However, larger quantities of oxygen produce a greater change in Q suggesting that this conduction process is affected by oxygen.

The change from the linear curve B to the curves with two linear sections B_1 - B_2 on poisoning with oxygen lends support tothe explanation given in Chapter 7 page 84 to account for the linearity of

of the conductivity curve of BaSr8 after 170 hours operation. This was to the effect that the cross section of the ionic conduction process was so high in this cathode that at all temperatures below 600°K ionic conduction was predominant. The fact that Q does not change appreciably for small additions of oxygen suggests that the value of Q given in the tables is the activation energy of the low temperature conduction process in this cathode. This would be in agreement with the values obtained after correction for several other cathodes as described in Chapter 7.

Conclusions.

The results of poisoning experiments described in this Chapter support the suggestion that oxygen poisoning is partly a surface phenomenon at temperatures below 600°K. The value of the temperature dependence of the extra low temperature process was found to increase appreciably on admitting even small quantities of oxygen to the cathode. This accords with the suggestion that conductivity in this temperature region is partly due to the movement of barium ions over the surfaces of the crystal grains, for the presence of oxygen on such surfaces would impede the movement of the barium ions.

However, the admission of larger quantities of oxygen to the cathode affects the value of Q suggesting that the second low temperature conduction process is impaired by oxygen, but not so readily as the surface process.

It is interesting to speculate on the nature of the second conductivity mechanism and so to see how this might then be affected by

oxygen. If excess (*N*-type) semiconduction in the predominant process oxygen could reduce the conductivity in two ways; either by entering the crystal lattice and occupying donor sites (on the assumption that these are oxygen ion vacancies) or by diffusing into the cracks between crystals thus forming a barrier to crystal to-crystal conduction. This latter process could still be the mechanism of oxygen poisoning even if the bulk conduction process in the crystal grains were not N-type excess semiconduction.

CHAPTER 12

DISCUSSION OF RESULTS

Introduction.

In this Chapter the information available from conductivity measurements and poisoning experiments described in the preceeding sections is collated. This leads to a clearer understanding of the conductivity processes which occur in oxide coated cathodes in the temperature range 290 - 1000°K. Some suggestions for further experimental work are also included.

The work of Loosjes and Vink (45) demonstrated that the conductivity could be expressed as the sum of two exponential terms thus,

$$\sigma = \sigma_1 \exp\left(\frac{-\phi_1}{kT}\right) + \sigma_2 \exp\left(\frac{-\phi_2}{kT}\right)$$

implying that two conduction mechanisms operate in parallel. One of these was the predominant process above about 700°K, the other was predominant below that temperature. A discussion of the results obtained in the investigations reported in sections 2 and 3 of this thesis can then be divided conveniently into two sections; behaviour of the oxide cathode above ~ 700°K and behaviour below that temperature.

1. Behaviour of the oxide-cathode in the high temperature region.

The conductivity measurements made on samples of barium oxide and barium strontium (BaSr)O cathodes give results very similar to those described by Loosjes and Vink (fig. 4.3) and several other authors. At temperatures above about 700°K Loosjes and Vink found that the slope of the conductivity line was very similar to the work function of the cathode determined from a Richardson plot of emission measure-

ments. This led to the conclusion that above about 700°K the predominant conduction mechanism was one of thermionic emission in the pores of the oxide coating (pore conduction). Evidence for pore conduction has been afforded more recently by measurements of the Hall effect (47) and thermoelectric effect (42) in oxide cathodes. The agreement between the activation energy of the conduction process and the work function of the cathode, which was obtained by Loosjes and Vink, was not observed by other authors. This is also the case in the measurements reported in Chapters 5 and 6. However, little importance is attached to this disagreement, for the measurement of the work function, which is temperature dependent, can only be made over a range of temperature not coincident with that over which the high temperature conductivity is measured. In the results reported in these Chapters, therefore, no deductions are made from evidence afforded by Richardson plots.

The oxygen and sulphur poisoning experiments described in Section 3 provided additional support to the pore conduction theory. At higher temperatures, in these experiments, the conductivity is reduced to an extent similar to, or greater than, the reduction of the emission, when oxygen gas or sulphur vapour is admitted to the cathode. In addition, during the period immediately after poisoning, the conductivity shows a recovery characteristic very similar to that of the emission in agreement with the results of Shepherd (64).

The sulphur poisoning experiments are of additional interest in that they show that a cathode, poisoned by small quantities of sulphur, will recover completely at temperatures above about 800°K. This

suggests that small quantities of sulphur vapour arising from impurities in the metal or insulating materials of commercial valves, should not prove deleterious to the oxide cathode under normal operating conditions.

Further evidence for the pore conduction theory is provided by measurements of conductivity at elevated temperatures. Above 1000°K the slope of the conductivity line returns to a lower value. Occasionally this phenomenon may be observed at lower temperatures e.g. fig. (5.16) and fig. (6.6) where the upper bend is evident. This is interpreted to be due to saturation of the electron emission in the pores and probably explains the transitions from one slope to another at ~1000°K observed by Hannay et al (58).

Thus it is well established that pore conduction is the predominant conduction mechanism in oxide coated cathodes at temperatures above 700°K and the results recorded in this work are in good agreement with this theory.

2. The Behaviour of the Oxide Cathode at temperatures below 700°K.

No detailed investigation of the conductivity of the oxide layer at temperatures below 700°K has been reported. Loosjes and Vink suggested that in the low temperature region the predominant conduction process would be conduction through the crystal grains limited by barrier layers at the crystal surfaces. This "bulk" conduction, in principal, could be either by movement of ions or electrons and it would be difficult to distinguish between these two carriers. But other processes may contribute to the conduction mechanism such as

ion movement over the surfaces of the crystal grains or electron movement in surface energy states.

From time to time (12)(49) evidence has been afforded which suggests that conduction occurs in a film of barium, though this has never been widely accepted. It is possible that this process could operate in parallel with another conduction process, e.g. electronic conduction through the crystal grains or in surface energy states.

An investigation of the low temperature conduction process is thus complicated by the possibility of so many contributory mechanisms and a systematic investigation would prove to be very difficult. The measurements reported in Sections 2 and 3 of this work do not purport to be even an attempt at such an investigation but some additional information has emerged from these experiments which assists in an understanding of the conduction process at low temperatures. This is discussed below.

In Section 2 conductivity measurements are described which indicate that at least two conduction processes are operating at 500°K. a temperature at which the contribution from the high temperature pore conduction mechanism is very slight. One of these processes appears to be the predominant conduction process at temperatures below 400°K. Experiments show that this process is adversely affected by the presence of oxygen on the surfaces of the crystal grains but is considerably enhanced by the presence of barium. The average value of the activation energy (L) of this extra low temperature conduction process is found to be 0.12eV although it is observed to be much less than this when barium is present in excessive quantities.

experiments to suggest this either. The shape of the poisoning characteristics does not give an indication that oxygen or sulphur diffuses into the oxide grains and reduces the conductivity by occupying vacant lattice (donor) sites.

The admission of oxygen or sulphur to a cathode increases the slope of both sections of the conductivity v. temperature line, implying that both conductivity processes are impaired by oxygen. This can be explained in terms of barriers between the crystallites. A bulk conduction process will depend upon the nature of the contact between adjacent crystals in addition to the actual mechanism of electron transfer in the crystals. Oxygen or sulphur in a poisoning attack can diffuse into and become lodged in crystal-crystal contacts and thus reduce the conductivity by trapping electrons. The recovery of the cathode at elevated temperatures with negative ion emission tends to support this view. It is not necessary, therefore, to introduce a semiconductor theory to account for the results obtained in poisoning a cathode at low temperatures.

The problem of interpreting the low value of Q still remains therefore. It cannot be concluded on the evidence presented in this work that semiconduction does not occur as a contributory conduction process. However, the low value of Q argues for some other mechanism. It is interesting to follow up the suggestion of Plumlee (66) that OH^-e centres are responsible for the semiconducting properties of oxide cathodes. Movement of donors then occurs by proton transfer

An interpretation of this conduction process in terms of the movement of barium ions on or near to the surfaces of the crystal grains is in agreement with the experimental evidence, and with a value of 0.16 ± 0.03eV obtained by Redington (68) for the activation energy of diffusion of barium on the surface of barium oxide.

There has been a tendency in the literature (47)(42) to interpret the lower section of the log conductivity v. reciprocal temperature curve in terms of 'normal' semiconduction. It is reasonable to suppose that the oxide is an excess N-type semiconductor since an excess of barium is necessary for normal operation of the oxide as an electron emitter, although no correlation has been found between excess barium content and thermionic emission (16). However, the very small values of activation energy (Q) of the low temperature conduction process obtained in the measurements described in section 2, do not support such an interpretation. It has been observed in Chapter 2 that if Q is found to be less than 0.25eV the simple theory of N-type excess semiconductors cannot be used to account for the slope of the conductivity line.

The values of Q obtained from the experiments described in Section 2 after correction for the extra-low temperature conduction process lie very close to 0.25eV. This value was obtained in all the cathodes employed and may be regarded as a typical value for well activated mixed oxide (BaSr)O coatings. It cannot be concluded therefore that the other low temperature conduction process is N-type excess semiconduction. Again there is no evidence from low temperature poisoning

from one oxygen atom to another. The activation energy of such a process would be very low e.g. in water the transition $H_2O \longrightarrow H_3O^+$ requires 0.25eV. Could the low value of Q be explained by proton transfer within the crystals? It would be difficult to show this experimentally.

Further Work.

It would be of immediate advantage to extend these conductivity measurements to further samples of barium oxide cathodes. The indications from fig. 7.1 are that a similar extra-low temperature conduction process occurs in barium oxide. Comparison of the value of Q (corrected) with values of Q obtained from work on single crystals of BaO would then at least indicate the magnitude of the differences involved.

Measurement of the conductivity of the oxide layer by a different method would also be of value in confirming the effects observed by the author using probe-tubes. One such method, employing two 'button' cathodes with the oxide layer between themwould also permit the measurement of the thermoelectric effect provided the temperature difference between the two buttons could be maintained with sufficient precision.

A method which permits the mechanical pressure on the oxide layer to be altered would also be useful in investigating the importance of the area of contact between the crystallites. An apparatus which this effect could be studied has been described by Hensley (71). One

button coated with oxide was mounted so that its position relative to a similarly coated button could be adjusted outside the vacuum tube by means of tonbac bellows. Extensive measurements in the low temperature range were not made by Hensley since the apparatus was designed to test the pore conduction theory with the cathodes first touching and then separated by a small gap.

It is thought that the measurements made on the poisoning effect of sulphur and oxygen are not sufficiently quantitative. Improvements in this respect might be made by admitting known quantities of gas into the vacuum tube from small sealed-off tubes. The behaviour of the cathode at known pressures of oxygen or sulphur vapour could then be studied particularly in the low temperature region.

The barium deposition experiments and oxygen and sulphur poisoning experiments could be improved and rendered less ambiguous if a mass-spectrometer technique were used to admit ions of known mass to the cathode. Such a method gives of greater control over the experimental conditions than is obtained in the experiments described in this work and should lead to more precise conclusions. A mass spectrometer, with these capabilities, is under the course of construction in this laboratory.

APPENDIX I

AN A.C. TECHNIQUE FOR THE MEASURING OF PROBE CURRENT-VOLTAGE CHARACTERISTICS

Introduction.

The curvature of the probe I-V characteristics of partially activated cathodes was reported in Chapter 5, but this effect was not investigated any further at that stage. In the following paragraphs a technique is described which enables the curvature to be studied in greater detail.

Fig. 5.1 and fig. 5.5 show that the curvature is most pronounced in the positive region. It is difficult to interpret such curvature without further information, particularly in view of the assymmetrical field which exists between the helical probe wire and the cylindrical nickel core. The application of larger probe potentials might assist in showing whether curvature also occurs in the negative region. However, during the time necessary for D.C. measurements to be made, with larger probe potentials, the probe or the oxide layer could become overheated and give rise to extraneous effects. This difficulty may be overcome by the use of an alternating probe potential which is applied only for a short time. During this time the I-V characteristic is displayed on a C.R.O. and photographed. Tomlinson (41) has pointed out that this method has the added advantage that a "zero-time" characteristic is thus obtained.

FIG. A1.

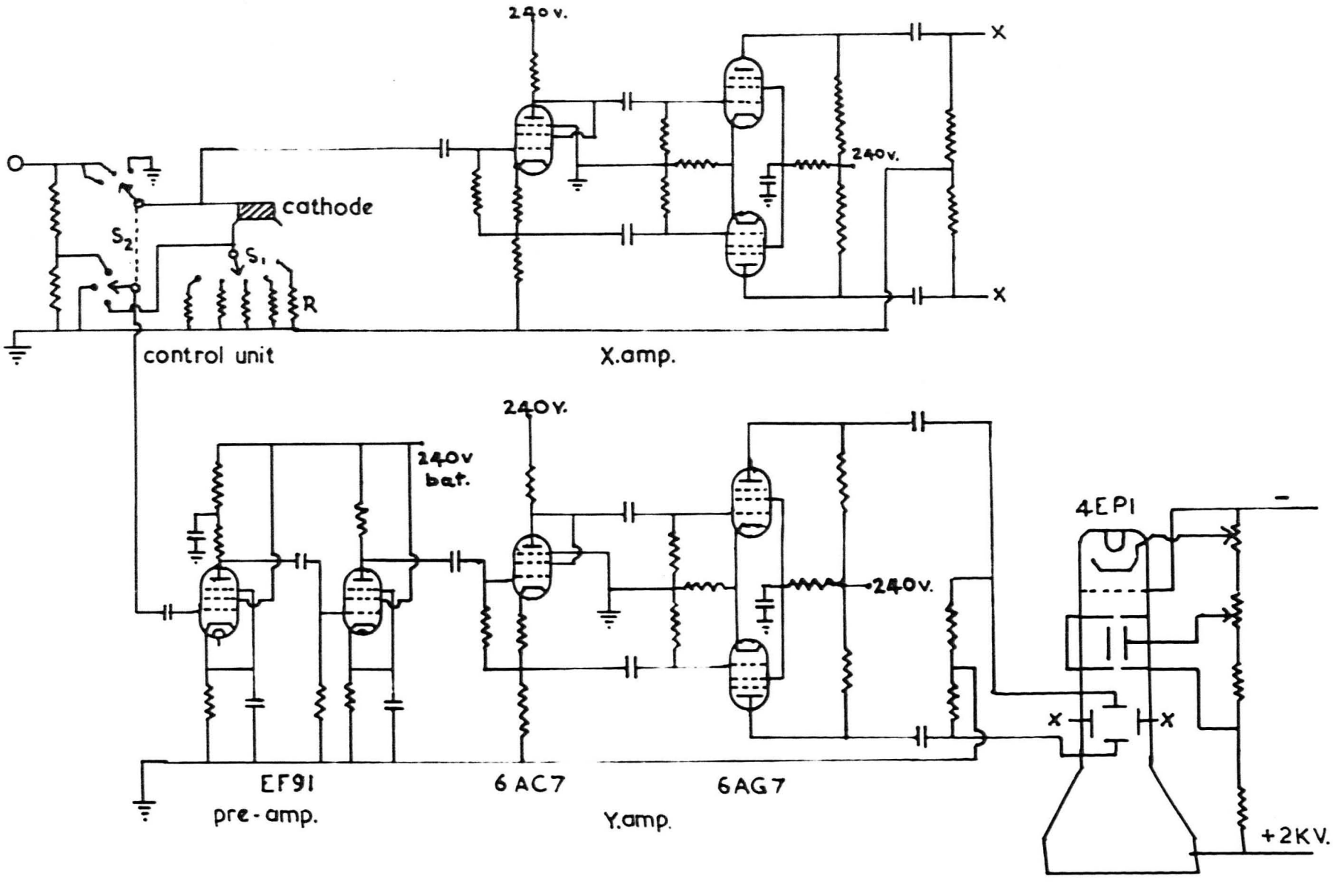
240v.
X
240v.
cathode
S2
S1
R
X
control unit
X.amp.
240v.
240v
bat.
240v.
4EP1
-
x
x
EF91
pre-amp.
6AC7
6AG7
Y.amp.
+2KV.

Experimental

The experimental arrangements was designed around an Emitron 4 EP1 cathode ray tube. This tube has a flat screen and a phosphor suitable for photographing.

Two similar amplifiers were designed to prove push-pull deflection at each pair of deflector plates. In addition a preamplifier was used to amplify the current waveform before it was applied to the Y amplifier. Fig. A1 shows the circuits in detail. In order to improve the signal-to-noise ratio in the first stage of the pre-amplifier both the EF91 heater and anode potentials were derived from batteries. The rest of the equipment operated with conventional stabilised power supplies.

The source of an alternating voltage used in these measurements was an Airmec Signal Generator type 702. This provided a signal of adjustable amplitude between 0 and 20 volts peak to peak, and of adjustable frequency from 30 to 30,000 cps. The output from this unit was monitored by a Solartron CD 568 oscilloscope and all voltage and current measurements were referred to the internal meter in this instrument. This was claimed by the manufacturers to have an accuracy of better than 5% which was adequate for the work undertaken.

The control unit contained a switch S_1 which selected the size of the resistance R in series with the cathode under test. The potential developed across R was proportional to the cathode resistance and this was fed to the preamplifier and thence to the Y amplifier and C.R.T. At the same time the a.c. signal was applied to the input of

FIG.AP1.

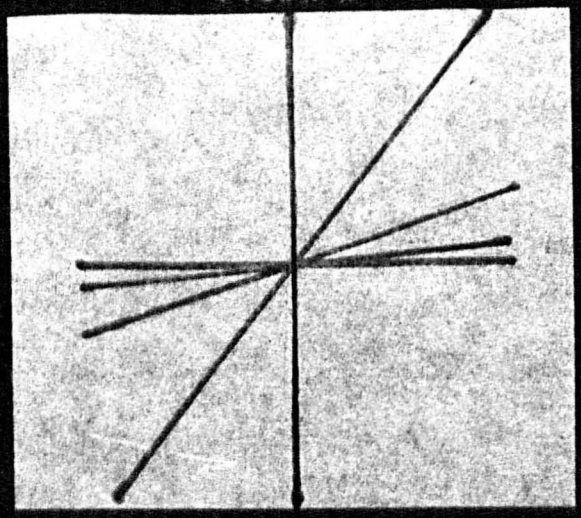

FIG.AP3

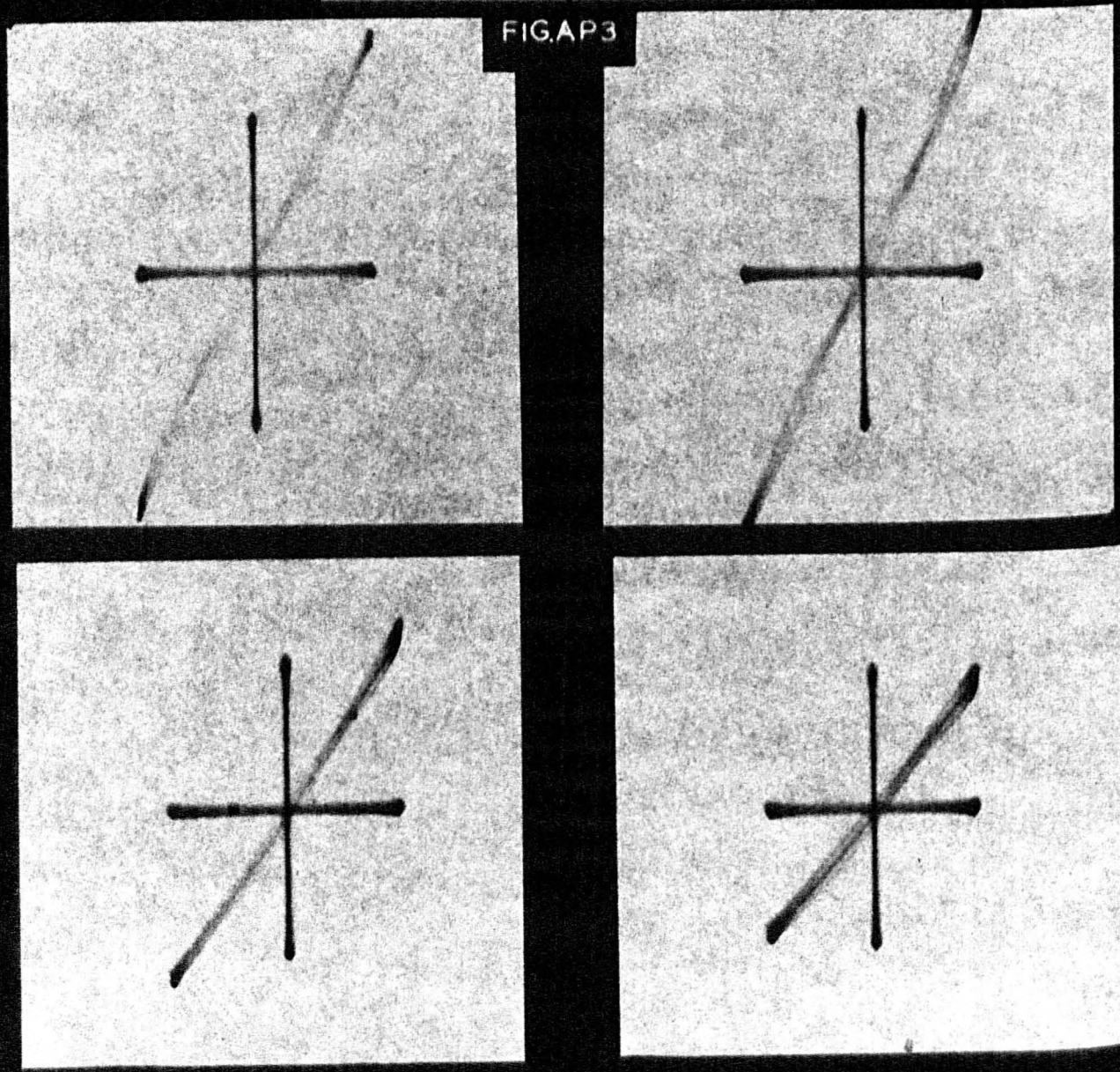

the X amplifier. In this way a voltage current characteristic was displayed on the screen of the C.R.T. The value of R was selected in conjunction with the a.c. voltage and the settings of the amplifier attenuators, so as to give a trace about 2" in length. The switch S_2 in the control unit provided a means whereby the X and Y axes and the characteristics could be displayed separately. The axes were used for calibration purposes; a fraction of the a.c. voltage $\left(\frac{1}{100}\text{th}\right)$ being fed into the Y amplifier through the preamplifier and the total voltage being fed to the X amplifier. This made it unnecessary to calibrate the attenuators and amplifiers since the calibration axes could be included in each photograph taken. Only the value of R had to be known accurately and so each resistor was measured against a standard, using a Muirhead potentiometer.

A Cossor oscilloscope camera type 1428 was used to photograph the trace on Ilford 5B52 Recording Film. An exposure time of about $\frac{1}{2}$ second was found to be adequate with 2000 volts on the P.D.A. electrode of the cathode ray tube.

Preliminary Experiments.

In order to ensure that non linearity was not introduced by the amplifiers and their associated circuitry a preliminary experiment was performed using a 15K Ω resistance to simulate the probe-base resistance of an oxide coated cathode. Fig. AP1 shows the results obtained with different values of R, the current sampling resistance. The characteristics are linear showing that non-linearity is not introduced by the amplifiers, etc.

FIG. AP2

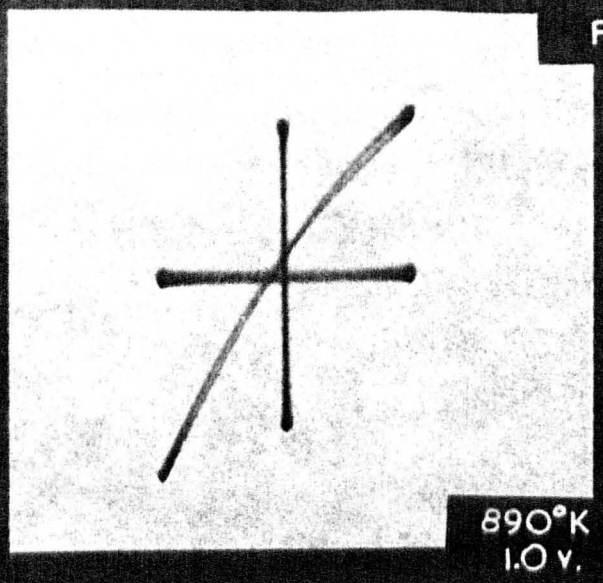

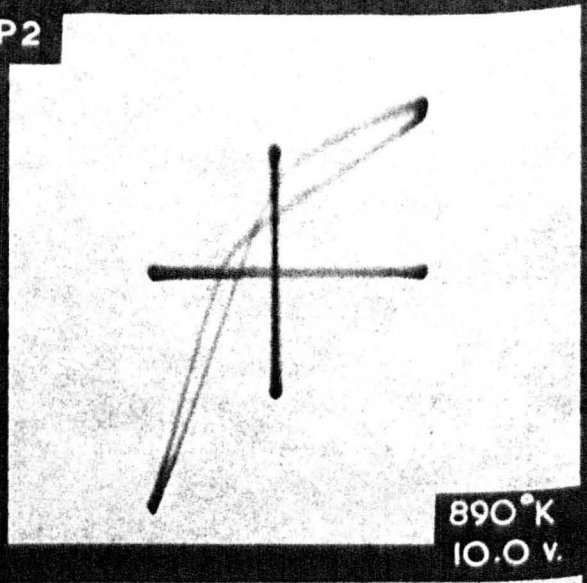

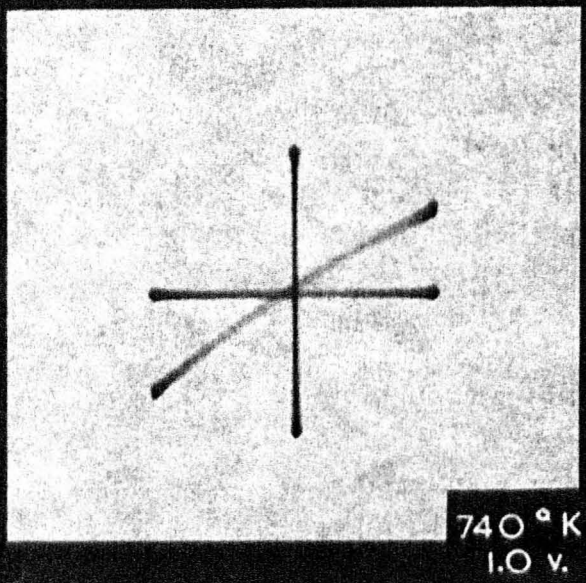

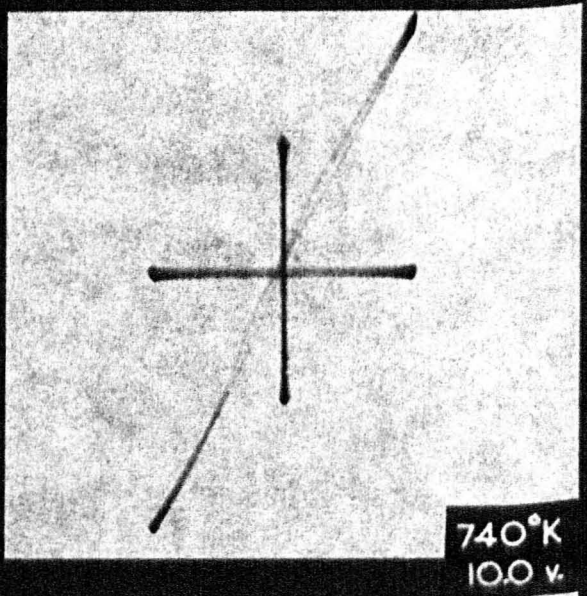

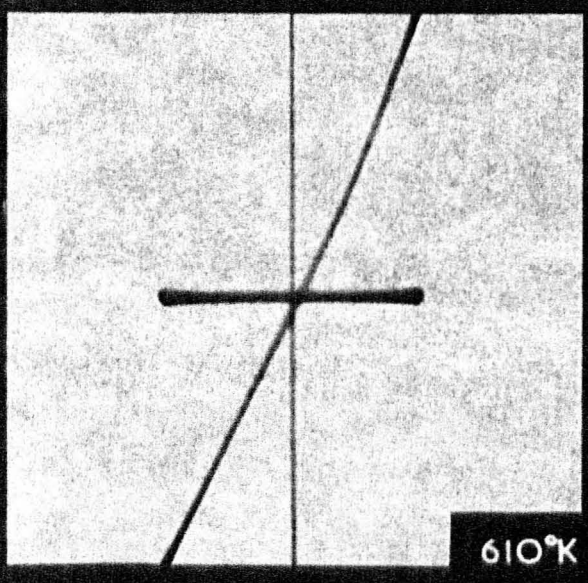

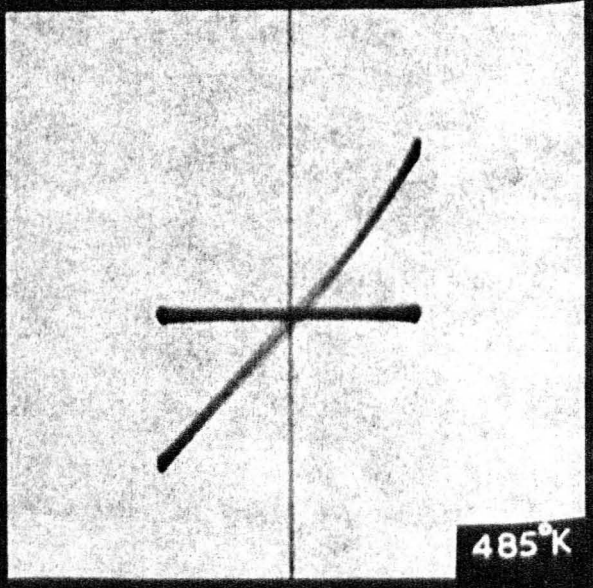

Probe-Base I-V Characteristics.

The 15KΩ resistance was replaced by the probe-base resistance of cathode BaSr8. It was necessary to employ D.C. on the heater of this cathode in order to prevent a.c. pick-up and consequent broadening of the trace on the C.R.T. A few of the I-V characteristics are given in fig. AP2. The a.c. voltage applied and the current sampling resistance together with the temperature are given with each characteristic.

The non-linearity of probe I-V characteristics for large applied voltages is clearly illustrated by these preliminary measurements. At 890°K even with only 1.0 volt applied curvature is evident. With 10 volts the curvature is most pronounced but 'phase' loops make obscure the true characteristic.

At 740°K just within the high temperature region the curvature with an unput of 1.0 volts is not very pronounced. However, with 10 volts applied an I-V characteristic very similar to that reported by Tomlinson (41) is obtained. This shows linearity at extreme positive and negative potentials but exhibits a higher slope section near to the origin. Tomlinson explained this behaviour in terms of saturation of the pore conduction mechanism at higher applied potentials and suggested a new conduction model for the tube which is described in Chapter 2.

At lower temperatures 610°K and 485°K the I-V characteristics with 10 volts input are not linear but exhibit slight curvature towards the current axis in the positive region. This effect has been noted by King (69) who employed a slightly different method. He was

FIG. AP4

BaSr6 LOW TEMPERATURE CONDUCTIVITY

measured by a.c. technique.

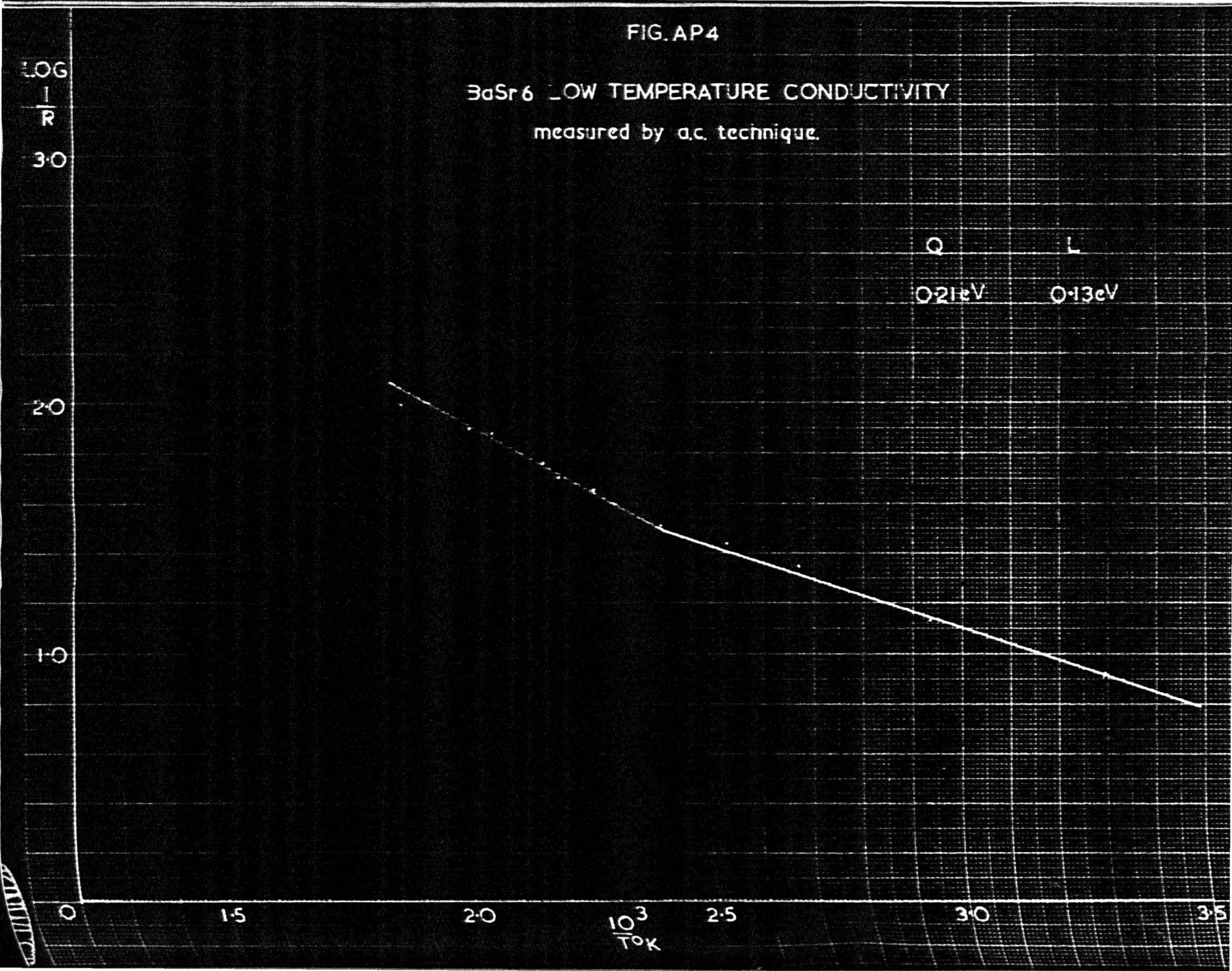

FIG.AP 5.

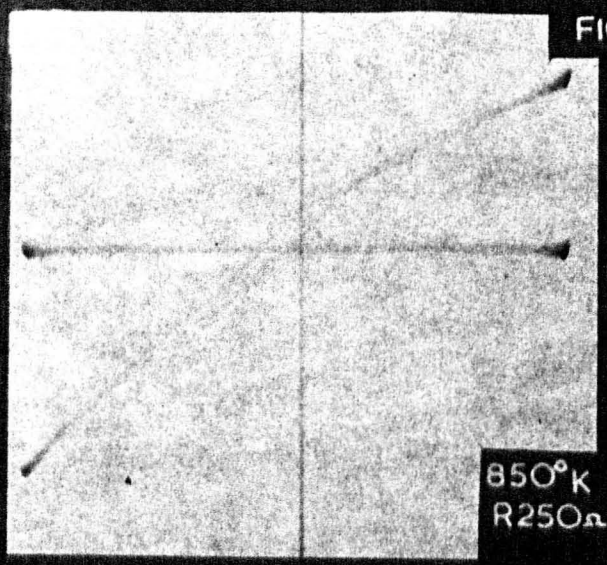
850°K
R250Ω

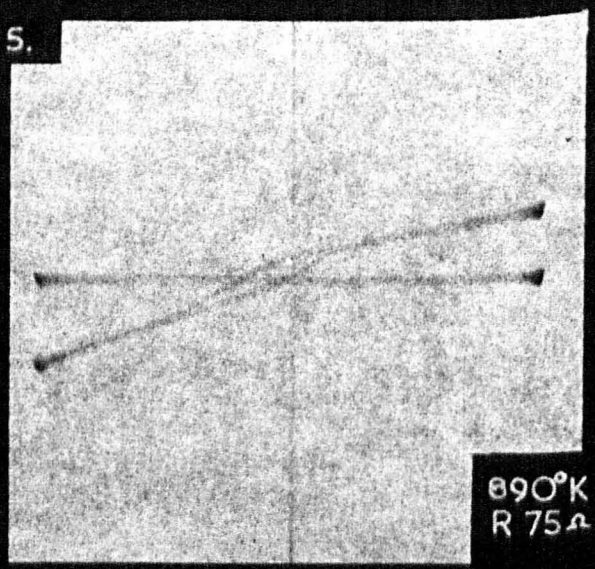
890°K
R 75Ω

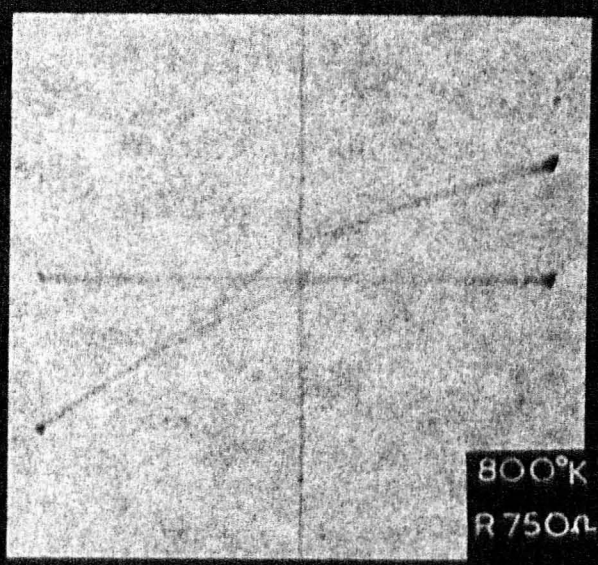
800°K
R 750Ω

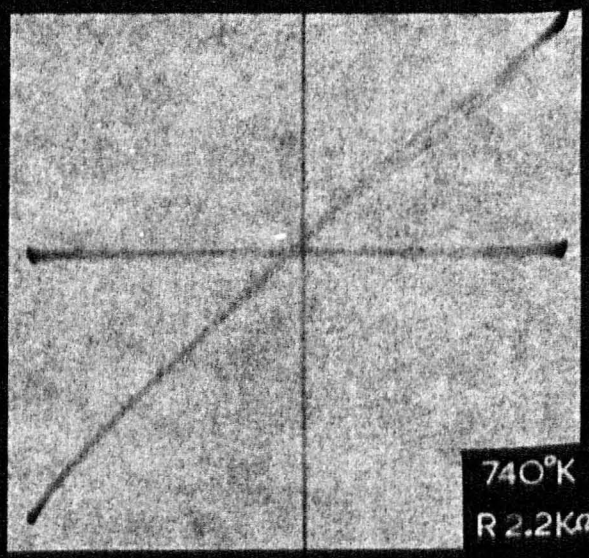
740°K
R 2.2KΩ

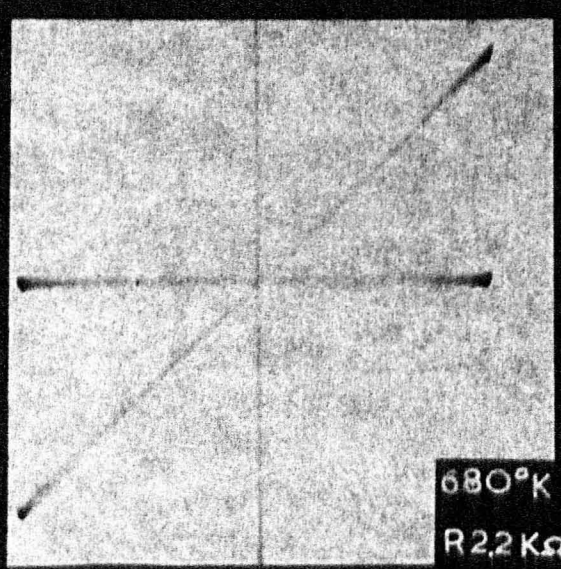
680°K
R 2.2 KΩ

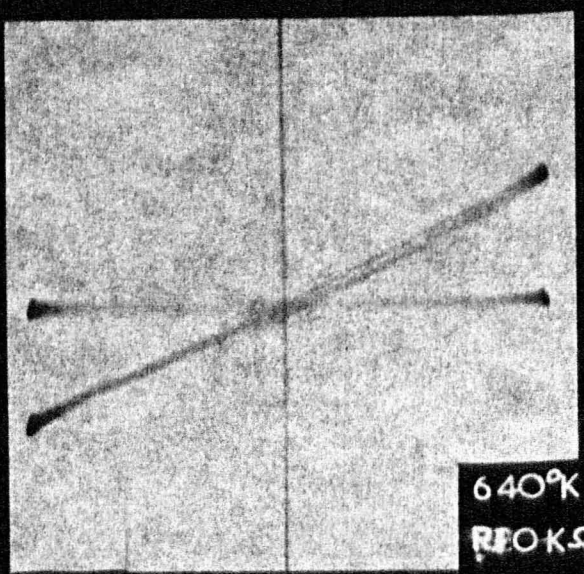
640°K
R 10 KΩ

not able to explain this but suggested that it might arise due to transitional resistances between the crystal grains or increased electron mobility at high field strengths.

Further Measurements.

A series of measurements were made on cathode BaSr6 throughout the low temperature range in order to construct a $\log 1/R$ vs. $1/T$ curve which might then be compared with the curves obtained by d.c. measurements. Some of the characteristics are shown in fig. AP3. Fig AP4 shows the conductivity line constructed from these measurements. The agreement with the d.c. measurements (fig. 7.4) is very good although the precision is limited by the broadening of the displayed characteristic at lower temperatures. However, the extra-low temperature section with slope of 0.13eV is obtained in agreement with the value of 0.12 eV obtained from the d.c. measurements.

The limit of sensitivity of this method at an input potential of 10 volts lies very close to that of the d.c. method with an input of 0.1 volts. Without very careful screening of the tube under test and all its associated circuitry it would not be possible to improve upon this figure.

Measurements on BaSr10.

Some measurements were attempted on this cathode before it was fully activated. These are given in fig. AP5. An input of 20 volts was used since this was found to show up the curvature. In the high temperature region the characteristics are curved near the origin but exhibit linearity at higher positive and negative potentials, again

FIG. AP6

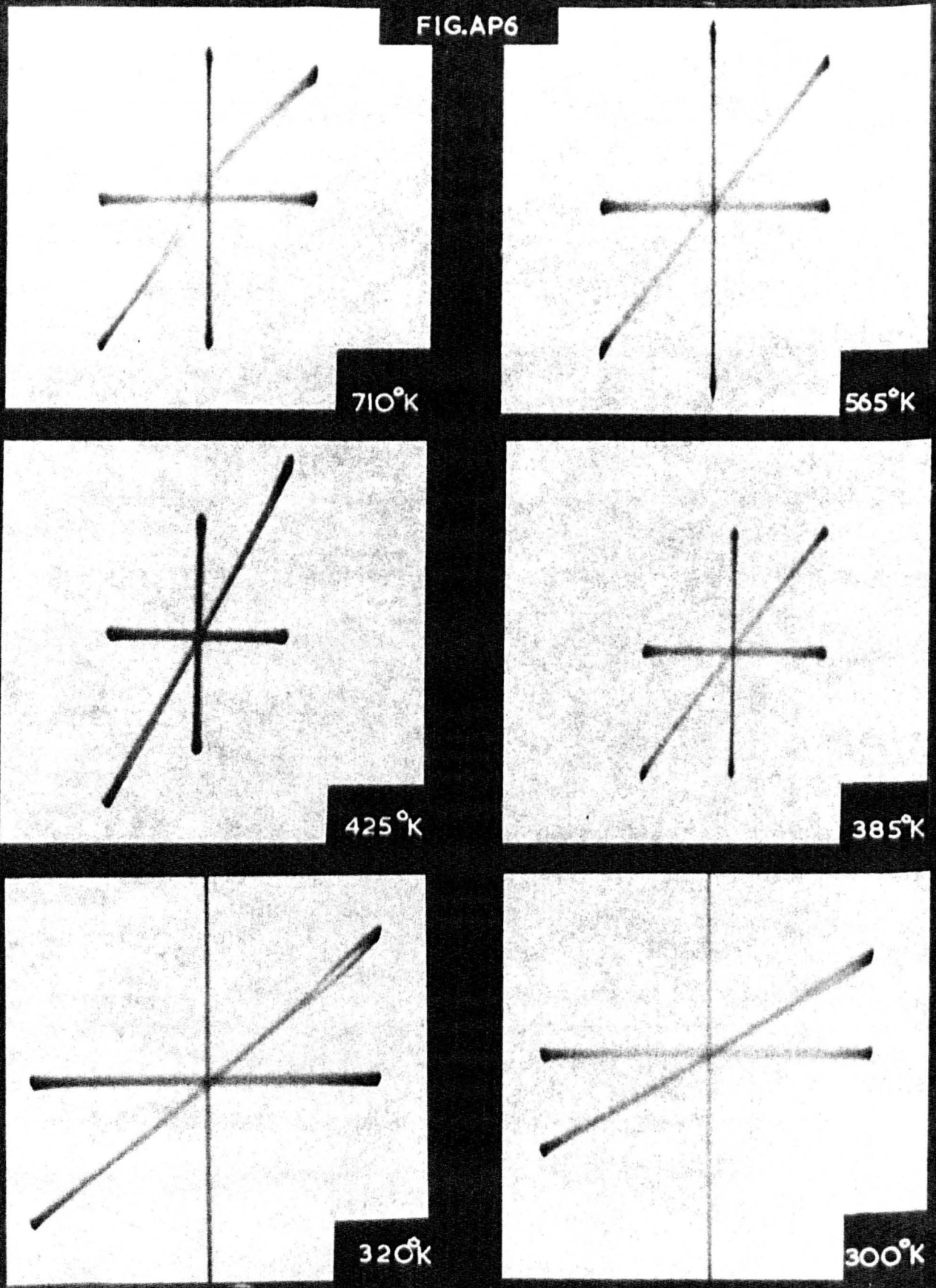

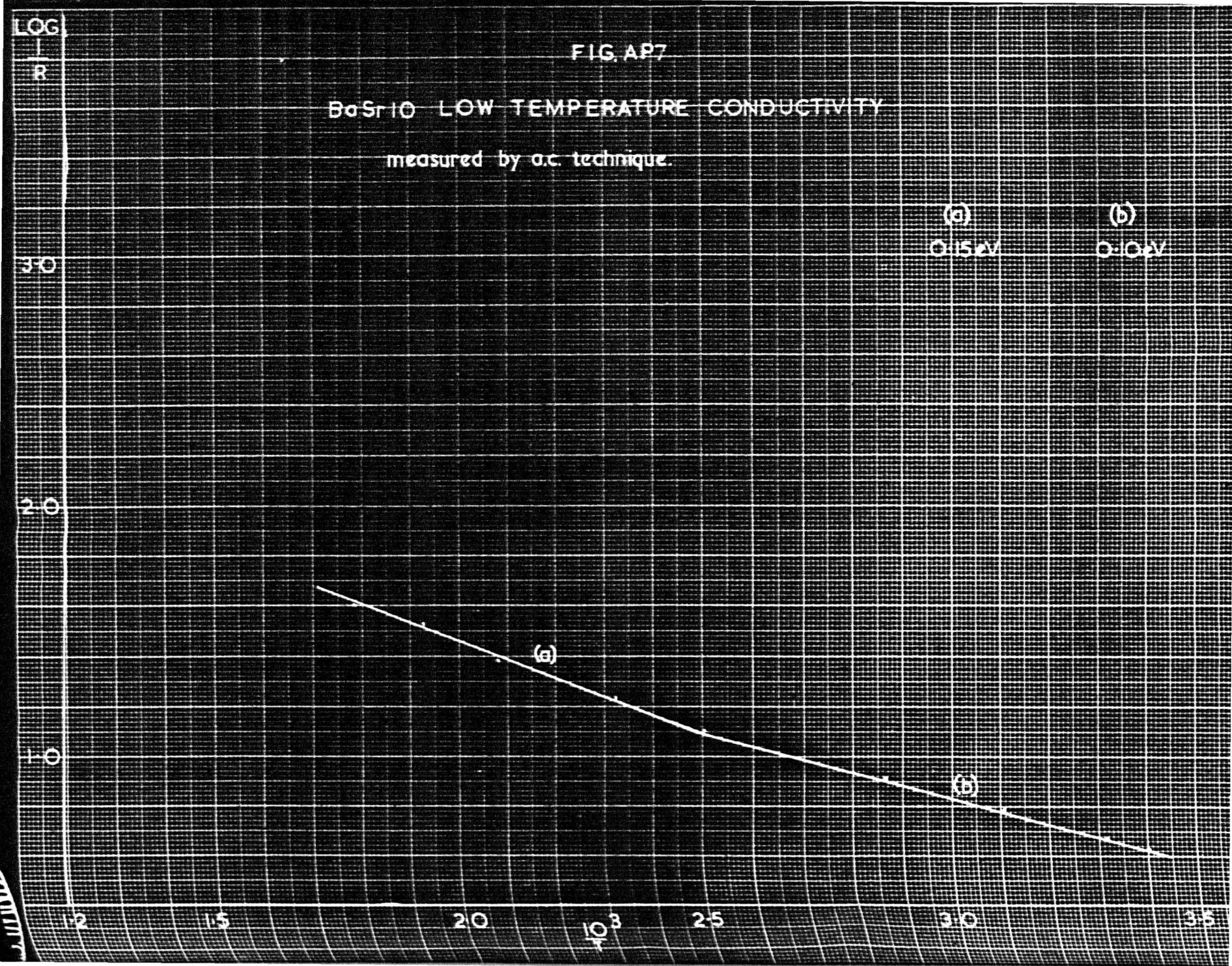
FIG. AP7
BaSr10 LOW TEMPERATURE CONDUCTIVITY
measured by a.c. technique.
LOG 1/R
(a)
0·15eV
(b)
0·10eV
3·0
2·0
1·0
(a)
(b)
1·2
1·5
2·0
10³/T
2·5
3·0
3·5

in agreement with Tomlinson. However, these characteristics are those of a partially activated cathode. Under d.c. conditions considerable curvature of the characteristics was obtained in agreement with results on nearly all the probe tube measurements described in Section 2 of this work. These results tend to confirm the suggestion made in Chapter 5 that temperature saturation of the pore conduction mechanism occurs at lower potentials when the cathode is partially activated. Cathode BaSr10 was eventually fully activated and the I-V characteristics obtained in this state are shown in fig. AP6. The curvature at higher temperature is less than in the unactivated state. At the lowermost temperatures 20 volts input was employed. This revealed a curvature of the characteristics towards the I-axis as obtained in the measurements on BaSr8.

A conductivity curve (fig. AP7) was constructed from these measurements. This exhibited a bend at $\sim 400^{\circ}K$ in agreement with previous measurements.

Discussion.

The a.c. technique appears to be a useful method of measuring probe I-V characteristics although it has a limited sensitivity at lower temperatures (high cathode resistance) due to extraneous pick-up affecting the displayed characteristic.

Very little may be deduced from the shape of the I-V characteristics. However, the results reported by Tomlinson and King have been reproduced in these measurements.

A completely satisfactory explanation of the curvature of the I-V characteristics when the cathode is poorly activated has not emerged from these measurements. This problem would be investigated more readily if a symmetrical field across the oxide layer could be obtained e.g. by employing two button cathodes. This a.c. technique would then prove to be of great value in obtaining "zero time" characteristics and the shape of the curves would be more amenable to theoretical treatment since the geometry of the electrodes would be well defined. This is not the case with probe tubes so that the measurements at the best can only have a qualitative value.

ACKNOWLEDGMENTS

My thanks are due to the following:-

Professor F. A. Vick, O.B.E. for helpful discussion and guidance during this work.

The University College of North Staffordshire for the laboratory facilities provided.

My colleagues in the Physics Department, U.C.N.S. for useful discussion on many of the problems involved.

Mr. F. Rowerth and Mr. B. Bloor of the University College Technical Staff for assistance with photographic work.

REFERENCES

1.	Grey, E.	Nature	165.	773	1950
2.	Kawamura	J.Phys.Soc.Japan	3.	301.	1948
3.	Yamaka Eiso	J.App.Phys.	23.	9. 937	1952
4.	Prescott & Marrison	J.Amer.Chem.Soc.	60	3047	1938
5.	Eisenstein	J.App.Phys.	20.	776	1949
6.	Forman	Phys.Rev.	96.	6. 1479	1954
7.	Wagener	Proc.Phys.Soc.	B 66.	400	1953
8.	Arnold	Phys.Rev.	70		1920
9.	Fineman & Eisenstein	J.App.Phys.	17	663	1946
10.	Rooksby	G.E.C. Journal	11	83	1940
		Nature	159	609	1947
11.	Rittner	Philips Res.Reps.	8.	3. 161	1953
12.	Becker	Phys.Rev.	34	1323	1929
13.	Shepherd	Brit.J.App.Phys.	4	70	1953
14.	Wooten, Ruckle & Moore	J.App.Phys.	26	1	1955
15.	Darbyshire, J.A.	Proc.Phys.Soc.	50	964	1938
16.	Moore, Wooten and Morrison	J.App.Phys.	26	8	1955
17.	Lowery, E.F.	Phys.Rev.	35	1367	1930
18.	Becker, J.A.	Phys.Rev.	34	1323	1929
19.	Becker & Sears, R.W.	Phys.Rev.	38	2193	1931
20.	Darbyshire	Proc.Phys.Soc.	50	964	1938
21.	Huber & Wagener	Z.Techn.Phys.	23	1	1942
22.	Wilson, M.A.	Proc.Roy.Soc.	A 134	277	1931

23.	Fowler, R.H.	Statistical Mechanics	C.U.P.		p.399	1936
24.	Sproull, R.L.	Phys.Rev.	67		166	1945
25.	Coomes, E.A.	J.App.Phys.	17		647	1946
26.	Wright, D.A.	Proc.Phys.Soc.	62B		398	1949
27.	Fan, M.Y.	J.App.Phys.	14		552	1943
28.	Hung, C.S.	J.App.Phys.	21		37	1950
29.	Schottky	Ann.der Physik	44		1011	1914
30.	Wright & Woods	Proc.Phys.Soc.		B	134	1952
31.	Morgulis, N.	J.Phys.U.S.S.R.	11		67	1947
32.	Metson, G.M.	Proc.Phys.Soc.	62B		589	1949
33.	Deb, S.	Indian J.Phys.	25		197	1951
34.	Vick & Walley	Proc.Phys.Soc.	B 47		170	1954
35.	Wright, D.A.	Brit.J.App.Phys.	1		150	1950
36.	Feaster, G.R.	J.App.Phys.	20		415	1949
37.	Nergaard	R.C.A.Rev.	13	4	464	1952
38.	Becker	Phys.Rev.	34		1323	1925
39.	Becker & Sears	Phys.Rev.	38		2193	1931
40.	de Vore, H.B.	Phys.Rev.	83		805	1951
41.	Tomlinson, T.B.	J.App.Phys.	25		720	1954
42.	Young, J.R.	J.App.Phys.	23		10	1952
43.	Plumlee, R.H.	R.C.A.Rev.	17		190	1956
44.	Nishibori & Kawamura	Proc.Phys.Maths.Soc. Japan	22		378	1940
45.	Loosjes and Vink	Philips Res.Reports	4		449	1949
46.	Nakai Inuishi & Tsung-che	J.Phys.Soc.Japan	10	6	437	1955

47.	Forman	Phys.Rev.	96	6	1479	1954
48.	Sparks and Philipp	J.App.Phys	24		4	1953
49.	Hughes and Coppola	Phys.Rev.	88		364	1952
50.	Wright, D.A.	Brit.J.App.Phys.	1		150	1950
51.	Sproull & Tyler	Semiconducting Materials Butterworths			p. 122	1951
52.	Doloff, R.T.	J.App.Phys.	27		1418	1956
53.	Shockley	Phys.Rev.	56		317	1939
54.	Wright, D.A.	Semiconductors Methuen			p. 57	1955
55.	Seitz, F.	Modern Theory of Solids McGraw-Hill			p.325	1940
56.	Fritzch, O.	Ann.Physik	22		375	1935
57.	Mott and Gurney	Electronic Processes in Ionic Crystals O.U.P.			p.166	1940
58.	Hannay, McNair & White	J.App.Phys.	20		669	1949
59.	Duckworth, A.	Ph.D.Thesis Manchester University unpublished				1951
60.	Koller	Phys.Rev.	25		671	1925
61.	Kawamura quoted in (62)					
62.	Arizumi & Narita	J.Phys.Soc.Japan	3		356	1949
63.	Metson	Nature	164		540	1949
64.	Shepherd	Brit.J.App.Phys.	4		70	1953
65.	Stahl, H.A.	App.Sci.Res.	B 1		397	1950
66.	Plumlee, R.H.	R.C.A. Rev.	17		231	1956
67.	Pauling	Nature of the Chemical Bond O.U.P.			p. 65	1940

68.	Redington	Phys.Rev.	87	1066	1952
69.	King, R.E.J.	Research	9	89	1956
70.	Stoll, S.J.	Brit.J.App.Phys.	7	94	1956
71.	Hensley	J.App.Phys.	27	286	1956